Volume 73A
Number 1
Jan.–Feb. 1969

Physics and Chemistry

U.S. DEPARTMENT OF COMMERCE

SECTION A

JOURNAL OF RESEARCH

NATIONAL BUREAU OF STANDARDS

Journal of Research
of the
National Bureau of Standards

A. Physics and Chemistry

Jan.–Feb. • 1969

VOLUME • 73A

NUMBER • 1

Editor: C. W. Beckett

Associate Editor: D. D. Wagman

Publication dates:
Feb. 1, Apr. 1, June 1, Aug. 1, Oct. 1, Dec. 1, 1969

JOURNAL OF RESEARCH

The National Bureau of Standards Journal of Research reports research and development in the fields of activity shown at right. Also included from time to time are survey articles on topics closely related to the Bureau's scientific and technical program.

The Journal is published in three separate sections as follows:

A. Physics and Chemistry

Contains papers of interest primarily to scientists working in these fields. Issued six times a year. Annual subscription: domestic, $6.00; foreign, $7.25. Single copy, $1.00.

B. Mathematical Sciences

Presents studies and compilations designed mainly for the mathematician and the theoretical physicist. Issued quarterly. Annual subscription: domestic, $2.25; foreign, $2.75. Single copy, 75c.

C. Engineering and Instrumentation

Reports research and development results of interest chiefly to the engineer and the applied scientist. Issued quarterly. Annual subscription: domestic, $2.75; foreign, $3.50. Single copy, 75c.

NATIONAL BUREAU OF STANDARDS

The National Bureau of Standards[1] was established by an act of Congress March 3, 1901. Today, in addition to serving as the Nation's central measurement laboratory, the Bureau is a principal focal point in the Federal Government for assuring maximum application of the physical and engineering sciences to the advancement of technology in industry and commerce. To this end the Bureau conducts research and provides central national services in three broad program areas and provides central national services in a fourth. These are: (1) basic measurements and standards, (2) materials measurements and standards, (3) technological measurements and standards, and (4) transfer of technology.

The Bureau comprises the Institute for Basic Standards, the Institute for Materials Research, the Institute for Applied Technology, and the Center for Radiation Research.

THE INSTITUTE FOR BASIC STANDARDS provides the central basis within the United States of a complete and consistent system of physical measurement, coordinates that system with the measurement systems of other nations, and furnishes essential services leading to accurate and uniform physical measurements throughout the Nation's scientific community, industry, and commerce. The Institute consists of an Office of Standard Reference Data and a group of divisions organized by the following areas of science and engineering:

Applied Mathematics—Electricity—Metrology—Mechanics—Heat—Atomic Physics—Cryogenics[2]—Radio Physics[2]—Radio Engineering[2]—Astrophysics[2]—Time and Frequency.[2]

THE INSTITUTE FOR MATERIALS RESEARCH conducts materials research leading to methods, standards of measurement, and data needed by industry, commerce, educational institutions, and government. The Institute also provides advisory and research services to other government agencies. The Institute consists of an Office of Standard Reference Materials and a group of divisions organized by the following areas of materials research:

Analytical Chemistry—Polymers—Metallurgy—Inorganic Materials—Physical Chemistry.

THE INSTITUTE FOR APPLIED TECHNOLOGY provides for the creation of appropriate opportunities for the use and application of technology within the Federal Government and within the civilian sector of American industry. The primary functions of the Institute may be broadly classified as programs relating to technological measurements and standards and techniques for the transfer of technology. The Institute consists of a Clearinghouse for Scientific and Technical Information,[3] a Center for Computer Sciences and Technology, and a group of technical divisions and offices organized by the following fields of technology:

Building Research—Electronic Instrumentation—Technical Analysis—Product Evaluation—Invention and Innovation—Weights and Measures—Engineering Standards—Vehicle Systems Research.

THE CENTER FOR RADIATION RESEARCH engages in research, measurement, and application of radiation to the solution of Bureau mission problems and the problems of other agencies and institutions. The Center for Radiation Research consists of the following divisions:

Reactor Radiation—Linac Radiation—Applied Radiation—Nuclear Radiation.

[1] Headquarters and Laboratories at Gaithersburg, Maryland, unless otherwise noted; mailing address Washington, D.C. 20234.
[2] Located at Boulder, Colorado 80302.
[3] Located at 5285 Port Royal Road, Springfield, Virginia 22151.

U.S. DEPARTMENT OF COMMERCE
NATIONAL BUREAU OF STANDARDS
A. V. Astin, Director

Order all publications from the Superintendent of Documents
U.S. Government Printing Office, Washington, D.C. 20402.
Use of funds for printing this publication approved by the Director of the Bureau of the Budget (June 22, 1966).

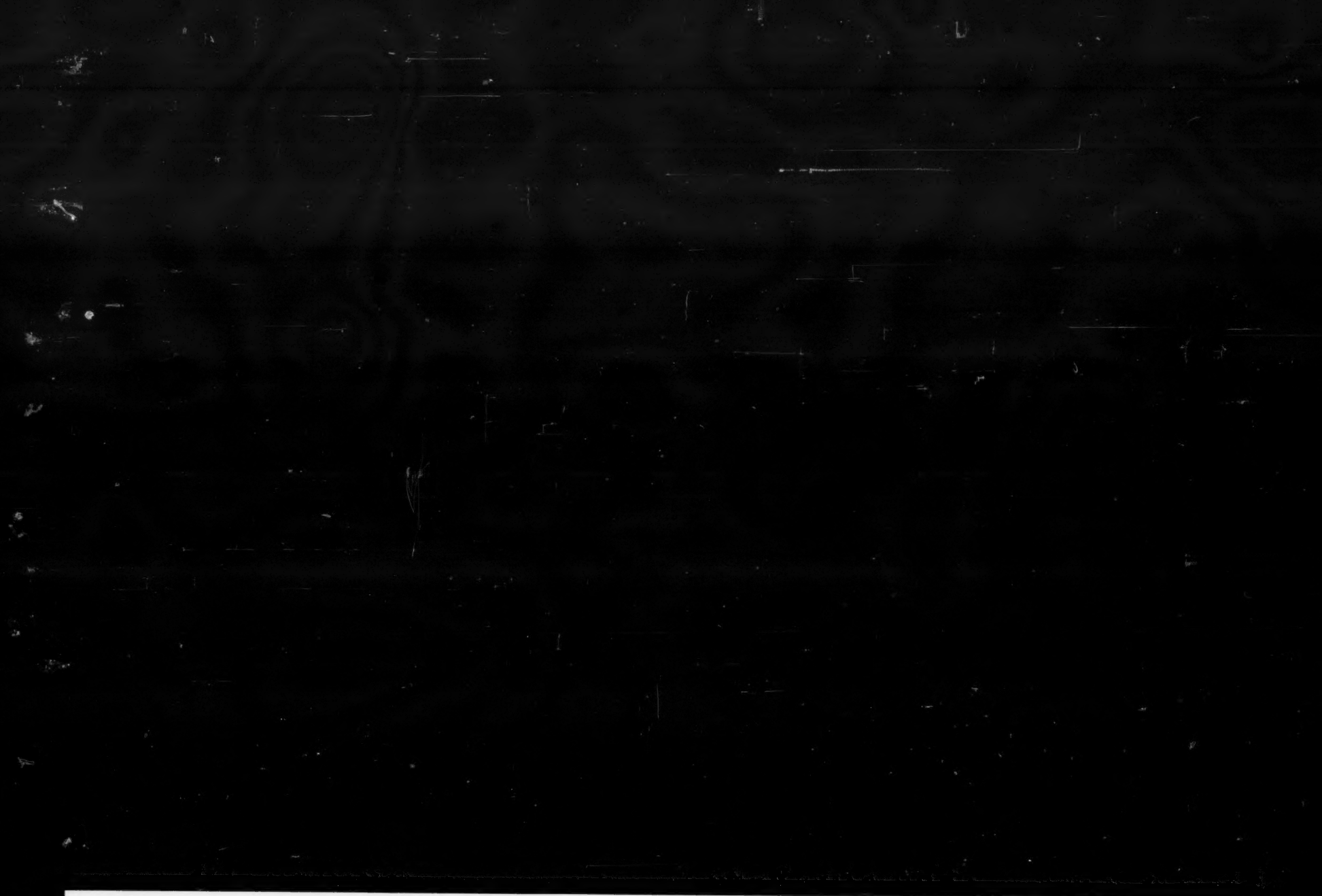

JOURNAL OF RESEARCH of the National Bureau of Standards—A. Physics and Chemistry
Vol. 73A, No. 1, January–February 1969

Specific Heats of Oxygen at Coexistence*

Robert D. Goodwin and Lloyd A. Weber****

Institute for Basic Standards, National Bureau of Standards, Boulder, Colorado 80302

(August 8, 1968)

Specific heats of saturated liquid, along the coexistence path, are useful for computing thermodynamic properties throughout the compressed liquid phase. We report 86 experimental heat capacities of oxygen for the two-phase system, liquid plus vapor, from the triple-point to near the critical-point and corresponding derived values for the liquid phase. These results are represented by a formula which can be integrated for heat absorbed and for entropy. The changes in value of internal energy, enthalpy, and entropy of the saturated liquid are tabulated from the triple-point to the critical-point.

Key Words: Coexistence; experimental; heat capacity; liquid phase; oxygen; saturated liquid; specific heat.

List of Symbols

A, B, C, r	constants for eq (5.1).
A_i	coefficients for liquid density formula.
B_i	coefficients for rectilinear diameter formula.
C_i	coefficients of formula for C_b.
D_i, E_i	binomial coefficients (appendix IV).
C_a	gross heat capacity adjusted for curvature.
C_b	heat capacity of empty calorimeter bomb.
$\bar{C}$	specific heat, two-phase sample, adjusted for curvature.
$\bar{C}_v$	specific heat of two-phase sample at constant total volume.
C_σ	specific heat of liquid on coexistence path.
E	internal energy.
E_b	volt-box output potential.
E_s	potential across standard resistor for heater current.
H	enthalpy.
ΔH_v	heat of vaporization.
J	the joule.
k	conversion factor, 0.101325 J/cm³ atm.
N	total g moles of fluid in bomb plus capillary tube.
N_b	g moles of fluid in the bomb.
N_c	g moles of fluid in the capillary tube.
P	pressure, 1 atm = 0.101325 MN/m².
Q	heat energy; also calorimetric heat input.
$Q/\Delta T$	unadjusted, gross heat capacity.
R_b	volt-box input resistance.
R_l	input lead-wire resistance.
ρ	density.
S	entropy.
t	time.
T	temperature, Kelvin.
T_1, T_2	initial and final temperatures of a heating interval.
T_a	average temperature in ΔT.
T_c	critical-point temperature, 154.77 K. [17]
T_t	triple-point temperature, 54.3507 K. [17, 18]
ΔT	calorimetric temperature increment, deg. Celsius.
v	molal volume, $1/\rho$.
V_b	volume of the calorimeter bomb.
V_l	total liquid volume.

1. Introduction

This work is part of a program on thermodynamic properties of oxygen. For gaseous states the temperature dependence of these properties may be obtained from spectroscopically derived specific heats at zero density [1][1] combined with accurate PVT data. For compressed liquid states, however, additional data are required. Useful among these are specific heats of saturated liquid, $C_\sigma(T)$, along the coexistence path. In the present report we give experimental results from near the triple-point to near the critical-point. We give an empirical formula for temperature dependence of these results, and the integrals in analytical form which we use for calculating the heat absorbed and the change in value of entropy on this path. We tabulate also the energy and enthalpy. Our results for specific heats in single-phase domains will be reported separately. In a forthcoming publication by one of us (L.A.W.), the present results are used

*This work was carried out at the National Bureau of Standards under the sponsorship of the National Aeronautics and Space Administration Fund Transfer R-06-006-046.
**Cryogenics Division, NBS Boulder Laboratories, Boulder, Colorado 80302.
[1] Figures in brackets indicate the literature references at the end of this paper.

with extensive *PVT* data to construct a complete thermodynamic network for oxygen from the triple-point to 300 K at pressures to 300 atm.

2. Apparatus and Procedures

2.1. Apparatus

The calorimeter is the same as used previously for hydrogen [2, 3], except that nearly all of the internal electric wires were replaced (following a relocation of our laboratory). In brief, the spherical sample-holder of type 316 stainless steel is about 2 in in diameter. It is filled via a stainless steel capillary tube 34 in long, $\frac{1}{16}$ in o.d. and 0.006 in i.d., terminating in a shutoff valve on top of the cryostat. A lightweight, cylindrical copper case on the sphere protects the 100 Ω electric heater (wound on the sphere) and serves as the reference temperature for two thermopiles (100 μV/deg C) controlling a guard ring and the adiabatic shield. For control of each of these shields we use a commercial, electronic "controller," giving automatic reset and rate sensitivity, in addition to our previous equipment. We observe the relative shield temperatures continuously on a recorder.

Temperature of the sample-holder is measured with the same platinum resistance thermometer (NBS 1955 scale) and 6-dial, μV potentiometer. Pressures are measured with the same dead-weight gage (piston diameters recently recalibrated), accurate to about one part in 10,000. For safety, oil of the gage is separated from the oxygen by nitrogen gas between two null-diaphragms. Filling pressures are corrected for hydrostatic pressure of cold oxygen in the capillary tube.

We obtain the calorimetric heating rate from simultaneous readings of potential and current. Potential wires are connected at the heater in a manner to account for heat developed in the current-carrying wires between shields and calorimeter [4, 5]. The potential wires lead to a potential-divider (volt-box). We correct for resistance of these potential wires, and for current drawn by the volt-box. The heater current is measured potentiometrically by means of a calibrated, standard resistor and a type K–3 potentiometer.

Time of the heating interval, Δt, is measured by an electronic counter (quartz piezoelectric oscillator) accurate to better than one part in a million. This counter is switched on and off by the potential across the calorimeter heater. An intervening transmitting circuit, of 22 megohm input impedance, gives the counter a signal independent of the heater potential.

2.2. Procedures for the Sample

The commercial high-purity oxygen (maximum nominal impurities 0.01%) is taken from a steel cylinder at about 130 atm. At this pressure the oxygen flows through a molecular sieve trap at 76 K, and is admitted slowly to the calorimeter bomb until this pressure also is near 130 atm. The amount of sample is fixed by the selected bomb temperature. A steady state exists after 30 min, when we measure temperature and pressure. We then immediately close the cryostat valve, and begin cooling the bomb into the region of two phases for the contained oxygen.

2.3. Procedure for a Heat Measurement

We measure five temperatures, $T(t)$, in several minutes immediately preceding a heat. They are extrapolated linearly to obtain T_1 at the midtime, t_a, of the heating interval. For a temperature rise of about 5 °C in 10 min we use currents from 0.04 to 0.12 A, dependent on the amount of sample. We average electric power from three pairs of potential and current readings. Shield temperatures as shown on the recorder lag about 0.005 °C at the start, recovering to within 0.001 °C of the calorimeter in about a minute. The opposite behavior follows ending of a heat. We then observe temperature drift of the calorimeter on another recorder. In about 20 min the temperature no longer increases, and may begin a very slow decrease (imperfect adiabatic shielding), when we take another five values for $T(t)$ over about 5 min. They are extrapolated linearly to obtain T_2 at t_a.

3. Calculations and Adjustments

3.1. Amount of Sample

Given the filling conditions P and T, we use an equation of state, appendix V, to calculate the one-phase density with an uncertainty of about 0.1 percent. By use of our bomb volume (uncertainty 0.1%, appendix I) we then have the amount of sample in the bomb. We sum amounts over the length of the capillary tube by use of estimated temperatures in appendix II, and above equation of state. Sum of amounts in bomb and capillary is N, total gram moles in the closed system, with maximum uncertainty of 0.2 percent.

3.2. The PVT Conditions

We use the average temperature for a specific heat observation, $T_a = (T_1 + T_2)/2$, to calculate pressure P_a from the vapor-pressure equation (appendix VI). First and second derivatives of $P(T)$ also are calculated at T_a. Volume of the bomb, V_b, and dV_b/dT are calculated at T_a, P_a (appendix I). Amount of sample in the bomb is $N_b = N - N_c$ where N_c is amount in the capillary tube at T_a, P_a. The increased amount in capillary tube, δN_c, is amount at T_2, P_2 less amount at T_1, P_1. Average density of the sample is defined $\rho_{av} \equiv N_b/V_b$.

Density of the liquid phase, ρ_l mole/cm³, and the derivative versus T, we obtain from the function (L.A.W.) of table 1. By use of the function for rectilinear diameter (L.A.W.) table 2, we obtain the vapor density, ρ_g. Relative volume of liquid in the bomb then is

$$V_l/V_b = (\rho_{av} - \rho_g)/(\rho_l - \rho_g), \qquad (3.1)$$

where V_l is absolute (not molal) volume of the liquid phase.

3.3. Gross, Tare, and Net Heat Capacities

Corresponding to the temperature rise ΔT, the total heat absorbed is Q joules, calculated from volt-box potential E_b, potential E_s across the standard resistor (both in volts), and time Δt, seconds,

$$E_x \equiv E_b \cdot (1+R_l/R_b)/K, \tag{3.2}$$

$$I_b = E_x/(R_b+R_l), \tag{3.3}$$

$$Q = E_x \cdot [E_s/R_s - I_b] \cdot \Delta t. \tag{3.4}$$

In (3.4), $R_s = 1.000\,004\ \Omega$, $R_b = 225{,}000\ \Omega$ is volt-box input resistance, $R_l = 30\ \Omega$ is resistance of the potential wires between heater and volt-box, and $K = 1/2000$ is the volt-box ratio (0.02% accuracy). Potentiometer accuracies for E_b and E_s are 0.01 percent and 0.015 percent. Uncertainty in Q therefore is about 0.05 percent.

TABLE 1. *Densities ρ_l of saturated liquid oxygen*

$$\rho_l = \rho_c + 10^{-6} \cdot \sum_{n=1}^{7} A_n \cdot x^n$$

where $x \equiv (T_c - T)^{1/3}$.

$T_c =$ 154.77 K	$\rho_c =$ 0.01362 mol/cm³
$A_1 = 3419.8$	$A_2 =$ 516.52
$A_3 =$ 319.91	$A_4 = -275.099$
$A_5 =$ 92.846 5	$A_6 =$ −14.724 0
$A_7 =$ 0.927 88	

TABLE 2. *Rectilinear diameter for oxygen*

$$(\rho_l + \rho_g)/2 = \rho_c + 10^{-3} \cdot \sum_{n=1}^{8} B_n \cdot x^n$$

where $x \equiv (T_c - T)/100$.

$T_c =$ 154.77 K	$\rho_c =$ 0.01362 mol/cm³
$B_1 =$ 5.892	$B_2 =$ 3.256
$B_3 = -14.031$	$B_4 = 43.814$
$B_5 = -75.269$	$B_6 = 71.788$
$B_7 = -36.405$	$B_8 =$ 7.727

As discussed below, the value of ΔT depends on the temperature scale, on extrapolations in time, and randomly on use of the potentiometer dials. We take the nominal uncertainty in ΔT to be $(0.1\%) \cdot (5/\Delta T)$. Uncertainty in the observed gross heat capacity, $Q/\Delta T$, therefore is roughly 0.15 percent.

An uncertainty in ΔT of roughly 0.05 percent is probable, based on uncertainties in slope of the temperature scale relative to the thermodynamic scale [7]. The statistical uncertainty in temperature increment, $\Delta T = T_2 - T_1$, obtained from least squares fitting of the $T(t)$ data, usually is near 0.01 percent, with rare values of 0.03 percent. Possible uncertainties arising from accuracy of the potentiometer for $\Delta T = 5.0$ °C, are given by the last column of table 3. Values this large arise only by chance if the uppermost dial of the potentiometer is changed in obtaining ΔT. Most frequently the uncertainties will be 0.1 to 0.01 of these values. R. E. Barieau kindly pointed out that this uncertainty could be diminished by an autocalibration of the potentiometer.

TABLE 3. *Uncertainties of temperatures derived from the potentiometer accuracy, k = 0.01 percent, and characteristics of the platinum resistance thermometer*

		$\delta T = k \cdot R \cdot dT/dR$		
T, K	R, Ω	dR/dT	δT	$(\delta T/5.0)$, %
50	1.923	0.095	0.002	0.04
100	7.305	.110	.007	.13
150	12.72	.107	.012	.24
200	17.99	.104	.017	.35
300	28.23	.101	.028	.56

We measured 68 tare heat capacities C_b of the empty calorimeter bomb from 55 to 300 K, in J/K. They were adjusted for curvature by application of a cubic expression in three separate ranges of T. After investigating various ways to utilize Debye functions, we represent these data more simply by

$$\mathrm{Log}_e(C_b/50) = \sum_{i=1}^{8} C_i \cdot (100/T)^{i-1}, \tag{3.5}$$

with an rms relative deviation of 0.11 percent. Table 4 gives values for coefficients, C_i. For this report the deviation applies to values of C_b from 20 to 67 J/K in the range $55 \leq T < 155$ K. For any quantity of sample, therefore, absolute uncertainty in the quantity $[Q/\Delta T - C_b]$ will range from 0.02 to 0.07 J/K due to uncertainties in C_b alone over the above range of T.

TABLE 4. *Constants for C_b of the empty calorimeter, eq (3.5)*

$C_1 =$ 0.9625 75	$C_2 =$ −2.6479 48
$C_3 =$ 6.6945 41	$C_4 = -11.5636$ 585
$C_5 = 10.9871$ 61	$C_6 =$ −6.0136 545
$C_7 =$ 1.7776 616	$C_8 =$ −0.2195 491

3.4. Curvature Adjustment

If the specific heat is not a linear function of T, a curvature adjustment may be necessary to find its value at the average temperature T_a[5]. We have applied this adjustment to the gross heat capacities, assuming that their true behavior is represented by

$$C_a = C_1 + C_2 \cdot T_a + C_3 \cdot T_a^2 + C_4 \cdot T_a^3 + C_5/\sqrt{T_c - T_a}, \tag{3.6}$$

where T_c is the critical temperature. (The coefficients C_1, C_2 etc. are not related to those of table 4.) The experimental gross heat capacity at average temperature T_a then is

$$C_a = Q/\Delta T - \{C_3/12 + C_4 \cdot T_a/4 + (C_5/32)/(T_c - T_a)^{5/2}\} \cdot \overline{\Delta T}^2. \quad (3.7)$$

This formula is obtained by integrating (3.6), i.e., $C_a \equiv \delta Q/dT$, between the limits $(T_a - \Delta T/2)$ and $(T_a + \Delta T/2)$. Collection of terms then yields two parts for Q, $C_a(T_a)$ the desired heat capacity at T_a, and a correction term which is a function of T_a and of ΔT. Coefficients in (3.6) are found by least squares, using $C_a = Q/\Delta T$. The difference between C_a and $Q/\Delta T$ is found to be small compared with various uncertainties and therefore could be neglected in the present work. For brevity, we define results of the curvature adjustment on specific heat of the two-phase sample as follows (prior to adjustment for calorimeter volume expansion),

$$\bar{C} = (C_a - C_b)/N_b, \quad (3.8)$$

with uncertainty of roughly 0.5 percent when $C_a \approx 2 \cdot C_b$.

3.5. Expansion and Capillary Adjustments

The bomb expands during the calorimetric interval ΔT. An adjustment to find specific heat at constant volume has been described [8, 9]. The capillary tube absorbs an amount of vapor, δN_c, which must boil away from liquid in the bomb. Combining these adjustments we obtain C_v for the two-phase sample,

$$\bar{C}_v = \bar{C} - \{T_a(dP/dT)(dV_b/dT) + \delta N_c \cdot \Delta H_v/\Delta T\}/N_b. \quad (3.9)$$

For this expression, we describe the heat of vaporization in joules per mole by use of $x \equiv (1 - T_a/T_c)$,

$$\Delta H_v = x^{0.4} \cdot (1.05 - 0.2 \cdot x) \cdot 10^4. \quad (3.10)$$

For computing overall uncertainty (see below), we take the following rough estimates,

$$(dP/dT),\ 0.5\%, \qquad (dV/dT),\ 2.0\%$$

$$\delta N_c,\ 100.0\%, \qquad \Delta H_v,\ 2.0\%.$$

A large uncertainty is assumed for δN_c because temperature along the capillary tube is poorly defined. A portion of the total capillary volume of 0.015 cm³ is outside the cryostat, at room temperature.

3.6. Calculation for C_σ

At sufficiently low temperatures one may observe directly C_σ, the heat capacity of the condensed phase at its own (negligible) vapor pressure. Otherwise C_σ is related to $\bar{C}_v$ of the two-phase system via PVT properties [8, 10]

$$C_\sigma = \bar{C}_v + (T/\rho) \cdot \{(-d\rho/dT)(dP/dT)/\rho - ((V_b \cdot \rho/N_b) - 1) \cdot d^2P/dT^2\}, \quad (3.11)$$

where ρ referes to the liquid phase. At the critical point $(-d\rho/dT) = \infty$. If the bomb is completely filled with liquid, $V_b \cdot \rho/N_b = 1$. For computing overall uncertainty (see below), we take the following rough estimates

$$\rho,\ 0.1\% \qquad V_b/N_b,\ 0.2\%$$

$$d\rho/dT,\ 1.0\% \qquad d^2P/dT^2,\ 5.0\%.$$

4. Experimental Results

Table 5 gives loading conditions for the sample in five experimental runs. Temperature and pressure, obtained by computation from laboratory observations, in effect are direct measurements. Volume of the bomb is computed, appendix I. Density is obtained by iterating the equation of state [6]. Total g moles, N, includes a few ten-thousandths in the capillary tube.

Table 6 gives the experimental conditions, the specific heats, and the uncertainties (errors) for each measurement (point) of the five experimental runs. Under ID is given the run number, followed by two digits for the point in that run. Temperature is the average, T_a. Pressure, bomb volume, and density are calculated, section 3. This density is the defined average, $\rho_{av} = N_b/V_b$. The sixth column gives ΔT, followed by $Q/\Delta T$, its value adjusted for curvature, and the tare heat capacity from (3.5). Next is $\bar{C}_v$ for the two-phase system, obtained via the adjustment of (3.9), and then C_σ calculated via (3.11), both in J/(mol K). The last two columns give uncertainties for $\bar{C}_v$ and for C_σ in percent, calculated by methods of appendix III.

TABLE 5. *Loading conditions for the samples*

Run	T, K	P, atm	V, cm³	ρ, mol/l	N, mol
2	197.279	131.432	73.133	13.128	0.9602
3	139.255	129.352	72.950	28.679	2.0924
5	173.070	129.980	73.054	20.223	1.4775
20	180.928	123.245	73.072	16.833	1.2302
32	137.181	106.345	72.934	28.633	2.0882

TABLE 6. *Experimental specific heats, saturated liquid oxygen*

ID	Temp. K	Pres. atm.	V_b cm³	Dens. mol/l	DEL T K	DQ/DT J/deg	$DQDTA$ J/deg	Tare J/deg	C_v J/M–K	CSAT J/M–K	Errors C_v	Percent CSAT
201	56.948	0.003	72.669	13.214	2.754	74.096	74.096	22.910	53.307	53.243	0.580	0.587
202	60.157	.007	72.672	13.213	3.673	76.465	76.466	25.185	53.404	53.280	.527	.541
203	60.357	.008	72.672	13.213	3.645	76.628	76.629	25.326	53.428	53.298	.529	.543
204	63.936	.018	72.677	13.212	3.525	79.350	79.350	27.835	53.649	53.405	.550	.577
205	67.925	.042	72.682	13.211	4.481	82.261	82.261	30.578	53.824	53.377	.516	.566
206	72.313	.092	72.688	13.210	4.309	85.477	85.477	33.501	54.129	53.345	.538	.626
207	76.537	.181	72.695	13.209	4.151	88.651	88.650	36.199	54.624	53.390	.558	.697
208	80.914	.335	72.702	13.208	4.614	92.088	92.087	38.860	55.430	53.591	.548	.756
247	81.735	.374	72.704	13.207	.936	92.488	92.488	39.344	55.344	53.376	1.291	1.543
209	85.426	.590	72.710	13.206	4.427	95.857	95.856	41.459	56.648	54.041	.564	.860
248	83.340	.458	72.707	13.207	2.276	93.826	93.826	40.276	55.767	53.532	.749	1.011
210	87.465	.745	72.714	13.205	4.377	97.515	97.513	42.585	57.201	54.201	.570	.911
211	91.759	1.176	72.723	13.204	4.228	100.793	100.791	44.859	58.246	54.336	.585	1.032
212	95.904	1.752	72.732	13.202	4.088	104.017	104.014	46.933	59.441	54.561	.598	1.160
213	100.224	2.557	72.742	13.200	4.580	107.561	107.558	48.972	61.006	55.036	.578	1.266
214	104.683	3.649	72.752	13.198	4.432	111.194	111.190	50.953	62.724	55.572	.588	1.417
215	109.022	5.011	72.763	13.196	4.280	114.936	114.931	52.764	64.730	56.397	.597	1.567
216	113.688	6.856	72.776	13.194	5.087	118.950	118.942	54.592	66.999	57.402	.564	1.682
217	118.664	9.323	72.790	13.192	4.899	123.492	123.484	56.412	69.827	58.951	.569	1.847
218	123.185	12.070	72.803	13.189	3.846	127.721	127.715	57.958	72.617	60.725	.619	2.043
219	127.626	15.294	72.817	13.187	5.079	132.040	132.026	59.383	75.615	62.979	.558	2.091
220	132.584	19.576	72.834	13.183	4.881	137.197	137.178	60.872	79.419	66.468	.561	2.204
221	137.495	24.605	72.851	13.180	5.115	142.744	142.710	62.249	83.733	71.438	.547	2.265
222	143.712	32.240	72.875	13.176	5.273	151.443	151.349	63.863	91.026	82.803	.532	2.274
223	148.798	39.696	72.896	13.172	4.954	161.666	161.307	65.087	100.099	104.910	.529	2.174
224	152.389	45.729	72.912	13.169	2.288	174.037	173.290	65.903	111.709	159.122	.702	2.035
301	57.563	.004	72.669	28.793	2.150	134.441	134.440	23.348	53.094	53.080	.563	.565
302	60.020	.007	72.672	28.792	2.769	136.329	136.328	25.089	53.164	53.142	.505	.508
303	63.138	.015	72.676	28.790	3.473	138.737	138.735	27.279	53.268	53.229	.466	.471
304	67.026	.035	72.681	28.788	4.309	141.548	141.546	29.966	53.327	53.259	.438	.446
305	71.253	.077	72.687	28.786	4.146	144.316	144.314	32.805	53.293	53.179	.450	.466
306	71.610	.082	72.687	28.786	4.145	144.308	144.307	33.041	53.177	53.059	.451	.467
307	76.180	.171	72.694	28.783	5.008	147.560	147.559	35.975	53.329	53.146	.431	.456
308	81.112	.344	72.703	28.780	4.874	151.277	151.277	38.978	53.671	53.407	.441	.480
309	85.910	.624	72.711	28.776	4.757	155.073	155.074	41.729	54.170	53.827	.450	.504
310	91.013	1.090	72.721	28.772	5.466	158.927	158.929	44.473	54.700	54.289	.436	.508
311	96.412	1.835	72.733	28.768	5.353	162.482	162.484	47.179	55.105	54.663	.444	.535
312	101.694	2.885	72.745	28.763	5.231	166.132	166.133	49.639	55.672	55.272	.452	.560
313	106.854	4.290	72.758	28.758	5.115	169.825	169.823	51.873	56.367	56.113	.459	.582
314	111.605	5.980	72.770	28.753	5.817	173.190	173.184	53.791	57.055	57.073	.445	.577
315	117.372	8.629	72.786	28.747	5.738	177.526	177.510	55.952	58.087	58.690	.449	.587
316	123.021	11.961	72.803	28.740	5.585	182.011	181.979	57.904	59.286	60.874	.455	.588
501	58.515	.005	72.670	20.332	7.229	102.718	102.718	24.024	53.261	53.218	.386	.391
502	65.588	.026	72.679	20.330	6.924	107.935	107.935	28.979	53.437	53.289	.404	.421
503	72.387	.093	72.688	20.327	6.700	112.688	112.687	33.549	53.561	53.199	.420	.462
504	78.969	.257	72.699	20.324	6.483	117.578	117.577	37.695	54.064	53.369	.435	.517
505	85.485	.594	72.711	20.321	6.569	122.788	122.786	41.492	55.019	53.877	.442	.579
506	91.909	1.194	72.723	20.317	6.302	127.571	127.569	44.936	55.924	54.261	.455	.660
507	98.099	2.132	72.737	20.313	6.100	132.123	132.119	47.984	56.940	54.741	.466	.745
508	104.668	3.645	72.752	20.309	5.819	137.342	137.338	50.946	58.465	55.727	.477	.840
509	110.671	5.615	72.767	20.305	6.216	141.950	141.943	53.424	59.901	56.770	.472	.912
510	116.768	8.318	72.784	20.300	6.012	147.003	146.994	55.734	61.753	58.421	.479	.992
511	122.642	11.713	72.801	20.295	5.771	151.952	151.941	57.777	63.712	60.528	.486	1.060
512	128.503	15.996	72.820	20.290	6.071	157.421	157.401	59.654	66.131	63.681	.479	1.096
513	134.442	21.382	72.840	20.284	5.848	163.348	163.314	61.404	68.939	68.327	.483	1.122
514	139.909	27.392	72.860	20.278	5.129	169.472	169.416	62.892	72.051	75.118	.500	1.133
515	144.531	33.362	72.878	20.273	4.163	175.847	175.757	64.066	75.536	85.273	.532	1.133
2001	59.127	.006	72.671	16.928	4.948	90.069	90.069	24.458	53.334	53.266	.445	.452
2002	63.957	.018	72.677	16.927	4.748	93.761	93.761	27.849	53.578	53.414	.463	.482
2003	68.641	.048	72.683	16.926	4.631	97.212	97.212	31.062	53.771	53.444	.479	.516
2004	73.193	.107	72.689	16.924	4.486	100.365	100.364	34.073	53.886	53.315	.496	.561
2005	77.601	.212	72.697	16.922	4.348	103.626	103.625	36.858	54.273	53.377	.512	.615
2006	84.131	.505	72.708	16.920	5.535	108.880	108.878	40.729	55.396	53.858	.485	.662
2007	89.547	.935	72.718	16.917	5.322	113.143	113.141	43.704	56.442	54.244	.499	.755
2008	95.108	1.628	72.730	16.915	5.824	117.347	117.344	46.543	57.549	54.584	.492	.842

TABLE 6. *Experimental specific heats, saturated liquid oxygen*—Continued

ID	Temp. K	Pres. atm.	V_b cm³	Dens. mol/l	DEL T K	DQ/DT J/deg	$DQDTA$ J/deg	Tare J/deg	C_v J/M-K	CSAT J/M-K	Errors C_v	Percent CSAT
2009	101.059	2.740	72.743	16.911	6.105	122.031	122.026	49.352	59.070	55.226	.492	.952
2010	107.253	4.417	72.759	16.908	6.364	127.065	127.058	52.039	60.973	56.211	.490	1.072
2011	113.476	6.763	72.775	16.904	6.116	132.161	132.153	54.512	63.100	57.499	.498	1.206
2012	119.674	9.893	72.793	16.900	6.315	137.612	137.599	56.766	65.689	59.463	.495	1.318
2013	125.847	13.936	72.811	16.895	6.066	143.326	143.309	58.823	68.650	62.227	.500	1.424
2014	133.607	20.556	72.837	16.889	5.756	151.059	151.028	61.166	73.007	67.580	.505	1.518
2015	139.222	26.577	72.858	16.884	5.513	157.562	157.504	62.711	77.003	74.171	.507	1.546
2016	144.586	33.439	72.879	16.880	5.260	165.194	165.048	64.080	82.007	85.561	.508	1.531
2017	149.672	41.101	72.900	16.874	4.960	176.417	175.696	65.289	89.660	112.651	.506	1.442
3201	56.440	.003	72.668	28.736	3.670	133.850	133.848	22.547	53.301	53.290	.444	.446
3202	60.313	.008	72.672	28.734	4.084	136.722	136.721	25.296	53.360	53.336	.434	.437
3203	64.924	.023	72.678	28.732	4.364	140.173	140.172	28.521	53.468	53.417	.432	.439
3204	69.487	.056	72.684	28.730	4.772	143.206	143.205	31.631	53.431	53.337	.427	.440
3205	74.304	.128	72.691	28.727	4.876	146.489	146.489	34.788	53.492	53.336	.431	.453
3206	79.250	.268	72.699	28.724	5.032	150.113	150.114	37.865	53.754	53.519	.434	.468
3207	84.378	.520	72.708	28.720	5.254	154.102	154.103	40.869	54.226	53.904	.434	.483
3208	89.559	.937	72.718	28.716	5.122	157.864	157.865	43.710	54.666	54.266	.443	.510
3209	94.825	1.585	72.729	28.712	5.428	161.408	161.409	46.404	55.072	54.626	.441	.527
3210	100.347	2.583	72.742	28.707	5.635	165.171	165.171	49.029	55.616	55.187	.441	.546
3211	105.901	3.999	72.755	28.701	5.493	169.126	169.124	51.472	56.337	56.034	.448	.570
3212	111.610	5.982	72.770	28.696	5.321	173.243	173.237	53.793	57.193	57.196	.456	.590
3213	117.010	8.441	72.785	28.690	5.502	177.342	177.328	55.821	58.178	58.716	.454	.593
3214	122.534	11.642	72.801	28.683	5.572	181.691	181.663	57.741	59.331	60.791	.455	.590

UN = 0.2, UA = 0.15, UB = 0.1, UC = 2.5, UD = 102.0, UE = 1.6, UF = 0.3, UG = 5.0, UH = 0.1.

5. Formulation and Comparisons With Earlier Data

An analytical description of $C_\sigma(T)$ is required for computations. Using the reduced argument, $x \equiv (T_c - T)/(T_c - T_t)$ where T_c and T_t are critical-point and triple-point temperatures, we find that a plot of $C_\sigma \cdot x^{1/2}$ versus T is a straight line, except for a small deviation as $T \to T_c$, figure 1. In the following form, this deviation is described by a binomial, which can be expanded for term-by-term integration,

$$C_\sigma = [A + B \cdot x + C \cdot (1 - r \cdot x)^n]/x^{1/2}, \qquad (5.1)$$

with $n = 12$. We define $r \equiv (T_c - T_t)/T_c$, such that $(1 - r \cdot x) \equiv T/T_c$.

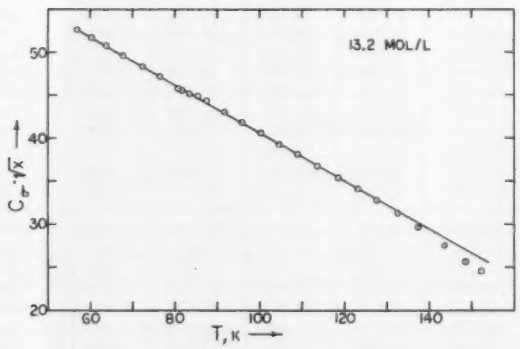

FIGURE 1. *Data of run No. 2 in coordinates of eq (5.1).*

This formula is similar to results obtained for a van der Waals fluid [16]. The weighted least squares determination of coefficients yields

$$A = 25.60277, \quad B = 27.71001, \quad C = -2.48274.$$

In table 7 the column PCNT is percent deviation of data, CSAT, from the calculated value, CALC. Weights, WT, are inversely proportional to the square of absolute errors obtained from the last column of table 6. In the last column of table 7, $D_2 \equiv (\text{CSAT-CALC})^2$ and column entries are $D2 \cdot WT$. For $n = 86$ data, the weighted, mean-square relative deviation is

$$\left\{ \sum^{n} (\Delta C_\sigma / C_\sigma)^2 \cdot WT \Big/ \sum^{n} WT \right\}^{1/2} \cdot 100 = 0.19\%.$$

The correspondingly weighted absolute mean-square deviation is 0.11 J/mol K.

TABLE 7. *Comparison of experimental specific heats with values calculated from eq (5.1)*

ID	Temp.	CSAT	CALC	PCNT	Weight	D2*WT	ID	Temp.	CSAT	CALC	PCNT	Weight	D2*WT
3201	56.440	53.290	53.294	−0.007	1.5956	0.002	2008	95.108	54.584	54.565	.034	.2872	.010
201	56.948	53.243	53.290	−.088	.5287	.115	212	95.904	54.561	54.645	−.154	.1675	.119
301	57.563	53.080	53.286	−.386	.5631	2.379	311	96.412	54.663	54.698	−.064	.5845	.072
501	58.515	53.218	53.280	−.117	.9487	.366	507	98.099	54.741	54.884	−.260	.3490	.712
2001	59.127	53.266	53.277	−.021	.7744	.010	213	100.224	55.036	55.143	−.194	.1418	.162
302	60.020	53.142	53.274	−.248	.6574	1.146	3210	100.347	55.187	55.159	.051	.9920	.079
202	60.157	53.280	53.274	.012	.5978	.002	2009	101.059	55.226	55.253	−.049	.2298	.017
3202	60.313	53.336	53.273	.118	1.6550	.652	312	101.694	55.272	55.340	−.123	.5364	.247
203	60.357	53.298	53.273	.047	.5929	.037	508	104.668	55.727	55.787	−.108	.2790	.102
303	63.138	53.229	53.272	−.081	.7318	.136	214	104.683	55.572	55.790	−.390	.1142	.542
204	63.936	53.405	53.274	.246	.5404	.927	3211	105.901	56.034	55.994	.071	.8828	.140
2002	63.957	53.414	53.274	.263	.7054	1.380	313	106.854	56.113	56.163	−.090	.4952	.125
3203	64.924	53.417	53.278	.261	1.6381	3.168	2010	107.253	56.211	56.237	−.045	.1823	.012
502	65.588	53.289	53.281	.014	.8563	.005	215	109.022	56.397	56.581	−.324	.0930	.313
304	67.026	53.259	53.292	−.061	.7887	.085	509	110.671	56.770	56.931	−.283	.2360	.612
205	67.925	53.377	53.300	.144	.5561	.329	314	111.605	57.073	57.143	−.123	.4881	.242
2003	68.641	53.444	53.308	.255	.6369	1.181	3212	111.610	57.196	57.145	.090	.7901	.209
3204	69.487	53.337	53.318	.035	1.6381	.058	2011	113.476	57.499	57.602	−.178	.1430	.151
305	71.253	53.179	53.345	−.310	.7449	2.043	216	113.688	57.402	57.656	−.441	.0793	.513
206	72.313	53.345	53.364	−.035	.4783	.016	510	116.768	58.421	58.528	−.183	.1950	.224
503	72.387	53.199	53.365	−.311	.7556	2.073	3213	117.010	58.716	58.603	.193	.7415	.946
2004	73.193	53.315	53.381	−.124	.5645	.247	315	117.372	58.690	58.717	−.046	.4557	.033
3205	74.304	53.336	53.406	−.131	1.5432	.753	217	118.664	58.951	59.143	−.324	.0637	.234
207	76.537	53.390	53.464	−.139	.4036	.223	2012	119.674	59.463	59.498	−.058	.1152	.014
2005	77.601	53.377	53.497	−.224	.4906	.702	3214	122.534	60.791	60.622	.278	.6991	1.988
504	78.969	53.369	53.543	−.324	.6373	1.920	511	122.642	60.528	60.669	−.232	.1637	.324
3206	79.250	53.519	53.553	−.063	1.4377	.163	316	123.021	60.874	60.834	.067	.4296	.070
208	80.914	53.591	53.617	−.048	.3559	.024	218	123.185	60.725	60.906	−.297	.0501	.164
308	81.112	53.407	53.625	−.407	.7097	3.375	2013	125.847	62.227	62.191	.058	.0926	.012
247	81.735	53.376	53.652	−.514	.1055	.802	219	127.626	62.979	63.179	−.317	.0448	.180
248	83.340	53.532	53.726	−.360	.2189	.820	512	128.603	63.681	63.711	−.047	.1474	.013
2006	84.131	53.858	53.765	.173	.4317	.373	220	132.584	66.468	66.670	−.302	.0367	.149
3207	84.378	53.904	53.778	.235	1.3263	2.112	2014	133.607	67.580	67.565	.022	.0710	.002
209	85.426	54.041	53.834	.384	.2823	1.206	513	134.442	68.327	68.354	−.039	.1199	.008
505	85.485	53.877	53.838	.073	.5302	.082	221	137.495	71.438	71.775	−.470	.0305	.347
309	85.910	53.827	53.862	−.064	.6535	.079	2015	139.222	74.171	74.199	−.038	.0579	.005
210	87.465	54.201	53.956	.455	.2555	1.538	514	139.909	75.118	75.292	−.231	.0995	.300
2007	89.547	54.244	54.096	.273	.3468	.759	222	143.712	82.803	83.275	−.567	.0229	.510
3208	89.559	54.266	54.097	.312	1.1755	3.359	515	144.531	85.273	85.609	−.392	.0792	.892
310	91.013	54.289	54.206	.153	.6383	.441	2016	144.586	85.561	85.776	−.251	.0453	.209
211	91.759	54.336	54.265	.130	.2061	.103	223	148.798	104.910	105.396	−.461	.0159	.374
506	91.909	54.261	54.278	−.031	.4291	.012	2017	149.672	112.651	112.502	.132	.0303	.067
3209	94.825	54.626	54.538	.162	1.0881	.845	224	152.389	159.122	157.151	1.254	.0081	3.136

Comparison with earlier data, which exist at temperatures up to the boiling-point, becomes possible by use of (5.1) for interpolation. Table 8 gives such data for saturated liquid oxygen, in J/mol K [11, 12, 4, 13], and compares them with our calculated results. The mean deviation of a few tenths of 1 percent from the data of Giauque and Johnston is within our accuracy.

Values for d^2P/dT^2 at saturation can be derived from two-phase heat capacities at two or more average densities [10]. Such data may be an aid to formulating an accurate vapor pressure equation, and R. E. Barieau brought this to our attention [14] almost simultaneously with the report of Yang and Yang [15]. For coexisting phases the relation is

$$\bar{C}_v/T = -d^2G/dT^2 + (d^2P/dT^2)\cdot v \qquad (5.2)$$

where G is the Gibbs free energy per mole and v is the average molal volume. We see that d^2P/dT^2 is obtained on isotherms as the slope of plots of $\bar{C}_v/T$ versus v. We now use this method only to show consistency between our experimental specific heats and available vapor pressure equations of high accuracy. We have compared two vapor pressure equations [6, 7] with each other, finding excellent agreement

in the second derivatives from the triple point to the boiling point.

Column 10 of table 6 gives the raw data, $\bar{C}_v$, for five runs at four significantly different average densities.

TABLE 8. *Comparison of calculated specific heats, J/mol K, with Euken, 1; Clusius, 2; Giauque, 3; Itterbeek, 4.*

ID	T, K	Refer.	Calcd.	Prcnt.
1	57.40	53.60	53.29	0.59
1	60.50	53.56	53.27	.54
1	65.10	53.39	53.28	.21
1	67.70	53.22	53.30	−.15
1	69.50	53.22	53.32	−.18
1	71.30	53.47	53.35	.23
1	73.00	52.80	53.38	−1.08
2	56.60	52.80	53.29	−.92
2	58.00	52.59	53.28	−1.30
2	59.70	52.13	53.28	−2.15
2	62.50	53.72	53.27	.84
2	65.10	54.14	53.28	1.62
2	65.50	52.47	53.28	−1.52
2	67.40	52.26	53.30	−1.94
2	67.60	53.68	53.30	.72
2	69.20	52.26	53.31	−1.98
2	70.10	53.30	53.33	−.05
2	71.00	52.43	53.34	−1.71
2	72.50	53.09	53.37	−.52
2	72.80	52.34	53.37	−1.94
3	56.95	53.38	53.29	.17
3	57.95	53.22	53.28	−.12
3	60.97	53.18	53.27	−.17
3	61.48	53.18	53.27	−.17
3	65.57	53.18	53.28	−.19
3	65.92	53.18	53.28	−.19
3	68.77	53.26	53.31	−.09
3	69.12	53.35	53.31	.07
3	70.67	53.43	53.34	.18
3	71.38	53.47	53.35	.23
3	73.31	53.60	53.38	.41
3	74.95	53.76	53.42	.63
3	75.86	53.56	53.45	.21
3	77.58	53.72	53.50	.42
3	78.68	53.68	53.53	.28
3	81.13	53.89	53.63	.49
3	82.31	53.81	53.68	.25
3	82.96	53.89	53.71	.34
3	84.79	54.10	53.80	.56
3	86.43	54.02	53.89	.24
3	86.61	54.18	53.90	.51
3	86.97	54.06	53.92	.25
3	87.32	54.02	53.95	.14
3	90.33	54.35	54.15	.36
4	70.00	53.40	53.33	.14
4	74.00	53.57	53.40	.32
4	78.00	53.73	53.51	.41
4	82.00	53.89	53.66	.42
4	86.00	54.06	53.87	.36
4	90.00	54.22	54.13	.17

For 50 points, Sumpct. = −0.08, Rmspct. = 0.81.

To interpolate onto isotherms, we represent the data for each run with a fourth order power series ($x = T/100$),

$$\bar{C}_v = A + B \cdot x + C \cdot x^2 + D \cdot x^3 + E \cdot x^4. \qquad (5.3)$$

The first row of table 9 identifies the experimental run. Second and third rows give density in mol/liter and the molal volume in cm³/mol respectively. Following rows give values for the coefficients in (5.3), followed by the rms deviation in percent. We then give selected isotherms of $\bar{C}_v$ and of $\bar{C}_v/T$, interpolated by use of eqs (5.3).

We obtain coefficients of (5.2) by least squares using the form

$$\bar{C}_v/T = A + B \cdot (k \cdot v), \qquad (5.2a)$$

such that $(-d^2G/dT^2) \equiv A$, and $(d^2P/dT^2) \equiv B$. Table 10 gives results on selected isotherms. The first three

TABLE 9. *Interpolation of* $\bar{C}_v$ *on isotherms*

ID =	2	20	5	32	3
Dens =	13.21	16.92	20.31	28.72	28.78
Vol =	75.71	59.11	49.23	34.82	34.74
A =	72.0792	76.3722	78.6311	67.1128	72.2048
B =	−69.9082	−94.5828	−108.3571	−60.9817	−82.8364
C =	80.7733	133.9037	163.3518	96.4842	128.5652
D =	−34.2514	−81.4570	−107.2576	−67.6495	−87.2916
E =	12.2039	24.5486	31.0169	20.6393	24.8471
Rms =	0.22	0.16	0.12	0.12	0.17
Temp	C_v	C_v	C_v	C_v	C_v
55	53.48	53.55	53.44	53.39	53.29
60	53.40	53.41	53.28	53.32	53.15
65	53.54	53.48	53.30	53.35	53.14
70	53.90	53.73	53.48	53.45	53.24
75	54.49	54.16	53.81	53.64	53.43
80	55.31	54.75	54.28	53.89	53.70
85	56.35	55.51	54.87	54.22	54.04
90	57.63	56.43	55.58	54.61	54.46
95	59.14	57.52	56.42	55.07	54.94
100	60.90	58.78	57.39	55.61	55.49
105	62.91	60.23	58.49	56.23	56.12
110	65.19	61.88	59.75	56.96	56.84
115	67.76	63.74	61.18	57.80	57.67
120	70.62	65.84	62.80	58.77	58.62
125	73.80	68.21	64.66	59.90	59.71
Temp	C_v/T	C_v/T	C_v/T	C_v/T	C_v/T
55	0.9724	0.9737	0.9717	0.9708	0.9688
60	.8899	.8902	.8879	.8887	.8859
65	.8237	.8228	.8199	.8207	.8176
70	.7701	.7676	.7640	.7636	.7606
75	.7266	.7221	.7175	.7152	.7124
80	.6914	.6844	.6785	.6737	.6713
85	.6630	.6531	.6455	.6378	.6358
90	.6403	.6270	.6176	.6067	.6051
95	.6225	.6055	.5939	.5797	.5783
100	.6090	.5878	.5739	.5561	.5549
105	.5992	.5736	.5570	.5355	.5345
110	.5927	.5625	.5431	.5178	.5167
115	.5892	.5543	.5320	.5026	.5015
120	.5885	.5487	.5234	.4898	.4885
125	.5904	.5456	.5173	.4792	.4777

columns give T, A, B, for (5.2a). The next column, $D2PDT2$, is the second derivative of Stewart's vapor pressure equation [6]. It is to be compared directly with the values in column B. Columns UA, UB are the absolute, statistical uncertainties in A, B, based only on deviations of the data from (5.2a). Maximum uncertainties in the $\bar{C}_v$ data of various runs, however, are about 0.5 percent (table 6). A probable uncertainty of 0.2 percent may be assigned to each run. One then finds that uncertainties of B for (5.2a) range from about 140 percent at 55 K to about 2 percent at 125 K. Within these bounds, the vapor pressure equation [6] and our specific heats are consistent at temperatures up to 125 K.

TABLE 10. *Coefficients* A *and* B *for eq (5.2a)*

Equation, $C_v/T = A + B \cdot (K \cdot V)$

Temp	A	B	D^2PDT^2	UA	UB
55	0.96750	0.00077	0.00014	0.00211	0.00039
60	.88471	.00074	.00039	.00209	.00039
65	.81494	.00116	.00088	.00221	.00041
70	.75500	.00198	.00169	.00215	.00040
75	.70261	.00314	.00286	.00195	.00036
80	.65613	.00461	.00439	.00170	.00032
85	.61438	.00636	.00624	.00145	.00027
90	.57646	.00835	.00836	.00122	.00023
95	.54175	.01055	.01070	.00105	.00019
100	.50978	.01295	.01321	.00093	.00017
105	.48024	.01551	.01586	.00089	.00017
110	.45290	.01823	.01862	.00092	.00017
115	.42763	.02107	.02148	.00098	.00018
120	.40436	.02401	.02445	.00107	.00020
125	.38305	.02705	.02753	.00116	.00022

6. Derived Thermodynamic Functions

We have used (5.1) for integrations along the coexistence path from triple point to critical point, as described in appendix IV. The thermodynamic functions are calculated via the following relations:

$$\Delta S = \int [C_\sigma/T] \cdot dT, \qquad Q = \int C_\sigma \cdot dT,$$

$$\Delta E = Q - \int P \cdot dv, \qquad \Delta H = Q + \int v \cdot dP.$$

The pressure-volume integrals were evaluated numerically by use of the vapor-pressure equation [6] and the liquid densities of table 1.

Table 11 presents our results at integral temperatures, at which are calculated the vapor-pressure, the saturated liquid density in mol/liter, and C_σ from (5.1) in J/mol K. Following columns give the molal increase of entropy, ΔS, the heat absorbed, $C \cdot DT$, the work, $P \cdot DV$, the increase of internal energy, ΔE, the work, $V \cdot DP$, and the increase of enthalpy, ΔH, all relative to the triple-point values. Throughout this table the unit of energy is the joule. Note that $H - H_t = E - E_t + Pv - (Pv)_t$, but at the triple point $(Pv)_t = 0.002$ J/mol, hence ΔH is numerically equal to $\Delta E + Pv$.

The probable uncertainty in these functions, obtained by integration, should not exceed that of C_σ for which we assess a probable error of 0.3 percent, as compared with maximum errors in table 6 from 0.5 to 2.2 percent.

7. Discussion

The accurate formulation of adjustment calculations for experimental specific heat measurements on a two-phase system is an exacting challenge [8, 10]. It therefore may be helpful to record the following details, pointed out by Barieau.

In eq (3.9) the adjustment for vapor entering the capillary tube is not rigorous. This vapor boils away from the liquid phase, and account should be taken of the diminished volume of liquid, an effect of increasing importance at temperatures approaching critical. In place of ΔH_v in eq (3.9) one should use ΔH_a, the heat of vaporization per mole of vapor leaving the vessel,

$$\Delta H_a = \Delta H_v \cdot \rho_l/(\rho_l - \rho_g) = T \cdot (dP/dT)/\rho_g, \quad (7.1)$$

where ρ_l, ρ_g are densities of saturated liquid and vapor. Note that ΔH_a does not vanish at the critical point. An adjustment to present data via eq (7.1), however, is not significant. At $T = 152$ K, for example, we have roughly $\Delta H_v = 2000$ J/mol, $\rho_l/(\rho_l - \rho_g) = 1.7$, and $\delta N_c/\Delta T = 2 \cdot 10^{-6}$ mol/deg for our capillary tube.

As noted by H. J. Hoge, several difficult adjustments are eliminated by performing experiments with relatively large and also with relatively small amounts of liquid in the calorimeter [8]. When two phases are present,

$$C_{\text{total}} = \text{Lim } (Q/\Delta T) = C_b - (N - N_c) \cdot T \cdot \frac{d^2G}{dT^2}$$

$$+ V_b \cdot T \cdot \frac{d^2P}{dT^2} + T \cdot \frac{dV_b}{dT} \cdot \frac{dP}{dT} + \Delta H_a \cdot \frac{dN_c}{dT}, \quad (7.2)$$

where G is the Gibbs free energy per mole. The difference of eq (7.2) for two amounts of sample, N_2 and N_1, is

$$C_2 - C_1 = -(N_2 - N_1) \cdot T \cdot d^2G/dT^2. \quad (7.3)$$

From eq (7.3) may be obtained the heat capacity of liquid along the coexistence path by use of PVT data whenever the latter are available,

$$C_\sigma = T \cdot dS/dT = -T \frac{d^2G}{dT^2} + \frac{T}{\rho}\left(\frac{d^2P}{dT^2}\right) - \frac{T}{\rho^2}\frac{d\rho}{dT} \cdot \frac{dP}{dT}, \quad (7.4)$$

where ρ and S refer to liquid.

In planning the present work we elected not to follow the above very attractive method. At temperatures approaching the critical temperature, the two

different filling densities eventually must approach the same value. In this region, d^2G/dT^2 from eq (7.3) might suffer the low accuracy expected in the difference of two large experimental values. Another practical impediment to eq (7.3) is the isothermal condition, which cannot be enforced experimentally for the two different fillings. Interpolation is required along each experimental run. Finally, for specific heats of the liquid at very low temperatures, the above filling densities are not optimum.

TABLE 11. *Thermodynamic properties, saturated liquid oxygen*

T, K	P, atm	Mol/l	CSAT	ΔS	$C \cdot DT$	$P \cdot DV$	ΔE	$V \cdot DP$	ΔH
54.351	0.001	40.842	53.313	0.000	0.00	0.000	0.00	0.000	0.00
55.000	.002	40.752	53.306	.633	34.61	.000	34.61	.001	34.61
60.000	.007	40.057	53.274	5.270	301.05	.000	301.05	.014	301.06
65.000	.023	39.359	53.278	9.534	567.42	.001	567.41	.055	567.47
70.000	.061	38.652	53.325	13.484	833.90	.003	833.90	.155	834.06
75.000	.143	37.936	53.423	17.166	1100.75	.008	1100.74	.371	1101.12
80.000	.297	37.208	53.581	20.618	1368.23	.019	1368.21	.786	1369.02
85.000	.561	36.463	53.811	23.873	1636.68	.042	1636.64	1.573	1638.19
90.000	.981	35.700	54.129	26.957	1906.49	.087	1906.40	2.694	1909.18
90.180	1.000	35.672	54.142	27.065	1916.23	.089	1916.14	2.748	1918.98
95.000	1.611	34.914	54.555	29.895	2178.15	.169	2177.98	4.504	2182.65
100.000	2.509	34.100	55.114	32.707	2452.26	.310	2451.95	7.142	2459.40
105.000	3.738	33.253	55.842	35.413	2729.57	.545	2729.02	10.840	2740.41
110.000	5.363	32.367	56.785	38.031	3011.03	.923	3010.11	15.862	3026.90
115.000	7.454	31.433	58.010	40.581	3297.89	1.517	3296.37	22.506	3320.39
120.000	10.082	30.439	59.617	43.082	3591.77	2.437	3589.33	31.118	3622.89
122.000	11.300	30.022	60.398	44.074	3711.77	2.932	3708.84	35.202	3746.97
124.000	12.621	29.592	61.277	45.063	3833.42	3.518	3829.91	39.692	3873.12
126.000	14.049	29.147	62.272	46.051	3956.95	4.215	3952.74	44.621	4001.57
128.000	15.591	28.686	63.402	47.041	4082.60	5.043	4077.56	50.022	4132.62
130.000	17.249	28.207	64.696	48.034	4210.67	6.029	4204.64	55.931	4266.60
132.000	19.031	27.706	66.189	49.032	4341.52	7.207	4334.31	62.390	4403.91
134.000	20.942	27.181	67.930	50.040	4475.59	8.618	4466.97	69.443	4545.04
136.000	22.986	26.628	69.982	51.062	4613.45	10.318	4603.13	77.143	4690.59
138.000	25.170	26.042	72.441	52.101	4755.79	12.381	4743.41	85.548	4841.34
140.000	27.501	25.416	75.443	53.164	4903.57	14.908	4888.66	94.727	4998.30
142.000	29.986	24.740	79.200	54.259	5058.06	18.041	5040.02	104.765	5162.83
144.000	32.631	24.000	84.063	55.399	5221.10	21.995	5199.11	115.766	5336.87
146.000	35.448	23.177	90.653	56.602	5395.45	27.105	5368.35	127.864	5523.32
148.000	38.446	22.236	100.210	57.896	5585.66	33.950	5551.71	141.239	5726.90
150.000	41.638	21.113	115.688	59.335	5800.13	43.669	5756.46	156.158	5956.29
151.000	43.312	20.445	127.975	60.142	5921.59	50.335	5871.25	164.319	6085.91
152.000	45.041	19.662	146.721	61.043	6058.19	59.059	5999.13	173.052	6231.24
153.000	46.828	18.688	180.235	62.103	6219.75	71.412	6148.34	182.485	6402.24
154.000	48.675	17.292	268.103	63.503	6434.78	92.343	6342.43	192.863	6627.64
154.770	50.140	13.620		66.148	6843.48	170.977	6672.50	202.000	7045.48

9. Appendix I. Volumes of the Calorimeter

For a spherical shell,

$$V/V_{1,0} = (l/l_1)^3 \cdot [1 + g(T) \cdot P]^3, \qquad (1)$$

where $V_{1,0}$ is our reference volume at $T = 100$ K, $P = 0$ atm. Length, l, may be a diameter (l_0 at $T = 0$, l_1 at $T = 100$ K) at $P = 0$. Function $g(T)$ includes the modulus of elasticity. We developed an approximation formula for thermal expansivity of type 316 stainless steel in the form

$$l/l_0 = 1 + f(T).$$

Dropping higher order terms from (1) we then have

$$V/V_R = 1 + 3 \cdot f(T) + 3 \cdot g(T) \cdot P, \qquad (2)$$

where

$$V_R = V_{1,0}/[1 + 3 \cdot f(100)].$$

For the elasticity, we use six unpublished values of $(\Delta V/\Delta P)/V$ obtained by Younglove and Diller for this

calorimeter from 40 to 300 K [3]. They are represented within their precision of a few percent by

$$(\Delta V/\Delta P)/V = k \cdot x^{1/3},\ \text{atm}^{-1},$$

where $x \equiv T/100$. Our description for the calorimeter volumes therefore is

$$V/V_R = 1 + 3 \cdot f(T) + k \cdot x^{1/3} \cdot P, \qquad (3)$$

where

$$f(T) = [C_1 + C_2 \cdot x] \cdot \exp\,[\alpha \cdot (1 - 1/x)],$$

with constants,

$$V_R = 72.657\ \text{cm}^3, \qquad C_1 = -0.0002\ 1461,$$

$$C_2 = +0.0005\ 9455, \qquad \alpha = 1.01062,$$

$$k = 0.0000111\ \text{atm}^{-1}.$$

The reference volume measured by Younglove and Diller was $V_{1,0} = 72.74$ cm³. We checked this volume at room temperature by expanding oxygen from the bomb at 3 atm into a calibrated, 130 cm³ glass flask, observing pressures on a commercial, helical-quartz *bourdon* gage. We used the equation of state derived by L.A.W. for these conditions, $Pv/RT = 1 - 0.195 \cdot P/T$, with units of atmospheres and degrees Kelvin. Our volume of 73.19 ± 0.1 cm³ at 297.3 K adjusts to $V_{1,0} = 72.6 \pm 0.1$ cm³. In our specific heat calculations we have used $V_{1,0} = 72.74$ cm³, assigning an uncertainty of 0.1 percent.

10. Appendix II. Estimated Temperatures Along the Capillary Tube

For a capillary tube which is thermally isolated except at its two ends, we may estimate temperatures by use of the temperature-dependent thermal conductivity, K, of stainless steel. We developed the approximation formula,

$$K/K_{100} = \exp\,[1.2 \cdot (1 - 10/T^{1/2})]. \qquad (1)$$

We placed (1) in the heat-flow equation, integrated numerically by computer, and developed an approximation formula for the results,

$$T_x = T_0 \cdot [1 + a \cdot x]^{2/3},$$

$$a \equiv [(T_1/T_0)^{3/2} - 1]. \qquad (2)$$

Here $x \equiv l/l_1$ is fraction of the distance from the cold end of a capillary tube of length l_1. Temperature at the cold end is T_0, at the hot end is T_1, and at position x it is T_x.

11. Appendix III. Method for Estimating Uncertainties (Errors)

We express the saturated liquid heat capacity in the following form,

$$C_\sigma = (A - B - C - D)/N_b + [E - (F - 1) \cdot G] \cdot H,$$

where

$$A \equiv C_a, \qquad B \equiv C_b, \qquad C \equiv k \cdot T \cdot (dP/dT) \cdot (dV_b/dT),$$

$$D \equiv \delta N_c \cdot \Delta H_v/\Delta T, \qquad E \equiv (-d\rho/dT) \cdot (dP/dT)/\rho,$$

$$F \equiv V_b \cdot \rho/N_b, \qquad G \equiv d^2P/dT^2, \qquad H \equiv k \cdot T/\rho,$$

$k = 0.101325$ J/mol-deg, ρ refers to the liquid phase.

Wherever a sum of terms occurs in brackets we sum absolute errors. For each product or ratio we sum relative errors. Uncertainties in A, B, etc., are symbolized UA, UB, etc., given in percent at the bottom of table 6. For A, alone, we introduce dependence on the interval, ΔT, $U_a = 0.05 + 0.10 \cdot (5/\Delta T)$. Results are given in the last two columns of table 6.

12. Appendix IV. Definite Integrals Used for Thermal Functions

Given A, B, C, r, and n for eq (5.1), define—

$$T_d \equiv (T_c - T_t), \qquad q \equiv r^{1/2}.$$

$$x \equiv (T_c - T)/T_d, \qquad z \equiv x^{1/2}.$$

The heat absorbed upon heating from the triple point is—

$$\int_{T_t}^{T} C_\sigma \cdot dT = T_d \cdot \{2A \cdot (1 - z) + 2B \cdot (1 - z^3)/3 + C \cdot \sigma_D\},$$

where

$$\sigma_D \equiv \sum_{i=1}^{n+1} 2D_i \cdot (1 - z^j)/j, \qquad j \equiv 2i - 1,$$

and the binomial coefficients are—

$$D_1 \equiv 1, \qquad D_{i+1} \equiv -D_i \cdot r \cdot (n + 1 - i)/i.$$

The increase of entropy upon heating from the triple point is—

$$\int_{T_t}^{T} (C_\sigma/T) \cdot dT = r \cdot [A \cdot F_a + B \cdot F_b + C \cdot \sigma_E],$$

where

$$F_a \equiv \lambda/q, \qquad F_b \equiv [\lambda - 2q \cdot (1 - z)]/q^3,$$

$$\lambda \equiv \ln\left[\frac{1+q}{1-q}\cdot\frac{1-q\cdot z}{1+q\cdot z}\right],$$

$$\sigma_E \equiv \sum_{i=1}^{n} 2E_i\cdot(1-z^j)/j, \qquad j\equiv 2i-1,$$

and the binomial coefficients are—

$$E_1 \equiv 1, \qquad E_{i+1} \equiv -E_i\cdot r\cdot(n-i)/i.$$

13. Appendix V

The equation of state from reference [6] is

$$\begin{aligned}P = {} & \rho RT + (n_1T + n_2 + n_3/T^2 + n_4/T^4 + n_5/T^6)\rho^2 \\ & + (n_6T^2 + n_7T + n_8 + n_9/T + n_{10}/T^2)\rho^3 \\ & + (n_{11}T + n_{12})\rho^4 + (n_{13} + n_{14}/T)\rho^5 \\ & + \rho^3(n_{15}/T^2 + n_{16}/T^3 + n_{17}/T^4)\ \exp(n_{25}\rho^2) \\ & + \rho^5(n_{18}/T^2 + n_{19}/T^3 + n_{20}/T^4)\ \exp(n_{25}\rho^2) \\ & + \rho^7(n_{21}/T^2 + n_{22}/T^3 + n_{23}/T^4)\ \exp(n_{25}\rho^2) \\ & + n_{24}\rho^{n_{28}+1}(\rho^{n_{28}} - \rho_c^{n_{28}})\ \exp[n_{26}(\rho^{n_{28}} - \rho_c^{n_{28}})^2 \\ & + n_{27}(T-T_c)^2].\end{aligned}$$

The coefficients of the equation of state, n_1 through n_{28}, taken from [6], are given in table 12. These coefficients were determined by a weighted least squares fit of the input experimental data. In this least squares fit, constraints for the critical point were imposed upon the equation of state. These constraints are listed in table 13; the fixed points are listed in table 14.

TABLE 12. *Coefficients for the equation*

T in K, P in atm, ρ in mol/liter

$R = 0.0820535$	$n_{10} = -3.59419602\times10$	$n_{19} = -2.67817667\times10^{3}$
$n_1 = 3.38759078\times10^{-3}$	$n_{11} = 1.02209557\times10^{-6}$	$n_{20} = 1.05670904\times10^{5}$
$n_2 = -1.31606223$	$n_{12} = 1.90454505\times10^{-4}$	$n_{21} = 5.63771075\times10^{-3}$
$n_3 = -7.38828523\times10^{3}$	$n_{13} = 1.21708394\times10^{-5}$	$n_{22} = -1.12012813$
$n_4 = 1.92049067\times10^{7}$	$n_{14} = 2.44255945\times10^{-3}$	$n_{23} = 1.46829491\times10^{2}$
$n_5 = -2.90260005\times10^{10}$	$n_{15} = 1.73655508\times10^{2}$	$n_{24} = 9.98868924\times10^{-4}$
$n_6 = -5.70101162\times10^{-9}$	$n_{16} = 3.01752841\times10^{5}$	$n_{25} = -0.00560$
$n_7 = 7.96822375\times10^{-6}$	$n_{17} = -3.49528517\times10^{7}$	$n_{26} = -0.157$
$n_8 = 6.07022502\times10^{-3}$	$n_{18} = 8.86724004\times10^{-1}$	$n_{27} = -0.350$
$n_9 = -2.71019658$		$n_{28} = 0.90$

TABLE 13. *Constraints imposed on the equation of state* [6]

P-ρ-T at the critical point $\begin{cases} P = 50.14 \text{ atm} \\ \rho = 13.333 \text{ mol/liter} \\ T = 154.77 \text{ K} \end{cases}$

$(\partial P/\partial\rho)_T = 0$ at the critical point

$(\partial^2 P/\partial\rho^2)_T = 0$ at the critical point

$(\partial P/\partial T)_\rho = dP/dT$ from appendix 6 at the critical point
$= 1.928386$ atm/K

TABLE 14. *Fixed point data* [6]

Critical pressure	50.14 atm
Critical temperature	154.77 K
Critical density	13.333 mol/liter
Normal boiling temperature (IPTS, fixed point)	90.18 K
Density saturated vapor at nbp	0.1396 mol/liter
Density saturated liquid at nbp	35.65 mol/liter
Triple point pressure	0.00150 atm
Triple point temperature	54.353 K

14. Appendix VI. The Vapor Pressure Equation from [6]

The vapor pressure equation is [P in atm, T in K]:

$$\ln P = a_0 + a_1T + a_2T^2 + a_3T^3 + a_4T^4 + a_5T^5 + a_6T^6 + a_7T^7.$$

TABLE 15. *Coefficients for the vapor pressure equation*

$a_0 = -6.25967185\times10$	$a_4 = -4.09349868\times10^{-6}$
$a_1 = 2.47450429$	$a_5 = 1.91471914\times10^{-8}$
$a_2 = -4.68973315\times10^{-2}$	$a_5 = -5.13113688\times10^{-11}$
$a_3 = 5.48202337\times10^{-4}$	$a_7 = 6.02656934\times10^{-14}$

8. References

[1] Woolley, H. W., Thermodynamic properties of molecular oxygen, ASTIA Document AD 19900 (June 1953).

[2] Goodwin, R. D., Apparatus for determination of *PVT* relations and specific heats of hydrogen to 350 atm at temperatures above 14 °K, J. Res. NBS **65C** (Engr. and Instr.) No. 4, 231–243 (1961).

[3] Younglove, B. A., and Diller, D. E., The specific heat of saturated liquid parahydrogen from 15 to 32 °K, Cryogenics **2** (No. 5), 283 (1962).

[4] Giauque, W. F., and Johnston, H. L., The heat capacity of oxygen from 12 °K to its boiling point and its heat of vaporization. The entropy from spectroscopic data. J. Am. Chem. Soc. **51**, 2300–2321 (1929).

[5] Scott, R. B., Meyers, C. H., Rands, R. D., Jr., Brickwedde, F. G., and Bekkedahl, N., Thermodynamic properties of 1,3-butadiene in the solid, liquid, and vapor states, J. Res. NBS **35**, 39–85 (1945) RP1661.

[6] Stewart, R. B., The Thermodynamic Properties of Oxygen, Dissertation, Dept. of Mech. Engr'g., Univ. of Iowa, June 1966.

[7] Muijlwijk, R., Moussa, M. R., and Van Dijk, H., The vapour pressure of liquid oxygen, Physica **32**, 805 (1966).

[8] Hoge, H. J., Heat capacity of a two-phase system, with applications to vapor corrections in calorimetry, J. Res. NBS **36**, 111 (1946) RP1693.

[9] Walker, P. A., The equation of state and specific heat of liquid argon, Thesis, Queen Mary College, Univ. of London (1956).

[10] Rowlinson, J. S., Liquids and Liquid Mixtures (Butterworths, London. 1959).

[11] Eucken, A., Uber das thermische Verhalten einiger komprimierter und kondensierter Gase bei tiefen Temperaturen, Verhandl. Deut. Physik. Ges. **18**, 4–17 (1916).

[12] Clusius, K., Uber die spezifische Wärme einiger kondensierter Gase zwischen 10° abs und ihrem Tripelpunkt, Z. physik. Chem. (Leipzig) **B3**, 41–79 (1929).

[13] Van Itterbeek, A., and Van Dael, W., Properties of some cryogenic liquids from sound velocity data, Advances in Cryogenic Engineering **9**, 207–216 (1963).

[14] Barieau, R. E., Helium Research Center, U.S. Bureau of Mines, Amarillo, Texas 79106, private communication, Jan. 14, 1965.

[15] Yang, C. N., and Yang, C. P., Critical point in liquid-gas transitions, Phys. Rev. Letters **13(9)**, 303–305 (1964).

[16] Barieau, R. E., Thermodynamic properties of a van der Waals fluid in the two-phase region, U.S. Bureau of Mines Report RI 6950, June 1967.

[17] Hoge, H. J., Vapor pressure and fixed points of oxygen and heat capacity in the critical region, J. Res. NBS **44**, 321–345 (1950) RP2081.

[18] Weber, L. A., Thermodynamic and related properties of oxygen from the triple point to 300 K at pressures to 330 atmospheres, internal report, June 20, 1968.

(Paper 73A1–529)

JOURNAL OF RESEARCH of the National Bureau of Standards—A. Physics and Chemistry
Vol. 73A, No. 1, January–February 1969

Specific Heats C_v of Fluid Oxygen from the Triple Point to 300 K at Pressures to 350 Atmospheres*

Robert D. Goodwin and Lloyd A. Weber****

Institute for Basic Standards, National Bureau of Standards, Boulder, Colorado 80302

(August 15, 1968)

Experimental specific heats at constant volume for oxygen in single phase domains are reported from the triple point to 300 K at pressures to 350 atmospheres. An empirical equation with seven constants describes these specific heats over the entire domain of ρ-T coordinates to within the experimental accuracy of 1 to 2 percent. Values for the terminal slopes of PVT isochores at the coexistence boundary, $(\partial P/\partial T)_v$, are derived for the liquid.

Key Words: Compressed liquid; heat capacities; liquid; oxygen; specific heats; thermodynamic properties.

List of Symbols

C_b	heat capacity of empty calorimeter bomb.
$C_v(\rho, T)$	specific heat of the sample.
$C_v^\circ(T)$	specific heat in ideal gas states.
C_x	adjustment for bomb expansion.
J	the joule.
k	conversion factor, 0.101325 J/cm³ atm.
L	the liter, 1,000 cm³.
N	total moles of fluid in bomb plus capillary tube.
N_b	moles of fluid in the bomb.
N_c	moles of fluid in the capillary tube.
P	pressure. 1 atm = 0.101325 MN/m².
Q	calorimetric heat input.
$Q/\Delta T$	gross heat capacity.
ρ	density.
ρ_c	critical density, 13.62 mol/l.
σ	density reduced at the critical point.
t	time.
T	temperature, Kelvin, NBS 1955 scale.
T_1, T_2	temperature at start and end of heating interval.
T_c	critical-point temperature, 154.77 K.
$\Delta T \equiv T_2 - T_1$	calorimetric temperature increment.
v	molal volume, $1/\rho$.
V_b	volume of the calorimeter bomb.
x	temperature reduced at the critical point.

1. Introduction

Specific heats are basic data for the computation of thermodynamic properties in the compressed liquid domain, yet for oxygen these data apparently never have been measured [1].[1] In the present report we give our results for C_v over the entire fluid domain below 300 K and below 350 atm. Many details of the experimental work are given in our companion publication on specific heats along the liquid-vapor coexistence path [2]. In forthcoming reports we give thermodynamic properties based on the current measurements.

2. Experimental Method

The calorimeter and cryostat are the same as used for the two-phase observations [2]. Briefly, the calorimeter is a spherical shell of stainless steel, 2 in in diameter, surrounded by adiabatic shields maintained at the calorimeter temperature by automatic controls. The amount of sample is determined from an observed temperature T and pressure P in a single-phase domain; from the bomb volume at this T, P; and from the fluid density derived from an equation of state [1]. The method for measuring calorimetric heat is identical with that of [2] as is the tare heat capacity of the empty calorimeter bomb. The computational method of adjusting for expansion of the bomb during a heating interval also is the same except that the required pressure increase in the bomb is estimated.

*This work was carried out at the National Bureau of Standards under the sponsorship of the National Aeronautics and Space Administration Fund Transfer R–06–006–046.
**Cryogenics Division, NBS Boulder Laboratories, Boulder, Colorado 80302.

[1] Figures in brackets indicate the literature references at the end of this paper.

3. Calculation of C_v From Laboratory Observations

To adjust for expansion of the bomb we estimate the pressure at T_1 and at T_2. An iterative method minimizes the difference $|\rho - \rho_e|$ where density ρ is obtained from contents and volume of the bomb,

$$\rho = [N - N_c(P, T)]/V_b(P, T), \tag{1}$$

and density ρ_e is used in the equation of state $P(\rho_e, T)$ to obtain the pressure. For the capillary tube we obtain $N_c(P, T)$ by summing over both liquid and gaseous phases whenever a meniscus exists in this tube. The capillary volume is about $0.0002 \cdot V_b$.

The densities ρ_1, ρ_2 obtained in this way at T_1, T_2 already recognize fluid in the capillary tube. We therefore use them in the adjustment C_x for bomb expansion as follows (appendix I),

$$\Delta v \equiv 1/\rho_2 - 1/\rho_1,$$

$$C_x \equiv k \cdot [T_2 \cdot (\partial P/\partial T)_2 - \Delta P/2] \cdot \Delta_v/\Delta T. \tag{2}$$

Our experimental data thus are reduced by the equation,

$$C_v = [Q/\Delta T - C_b]/N_b - C_x \tag{3}$$

with no curvature adjustments [2]. Only for datum No. 225 near critical is the adjustment significant: this datum should be reduced to 46.4 J/mol-K in table 2. The maximum uncertainties (errors) in C_v are calculated as in [2], using the same estimates for uncertainty of individual variables.

4. Experimental Results

The locus of each specific heat observation is given by figure 1 in density-temperature coordinates. The observations extend from the coexistence envelope at low temperatures to the 350-atm boundary of pressure at high temperatures. The amount of sample for each experimental run (horizontal line on fig. 1) is calculated from the loading conditions of table 1. The total number of moles N given in the last column includes a few ten thousandths in the capillary tube.

Table 2 gives experimental results. Identification in the first column is the run number followed by two digits for the point of that run. Next are the observed temperature, the estimated pressure, and the calculated density at this pressure. The bomb volume V, BMB and DV/DT for the bomb are calculated at T, P as in [2]. The seventh column DEL T is the experimental temperature increment, ΔT. Following columns are the gross heat capacity $Q/\Delta T$, the tare heat capacity of the empty calorimeter, and the adjusted specific heat of the oxygen sample computed

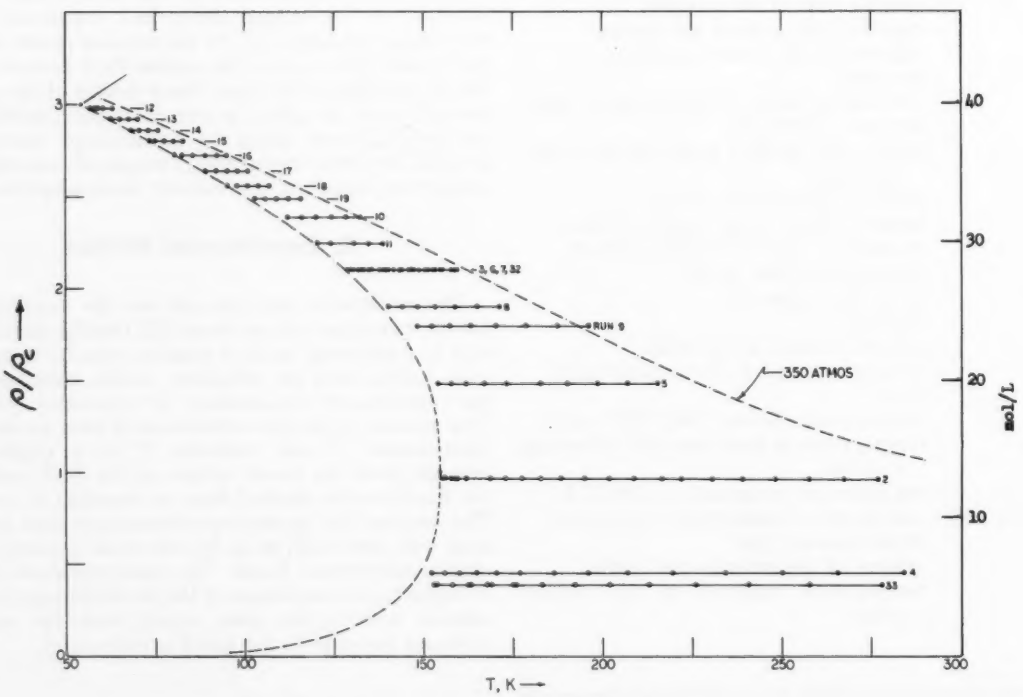

FIGURE 1. *Locus of* C_v *data in* $\rho - T$ *coordinates.*

by eq (3). The last column is estimated maximum relative uncertainty (error), in percent. This increases rapidly with diminishing interval ΔT and with diminishing amount of sample. A comparison of runs 3, 6, 7, 32, all at the same density, shows that these estimates of error are realistic.

The behavior of these specific heats is illustrated in figure 2 by plots of selected runs (isochores). For a wide range of densities about the critical density the specific heat increases sharply as temperature diminishes toward the coexistence envelope. At densities far removed from critical, however, the temperature dependence is relatively weak.

TABLE 1. *Loading conditions for the samples*

Run	T, K	P, ATM	V, cm³	D, Mol/l	N, Mol
2	197.279	131.432	73.133	13.128	0.9602
3	139.255	129.352	72.950	28.679	2.0924
4	200.125	76.159	73.086	6.110	0.4467
5	173.070	129.980	73.054	20.223	1.4775
6	139.083	128.514	72.949	28.696	2.0936
7	138.976	127.012	72.948	28.688	2.0929
8	148.103	96.998	72.947	25.893	1.8890
9	173.955	187.207	73.112	23.090	1.6884
10	116.705	125.967	72.884	32.557	2.3731
11	131.071	159.226	72.953	30.621	2.2341
12	59.069	122.822	72.754	40.632	2.9565
13	65.450	120.256	72.763	39.783	2.8950
14	71.341	114.230	72.769	38.974	2.8364
15	76.877	108.612	72.775	38.202	2.7805
16	85.691	138.618	72.817	37.157	2.7060
17	94.357	145.740	72.843	36.010	2.6234
18	102.979	156.273	72.873	34.875	2.5417
19	109.048	141.669	72.877	33.884	2.4696
32	137.181	106.345	72.934	28.633	2.0882
33	207.639	71.974	73.106	5.253	0.3841

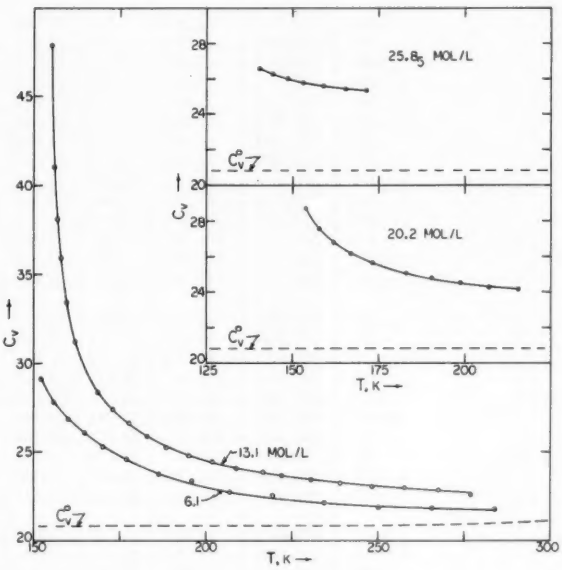

FIGURE 2. *Selected isochores of* C_v *data.*

TABLE 2. *Experimental specific heats*

ID	T, K	P, atm	Dens. mol/l	V, bmb cm³	DV_b/DT cm³/deg	Del T K	DQ/DT J/deg	Tare J/deg	C_p J/M-K	Error percent
225	155.297	51.144	13.166	72.925	0.0047	0.764	112.656	66.536	47.883	2.077
226	155.970	52.427	13.166	72.928	.0047	0.812	106.171	66.679	40.978	2.173
227	156.753	53.920	13.165	72.932	.0047	0.830	103.576	66.844	38.103	2.237
228	157.829	55.971	13.164	72.937	.0047	1.414	101.692	67.069	35.905	1.592
229	159.558	59.267	13.163	72.945	.0047	2.106	99.644	67.423	33.402	1.311
230	162.067	64.054	13.160	72.957	.0048	2.991	98.042	67.923	31.208	1.145
231	168.678	76.686	13.154	72.989	.0049	3.947	96.558	69.170	28.354	1.090
232	172.876	84.734	13.151	73.010	.0049	4.554	96.375	69.912	27.385	1.061
233	177.619	93.820	13.146	73.033	.0050	5.036	96.396	70.709	26.571	1.051
234	182.951	104.018	13.141	73.060	.0050	5.737	96.521	71.556	25.811	1.034
235	188.633	114.906	13.136	73.089	.0051	6.284	96.805	72.407	25.213	1.029
236	195.116	127.315	13.130	73.122	.0052	6.853	97.260	73.319	24.729	1.025
237	201.815	140.083	13.124	73.157	.0052	6.741	97.840	74.202	24.404	1.048
238	208.788	153.339	13.117	73.193	.0053	7.397	98.351	75.065	24.028	1.040
239	216.716	168.371	13.109	73.235	.0054	8.697	99.094	75.984	23.835	1.012
240	222.219	178.853	13.104	73.265	.0054	8.676	99.500	76.588	23.621	1.025
241	230.717	194.880	13.096	73.311	.0055	8.624	100.165	77.471	23.384	1.043
242	239.156	210.642	13.087	73.357	.0055	9.367	100.833	78.295	23.211	1.036
243	248.314	227.681	13.078	73.408	.0056	9.298	101.488	79.138	23.003	1.053
244	257.729	245.185	13.069	73.461	.0056	9.901	102.259	79.955	22.943	1.048
245	267.382	263.047	13.059	73.515	.0057	9.883	102.936	80.749	22.810	1.061
246	276.983	280.719	13.049	73.570	.0057	9.810	103.453	81.497	22.557	1.079
317	130.692	45.629	28.719	72.852	.0115	4.180	117.358	60.316	26.501	0.710
318	134.835	86.416	28.700	72.899	.0117	4.155	118.134	61.515	26.279	.722
319	138.945	126.677	28.680	72.947	.0119	4.115	119.032	62.638	26.149	.734
320	143.490	169.947	28.659	73.000	.0121	4.071	120.315	63.808	26.181	.745

324-194 O-69—2

TABLE 2. *Experimental specific heats*—Continued

ID	T, K	P, atm	Dens. mol/l	V, bmb cm³	DV_b/DT cm³/deg	Del T K	DQ/DT J/deg	Tare J/deg	C_v J/M-K	Error percent
321	147.531	208.734	28.640	73.048	.0122	4.065	121.052	64.790	26.045	.754
322	151.493	246.338	28.621	73.096	.0123	4.038	121.854	65.703	25.975	.762
323	155.489	283.838	28.602	73.144	.0123	4.010	122.640	66.577	25.917	.771
324	159.453	320.561	28.583	73.191	.0124	3.987	123.419	67.402	25.881	.779
401	152.179	42.261	6.126	72.908	.0035	3.667	78.902	65.856	29.116	1.842
402	155.794	44.979	6.124	72.921	.0036	3.654	79.105	66.642	27.809	1.932
403	160.002	48.086	6.123	72.936	.0036	4.858	79.536	67.512	26.825	1.784
404	164.797	51.575	6.122	72.954	.0036	4.830	80.129	68.450	26.050	1.851
405	170.195	55.441	6.120	72.973	.0037	6.065	80.766	69.443	25.253	1.770
406	176.883	60.164	6.118	72.998	.0037	7.453	81.616	70.588	24.586	1.719
407	186.560	66.896	6.115	73.034	.0038	8.851	82.742	72.102	23.712	1.720
408	196.057	73.392	6.112	73.070	.0038	10.315	83.926	73.446	23.349	1.704
409	207.059	80.831	6.108	73.113	.0039	11.906	85.051	74.856	22.704	1.718
410	219.594	89.217	6.104	73.162	.0040	14.076	86.411	76.303	22.502	1.703
411	234.502	99.074	6.099	73.222	.0040	16.083	87.771	77.847	22.080	1.721
412	250.222	109.382	6.093	73.285	.0041	15.818	89.133	79.307	21.849	1.768
413	265.673	119.428	6.088	73.348	.0041	15.564	90.424	80.611	21.810	1.801
414	284.186	131.436	6.082	73.425	.0042	22.098	91.825	82.036	21.743	1.743
516	154.095	54.534	20.260	72.925	.0065	3.557	109.070	66.277	28.687	0.861
517	157.860	69.185	20.253	72.950	.0066	4.052	108.211	67.075	27.548	.841
518	162.027	85.593	20.245	72.978	.0068	4.604	107.931	67.915	26.773	.821
519	167.104	105.862	20.235	73.012	.0069	5.636	108.019	68.882	26.160	.784
520	173.286	130.879	20.222	73.056	.0071	6.818	108.375	69.983	25.635	.758
521	182.885	169.899	20.203	73.125	.0073	7.424	109.089	71.546	25.030	.762
522	190.402	200.537	20.187	73.180	.0074	8.030	109.875	72.662	24.786	.759
523	198.662	233.997	20.170	73.242	.0076	8.631	110.597	73.793	24.489	.759
524	207.168	268.288	20.152	73.306	.0077	8.559	111.373	74.869	24.263	.773
525	215.586	301.941	20.134	73.371	.0078	8.488	112.233	75.857	24.159	.784
601	129.811	37.509	28.740	72.842	.0115	3.266	117.622	60.052	26.746	.776
602	133.528	74.090	28.722	72.885	.0117	4.191	118.258	61.144	26.503	.715
603	137.687	114.969	28.703	72.933	.0119	4.158	119.135	62.301	26.348	.727
604	141.772	154.822	28.683	72.981	.0120	4.123	119.959	63.374	26.208	.738
605	146.114	196.833	28.663	73.032	.0121	4.601	120.928	64.452	26.134	.718
606	150.669	239.909	28.641	73.087	.0123	4.556	121.869	65.517	26.071	.728
607	154.966	279.917	28.621	73.138	.0124	4.084	122.699	66.465	25.983	.764
608	159.013	317.536	28.601	73.187	.0124	4.056	123.490	67.312	25.941	.772
706	128.832	27.695	28.736	72.831	.0114	1.235	116.949	59.755	26.563	1.311
701	130.025	39.312	28.730	72.844	.0115	3.309	117.328	60.116	26.580	0.774
702	134.223	80.690	28.710	72.893	.0117	5.111	118.134	61.342	26.354	.672
703	139.804	135.185	28.684	72.957	.0119	6.140	119.373	62.864	26.197	.647
704	146.427	198.814	28.653	73.036	.0121	7.147	120.813	64.527	26.058	.633
705	153.498	265.658	28.619	73.120	.0123	7.036	122.247	66.147	25.940	.645
801	140.433	41.159	25.920	72.874	.0094	3.443	114.237	63.029	26.569	.800
802	144.299	69.148	25.906	72.911	.0096	4.335	114.672	64.009	26.260	.743
803	148.597	100.417	25.891	72.952	.0097	4.315	115.265	65.040	26.003	.755
804	153.298	134.674	25.874	72.998	.0099	5.247	115.933	66.103	25.769	.717
805	159.026	176.397	25.854	73.054	.0101	6.277	116.864	67.315	25.593	.690
806	165.241	221.439	25.831	73.117	.0103	6.228	117.775	68.534	25.404	.702
807	171.390	265.204	25.809	73.179	.0104	6.159	118.795	69.654	25.335	.712
901	148.563	49.065	23.158	72.904	.0078	3.472	111.380	65.032	27.063	.836
902	152.486	70.121	23.148	72.935	.0079	4.430	111.376	65.924	26.510	.775
903	157.402	96.826	23.135	72.974	.0081	5.460	111.703	66.980	26.056	.736
904	163.303	128.912	23.119	73.023	.0083	6.544	112.244	68.164	25.651	.711
905	170.379	167.584	23.100	73.082	.0085	7.701	113.034	69.475	25.311	.695
906	178.665	212.816	23.077	73.153	.0087	8.963	113.961	70.879	25.001	.684
907	187.541	261.017	23.052	73.231	.0089	8.897	114.947	72.247	24.743	.698
908	196.331	308.226	23.027	73.308	.0090	8.810	115.944	73.483	24.579	.710
1001	108.879	10.276	32.611	72.766	0.0154	2.682	144.011	52.706	37.350	0.691
1002	112.214	60.010	32.588	72.816	.0154	3.998	122.680	54.028	27.778	.670
1003	116.182	118.880	32.560	72.875	.0155	3.956	123.831	55.520	27.617	.683
1004	120.105	175.140	32.533	72.934	.0157	3.913	125.072	56.916	27.568	.695
1005	124.452	236.551	32.503	73.000	.0159	4.807	126.438	58.374	27.472	.658
1006	128.570	293.382	32.475	73.064	.0159	3.930	127.509	59.674	27.404	.711
1007	132.456	345.654	32.449	73.123	.0159	3.884	128.793	60.835	27.405	.720

TABLE 2. *Experimental specific heats* – Continued

ID	T, K	P, atm	Dens. mol/l	V, bmb cm³	DV_b/DT cm³/deg	Del T K	DQ/DT J/deg	Tare J/deg	C_v J/M-K	Error percent
1101	120.598	34.060	30.681	72.814	.0134	3.252	119.834	57.086	27.145	.750
1102	124.251	77.714	30.660	72.862	.0134	4.078	120.649	58.308	26.970	.696
1103	130.736	155.031	30.623	72.949	.0137	4.093	122.320	60.329	26.782	.710
1104	134.797	202.264	30.600	73.003	.0138	4.062	123.406	61.504	26.702	.720
1105	138.824	249.075	30.577	73.057	.0139	4.026	124.403	62.605	26.638	.730
1201	56.368	31.319	40.670	72.689	.0266	2.189	136.052	22.495	36.444	.660
1202	58.917	116.769	40.634	72.751	.0268	2.909	133.675	24.309	35.190	.602
1203	57.897	82.169	40.649	72.726	.0267	2.561	133.302	23.585	35.202	.629
1204	60.442	169.884	40.612	72.787	.0269	2.535	134.526	25.387	34.989	.642
1205	62.967	251.014	40.578	72.849	.0271	2.530	135.948	27.159	34.995	.652
1301	62.590	31.232	39.821	72.697	.0253	2.525	135.336	26.896	35.516	.640
1302	65.138	109.378	39.787	72.756	.0255	2.576	132.643	28.668	34.171	.652
1303	67.705	186.200	39.754	72.815	.0256	2.566	132.990	30.429	33.533	.665
1304	70.233	262.996	39.721	72.874	.0257	2.528	134.959	32.130	33.603	.677
1401	68.103	20.551	39.015	72.698	.0241	2.453	139.280	30.699	36.401	.654
1402	70.626	94.552	38.983	72.753	.0242	2.604	131.137	32.391	32.993	.667
1403	73.222	166.234	38.951	72.811	.0243	2.597	132.251	34.092	32.902	.678
1404	75.794	235.407	38.921	72.868	.0244	2.555	133.549	35.733	32.638	.692
1501	72.907	3.541	38.249	72.691	.0229	1.469	148.023	33.888	39.092	.840
1502	74.969	58.588	38.224	72.735	.0229	2.665	129.376	35.211	32.211	.674
1503	77.616	126.868	38.194	72.791	.0230	2.641	130.468	36.867	31.904	.687
1504	80.237	195.252	38.164	72.847	.0231	2.614	131.740	38.458	31.779	.699
1505	82.818	261.059	38.134	72.902	.0232	2.585	133.216	39.975	31.748	.710
1601	80.108	5.857	37.217	72.705	.0214	2.010	146.516	38.381	38.279	.732
1602	82.640	67.258	37.189	72.756	.0214	3.064	128.741	39.872	31.172	.659
1603	85.671	137.879	37.158	72.816	.0215	3.029	130.090	41.596	31.124	.671
1604	89.014	214.296	37.123	72.883	.0216	3.673	131.574	43.420	30.882	.634
1605	92.303	287.554	37.089	72.949	.0217	2.922	132.853	45.138	30.812	.702
1606	95.052	346.307	37.061	73.005	.0218	2.593	133.954	46.516	30.599	.747
1701	89.205	38.784	36.059	72.747	.0198	3.071	127.701	43.522	30.522	.673
1702	92.249	102.328	36.030	72.803	.0198	3.024	128.105	45.110	30.173	.689
1703	95.257	163.556	36.002	72.859	.0199	2.998	129.212	46.617	29.942	.701
1704	98.232	224.501	35.973	72.915	.0200	2.969	130.292	48.047	29.792	.713
1705	100.982	279.569	35.947	72.967	.0200	2.540	131.390	49.318	29.718	.770
1801	95.085	9.674	34.943	72.736	.0182	2.325	143.109	46.532	36.569	.720
1802	97.805	60.228	34.920	72.783	.0183	3.124	125.443	47.845	29.177	.697
1803	100.912	117.381	34.893	72.837	.0183	3.096	126.360	49.286	28.914	.709
1804	103.990	174.180	34.867	72.890	.0184	3.067	127.467	50.653	28.800	.721
1805	107.030	229.235	34.841	72.944	.0185	3.036	128.575	51.946	28.708	.732
1901	102.977	40.081	33.932	72.778	.0170	3.112	124.268	50.210	28.681	.711
1902	106.074	93.034	33.907	72.828	.0170	3.092	124.934	51.546	28.423	.723
1903	109.146	143.256	33.883	72.878	.0171	3.060	126.022	52.814	28.395	.734
1904	112.406	195.782	33.858	72.932	.0172	3.488	127.224	54.102	28.282	.705
1905	115.869	252.214	33.831	72.989	.0174	3.451	128,404	55.406	28.202	.717
3215	129.470	31.078	28.669	72.836	.0114	1.904	117.407	59.949	26.757	1.007
3216	132.006	55.993	28.657	72.865	.0115	3.216	117.856	60.704	26.613	0.788
3217	135.669	91.698	28.639	72.906	.0117	4.166	118.642	61.748	26.466	.721
3218	140.018	134.022	28.619	72.957	.0119	4.589	119.623	62.920	26.350	.706
3219	144.268	175.030	28.599	73.007	.0120	4.567	120.439	64.001	26.202	.716
3220	148.803	217.859	28.578	73.060	.0121	4.566	121.420	65.088	26.146	.724
3221	153.319	259.958	28.556	73.114	.0123	4.528	122.265	66.108	26.029	.734
3222	157.769	301.385	28.535	73.168	.0123	4.456	123.186	67.056	25.998	.744
3301	153.683	40.658	5.268	72.911	.0034	3.974	76.126	66.188	25.789	2.225
3302	157.856	43.222	5.267	72.925	.0035	4.481	76.804	67.074	25.242	2.177
3303	162.538	46.053	5.265	72.942	.0035	5.023	77.530	68.015	24.681	2.146
3304	167.824	49.204	5.264	72.960	.0035	5.670	78.393	69.015	24.324	2.104
3305	175.869	53.924	5.262	72.989	.0036	6.997	79.464	70.420	23.450	2.060
3306	183.525	58.348	5.260	73.016	.0036	8.471	80.576	71.644	23.154	2.000
3307	192.262	63.335	5.257	73.048	.0037	9.183	81.705	72.924	22.756	2.018
3308	202.057	68.848	5.255	73.085	.0037	10.605	82.915	74.233	22.494	1.999
3309	213.082	74.992	5.252	73.126	.0038	12.226	84.166	75.570	22.262	1.986

TABLE 2. *Experimental specific heats*—Concluded

ID	T, K	P, atm	Dens. mol/l	V, bmb cm^3	DV_b/DT cm^3/deg	Del T K	DQ/DT J/deg	Tare J/deg	C_v J/M-K	Error percent
3310	226.034	82.147	5.248	73.176	.0038	13.984	85.532	76.991	22.111	1.979
3311	240.759	90.217	5.244	73.233	.0039	15.816	86.903	78.446	21.885	1.986
3312	257.791	99.456	5.239	73.300	.0040	18.628	88.403	79.961	21.834	1.973
3313	278.133	110.390	5.233	73.381	.0040	22.722	89.996	81.585	21.743	1.964
3314	157.576	43.049	5.267	72.924	.0035	4.964	76.716	67.016	25.166	2.095
3315	162.898	46.267	5.265	72.943	.0035	5.785	77.539	68.085	24.524	2.051
3316	168.890	49.834	5.264	72.964	.0035	6.325	78.540	69.208	24.203	2.041
3317	175.475	53.694	5.262	72.987	.0036	6.999	79.473	70.354	23.645	2.043

UN = 0.20, UQ = 0.05, UT = 0.10, UB = 0.10, UP = 0.10, UPP = 1.00. UV = 0.20.

5. Representation of the Data

These C_v data will be useful for computations only if they can be interpolated. This is difficult with two independent variables, and is exceptionally difficult when these variables do not fill a rectangular array, as at present (fig. 1). We have developed an "equation of state" for these oxygen C_v data, using density and temperature as arguments. We postulate a temperature dependence on isochores, allowing behavior of the density dependent parameters in the equation to be imposed by the data. We first present the proposed equation, discussing its genesis later on.

As seen below, the equation has at least five exponents, α, β, γ, δ, ϵ, all of which must be selected. There remain eight arbitrary constants. Define $x \equiv T/T_c$, $\sigma \equiv \rho/\rho_c$. Let $A(\sigma)$ and $B(\sigma)$ be density dependent parameters, and let $W(\sigma, T)$ give nonanalytic behavior at the critical point. The equation then is

$$C_v = C_v^\circ + A \cdot [(1-B) \cdot x^\alpha + B \cdot W \cdot x^\beta] \cdot \qquad (4)$$

From [6] we use

$$C_v^\circ(T) = 20.8 + 0.04 \cdot x^3, \text{ J/mol deg.}$$

We find the descriptions,

$$A(\sigma) \equiv A_1 \cdot \sigma + A_2 \cdot \sigma^2 + A_3 \cdot \sigma^3 + A_4 \cdot \sigma^4 + A_5 \cdot \sigma^5, \qquad (4\text{–a})$$

$$B(\sigma) \equiv \exp[-B_1 - B_2 \cdot \sigma^\gamma] \cdot \qquad (4\text{–b})$$

Defined functions in (4) are

$$T_0(\sigma) \equiv T_c \cdot \exp[-C_1 \cdot (\sigma-1)^\delta \cdot \ln(\sigma)], \qquad (4\text{–c})$$

$$W(\sigma, T) \equiv [T/T_0 - 1]^{-\epsilon}. \qquad (4\text{–d})$$

Following are values of the constants for eq (4):

$\alpha = -1/4$	$A_1 = 13.3714$	$B_1 = 0$
$\beta = -3$	$A_2 = -12.917566$	$B_2 = 1/4$
$\gamma = +3$	$A_3 = 5.054888$	$C_1 = 4/3 \cdot$
$\delta = +3$	$A_4 = -0.761749$	
$\epsilon = +1/3$	$A_5 = 0.052853$	

Table 3 gives the proof of this practical pudding, a comparison of experimental and calculated values for $C_v(\rho, T)$ over the entire $\rho - T$ domain. The mean relative deviation of 0.47 percent for 151 data is comparable with uncertainty of the data (table 2). In this table 3 the experimental data for C_v have been adjusted to a constant density on each run by use of eq (4). The adjustments are smaller than the uncertainty in each point.

A linear form is obtained from eq (4) upon multiplying by $x^{1/4}$. Figure 3 illustrates data of run No. 2 at near critical density in these coordinates. We substitute $(x-1)^{-1/3}$ for $W(\rho, T)$ at this density. Temperature decreases to the right, with critical temperature at infinity. Vertical uncertainties shown for three points at the right arise from the C_v data. Horizontal uncertainties correspond to 0.2 K difference between our value for T_c and that of Voronel' et al. [8].

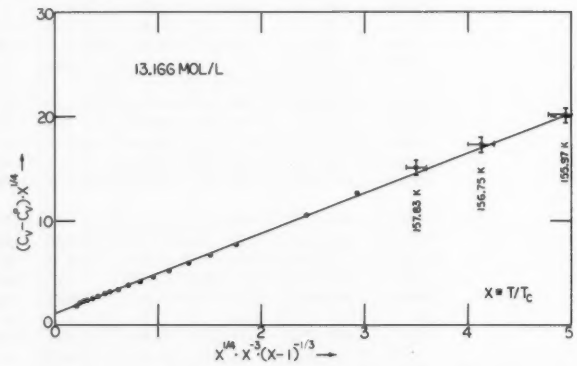

FIGURE 3. *Data of run No. 2 in coordinates of eq (4).*

Briefly, we arrived at eq (4) as follows. As the equation must be relatively simple, due to disposition of the data, we seek a mixture of weak and strong temperature dependencies only. For the former we may take $T^{-1/4}$ from the Lennard-Jones description of the second virial coefficient [7]. For the latter we include T^β, finding $\beta = -3$ by trial, in agreement with the Beattie-Bridgeman equation of state for domains away from critical [7]. For the nonanalytic part of the latter we at first explored

TABLE 3. *Experimental and calculated* C_v

ID	DEN	TEMP	C_v	CALC	PCNT
3301	5.268	153.683	25.79	26.01	−0.86
3314	5.268	157.576	25.17	25.49	−1.28
3302	5.268	157.856	25.24	25.46	−.85
3303	5.268	162.538	24.68	24.93	−1.01
3315	5.268	162.898	24.53	24.90	−1.49
3304	5.268	167.824	24.33	24.44	−.47
3316	5.268	168.890	24.21	24.35	−.60
3317	5.268	175.475	23.65	23.87	−.91
3305	5.268	175.869	23.45	23.84	−1.62
3306	5.268	183.525	23.16	23.40	−1.02
3307	5.268	192.262	22.76	23.00	−1.03
3308	5.268	202.057	22.50	22.65	−.67
3309	5.268	213.082	22.27	22.36	−.40
3310	5.268	226.034	22.12	22.10	.07
3311	5.268	240.759	21.89	21.89	−.01
3312	5.268	257.791	21.84	21.73	.50
3313	5.268	278.133	21.75	21.61	.64
402	6.124	155.794	27.81	27.18	2.32
403	6.124	160.002	26.83	26.42	1.53
404	6.124	164.797	26.05	25.72	1.29
405	6.124	170.195	25.26	25.08	.69
406	6.124	176.883	24.59	24.45	.56
407	6.124	186.560	23.72	23.76	−.20
408	6.124	196.057	23.35	23.26	.39
409	6.124	207.059	22.71	22.83	−.54
410	6.124	219.594	22.51	22.47	.15
411	6.124	234.502	22.09	22.17	−.39
412	6.124	250.222	21.85	21.95	−.45
413	6.124	265.673	21.82	21.81	.04
414	6.124	284.186	21.75	21.69	.26
225	13.166	155.297	46.40	47.01	−1.29
226	13.166	155.970	40.98	40.72	.64
227	13.166	156.753	38.10	37.56	1.44
228	13.166	157.829	35.90	35.17	2.10
229	13.166	159.558	33.40	32.94	1.40
230	13.166	162.067	31.21	31.04	.54
231	13.166	168.678	28.35	28.41	−.19
232	13.166	172.876	27.38	27.42	−.13
233	13.166	177.619	26.57	26.59	−.08
234	13.166	182.951	25.81	25.89	−.29
235	13.166	188.633	25.21	25.31	−.36
236	13.166	195.116	24.73	24.79	−.23
237	13.166	201.815	24.41	24.37	.17
238	13.166	208.788	24.03	24.01	.08
239	13.166	216.716	23.84	23.69	.62
240	13.166	222.219	23.63	23.51	.50
241	13.166	230.717	23.39	23.28	.50
242	13.166	239.156	23.22	23.09	.58
243	13.166	248.314	23.02	22.92	.40
244	13.166	257.729	22.96	22.79	.74
245	13.166	267.382	22.83	22.68	.65
246	13.166	276.983	22.57	22.59	−.08
516	20.260	154.095	28.69	28.69	−0.02
517	20.260	157.860	27.54	27.75	−.74
518	20.260	162.027	26.77	27.04	−1.00
519	20.260	167.104	26.15	26.42	−.99
520	20.260	173.286	25.63	25.87	−.92
521	20.260	182.885	25.03	25.27	−.96
522	20.260	190.402	24.78	24.93	−.59
523	20.260	198.662	24.49	24.65	−.63
524	20.260	207.168	24.27	24.42	−.61
525	20.260	215.586	24.17	24.24	−.29
901	23.158	148.563	27.06	26.66	1.52
902	23.158	152.486	26.51	26.35	.61
903	23.158	157.402	26.05	26.03	.10
904	23.158	163.303	25.65	25.71	−.27

TABLE 3. *Experimental and calculated* C_v—Continued

ID	DEN	TEMP	C_v	CALC	PCNT
905	23.158	170.379	25.31	25.42	−.44
906	23.158	178.665	25.00	25.15	−.59
907	23.158	187.541	24.74	24.92	−.70
908	23.158	196.331	24.58	24.74	−.64
801	25.920	140.433	26.57	26.19	1.44
802	25.920	144.299	26.26	26.04	.84
803	25.920	148.597	26.00	25.89	.42
804	25.920	153.298	25.77	25.75	.07
805	25.920	159.026	25.59	25.60	−.03
806	25.920	165.241	25.40	25.46	−.21
807	25.920	171.390	25.34	25.34	−.01
3215	28.669	129.470	26.76	26.49	1.01
3216	28.669	132.006	26.61	26.42	.73
3217	28.669	135.669	26.47	26.33	.51
3218	28.669	140.018	26.35	26.24	.44
3219	28.669	144.268	26.21	26.15	.21
3220	28.669	148.803	26.16	26.07	.32
3221	28.669	153.319	26.04	26.00	.17
3222	28.669	157.769	26.02	25.93	.32
317	28.719	130.692	26.50	26.46	.15
318	28.719	134.835	26.28	26.36	−.30
319	28.719	138.945	26.15	26.27	−.44
320	28.719	143.490	26.19	26.18	.04
321	28.719	147.531	26.05	26.10	−.19
322	28.719	151.493	25.99	26.04	−.19
323	28.719	155.489	25.93	25.97	−.17
324	28.719	159.453	25.90	25.92	−.07
706	28.736	128.832	26.56	26.51	.19
701	28.736	130.025	26.58	26.48	.38
702	28.736	134.223	26.36	26.37	−.07
703	28.736	139.804	26.20	26.25	−.19
704	28.736	146.427	26.07	26.12	−.22
705	28.736	153.498	25.95	26.01	−.21
601	28.740	129.811	26.75	26.49	.98
602	28.740	133.528	26.50	26.39	.42
603	28.740	137.687	26.35	26.30	.20
604	28.740	141.772	26.21	26.21	.00
605	28.740	146.114	26.14	26.13	.04
606	28.740	150.669	26.08	26.05	.11
607	28.740	154.966	26.00	25.99	.04
608	28.740	159.013	25.96	25.93	.12
1101	30.681	120.598	27.15	27.04	0.39
1102	30.681	124.251	26.97	26.96	.05
1103	30.681	130.736	26.79	26.83	−.15
1104	30.681	134.797	26.72	26.76	−.17
1105	30.681	138.824	26.66	26.70	−.15
1002	32.588	112.214	27.78	27.81	−.11
1003	32.588	116.182	27.63	27.73	−.37
1004	32.588	120.105	27.58	27.65	−.25
1005	32.588	124.452	27.50	27.58	−.29
1006	32.588	128.570	27.44	27.51	−.25
1007	32.588	132.456	27.45	27.45	.00
1901	33.932	102.977	28.68	28.58	.35
1902	33.932	106.074	28.43	28.51	−.28
1903	33.932	109.146	28.41	28.45	−.11
1904	33.932	112.406	28.31	28.38	−.24
1905	33.932	115.869	28.24	28.32	−.25
1802	34.920	97.805	29.18	29.20	−.09
1803	34.920	100.912	28.93	29.13	−.70
1804	34.920	103.990	28.83	29.06	−.81
1805	34.920	107.030	28.75	29.00	−.86

TABLE 3. *Experimental and calculated* C_v—Continued

ID	DEN	TEMP	C_v	CALC	PCNT
1701	36.059	89.205	30.52	30.10	1.41
1702	36.059	92.249	30.19	30.02	.58
1703	36.059	95.257	29.98	29.94	.13
1704	36.059	98.232	29.84	29.86	−.07
1705	36.059	100.982	29.78	29.80	−.04
1602	37.189	82.640	31.17	31.06	.35
1603	37.189	85.671	31.15	30.97	.57
1604	37.189	89.014	30.93	30.87	.19
1605	37.189	92.303	30.88	30.77	.35
1606	37.189	95.052	30.69	30.70	−.04
1502	38.224	74.969	32.21	32.13	.24
1503	38.224	77.616	31.93	32.03	−.33
1504	38.224	80.237	31.83	31.94	−.35
1505	38.224	82.818	31.82	31.85	−.09
1402	38.983	70.626	32.99	32.96	.10
1403	38.983	73.222	32.93	32.85	.25
1404	38.983	75.794	32.69	32.74	−.15
1302	39.787	65.138	34.17	33.96	.61
1303	39.787	67.705	33.57	33.83	−.79
1304	39.787	70.233	33.67	33.72	−.13
1203	40.649	57.897	35.20	35.24	−.12
1202	40.649	58.917	35.21	35.18	.07
1204	40.649	60.442	35.03	35.09	−.17
1205	40.649	62.967	35.08	34.94	.38

NPP = 151, Pct = 0.47.

the logarithmic form suggested by Voronel' et al., for oxygen near the critical point [8]. When this failed, we used a power ϵ in the expression

$$W \equiv (T/T_c - 1)^{-\epsilon},$$

as discussed by Fisher [9]. In this expression we obviously cannot use T_c on isochores departing from the critical density. Instead we must use $T_0(\sigma)$, a locus inside the coexistence envelope (fig. 1), touching it at the critical point. Through eq (4–c) the shape of this locus is adjusted by constant C_1. The first three derivatives vanish at the critical density (we explored $\delta = 1, 3, 5$). We hope soon to report on a *PVT* equation of state incorporating eq (4–d) for nonanalyticity at the critical point.

When coefficients for the two temperature dependent terms in eq (4) are found by least squares, they are worthless because they have large amplitudes mostly of opposite sign and their density dependence is irregular. We therefore seek data for B by trial on each isochore, obtaining A as an average. Equations (4–a), and (4–b) result from an examination of these data. As a final step, we iterate simultaneously for ϵ, B_2, and C_1, with $A(\sigma)$ constrained to eq (4–a) by least squares. Rounding these constants to the final values has an insignificant effect on the mean deviation. Constant B_1 must exceed zero if the second virial coefficient vanishes at high temperature by a $T^{-1/4}$ dependence, but our computer experiments with the present data give $B_1 = 0$. Equation (4) gives a finite value for $(\partial P/\partial T)_\rho$ at the critical point, a result derived from the thermodynamic relation

$$(\partial^2 P/\partial T^2)_\rho = -\rho^2 \cdot (\partial C_v/\partial \rho)_T/T.$$

Simplification of eq (4) is possible at the cost of increased deviations on low-density isochores near saturation. A plot of the data for $A(\sigma)$ is qualitatively a cubic in σ. The expression for $T_0(\sigma)$, eq (4–c), has the most simple, acceptable behavior at the origin when constant $C_1 = 1$. In this case C_1 is not an arbitrary constant. With these considerations we present the following results to show that $C_v(\sigma, T)$ might be described with fewer arbitrary constants than for eq (4) above. More accurate data are required at the low densities for a test of this possibility.

Constants for simplified eq (4)

Assuming these values—

$\alpha = -1/4$	$A_4 = 0$
$\beta = -3$	$A_5 = 0$
$\gamma = +3$	$B_1 = 0$
$\delta = +3$	$C_1 = 1$

We find the following values—

$\epsilon = 0.360$	$A_1 = 10.2672$
$B_2 = 0.331$	$A_2 = -7.39130$
	$A_3 = 1.75627$

Mean relative deviation for 152 C_v data is 0.63 percent.

These constants are *not* used in the following calculations

Data of Voronel' et al. [8], are given in table 4 on an isochore near critical density, and are compared with calculated values from eq (4). Our experimental data from table 2 agree better with Voronel' et al., than do our calculated values, suggesting that $W(\sigma, T)$ is not optimized for densities near critical. Necessary accuracy is lacking, however, for a critical comparison, because the respective critical point constants do not agree, and our experiments were not designed for high precision near the critical point.

TABLE 4. *Comparisons of* C_v *on a near-critical isochore*

T, K	Dens Mol/l	C_v, J/mol-K		
		Vrnl	Calc	Pcnt
155.000	12.7625	51.60	55.64	−7.26
155.120	12.7625	49.90	51.19	−2.52
155.130	12.7625	51.70	50.91	1.55
155.270	12.7625	50.10	47.84	4.73
155.380	12.7625	48.00	46.12	4.08
155.450	12.7625	46.90	45.23	3.70
155.640	12.7625	44.20	43.30	2.08
155.830	12.7625	44.60	41.86	6.55
156.860	12.7625	39.00	37.48	4.07
158.910	12.7625	32.80	33.79	−2.93
159.600	12.7625	34.50	33.04	4.42
160.140	12.7625	33.30	32.54	2.35

6. Derived Values for $(\partial P/\partial T)_v$ at Saturation

An interesting and valuable calculation can be performed now that we have analytical descriptions for C_σ, the specific heat of liquid along the coexistence path [2], and for C_v in one-phase domains. The thermodynamic relation [10],

$$C_\sigma = C_v + k \cdot T \cdot (-d\rho/dT)_\sigma \cdot (\partial P/\partial T)_v/\rho^2, \qquad (5)$$

contains temperature dependence of liquid density on the coexistence path $(d\rho/dT)_\sigma$ given in [2], and $(\partial P/\partial T)_v$ the terminal slopes of PVT isochores at the coexistence boundary. These slopes cannot be estimated with confidence by extrapolating PVT data because in just this terminal region the isochores may have maximum curvature. Yet these slopes are required data for thermal computations on isotherms extending from saturated liquid states into compressed liquid states.

Table 5 gives our computation of $(\partial P/\partial T)_v$ for liquid at the coexistence boundary under the heading CALCD. In column WEBER are values derived from *PVT* data [3], and in column ROWLN are some earlier values derived by J. S. Rowlinson [10]. With uncertainties of about 1 percent each in C_σ and in C_v, the uncertainty in $(C_\sigma - C_v)$ is about 3 percent when $C_\sigma \approx 2 \cdot C_v$. To this, add 1 percent uncertainty in $(d\rho/dT)_\sigma$ to obtain about 4 percent total uncertainty in the derived values for $(\partial P/\partial T)_v$. Agreement among the last three columns of table 5 is excellent.

TABLE 5. *Derived terminal values of* $(\partial P/\partial T)_v$ *for liquid*

T, K	P, atm	Mol/l	$D\rho/DT$ Mol/l K	CSAT J/mol-K	C_v J/mol-K	DP/DT, atm/K		
						CALCD	WEBER	ROWLN
54.351	0.001	40.842	−0.1384	53.31	35.69	38.57	38.93	.....
55.000	.002	40.752	−.1385	53.31	35.54	38.22	38.56	.....
60.000	.007	40.057	−.1392	53.27	34.51	35.58	35.77	36.60
65.000	.023	39.359	−.1404	53.28	33.56	33.02	33.14	33.90
70.000	.061	38.652	−.1421	53.33	32.70	30.57	30.65	31.20
75.000	.143	37.936	−.1444	53.42	31.90	28.23	28.30	28.80
80.000	.297	37.208	−.1472	53.58	31.17	26.01	26.09	26.50
85.000	.561	36.463	−.1506	53.81	30.49	23.90	24.00	24.50
90.000	.981	35.700	−.1548	54.13	29.85	21.91	22.03	22.30
90.180	1.000	35.672	−.1550	54.14	29.83	21.84	21.96	22.20
95.000	1.611	34.914	−.1598	54.55	29.27	20.03	20.17	.....
100.000	2.509	34.100	−.1659	55.11	28.73	18.26	18.42	.....
105.000	3.738	33.253	−.1730	55.84	28.[illegible]	16.58	16.75	.....
110.000	5.363	32.367	−.1817	56.78	27.78	15.00	15.17	.....
115.000	7.454	31.433	−.1923	58.01	27.37	13.51	13.67	.....
120.000	10.082	30.439	−.2055	59.62	27.00	12.09	12.23	.....
125.000	13.321	29.372	−.2224	61.76	26.69	10.74	10.84	.....
130.000	17.249	28.207	−.2448	64.70	26.44	9.44	9.61	.....
135.000	21.947	26.909	−.2763	68.91	26.29	8.16	8.25	.....
140.000	27.501	25.416	−.3247	75.44	26.31	6.89	6.90	.....
145.000	34.018	23.601	−.4110	87.09	26.71	5.57	5.58	.....
150.000	41.638	21.113	−.6247	115.69	28.50	4.09	4.14	.....
151.000	43.312	20.445	−.7174	127.97	29.48	3.75		
152.000	45.041	19.662	−.8600	146.72	31.14	3.37	3.51	.....
153.000	46.828	18.688	−1.1189	180.23	34.64	2.93		
154.000	48.675	17.292	−1.8252	268.10	49.22	2.30	2.72	.....

7. Appendix I. Adjustment for Expansion of the Calorimeter Bomb

This derivation is similar to that of P. A. Walker [4]. With reference to figure 4, we want Q_{AB} at constant volume for a given $\Delta T = T_2 - T_1$, but we observe Q_{AC} due to the increase ΔV of bomb volume. From thermodynamics,

$$\Delta E_{AC} = Q_{AC} - \int_A^C P \cdot dV. \qquad (a\text{–}1)$$

Along path ABC, however,

$$\Delta E_{AC} = \int_A^B \left(\frac{\partial E}{\partial T}\right)_{V_1} dT + \int_B^C \left(\frac{\partial E}{\partial V}\right)_{T_2} \cdot dV. \qquad (a\text{–}2)$$

Combining (a–1) and (a–2) with the thermodynamic equation of state,

$$(\partial E/\partial V)_T = T \cdot (\partial P/\partial T)_v - P, \qquad (a\text{–}3)$$

we obtain

$$Q_{AB} - Q_{AC} = \int_B^C P \cdot dV_{T_2} - \int_A^C P dV - T_2 \cdot \int_B^C \left(\frac{\partial P}{\partial T}\right)_V dV. \qquad (a\text{–}4)$$

Sum of the first two terms on the right of (a–4) is the area of triangle ABC, which is approximately $\Delta P \cdot \Delta V/2$. Hence

$$Q_{AB} = Q_{AC} + \left[\Delta P/2 - T_2 \cdot \left(\frac{\partial P}{\partial T}\right)_V\right] \cdot \Delta V \qquad (a\text{–}5)$$

where $(\partial P/\partial T)_V$ at T_2 is a mean over ΔV. For sufficiently small interval about T, however, (a–5) becomes simply

$$(Q/\Delta T)_{AB} = (Q/\Delta T)_{AC} - T \cdot (\partial P/\partial T)_V \cdot \Delta V/\Delta T. \qquad (a\text{–}6)$$

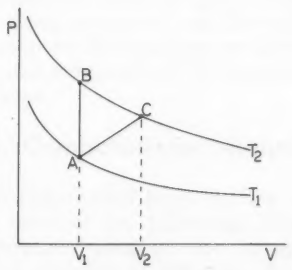

FIGURE 4. P–V *diagram for appendix I.*

We accounted for fluid forced into the capillary tube as described in the main text above eq (2). R. E. Barieau subsequently has given a careful derivation for these adjustments with the following result

$$C_v = \left[\text{Lim}\left(\frac{Q}{\Delta T}\right) - C_b\right]\frac{1}{N_b} - T\cdot\left(\frac{\partial P}{\partial T}\right)_\rho \cdot \frac{dv}{dT}. \quad \text{(a-7)}$$

where

$$\frac{dv}{dT} = \frac{1}{N_b}\left[\frac{dV_b}{dT} + \frac{V_b}{N_b}\cdot\frac{dN_c}{dT}\right]. \quad \text{(a-8)}$$

For our eq (2) we calculated density in the bomb as

$$\rho = (N - N_c)/V_b, \quad \text{(a-9)}$$

and the value of Δv for eq (2) as

$$\Delta v = 1/\rho_2 - 1/\rho_1. \quad \text{(a-10)}$$

From (a-9) and (a-10) one obtains

$$\Delta v = [N\cdot\Delta V_b + V_b\cdot\Delta N_c]/(N - N_{c_2})(N - N_{c_1}), \quad \text{(a-11)}$$

or very closely for a small capillary tube,

$$\Delta v/\Delta T \approx \frac{1}{N_b}\left[\Delta V_b + V_b\cdot\Delta N_c/N_b\right]/\Delta T. \quad \text{(a-12)}$$

This is the same as (a-8) for small intervals.

8. References

[1] Stewart, R. B., The Thermodynamic Properties of Oxygen, Dissertation, Dept. of Mech. Eng., Univ. of Iowa, June, 1966.

[2] Goodwin, R. D. and Weber, L. A., Specific heats of oxygen at coexistence, J. Res. NBS **73A** (Phys. and Chem.), No. 1 (1969).

[3] Weber, L. A., Internal report, June 20, 1968.

[4] Walker, P. A., The Equation of State and the Specific Heat of Liquid Argon, Ph. D. Thesis, Queen Mary College, Univ. of London, 1956.

[5] Hoge, H. J., Heat capacity of a two-phase system, with applications to vapor corrections in calorimetry, J. Res. NBS **36,** 111 (1946) RP.

[6] Woolley, H. W., Thermodynamic functions for molecular oxygen in the ideal gas state, J. Res. NBS **40,** 163–68 (1948) RP.

[7] Beattie, J. A. and Stockmayer, W. H., The Thermodynamics and Statistical Mechanics of Real Gases, Chapter II in States of Matter, H. S. Taylor and S. Glasstone, editors (D. van Nostrand Co., Inc., New York, N.Y., 1951).

[8] Voronel', A. V., Chashkin, Yu. R., Popov, V. A., and Simkin, V. G., Measurement of the Specific Heat C_v of Oxygen near the Critical Point, Soviet Phys.–JETP **18** (2), 568–9 (1964).

[9] Fisher, M. E., Correlation functions and the critical region of simple fluids, J. Math. Phys. **5** (7), 944–961 (1964).

[10] Rowlinson, J. S., Liquids and Liquid Mixtures (Butterworths, London, 1959).

(Paper 73A1–530)

JOURNAL OF RESEARCH of the National Bureau of Standards—A. Physics and Chemistry
Vol. 73A, No. 1, January–February 1969

Thermodynamic Properties of Fluid Oxygen at Temperatures to 250 K and Pressures to 350 Atmospheres on Isochores at 1.3 to 3.0 Times Critical Density *

Robert D. Goodwin**

Institute for Basic Standards, National Bureau of Standards, Boulder, Colorado 80302

(August 20, 1968)

The starting point for these calculations is liquid oxygen at the triple point. An analytical formula is used for specific heats of saturated liquid along the coexistence path to obtain internal energies and entropies of the saturated liquid. With these initial values, the calculations next are made as a function of temperature along isochores, using an "equation of state" for the specific heats $C_v(\rho, T)$ in the single-phase domain. Enthalpies are obtained by adding Pv to the internal energies. Results are tabulated at uniform densities and temperatures. Based on uncertainties of one percent in the specific heat data, the uncertainty of thermal properties also is taken to be 1 percent.

Key Words: Compressed liquid; enthalpy; entropy; internal energy; oxygen; saturated liquid; thermodynamic properties.

List of Symbols

$C_\sigma(T)$	specific heat of liquid along the coexistence path.
$C_v(\rho, T)$	specific heat at constant volume in the single phase domain.
$C_v^\circ(T)$	specific heat at constant volume in the ideal gas states.
D	density, on the computer-printed tables.
E	internal energy. E_0° for ideal gas state at $T=0$.
E_t	internal energy of liquid at the triple point.
H	enthalpy.
H_t	enthalpy of liquid at the triple point.
J	the Joule.
k	conversion factor, 0.101325 J/(cm³-atm).
L	the liter, 1000 cm³.
P	pressure. 1 atm = 0.101325 MN/m².
ρ	density.
ρ_c	0.01362 mol/cm³ at the critical point [1].
S	entropy.
S_t	entropy of liquid at the triple point.
T	temperature, K (NBS 1955).
T_c	154.77 K at the critical point [6].
T_t	54.3507 K at the triple point [1].
v	$1/\rho$ molal volume.

1. Introduction

We recently have completed PVT and C_v measurements on oxygen at temperatures to 300 K and pressures to 350 atm, data needed for calculating thermodynamic properties [1, 2, 3]. The computation of a self-consistent thermodynamic network is an intricate and time-consuming labor [4]. In the present report, we use specific heat data in compressed liquid states to obtain thermodynamic properties along paths at constant density (isochores), beginning at the saturated liquid. We consider these results to be preliminary because the same properties can be calculated along alternate routes, as for example on isotherms by use of PVT data, and a measure of the consistency remains to be established.

2. Computational Methods

Figure 1 is reproduced here to show the computational paths used in the following. This figure is a density-temperature diagram for oxygen, including the locus for a pressure of 350 atm. The small circles locate experimental C_v measurements along isochores [3]. We start our calculations with $E=E_t$ and $S=S_t$ at the liquid triple point, located on figure 1 near $T=54$ K and $\rho/\rho_c=3.0$, calculating the change in values of E and of S with increasing T along the saturated liquid path, down to various rounded densities. We then calculate the change in values

*This work was carried out at the National Bureau of Standards under the sponsorship of the National Aeronautics and Space Administration Fund Transfer R-06-006-046.
**Cryogenics Division, NBS Boulder Laboratories, Boulder, Colorado 80302.

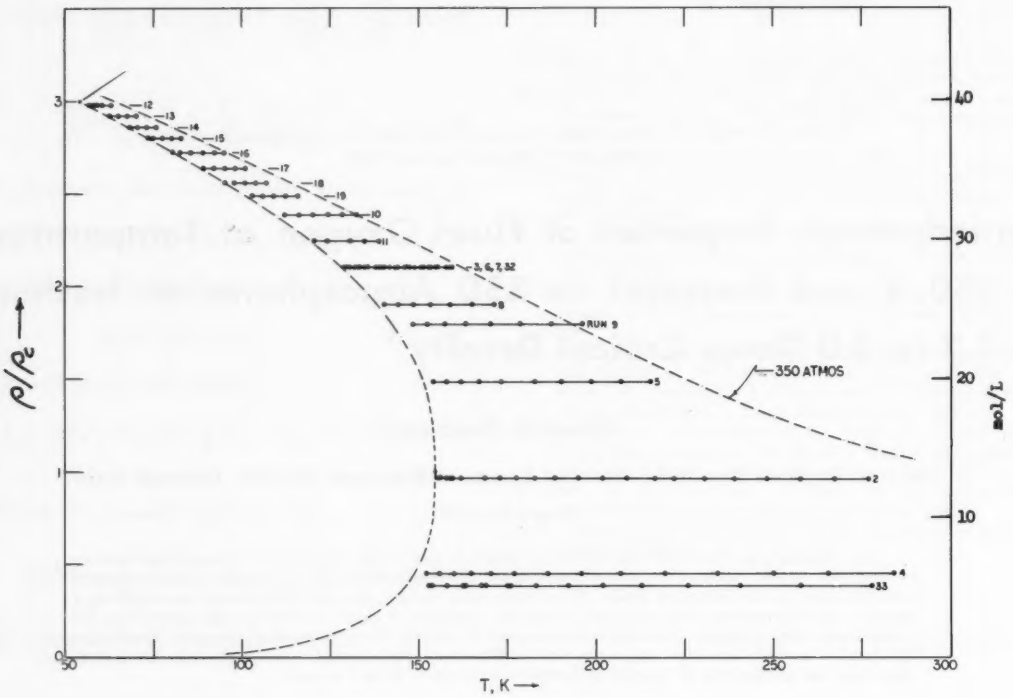

FIGURE 1. *Locus of* C_v *data in* ρ-T *coordinates.*

of E and of S with increasing T at constant density up to 350 atm. On either of these paths we have

$$E = E_t + \int C \cdot dT + \int [P/\rho^2]_\sigma \cdot d\rho, \tag{1}$$

$$H = E + P/\rho, \tag{2}$$

$$S = S_t + \int C \cdot dT/T, \tag{3}$$

where $C \equiv C_\sigma(T)$ for the saturated liquid path, and $C \equiv C_v(\rho, T)$ on the isochores (ρ = constant).

Whereas E_t and S_t may be set at zero, we believe the results will be more useful if they are on the basis of ideal gas states. We therefore take values for E_t and for S_t derived in [1] via *PVT* data and specific heats relative to data of Woolley for the ideal gas states [5],

$$E_t \equiv E_{tp} - E_0^\circ = -6189.6 \text{ J/mol},$$

$$H_t = E_t, \quad S_t = 67.00 \text{ J/mol deg},$$

where E_{tp} refers to liquid at the triple point. Note that $H_t = E_t$ within uncertainty of the data due to the very low triple point value of the $P \cdot v$ product.

On the saturated liquid path we perform the calculations of (1), (2), and (3) by use of the analytical formula for $C_\sigma(T)$ in [2], the vapor pressure equation $P(T)$ reproduced in [2] from [6], and the formula for densities of saturated liquid $\rho(T)$, table 1 in [2]. Along the isochores we perform the calculations of (1) and (3) by use of the analytical formula for $C_v(\rho, T)$ in [3]. For the calculation (2) we used pressures tabulated for us by Lloyd A. Weber from his *PVT* interpolation programs [1].

3. Description of the Tables

Each table describes a surface in three dimensions. Independent variables are density increasing to the right and temperature increasing downwards. Uniform values of these variables are the same in corresponding tables for pressure, internal energy, enthalpy and entropy. The range of densities from 18.00 to 40.00 mol/liter is broken into three tables, a, b, c due to printing limitations. In every table the first row gives the isochore density, D, in mol/liter, and the second row gives the temperature at saturation TSAT in K for this liquid density. This temperature is found by trial to minimize the difference between the isochore density D and that calculated by the formula $\rho(T)$ for saturated liquid. The first column in every table gives temperatures, K (NBS 1955) along the isochores.

In table 1 for pressures, the third row gives the vapor pressure PS in atmospheres at TSAT, and table entries are the pressure in atmospheres. As all experimental data for *PVT* and for C_v terminate at a pressure near 350 atm, all entries in tables 2, 3, and 4 which correspond to a table 1 pressure greater than 350 atm necessarily are extrapolated and therefore are subject to unknown error. Horizontal lines in the tables help to locate this limit.

TABLE 1–a. *Pressures*

D, mol/l =	18.00	19.00	20.00	21.00	22.00	23.00	24.00	25.00	26.00
TSAT, K =	153.55	152.71	151.59	150.18	148.45	146.40	144.00	141.25	138.14
PS, atm =	47.842	46.300	44.326	41.934	39.153	36.031	32.632	29.035	25.328
Temp., K	Pressure, atm								
140.00	.....	.....	.....	.....	.....	.....	.....	.....	39.085
145.00	.....	.....	.....	.....	.....	.....	38.498	53.788	76.333
150.00	.....	.....	.....	.....	46.245	54.786	67.983	87.137	113.724
155.00	52.070	53.789	56.857	61.919	69.778	81.395	97.905	120.627	151.077
160.00	67.121	70.660	75.825	83.266	93.786	108.352	128.105	154.366	188.622
165.00	82.689	88.035	95.253	105.005	118.099	135.510	158.386	188.051	225.989
170.00	98.539	105.694	114.946	126.969	142.589	162.791	188.731	221.726	263.238
175.00	114.552	123.522	134.802	149.078	167.186	190.123	219.057	255.323	300.395
180.00	130.694	141.473	154.761	171.263	191.831	217.481	249.383	288.815	337.050
185.00	146.902	159.492	174.797	193.534	216.552	244.852	279.615	322.220	374.285
190.00	163.162	177.573	194.888	215.828	241.248	272.165	309.794	355.611	411.425
195.00	179.478	195.702	215.002	238.108	265.890	299.410	339.991	389.318	
200.00	195.788	213.819	235.111	260.398	290.533	326.516	369.535		
205.00	212.117	231.947	255.203	282.615	315.005	353.305	398.571		
210.00	228.445	250.074	275.295	304.831	339.477	380.094			
215.00	244.750	268.123	295.340	327.444	365.949				
220.00	261.055	286.173	315.385	350.056	392.421				
225.00	277.352	304.190	335.157	371.495					
230.00	293.649	322.207	354.929	392.934					
235.00	309.873	339.837	373.251						
240.00	326.096	357.468							
245.00	343.070	377.886							
250.00	360.045								
255.00	376.286								

TABLE 1–b. *Pressures*

D, mol/l =	27.00	28.00	29.00	30.00	31.00	32.00	33.00	34.00
TSAT, K =	134.67	130.84	126.65	122.11	117.22	112.00	106.45	100.60
PS, atm =	21.609	17.979	14.535	11.367	8.550	6.139	4.166	2.638
Temp., K	Pressure, atm							
102.00								29.667
104.00								65.752
106.00								101.527
108.00							30.406	136.999
110.00							62.709	172.177
112.00						6.762	94.781	207.070
114.00						35.830	126.631	241.685
116.00						64.733	158.267	276.030
118.00					18.915	93.478	189.696	310.115
120.00					44.877	122.074	220.927	343.946
122.00					70.740	150.528	251.967	377.533
124.00				33.378	96.513	178.848	282.825	410.883
126.00				56.581	122.201	207.042	313.508	444.004
128.00			28.543	79.745	147.813	235.116	344.024	
130.00			49.627	103.086	173.229	262.850	374.741	
132.00		28.909	70.428	126.063	198.490	290.487	404.938	
134.00		47.502	91.174	148.980	223.649	318.756	438.716	
136.00	32.682	66.191	111.835	171.819	248.862	346.201		
138.00	49.366	84.800	132.456	194.604	273.920	373.487		
140.00	66.033	103.378	153.066	217.373	298.911	400.622		
142.00	82.733	121.927	173.573	240.040	324.046	428.652		
144.00	99.404	140.436	193.999	262.348	347.989			
146.00	116.047	159.041	214.665	284.943	372.019			
148.00	132.754	177.509	235.041	307.518	397.287			
150.00	149.391	195.957	255.415	329.926	421.828			
152.00	165.976	214.305	275.633	352.120				
154.00	182.682	232.815	296.056	374.560				
156.00	199.220	251.279	316.041	393.321				
158.00	215.870	269.464	336.581	420.240				
160.00	232.482	287.542	355.111					
162.00	248.994	305.660	374.735					
164.00	265.507	323.779	394.359					
166.00	281.981	341.913	414.344					
168.00	298.415	360.064						
170.00	314.848	378.216						
172.00	331.239	396.189						
174.00	347.630	414.162						
176.00	363.687							

In table 2 for internal energies the third row gives E_s, the change in value of internal energy of saturated liquid from the triple point temperature up to the saturation temperature TSAT for each isochore. Total E at each such point is $E_t + E_s$. Table entries are the internal energy, E in J/(mol).

In table 3 for enthalpies the third row gives H_s, the change in value of enthalpy of saturated liquid from T_t up to TSAT. Total H at each such point is $H_t + H_s$. Table entries are the enthalpy, H in J/(mol).

In table 4 for entropies, the third row gives S_s, the change in value of entropy of saturated liquid from T_t up to TSAT. Total S at each such point is $S_t + S_s$. Table entries are the entropy, S in J/(mol deg).

4. Comparisons and Estimate of Accuracy

The compendium of thermal properties of oxygen by R. B. Stewart [6] is invaluable because it provides independent computations with which to compare our results. Stewart used an analytical equation of state to effect the computations using, among other data, Woolley's ideal gas (thermal) functions and early *PVT* data of L. A. Weber [1]. Our specific heat data, however, had not then been obtained.

Table 5 gives comparisons with results interpolated from Stewart's tabulations on isobars. The first two columns give density on three isochores and two temperatures on each. The rounded pressure is included for convenience in the third column. The last three columns give the relative deviation in percent of Stewart's values for E, H, and S from our values. The excellent agreement of entropies is conspicuous. All deviations of E and of H are positive, such that a small change in our (or his) assigned value for E_t would suffice to diminish the mean of these deviations. Note that the relative deviations at $\rho = 26$ mol/l, $T = 175$ K appear large because both E and H have small values, tables 2, 3.

TABLE 1–c. *Pressures*

D, mol/l =	35.00	36.00	37.00	38.00	39.00	40.00
TSAT, K =	94.46	88.05	81.41	74.56	67.55	60.41
PS, atm =	1.531	0.796	0.358	0.133	0.039	0.008
Temp., K	Pressure, atm					
62.00						57.072
64.00						126.932
66.00						195.835
68.00					15.135	263.793
70.00					78.241	330.814
72.00					140.514	396.909
74.00					201.962	
76.00				42.206	262.595	
78.00				98.360	322.423	
80.00				153.806	381.456	
82.00			17.183	208.552	439.701	
84.00			67.713	262.606		
86.00			117.641	315.979		
88.00			166.978	368.680		
90.00		47.007	215.731	420.717		
92.00		91.884	263.910			
94.00		136.270	311.524			
96.00	34.780	180.173	358.581			
98.00	75.049	223.602	405.091			
100.00	114.921	266.566	451.062			
102.00	154.404	309.073				
104.00	193.506	351.132				
106.00	232.237	392.753				
108.00	270.604	433.943				
110.00	308.616					
112.00	346.281					
114.00	383.607					

TABLE 2–a. *Internal energies*

D, mol/l =	18.00	19.00	20.00	21.00	22.00	23.00	24.00	25.00	26.00
TSAT, K =	153.55	152.71	151.59	150.18	148.45	146.40	144.00	141.25	138.14
ES, J/mol =	6247.0	6101.7	5944.8	5776.2	5595.9	5403.6	5199.2	4982.4	4753.4
Temp., K	Energy, J/mol								
140.00									−1387.4
145.00							−963.9	−1108.7	−1256.9
150.00					−551.2	−689.5	−832.2	−978.4	−1127.3
155.00	109.2	−15.0	−144.3	−278.1	−415.9	−557.4	−702.0	−849.2	−998.4
160.00	264.6	132.1	−3.7	−142.2	−283.4	−427.0	−573.0	−720.9	−870.3
165.00	407.6	271.4	132.1	−9.4	−152.9	−298.1	−444.9	−593.3	−742.6
170.00	544.5	406.1	264.5	121.0	−24.0	−170.3	−317.8	−466.3	−615.6
175.00	677.6	537.6	394.6	249.7	103.6	−43.5	−191.4	−340.0	−488.9
180.00	807.7	666.8	522.7	376.9	230.0	82.5	−65.6	−214.1	−362.7
185.00	935.7	794.1	649.3	502.9	355.5	207.7	59.6	−88.7	−236.8
190.00	1061.9	919.9	774.7	627.8	480.2	332.3	184.3	36.3	−111.2
195.00	1186.7	1044.5	899.0	752.0	604.2	456.4	308.5	161.0	
200.00	1310.2	1168.0	1022.4	875.3	727.7	579.9	432.4		
205.00	1432.8	1290.6	1145.1	998.1	850.6	703.1	555.9		
210.00	1554.4	1412.4	1267.1	1120.3	973.0	825.8			
215.00	1675.3	1533.6	1388.5	1242.0	1095.0				
220.00	1795.6	1654.2	1509.5	1363.3	1216.7				
225.00	1915.2	1774.3	1629.9	1484.1					
230.00	2034.4	1893.9	1750.0	1604.7					
235.00	2153.1	2013.1	1869.8						
240.00	2271.5	2132.0							
245.00	2389.5	2250.6							
250.00	2507.1								
255.00	2624.5								

TABLE 2–b. *Internal energies*

D, mol/l =	27.00	28.00	29.00	30.00	31.00	32.00	33.00	34.00
TSAT, K =	134.67	130.84	126.65	122.11	117.22	112.00	106.45	100.60
ES, J/mol =	4512.0	4258.5	3992.9	3715.2	3425.5	3123.8	2810.3	2485.1
Temp., K	Energy, J/mol							
102.00								−3664.4
104.00								−3607.2
106.00								−3550.1
108.00							−3335.9	−3493.0
110.00							−3279.8	−3436.1
112.00						−3065.7	−3223.8	−3379.2
114.00						−3010.6	−3167.9	−3322.4
116.00						−2955.5	−3112.1	−3265.6
118.00					−2742.9	−2900.5	−3056.3	−3209.0
120.00					−2688.6	−2845.6	−3000.6	−3152.4
122.00					−2634.4	−2790.7	−2945.0	−3095.9
124.00				−2423.6	−2580.2	−2736.0	−2889.5	−3039.4
126.00				−2370.0	−2526.2	−2681.3	−2834.0	−2983.1
128.00			−2160.8	−2316.5	−2472.2	−2626.6	−2778.6	
130.00			−2107.7	−2263.1	−2418.3	−2572.1	−2723.3	
132.00		−1900.4	−2054.7	−2209.8	−2364.4	−2517.6	−2668.0	
134.00		−1847.7	−2001.8	−2156.5	−2310.7	−2463.1	−2612.8	
136.00	−1642.6	−1795.1	−1949.0	−2103.4	−2257.0	−2408.8		
138.00	−1590.1	−1742.6	−1896.3	−2050.3	−2203.3	−2354.5		
140.00	−1537.8	−1690.3	−1843.7	−1997.2	−2149.7	−2300.2		
142.00	−1485.6	−1638.0	−1791.2	−1944.3	−2096.2	−2246.0		
144.00	−1433.6	−1585.8	−1738.7	−1891.4	−2042.8			
146.00	−1381.6	−1533.7	−1686.3	−1838.5	−1989.3			
148.00	−1329.8	−1481.7	−1634.0	−1785.7	−1936.0			
150.00	−1278.0	−1429.8	−1581.7	−1733.0	−1882.7			
152.00	−1226.4	−1377.9	−1529.5	−1680.4				
154.00	−1174.8	−1326.1	−1477.4	−1627.7				
156.00	−1123.3	−1274.4	−1425.3	−1575.2				
158.00	−1071.9	−1222.8	−1373.3	−1522.7				
160.00	−1020.6	−1171.2	−1321.3					
162.00	−969.3	−1119.7	−1269.4					
164.00	−918.2	−1068.2	−1217.6					
166.00	−867.1	−1016.8	−1165.7					
168.00	−816.0	−965.4						
170.00	−765.0	−914.1						
172.00	−714.1	−862.9						
174.00	−663.2	−811.7						
176.00	−612.4							

TABLE 2–c. *Internal energies*

D, mol/l =	35.00	36.00	37.00	38.00	39.00	40.00
TSAT, K =	94.46	88.05	81.41	74.56	67.55	60.41
ES, J/mol =	2148.5	1801.1	1443.6	1077.2	703.1	323.0
Temp., K	Energy, J/mol					
62.00						−5812.0
64.00						−5743.4
66.00						−5675.1
68.00					−5471.5	−5606.9
70.00					−5405.4	−5539.0
72.00					−5339.5	−5471.2
74.00					−5273.7	
76.00				−5066.4	−5208.2	
78.00				−5002.6	−5142.7	
80.00				−4939.0	−5077.5	
82.00			−4727.6	−4875.6	−5012.3	
84.00			−4665.8	−4812.2		
86.00			−4604.1	−4749.0		
88.00			−4542.5	−4686.0		
90.00		−4329.9	−4481.0	−4623.0		
92.00		−4269.9	−4419.7			
94.00		−4210.0	−4358.4			
96.00	−3995.9	−4150.2	−4297.3			
98.00	−3937.4	−4090.5	−4236.2			
100.00	−3879.0	−4030.8	−4175.3			
102.00	−3820.6	−3971.3				
104.00	−3762.4	−3911.9				
106.00	−3704.2	−3852.6				
108.00	−3646.1	−3793.3				
110.00	−3588.1					
112.00	−3530.2					
114.00	−3472.4					

TABLE 3–a. *Enthalpies*

D, mol/l =	18.00	19.00	20.00	21.00	22.00	23.00	24.00	25.00	26.00
TSAT, K =	153.55	152.71	151.59	150.18	148.45	146.40	144.00	141.25	138.14
HS, J/mol =	6516.3	6348.6	6169.3	5978.6	5776.2	5562.4	5336.9	5100.1	4852.1
Temp., K	Enthalpy, J/mol								
140.00									−1235.1
145.00							−801.4	−890.7	−959.4
150.00					−338.2	−448.1	−545.2	−625.3	−684.1
155.00	402.3	271.8	143.8	20.7	−94.6	−198.8	−288.7	−360.3	−409.7
160.00	642.4	508.9	380.5	259.5	148.6	50.3	−32.1	−95.2	−135.2
165.00	873.0	740.9	614.6	497.2	391.1	298.9	223.7	168.9	138.1
170.00	1099.2	969.7	846.9	733.6	632.8	546.9	479.0	432.3	410.3
175.00	1322.4	1196.4	1077.5	969.0	873.6	794.1	733.5	694.9	681.8
180.00	1543.4	1421.3	1306.8	1203.2	1113.5	1040.6	987.2	956.5	950.9
185.00	1762.6	1644.7	1534.9	1436.7	1352.9	1286.4	1240.1	1217.3	1221.8
190.00	1980.4	1866.9	1762.0	1669.2	1591.3	1531.3	1492.2	1477.6	1492.1
195.00	2197.0	2088.1	1988.3	1900.8	1828.9	1775.4	1743.9	1738.9	
200.00	2412.4	2308.3	2213.6	2131.8	2065.8	2018.4	1992.5		
205.00	2626.8	2527.5	2438.0	2361.7	2301.4	2259.5	2238.6		
210.00	2840.4	2746.0	2661.8	2591.1	2536.5	2500.3			
215.00	3053.1	2963.5	2884.8	2821.9	2780.5				
220.00	3265.1	3180.3	3107.3	3052.3	3024.0				
225.00	3476.5	3396.5	3327.9	3276.6					
230.00	3687.4	3612.2	3548.2	3500.6					
235.00	3897.5	3825.4	3760.7						
240.00	4107.1	4038.3							
245.00	4320.7	4265.8							
250.00	4533.9								
255.00	4742.7								

TABLE 3–b. *Enthalpies*

D, mol/l =	27.00	28.00	29.00	30.00	31.00	32.00	33.00	34.00
TSAT, K =	134.67	130.84	126.65	122.11	117.22	112.00	106.45	100.60
HS, J/mol =	4593.1	4323.6	4043.7	3753.6	3453.4	3143.3	2823.1	2493.0
Temp., K	Enthalpy, J/mol							
102.00								−3576.0
104.00								−3411.3
106.00								−3247.5
108.00							−3242.5	−3084.7
110.00							−3087.3	−2922.9
112.00						−3044.3	−2932.8	−2762.1
114.00						−2897.1	−2779.1	−2602.1
116.00						−2750.5	−2626.1	−2443.0
118.00					−2681.1	−2604.5	−2473.9	−2284.8
120.00					−2541.9	−2459.0	−2322.3	−2127.4
122.00					−2403.2	−2314.1	−2171.4	−1970.8
124.00				−2310.8	−2264.8	−2169.7	−2021.1	−1815.0
126.00				−2178.9	−2126.7	−2025.7	−1871.4	−1659.9
128.00			−2061.0	−2047.2	−1989.0	−1882.2	−1722.3	
130.00			−1934.3	−1914.9	−1852.1	−1739.8	−1572.6	
132.00		−1795.7	−1808.6	−1784.0	−1715.7	−1597.8	−1424.6	
134.00		−1675.8	−1683.3	−1653.3	−1579.7	−1453.8	−1265.7	
136.00	−1519.9	−1555.6	−1558.3	−1523.0	−1443.5	−1312.6		
138.00	−1404.9	−1435.8	−1433.6	−1393.0	−1308.0	−1171.8		
140.00	−1290.0	−1316.2	−1308.9	−1263.0	−1172.7	−1031.7		
142.00	−1175.2	−1196.8	−1184.7	−1133.5	−1037.1	−888.7		
144.00	−1060.5	−1077.6	−1060.9	−1005.3	−905.3			
146.00	−946.1	−958.2	−936.3	−876.1	−773.4			
148.00	−831.6	−839.4	−812.8	−747.1	−637.4			
150.00	−717.4	−720.7	−689.3	−618.7	−503.9			
152.00	−603.5	−602.4	−566.5	−491.1				
154.00	−489.2	−483.6	−443.0	−362.7				
156.00	−375.7	−365.1	−321.1	−246.7				
158.00	−261.8	−247.7	−197.3	−103.3				
160.00	−148.1	−130.7	−80.6					
162.00	−34.9	−13.6	39.9					
164.00	78.2	103.5	160.3					
166.00	191.2	220.5	282.0					
168.00	303.9	337.5						
170.00	416.5	454.5						
172.00	529.0	570.8						
174.00	641.4	687.1						
176.00	752.4							

TABLE 3–c. *Enthalpies*

D, mol/l =	35.00	36.00	37.00	38.00	39.00	40.00
TSAT, K =	94.46	88.05	81.41	74.56	67.55	60.41
HS, J/mol =	2153.0	1803.4	1444.6	1077.5	703.2	323.1
Temp., K	Enthalpy, J/mol					
62.00						−5667.4
64.00						−5421.9
66.00						−5179.0
68.00					−5432.2	−4938.7
70.00					−5202.1	−4701.0
72.00					−4974.4	−4465.8
74.00					−4749.0	
76.00				−4953.9	−4525.9	
78.00				−4740.4	−4305.1	
80.00				−4528.9	−4086.4	
82.00			−4680.6	−4319.5	−3870.0	
84.00			−4480.3	−4112.0		
86.00			−4281.9	−3906.5		
88.00			−4085.2	−3702.9		
90.00		−4197.6	−3890.2	−3501.2		
92.00		−4011.3	−3696.9			
94.00		−3826.4	−3505.3			
96.00	−3895.2	−3643.1	−3315.3			
98.00	−3720.1	−3461.1	−3126.9			
100.00	−3546.3	−3280.6	−2940.1			
102.00	−3373.6	−3101.4				
104.00	−3202.2	−2923.6				
106.00	−3031.9	−2747.1				
108.00	−2862.7	−2571.9				
110.00	−2694.7					
112.00	−2527.7					
114.00	−2361.8					

TABLE 4–a. *Entropies*

D, mol/l =	18.00	19.00	20.00	21.00	22.00	23.00	24.00	25.00	26.00
TSAT, K =	153.55	152.71	151.59	150.18	148.45	146.40	144.00	141.25	138.14
SS, J/mol K =	62.81	61.77	60.66	59.47	58.21	56.85	55.40	53.84	52.17
Temp., K	Entropy, J/(mol deg)								
140.00									119.52
145.00							122.58	121.53	120.44
150.00					125.49	124.50	123.48	122.42	121.32
155.00	130.15	129.24	128.32	127.36	126.38	125.37	124.33	123.26	122.16
160.00	131.13	130.18	129.21	128.22	127.22	126.20	125.15	124.08	122.98
165.00	132.01	131.04	130.04	129.04	128.02	126.99	125.94	124.86	123.76
170.00	132.83	131.84	130.83	129.82	128.79	127.75	126.70	125.62	124.52
175.00	133.60	132.60	131.59	130.57	129.53	128.49	127.43	126.35	125.26
180.00	134.34	133.33	132.31	131.28	130.24	129.20	128.14	127.06	125.97
185.00	135.04	134.03	133.00	131.97	130.93	129.88	128.82	127.75	126.66
190.00	135.71	134.70	133.67	132.64	131.60	130.55	129.49	128.42	127.33
195.00	136.36	135.35	134.32	133.28	132.24	131.19	130.13	129.06	
200.00	136.98	135.97	134.94	133.91	132.87	131.82	130.76		
205.00	137.59	136.58	135.55	134.51	133.47	132.43	131.37		
210.00	138.18	137.16	136.14	135.10	134.06	133.02			
215.00	138.74	137.73	136.71	135.68	134.64				
220.00	139.30	138.29	137.27	136.23	135.20				
225.00	139.84	138.83	137.81	136.78					
230.00	140.36	139.35	138.33	137.31					
235.00	140.87	139.87	138.85						
240.00	141.37	140.37							
245.00	141.85	140.86							
250.00	142.33								
255.00	142.79								

324-194 O-69—3

TABLE 4–b. *Entropies*

D, mol/l =	27.00	28.00	29.00	30.00	31.00	32.00	33.00	34.00
TSAT, K =	134.67	130.84	126.65	122.11	117.22	112.00	106.45	100.60
SS, J/mol K =	50.38	48.45	46.37	44.13	41.70	39.06	36.18	33.04
Temp., K	Entropy, J/(mol deg)							
102.00								100.43
104.00								100.99
106.00								101.53
108.00							103.59	102.07
110.00							104.10	102.59
112.00						106.06	104.61	103.10
114.00						106.55	105.10	103.60
116.00						107.03	105.59	104.10
118.00					108.88	107.50	106.06	104.58
120.00					109.33	107.96	106.53	105.06
122.00					109.78	108.41	106.99	105.52
124.00				111.54	110.22	108.86	107.44	105.98
126.00				111.97	110.65	109.29	107.89	106.43
128.00			113.65	112.39	111.08	109.72	108.32	
130.00			114.07	112.80	111.50	110.15	108.75	
132.00		115.68	114.47	113.21	111.91	110.56	109.17	
134.00		116.08	114.87	113.61	112.31	110.97	109.59	
136.00	117.64	116.47	115.26	114.00	112.71	111.37		
138.00	118.02	116.85	115.64	114.39	113.10	111.77		
140.00	118.40	117.23	116.02	114.77	113.49	112.16		
142.00	118.77	117.60	116.39	115.15	113.87	112.55		
144.00	119.13	117.96	116.76	115.52	114.24			
146.00	119.49	118.32	117.12	115.88	114.61			
148.00	119.84	118.68	117.48	116.24	114.97			
150.00	120.19	119.03	117.83	116.60	115.33			
152.00	120.53	119.37	118.17	116.95				
154.00	120.87	119.71	118.52	117.29				
156.00	121.20	120.04	118.85	117.63				
158.00	121.53	120.37	119.18	117.96				
160.00	121.85	120.70	119.51					
162.00	122.17	121.02	119.83					
164.00	122.48	121.33	120.15					
166.00	122.79	121.64	120.46					
168.00	123.10	121.95						
170.00	123.40	122.25						
172.00	123.70	122.55						
174.00	123.99	122.85						
176.00	124.28							

TABLE 4-c. *Entropies*

D, mol/l =	35.00	36.00	37.00	38.00	39.00	40.00
TSAT, K =	94.46	88.05	81.41	74.56	67.55	60.41
SS, J/mol K =	29.58	25.77	21.55	16.85	11.58	5.64
Temp., K	Entropy, J/(mol deg)					
62.00	.....	.....	.....	.....	.....	73.53
64.00	.....	.....	.....	.....	.....	74.62
66.00	.....	.....	.....	.....	.....	75.67
68.00	.....	.....	.....	.....	78.80	76.68
70.00	.....	.....	.....	.....	79.76	77.67
72.00	.....	.....	.....	.....	80.69	78.62
74.00	.....	.....	.....	.....	81.59	
76.00	.....	.....	.....	84.46	82.46	
78.00	.....	.....	.....	85.29	83.31	
80.00	.....	.....	.....	86.10	84.14	
82.00	.....	.....	88.78	86.88	84.94	
84.00	.....	.....	89.52	87.64		
86.00	.....	.....	90.25	88.39		
88.00	.....	.....	90.96	89.11		
90.00	.....	93.43	91.65	89.82		
92.00	.....	94.09	92.32			
94.00	.....	94.74	92.98			
96.00	97.06	95.37	93.62			
98.00	97.66	95.98	94.25			
100.00	98.25	96.58	94.87			
102.00	98.83	97.17				
104.00	99.39	97.75				
106.00	99.95	98.32				
108.00	100.49	98.87				
110.00	101.02					
112.00	101.55					
114.00	102.06					

TABLE 5. *Comparisons of thermal properties [6]*

PVT state			$100 \cdot [G_s - G]/G$ [a]		
ρ, Mol/l	T, K	P, atm	E	H	S
18	180	131	+0.98	+0.58	+0.03
18	230	294	+0.47	+0.30	+0.04
26	145	76	+0.47	+0.87	+0.03
26	175	300	+2.33	+1.78	+0.05
34	104	66	+0.20	+0.26	+0.02
34	118	310	+0.18	+0.47	+0.01

[a] G represents E, H, or S. Values for G_s are from [6].

TABLE 6. *Comparisons of thermal properties [1]*

PVT state			$100 \cdot [G_w - G]/G$ [a]		
ρ, mol/l	T, K	P, atm	E	H	S
18	180	131	+0.81	+0.44	+0.03
18	230	294	+0.37	+0.21	+0.04
26	140	39	+0.35	+0.40	+0.03
26	175	300	+2.00	+1.41	+0.05
34	104	66	−0.09	−0.05	−0.03
34	118	310	−0.05	−0.09	−0.02

[a] G represents E, H or S. Values for G_w are from [1].

Table 6 gives analogous comparisons with properties interpolated from L. A. Weber's tabulations on isobars [1]. Weber also used Woolley's ideal gas functions. The recent *PVT* data were combined with some of the present specific heat data. His methods for describing portions of the *PVT* surface were quite different from the equation of state used by Stewart.

A discussion of the significance of deviations in tables 5 and 6 is not in the scope of this report. It requires a detailed analysis of uncertainties (in two independent variables) traced from experimental data through the computational steps. It is a common experience to find disagreements of roughly 5 percent between experimental specific heats and those derived from good *PVT* data via the second derivative, $(\partial^2 P/\partial T^2)_\rho$ [4]. For the values in tables 2, 3, and 4 we estimate a rough uncertainty of 1 percent, except for the small values near an inversion of sign, as follows. Our uncertainties for C_σ and C_v range from 0.5 to over 1.0 percent [2, 3]. Relative errors in the integrals, i.e., the thermal functions, generally should be less than in these integrands.

5. References

[1] Weber, L. A., Thermodynamic and related properties of oxygen from the triple point to 300 K at pressures to 330 atmospheres, Internal report, June 20, 1968.

[2] Goodwin, R. D., and Weber, L. A., Specific heats of oxygen at coexistence, J. Res. NBS **73A** (Phys. and Chem.) No. 1, (1969).

[3] Goodwin, R. D., and Weber, L. A., Specific heats C_v of fluid oxygen from the triple point to 300 K at pressures to 350 atm. J. Res. NBS **73A** (Phys. and Chem.) No. 1, (1969).

[4] Din, F., Thermodynamic Functions of Gases, Vol. **1** (Butterworths Scientific Publications, London, 1956).

[5] Woolley, H. W., Thermodynamic functions for molecular oxygen in the ideal gas state, J. Res. NBS **40,** 163–168 (1948), also ASTIA document AD 19900, June 30, 1953.

[6] Stewart, R. B., The thermodynamic properties of oxygen, Dissertation, Dept. Mech. Engr'g., Univ. of Iowa, June 1966.

(Paper 73A1–531)

JOURNAL OF RESEARCH of the National Bureau of Standards—A. Physics and Chemistry
Vol. 73A, No. 1, January–February 1969

Two New Standards for the pH Scale [1]

Bert R. Staples and Roger G. Bates

Institute for Materials Research, National Bureau of Standards, Washington, D.C. 20234

(July 9, 1968)

Two new primary standards for the NBS pH scale, supplementing the five already available, are proposed. The new reference solutions are the 0.05 molal solution of potassium dihydrogen citrate and a mixture of sodium bicarbonate and sodium carbonate, each 0.025 molal. The citrate solution has a pH of 3.776 at 25 °C and is more stable under certain conditions than either the tartrate or phthalate standards. The carbonate solution has a pH of 10.012 at 25 °C. It therefore extends the NBS pH scale above its present upper limit of 9.180 at this temperature. Reference values pH(S), based on emf measurements of cells with hydrogen electrodes and silver-silver chloride electrodes, have been assigned to these two standard solutions at 11 temperatures from 0 to 50 °C.

Key Words: Acidity; carbonate; citrate; emf; hydrogen electrode; pH; standards for pH.

1. Introduction

At present, the NBS standard pH scale is fixed in the range 3.5 to 9.5 by means of five primary standard solutions. The five reference solutions which define this conventional activity scale are listed in table 1 with the corresponding standard pH, designated pH(S), at 25 °C [1].[2]

The least suitable of the five primary standards is the solution of potassium hydrogen tartrate. Its chief disadvantage is its tendency to support the growth of molds [2]. Molds usually appear in the tartrate solution after a few days, and the pH may increase by as much as 0.1 unit. Likewise neither the phthalate solution nor the borax solution is an ideal pH standard. Although the former probably is used most extensively of all the primary pH standards, it has the disadvantage of being unstable in contact with the platinum-hydrogen electrode [3]. Since phthalate absorbs strongly in the ultraviolet region of the spectrum, this solution also finds limited application in many spectrophotometric methods for the determination of dissociation constants and in other studies of acid-base behavior.

Borax (sodium tetraborate decahydrate) has been found to lose some of its water of crystallization during storage. More important, the ionic strength of the solution is not as well known as might be desired, as a consequence of the tendency of boric acid to polymerize in solution. It is accordingly difficult to calculate pH(S) with certainty, as the calculation requires a knowledge of the ionic strength. Furthermore, an alkaline standard with a pH higher than that of the borax standard (9.18 at 25 °C) would be most useful. In view of the increasing uncertainties of the glass electrode response as the pH rises above 10, it would be most desirable to have an additional standard with pH(S) of 10 or greater.

TABLE 1. *Primary standards of the NBS pH scale*

Material	Molality	pH(S) at 25 °C
$KHC_4H_4O_6$ (tartrate)	satd. at 25 °C	3.557
$KHC_8H_4O_4$ (phthalate)	0.05	4.008
KH_2PO_4	0.025	6.865
Na_2HPO_4	0.025	
KH_2PO_4	0.008695	7.413
Na_2HPO_4	0.03043	
$Na_2B_4O_7 \cdot 10H_2O$ (borax)	0.01	9.180

The precise, electromotive force measurements leading to the assignment of pH(S) values to a solution 0.05 molal in potassium dihydrogen citrate and to another solution 0.025 molal in both sodium bicarbonate and sodium carbonate from 0 to 50 °C are described in this paper. These two reference solutions supplement the present primary standards, extending the standard scale to pH 10 at 25 °C and facilitating the standardization of hydrogen electrode pH cells at the lower end of the standard scale. In addition, the citrate solution can often be used advantageously in spectrophotometric studies where the phthalate solution is excluded.

[1] Presented before the Division of Analytical Chemistry of the American Chemical Society at its national meeting in San Francisco, California, on April 3, 1968.
[2] Figures in brackets indicate the literature references at the end of this paper.

2. Experimental Procedures

2.1. Potassium Dihydrogen Citrate

The potassium dihydrogen citrate was prepared and purified by M. Paabo according to the procedure given by Kolthoff [4]. Anhydrous granular citric acid, 1 mole of which was dissolved in 80 cm^3 of hot water, was neutralized with anhydrous reagent-grade potassium carbonate which had been dried previously at 205 °C. The recrystallized product was analyzed coulometrically and was found to assay 99.999 percent, with an uncertainty of 0.005 percent.

2.2. Carbonate Salts

The sodium carbonate ("primary standard" grade) was dried at 250 °C for 90 min and stored over calcium chloride and Drierite. Reagent-grade sodium bicarbonate was dried over a mixture of molecular sieves and Drierite for about two days at room temperature. Coulometric assay of these salts gave the following results: $NaHCO_3$, 99.95 percent; Na_2CO_3, 99.97 percent.

2.3. Methods and Results

With a few minor exceptions, the experimental techniques for the conduct of the precise emf measurements, including the design of the cells and the preparation of the electrodes, were the same as those described earlier [5, 6]. The solutions were prepared by weight from the buffer salts, a sample of fused potassium chloride low in bromide [7], and distilled water with a conductance less than $0.8 \times 10^{-6} \Omega^{-1}$ cm^{-1}. It was essential that the water used in preparing the carbonate solution be purged with carbon dioxide-free nitrogen before the salts were dissolved in it. A slow increase in emf with time, observed in the cells containing the carbonate buffer, was minimized by discontinuing the hydrogen flow overnight during the course of the experiments. This drift was probably due to the removal of carbon dioxide from the buffer solution by the constant passage of hydrogen gas over long periods of time.

The emf of the following cells without liquid junction was measured at 11 temperatures from 0 to 50 °C:

Pt;H_2(g, 1 atm), KH_2 citrate (0.05m), KCl (m_{Cl}), AgCl;Ag

and

Pt;H_2(g, 1 atm), $NaHCO_3$ (0.025m), Na_2CO_3 (0.025m), KCl (m_{Cl}), AgCl;Ag

where m_{Cl} was 0.005, 0.01, or 0.015 mol kg^{-1}. The measured values of the emf, corrected to a partial pressure of hydrogen of 1 atm, are summarized in table 2. Each entry in the table is the average emf of four to seven individual cells. In general, values for the individual cells varied from the average by several hundredths of a millivolt in the citrate series to a maximum of over 0.1 mV for some of the cells containing the carbonate buffer.

Values of the acidity function $p(a_H\gamma_{Cl})$ were calculated from the measured emf (E) of each cell at each of the three chloride concentrations by the equation

$$p(a_H\gamma_{Cl}) \equiv -\log\,(\gamma_H\gamma_{Cl}m_H) = \frac{(E-E^\circ)F}{RT\ln 10} + \log m_{Cl} \quad (1)$$

The standard emf E° of the cell is known over the temperature range of the measurements [8]. Limiting values of $p(a_H\gamma_{Cl})$, designated $p(a_H\gamma_{Cl})^\circ$, in the absence of chloride were obtained by extrapolating the average $p(a_H\gamma_{Cl})$ for each buffer-chloride mixture as a function of m_{Cl} to $m_{Cl}=0$. These limiting acidity functions are listed in tables 3 and 4. The extrapolation at 25 °C is shown in figure 1.

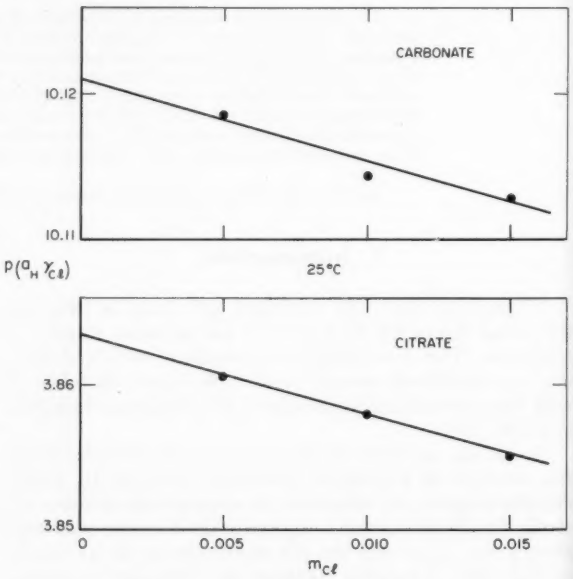

FIGURE 1. *The acidity function* $p(a_H\gamma_{Cl})$ *at 25 °C plotted as a function of the molality of chloride.*

An iterative procedure was used to calculate the ionic strengths. For this purpose, the three dissociation constants of citric acid [9], the second constant for carbonic acid [10], and the ionization constant of water [11] were used. The activity coefficient γ_i of each univalent ion i was taken equal to that for chloride as given by the convention [12]

$$-\log \gamma_{Cl^-} = \frac{A\sqrt{I}}{1+1.5\sqrt{I}} \quad (2)$$

in which A is the Debye-Hückel slope [6] and I is the ionic strength. Activity coefficients of bivalent and trivalent ions were approximated by $(\gamma_{Cl^-})^4$ and $(\gamma_{Cl^-})^9$, respectively, in accord with the valence factor in the Debye-Hückel equation. The activity coefficients and

TABLE 2. *Emf (E) of the cell* $Pt;H_2$ *(g, 1 atm), buffer-*KCl *soln.,* AgCl;Ag *from 0 to 50 °C, in volts*

KCl molality	E_0	E_5	E_{10}	E_{15}	E_{20}	E_{25}	E_{30}	E_{35}	E_{40}	E_{45}	E_{50}
Buffer: Potassium dihydrogen citrate (0.05 molal)											
0.015	0.54889	0.55086	0.55274	0.55463	0.55648	0.55828	0.56011	0.56190	0.56366	0.56539	0.56710
.01	.55851	.56062	.56272	.56477	.56688	.56878	.57087	.57277	.57478	.57666	.57849
.005	.57509	.57751	.57990	.58224	.58458	.58686	.58915	.59142	.59366	.59587	.59807
Buffer: $NaHCO_3$ (0.025 molal), Na_2CO_3 (0.025 molal)											
0.015	0.89957	0.90514	0.91094	0.91679	0.92261	0.92844	0.93435	0.94026	0.94621	0.95210	0.95803
.01	.90921	.91513	.92109	.92709	.93310	.93903	.94512	.95123	.95738	.96334	.96951
.005	.92558	.93199	.93822	.94451	.95085	.95707	.96349	.96991	.97633	.98289	.98908

TABLE 3. *Assignment of pH(S) values to the 0.05 molal solution of potassium dihydrogen citrate from 0 to 50 °C*

t	$p(a_H\gamma_{Cl})^\circ$	I	$-\log \gamma_{Cl^-}$	pa_H	pH(S) (calc.)
°C					
0	3.948_1	0.0527	0.0840	3.864	3.863
5	3.923_8	.0526	.0845	3.839	3.840
10	3.904_2	.0526	.0851	3.819	3.820
15	3.887_4	.0526	.0858	3.802	3.802
20	3.874_3	.0526	.0865	3.788	3.788
25	3.863_5	.0526	.0872	3.776	3.776
30	3.854_8	.0526	.0879	3.767	3.766
35	3.847_2	.0525	.0886	3.759	3.759
40	3.843_1	.0525	.0894	3.754	3.753
45	3.840_4	.0524	.0902	3.750	3.750
50	3.839_9	.0524	.0910	3.749	3.749

TABLE 4. *Assignment of pH(S) values to the solution 0.025 molal with respect to both sodium bicarbonate and sodium carbonate from 0 to 50 °C*

t	$p(a_H\gamma_{Cl})^\circ$	I	$-\log \gamma_{Cl^-}$	pa_H	pH(S) (calc.)
°C					
0	10.426_1	0.1	0.1055	10.321	10.317
5	10.348_8	.1	.1062	10.243	10.245
10	10.285_1	.0999	.1070	10.178	10.179
15	10.223_7	.0999	.1078	10.116	10.118
20	10.168_4	.0999	.1086	10.060	10.062
25	10.121_0	.0999	.1095	10.012	10.012
30	10.078_8	.0998	.1104	9.968	9.966
35	10.039_2	.0998	.1114	9.928	9.925
40	10.004_6	.0997	.1123	9.892	9.889
45	9.969_0	.0996	.1133	9.856	9.856
50	9.939_6	.0995	.1144	9.825	9.828

the ionic strength were calculated by successive approximations until neither varied by more than 1×10^{-6} from one approximation to the next. The calculations were simplified by the use of a time-shared computer with Dartmouth BASIC language.

A method for the resolution of overlapping dissociation constants has been described [9, 13] which simplifies the estimation of the ionic strength. The values of I for the citrate solution obtained by this method agreed to about 0.001 with those resulting from the iterative procedure.

The conventional pa_H values for the citrate buffer are given in table 3 along with related data from which they were derived. A similar summary for the carbonate buffer is given in table 4. In both instances, the pa_H was calculated from $p(a_H\gamma_{Cl})^\circ$ by the equation

$$pa_H = p(a_H\gamma_{Cl})^0 + \log \gamma_{Cl^-} \qquad (3)$$

where γ_{Cl^-} was defined by eq (2). In the NBS procedure for establishing pH standards, the conventional pa_H is taken equal to the standard value pH(S) of the operational definition of pH.

3. Discussion

The pH(S) values for the two new standards are plotted as a function of temperature in figure 2. The method of least squares and OMNITAB were utilized to fit pH(S) to an equation of the form

$$\text{pH(S)} = \frac{A}{T} + B + CT \qquad (4)$$

where T is the temperature in kelvins. The constants of this equation are listed in table 5, and the calculated pH(S) is included in tables 3 and 4. The standard deviation of the "experimental" pH(S) from the smoothed curve represented by eq (4) is 0.0007 unit for the citrate buffer and 0.0026 unit for the carbonate buffer.

The citrate is highly recommended as an additional primary pH standard by the long-term stability of both the solid potassium dihydrogen citrate and its aqueous solution and by the stability of citrate solutions in contact with the hydrogen electrode. In addition, this reference solution is convenient to prepare, as only one salt need be weighed. The pH(S) value assigned to the 0.05*m* solution of this salt at 25 °C is 3.776.

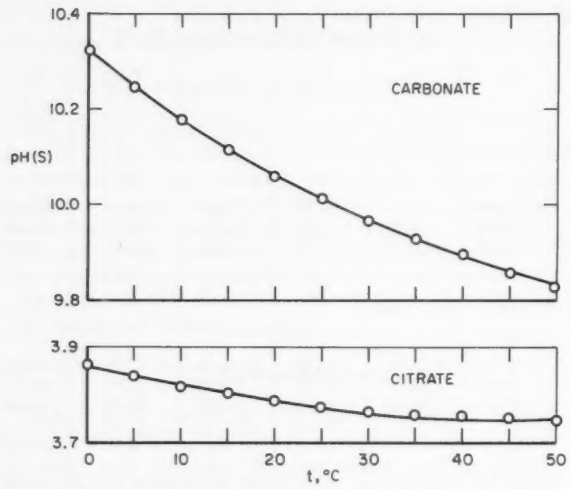

FIGURE 2. pH(S) *for the citrate and carbonate standards plotted as a function of temperature.*

TABLE 5. *Constants of eq (4)*

	Citrate standard	Carbonate standard
A	1280.4	2557.1
B	−4.1650	−4.2846
C	0.012230	0.019185

The carbonate buffer, 0.025 molal in sodium bicarbonate and sodium carbonate, is a useful primary standard for the high pH region. This solution is reasonably stable if protected from atmospheric carbon dioxide. Its assigned pH(S) is 10.012 at 25 °C.

The uncertainty of the assigned values of pH(S) can be estimated by combining the standard errors of the intercepts $p(a_H\gamma_{Cl})^\circ$ given in tables 3 and 4 with the estimated uncertainty in the standard emf and natural constants used in the calculation of $p(a_H\gamma_{Cl})$ and with the standard deviation of the experimental pH(S) from eq (4). The standard emf is known to better than 0.1 mV (0.0017 in pH) and, for all practical purposes, the values of R, T, and F contribute a negligible amount to the uncertainty of pH(S). Furthermore, the convention set forth in eq (2) is considered to be exact. The standard deviations of $p(a_H\gamma_{Cl})$ ranged from 0.0001 to 0.0015, while the standard deviation of the values of pH(S) from eq (4) was 0.0007 for the citrate buffer and 0.0026 for the carbonate buffer. Although the manner in which these individual errors are combined is to some extent a subjective matter, the total uncertainty in pH(S) is estimated to lie between 0.002 and 0.005 unit, being least for the citrate buffer near 25 °C and greatest for the carbonate buffer at 0 and 50 °C.

The group of primary pH standards that define the NBS scale should exhibit a satisfactory consistency when intercompared in any pH meter with liquid junction. If the standard scale of pH were not internally consistent, the experimental values of an "unknown" solution would depend upon the particular reference solution chosen to standardize the measuring instrument. Evidently no exact consistency can be expected when a liquid-junction potential is involved, because the standards have different ionic strengths and contain different ionic species whose mobilities are not the same.

To reveal the extent of the consistency, the new citrate and carbonate standards were intercompared with the equimolal phosphate standard [pH(S) = 6.865 at 25 °C] in a cell where two hydrogen electrodes were separated by a bridge of saturated potassium chloride solution [14]. The results displayed in figure 3 show that the pH indicated by this cell with liquid junction is higher than the assigned pH(S) for the citrate standard and lower for the carbonate standard. In each instance, the difference may amount to 0.01 pH unit in the temperature range 10 to 45 °C.

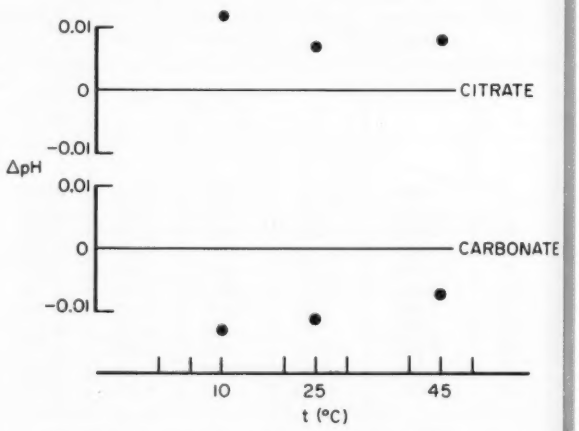

FIGURE 3. *Internal consistency of the standard* pH *scale.* Comparison of the new pH standards with the equimolal phosphate standard [pH(S) = 6.865 at 25 °C].

The citrate reference solution is most conveniently prepared by dissolving 11.41 g of pure potassium dihydrogen citrate in water and diluting to 1 liter at 25 °C. The carbonate reference solution can be made by dissolving 2.092 g of sodium bicarbonate and 2.640 g of sodium carbonate in carbon-dioxide-free water and diluting to 1 liter at 25 °C. The weights given above are weights in air. The compositions, densities, dilution values [15], buffer values [16], and pH-temperature coefficients for the two new pH standard solutions are summarized in table 6.

TABLE 6. *Properties of two standard reference solutions at 25 °C*

	Citrate standard	Carbonate standard
Molality	0.05	0.025 (each salt)
Molarity	0.04958	0.02492 (each salt)
Density, g ml^{-1}	1.00294	1.00135
Dilution value	+0.024	+0.079
Buffer value	0.034	0.029
dpH/dt	−0.0022	−0.0096

The authors are indebted to George Marinenko for performing the coulometric analyses of the buffer salts.

4. References

[1] Bates, R. G., J. Res. NBS **66A** (Phys. and Chem.) No. 2, 179 (1962).
[2] Bates, R. G., Anal. Chem. **23,** 813 (1951).
[3] Hamer, W. J., and Acree, S. F., J. Res. NBS **33,** 87 (1944) RP 1598.
[4] Kolthoff, I. M., Acid-Base Indicators, p. 253 (The Macmillan Co., New York, 1937).
[5] Gary, R., Bates, R. G., and Robinson, R. A., J. Phys. Chem. **68,** 1186 (1964).
[6] Bates, R. G., Determination of pH, ch. 9 and appendix (John Wiley & Sons, New York, N.Y., 1964).
[7] Pinching, G. D., and Bates, R. G., J. Res. NBS **37,** 311 (1946) RP 1749.
[8] Bates, R. G., and Bower, V. E., J. Res. NBS **53,** 283 (1954) RP 2546.
[9] Bates, R. G., and Pinching, G. D., J. Am. Chem. Soc. **71,** 1274 (1949).
[10] Harned, H. S., and Scholes, S. R., J. Am. Chem. Soc. **63,** 1706 (1941).
[11] Harned, H. S., and Owen, B. B., The Physical Chemistry of Electrolytic Solutions, 3d ed., ch. 15 (Reinhold Publishing Corp., New York, 1958).
[12] Bates, R. G., and Guggenheim, E. A., Pure Appl. Chem. **1,** 163 (1960).
[13] Bates, R. G., J. Am. Chem. Soc. **70,** 1579 (1948).
[14] Bates, R. G., Pinching, G. D., and Smith, E. R., J. Res. NBS **45,** 418 (1950) RP 2153.
[15] Bates, R. G., Anal. Chem. **26,** 871 (1951).
[16] Van Slyke, D. D., J. Biol. Chem. **52,** 525 (1922).

(Paper 73A1–532)

JOURNAL OF RESEARCH of the National Bureau of Standards—A. Physics and Chemistry
Vol. 73A, No. 1, January–February 1969

Calculation of Diffusion Coefficients in Ternary Systems from Diaphragm Cell Experiments*

P. R. Patel,** E. C. Moreno,** and T. M. Gregory**

Institute for Materials Research, National Bureau of Standards, Washington, D.C. 20234

(September 17, 1968)

Using a generalized least square procedure, a method is developed to estimate diffusion coefficients, D_{ij}, from concentration measurements made in a set of experiments of varying duration but with the same initial conditions. The method requires neither approximations nor restrictions in the flow equations. The D_{ij} and their errors are calculated simultaneously with the adjustment of the weighted observables—concentrations of the two solute components and time. A procedure is described to insure convergence in a given experimental set. The effect of the duration of the longest experiment, and errors in the observables on the estimated values of D_{ij} and their errors, are investigated. Application of the method to available data yielded values for D_{ij} in agreement with those previously calculated by more involved procedures.

Key Words: Diaphragm cell; diffusion coefficients; least squares calculation; ternary system.

1. Introduction

The methods reported for the calculation of diffusion coefficients in ternary systems from diaphragm cell data require either restrictions in the experimental conditions [1, 2][1] or approximations in the flux equations [3]. A new method is reported here that obviates the limitations of previous procedures when concentrations of the diffusing solutes are directly measured in the cell compartments. Although the present method was derived independently of a procedure recently reported by Cussler and Dunlop [4], the two approaches to the problem are similar. The present derivations, however, allow a more complete and direct treatment of the subject, particularly for the calculation of errors.

2. Theory

The general equations that define diffusion flows, $(J_i)_V$, in ternary systems relative to a volume-fixed frame of reference are [5, 6].

$$(J_i)_V = -\sum_{j=1}^{2} (D_{ij})_V \frac{\partial C_j}{\partial x} \qquad (i=1, 2) \tag{1}$$

in which $(D_{ij})_V$ are practical diffusion coefficients and C_j is the concentration of component j. Integration of eq (1), considering the conditions for the diaphragm cell, assuming linear concentration gradients and no changes in volume during the diffusion process, gives the general solution [7]

$$\Delta C_i = A_i e^{-\beta m_1 t} + B_i e^{-\beta m_2 t} \qquad (i=1, 2) \tag{2}$$

in which ΔC_i is the concentration difference (molar scale is used throughout these derivations) of component i between the two compartments at any time t, β is the cell constant and the other quantities are defined by

$$A_i = \frac{\Delta C_i^\circ (D_{ii} - m_2) + D_{ij}\Delta C_j^\circ}{m_1 - m_2} \qquad \left.\begin{array}{l} i=1, 2 \\ j=1, 2 \end{array}\right\} \tag{3}$$

$$B_i = \frac{\Delta C_i^\circ (D_{ii} - m_1) + D_{ij}\Delta C_j^\circ}{m_2 - m_1} \qquad \left.\begin{array}{l} \\ i \neq j \end{array}\right\} \tag{4}$$

$$m_1 = \tfrac{1}{2}[D_{11} + D_{22} + \sqrt{(D_{11}+D_{22})^2 - 4(D_{11}D_{22} - D_{12}D_{21})}]$$

$$m_2 = \tfrac{1}{2}[D_{11} + D_{22} - \sqrt{(D_{11}+D_{22})^2 - 4(D_{11}D_{22} - D_{12}D_{21})}] \tag{5}$$

*This investigation was supported in part by Research Grants DE-01819 and DE-02659 to the American Dental Association from the National Institute of Dental Research, and is part of the dental research program conducted by the National Bureau of Standards in cooperation with the Council on Dental Research of the American Dental Association; the National Institute of Dental Research; the Army Dental Corps; the Dental Sciences Division, School of Aerospace Medicine, USAF; and the Veterans Administration.

**Research Associates from the American Dental Association in the Dental Research Section, National Bureau of Standards, Washington, D.C. 20234.

[1] Figures in brackets indicate the literature references at the end of this paper.

In eqs (3) and (4), ΔC° denotes concentration differences at $t=0$, and D_{ij} are the integral cell diffusion coefficients.[2]

The calculation of D_{ij} is accomplished by a generalized least squares procedure [8] using eq (2) as the mathematical model. Thus, the condition equations are of the form

$$F=(X_1-X_2)-A_1e^{-\beta m_1 T}-B_1e^{-\beta m_2 T} \tag{6}$$

$$L=(Y_1-Y_2)-A_2e^{-\beta m_1 T}-B_2e^{-\beta m_2 T} \tag{7}$$

in which X and Y represent the concentrations of components 1 and 2, respectively, in the compartments indicated by their subscripts at the observation time T.[3]

If observations (determinations of X and Y) are made at the end of N diffusion experiments (with the same initial conditions) of duration T_1, T_2, . . ., T_N, then there will be $2N$ condition equations. The observations corresponding to different values of T are statistically independent, since for each duration, a new experiment is conducted. The number of condition equations may not be a multiple of 2, however, if either X or Y is not determined at the end of some of the experiments.

When observations are made in only one of the compartments, for example compartment 2, the condition equations take the form

$$F'=(\Delta X^\circ+2X_2^\circ-2X_2)-A_1e^{-\beta m_1 T}-B_1e^{-\beta m_2 T} \tag{8}$$

$$L'=(\Delta Y^\circ+2Y_2^\circ-2Y_2)-A_2e^{-\beta m_1 T}-B_2e^{-\beta m_2 T} \tag{9}$$

in which ΔX° and ΔY° are concentration differences for the two components at time $T=0$.

The aim of the procedure is to compute the adjustments of the observables and the corrections for the initial estimates of the diffusion coefficients in such a way that

$$F^{(n)}(x_1^{(n)}, x_2^{(n)}, t^{(n)}, \Delta x^\circ, \Delta y^\circ, D_{11}, D_{12}, D_{21}, D_{22}) \approx 0 \qquad (n=1, 2, \ldots, N) \tag{10}$$

and

$$L^{(n)}(y_1^{(n)}, y_2^{(n)}, t^{(n)}, \Delta x^\circ, \Delta y^\circ, D_{11}, D_{12}, D_{21}, D_{22}) \approx 0 \tag{11}$$

in which x, y, t, Δx°, and Δy° are adjusted observables, and D_{ij} are the final estimates of coefficients. This adjustment is done subject to the least squares criterion that the weighted sum of squares of the residuals (observed value − adjusted value) of the observables X, Y, T, ΔX°, and ΔY° be a minimum. In these derivations, the cell constant, β, is considered as an "external parameter," that is, a quantity obtained from independent experiments, and therefore, not susceptible of adjustment. However, the error in β is taken into account in the estimation of the error bounds for D_{ij}, as explained below.

Linearization of the condition equations (6) and (7) is done about the observed points (X_1, X_2, T, ΔX°, ΔY°, D_{11}°, D_{12}°, D_{21}°, D_{22}°) and (Y_1, Y_2, T, ΔX°, ΔY°, D_{11}°, D_{12}°, D_{21}°, D_{22}°) using the best available initial estimates, D_{ij}°, for the diffusion coefficients. A procedure to obtain good initial estimates for D_{ij} is described later.

The $2N$ reduced condition equations, resulting from the linearization mentioned above, may be written, in matrix notation,

$$BV+P\alpha=M \tag{12}$$

in which B is the matrix ($2N\times[5N+2]$) of the derivatives of the condition functions [6] and [7] with respect to the observables, V is the column vector ($[5N+2]\times 1$) of the residuals, P is the matrix ($2N\times 4$) of the derivatives of the condition functions with respect to D_{ij}, α is the column vector (4×1) of the corrections for the D_{ij}° (i.e., $\alpha_{ij}=D_{ij}^\circ-D_{ij}$) and M is the column vector ($2N\times 1$) of the values of the condition functions. The condition functions and their derivatives are evaluated using the experimental values of the observables and the initial estimates for the diffusion coefficients.

The sum of squares of the residuals, S^2, is given by

$$S^2=\tilde{V}WV \tag{13}$$

in which W is the diagonal matrix of the weights, W_{obs}, for the $5N+2$ observables and the tilde represents transposition. These weights are calculated from

$$W_{obs}=\frac{\sigma_{int}^2}{\sigma_{obs}^2} \tag{14}$$

in which σ_{obs} is the standard deviation for the observable in question and σ_{int} is an arbitrary constant conveniently selected for calculation purposes.

Minimization of S^2 (eq (13)) subject to the conditions (12), effected by the use of a Lagrange multiplier, Λ, and the subsequent elimination of V, results in $2N+4$ normal equations with $2N$ unknown λ's (the elements of column vector (Λ), and four unknown α_{ij}. As shown by Guest [9] this leads to the following equations:

$$\begin{bmatrix} R & P \\ \tilde{P} & 0 \end{bmatrix}\times\begin{bmatrix} \Lambda \\ \alpha \end{bmatrix}=\begin{bmatrix} M \\ 0 \end{bmatrix}$$

or (15)

$$G\times\begin{bmatrix} \Lambda \\ \alpha \end{bmatrix}=\begin{bmatrix} M \\ 0 \end{bmatrix}$$

in which $R=BW^{-1}\tilde{B}$, of dimension $2N\times 2N$.

[2] Usually, diffusion experiments in a diaphragm cell will yield values for integral diffusion coefficients. However, if ΔC_i° is selected sufficiently small, the calculated D_{ij} will approach the values for differential diffusion coefficients. The present treatment will apply equally well for such conditions. The functional relationships between the integral D_{ij} and concentration of the components in ternary systems are not known. Attempts have been made to solve this problem for some particular systems [P. F. Mijnlieff and H. A. Vreedenberg, J. Phys. Chem. **70**, 2158 (1966)] but a general analytical solution involves formidable mathematical difficulties.

[3] After the preparation of the present manuscript, J. Mandel, National Bureau of Standards suggested the use of the concentration differences in eqs (6) and (7) as observables, instead of working with individual concentration terms. The present procedure would apply equally well for this case.

The solution of the above system of equations yields

$$\begin{bmatrix} \Lambda \\ \alpha \end{bmatrix} = G^{-1} \begin{bmatrix} M \\ 0 \end{bmatrix}. \tag{16}$$

Since G^{-1} is symmetric, like G, it can be partitioned similarly as follows:

$$G^{-1} = \begin{bmatrix} Q & H \\ \tilde{H} & C \end{bmatrix}. \tag{17}$$

Then, the solutions for Λ and α can be written as,

$$\Lambda = QM$$

$$\alpha = \tilde{H}M$$

The values thus obtained for α_{ij} can be now used to calculate new estimates for D_{ij}, since

$$D_{ij} = D^{\circ}_{ij} - \alpha_{ij}. \tag{18}$$

These new estimates of D_{ij} are used iteratively as initial estimates (substituting for D°_{ij}) until convergence in S^2, calculated by eq (13), is obtained. At this point the final residuals are calculated from $V = \bar{W}^{-1}\tilde{B}\Lambda$. The error vector Δ, (ΔD_{11}, ΔD_{12}, ΔD_{21}, ΔD_{22}), can be found from the 4×4 error submatrix, $E = -C$, of G^{-1}:

$$\Delta = \sigma_{\text{ext}} \sqrt{E_{ij}} \tag{19}$$

in which the standard error, σ_{ext}, is given by $\sqrt{\{S^2/(2N-4)\}}$, $2N-4$ being the degrees of freedom.

A discrepancy between the ratio $\sigma^2_{\text{ext}}/\sigma^2_{\text{int}}$ and unity is an indication of disagreement between the variances assumed in the calculations (based on previous experience) and the error variances actually existing in the experiment [10].

The errors as obtained from eq (19) do not reflect the influence of the error, σ_β, in the independently determined cell constant β. Therefore, calculations are repeated using successively the values $\beta + \sigma_\beta$ and $\beta - \sigma_\beta$ for the cell constant. A t-test is then performed between the D_{ij} obtained in this fashion and those obtained when β was considered free of error. If the t-test indicates no significant difference, at a selected level of significance, the errors obtained for the D_{ij} with the assumption that $\sigma_\beta = 0$ may be adopted. Otherwise, a confidence band for the D_{ij} should be estimated.

A requirement for the convergence of the iterative procedure in the calculation of D_{ij} is that the initial estimates of these parameters be close to the final estimates. Various procedures have been suggested [11, 12, 13] to insure convergence in problems of this nature. In this investigation it was found that, for ternary systems, good initial estimates for only two of the four coefficients are required to insure convergence, their identity being determined by the initial experimental conditions. Three cases of initial conditions are possible in a ternary system: (1) Both diffusing components have nonzero concentration gradients; (2) Component 1 has a nonzero gradient and component 2 has a zero gradient; (3) Component 2 has a nonzero gradient and component 1 has a zero gradient. The two diffusion coefficients for which good initial estimates are required in each one of the three cases are: for case (1) D_{11} and D_{22}; for case (2) D_{11} and D_{21}; and for case (3) D_{22} and D_{12}. The initial estimates for the remaining 2 coefficients in each case can be taken as zero. In the flux equations (1) the main contribution to the flux of one component is given by those terms involving the component for which there is an initial concentration gradient. Then, ignoring, as a first approximation, those terms that contribute the least to the diffusion fluxes, performing the corresponding integrations, the resulting expressions may be written in the logarithmic form,

$$\ln \frac{\Delta C_i}{\Delta C^{\circ}_j} = -D_{ij}\beta t \qquad \begin{matrix} i = 1, 2 \\ j = 1, 2 \end{matrix} \tag{20}$$

which covers the three cases given above. The required initial estimates of the diffusion coefficients are then obtained by a simple linear regression using the appropriate experimental data. In this way, convergence was obtained after 4 to 6 cycles in all the cases tested.

3. Test of the Method

The procedure was thoroughly tested by constructing artificial "experimental" data. The condition functions (8) and (9) were used assuming a value of zero for X°_2 and Y°_2. Exact solutions of eqs (2) were obtained for different arbitrary sets of D_{ij}, β, and initial concentration differences. The "true" points thus obtained were transformed into "experimental" observations by the use of a table of normal deviates, and the foregoing method was applied to these data.[4] Thus the following factors affecting the estimated values for D_{ij} and their errors were investigated: (a) duration of the longest experiment in a given set of experiments, (b) number of experiments (total number of observations) in sets having the same duration for the longest experiment, and (c) errors in the observables.

For the case of binary systems, expressions have been reported [14, 15] to calculate an optimum experimental time at which the fractional error in the diffusion coefficient becomes minimum. Derivation of similar expressions for ternary systems involves such complexity that it is practically unmanageable. In the present investigation this subject was studied by calculations of D_{ij} for different sets of experiments, varying the duration of the longest experiment in each set. A sample of the results obtained is shown

[4] All the values given in the tables in this paper were calculated assuming that the relative precision in the determination of the observables (except time) remained constant. This situation is often found when concentrations are directly determined by chemical analyses; the volume of the aliquots is selected so as to analyze essentially the same amount of component in the samples. The adjustment procedure, however, is general and satisfactory results are also obtained by considering absolute precision.

in table 1. The time given at the top of each column corresponds to the longest experiment in a set consisting of eight experiments, the time increment for each successive experiment being one-eighth of the longest experiment. Values for the percent decrease of the initial concentration differences of components 1 and 2, R_1 and R_2, at the end of the longest experiment for a particular set are given in the second and third rows. In order to facilitate the interpretation of these calculations, the same random numbers were used to estimate the "experimental" observations for each set. For this reason, the ratio $\sigma^2_{ext}/\sigma^2_{int}$ is fairly constant in this table and, as might have been anticipated, its value is close to unity.

Table 1 shows that as the duration of the longest experiment increases, the estimated D_{ij} approach the values for the "true" diffusion coefficients. Furthermore, the last row in the table shows that there is a minimum in the sum of squares of the errors in D_{ij}, $\Sigma\Delta^2_{ij}$, corresponding to a set with an experiment of maximum duration between 200 and 600 hr. This type of calculation was also performed with a number of systems varying the initial conditions and the (true) values for D_{ij}. In all cases a minimum was found but its position varied from system to system and there was no apparent trend correlating the minimum with the parameters used or calculated. In some of the systems studied, the approach to and departure from the minimum value of $\Sigma\Delta^2_{ij}$ occurred very gradually as the duration of the longest experiment increased. In other systems, however, the valley region was very narrow. Typical examples of these features are shown in figure 1 in which the quantity $\Sigma\Delta^2_{ij}$ is plotted against the duration of the longest experiment in various experimental sets. Initial conditions and related param-

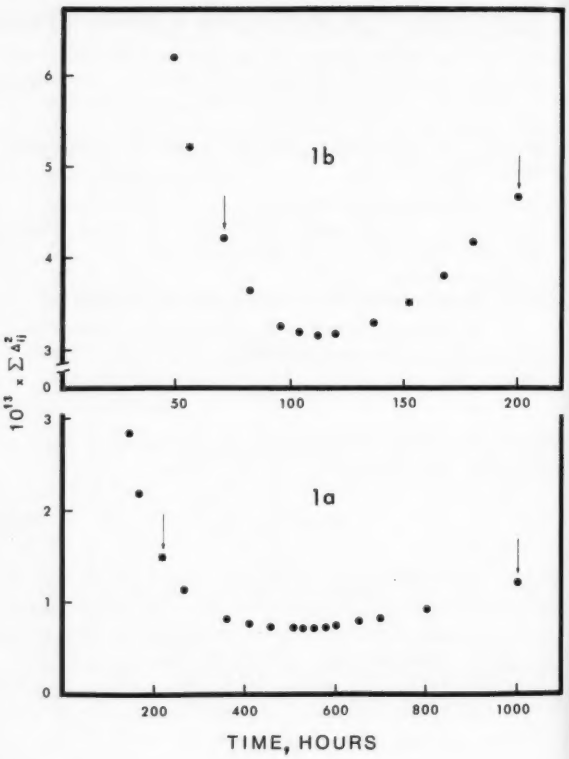

FIGURE 1. *Effect of duration of longest experiment on errors in* D_{ij}.
For both plots: Number of experiments per set, initial conditions, errors in observables, and cell constant, as given in table 1. For 1a, "true" D_{ij} as in table 1. For 1b, "true" $D_{ij} \times 10^5$: $D_{11}=8.0$, $D_{12}=1.0$, $D_{21}=-2.0$, $D_{22}=4.0$.

TABLE 1. *Effect of duration of the longest experiment on the estimated values and errors of the diffusion coefficients*

Duration of longest exp., hr*	24	120	216	312	408	504	600	800	True diff. coeffs.
$R_1=100\ \Delta X/\Delta X^\circ$	83.2	39.5	18.3	8.1	3.4	1.2	0.2	−0.3	.....
$R_2=100\ \Delta Y/\Delta Y^\circ$	90.5	61.2	42.0	29.1	20.4	14.3	10.1	4.9	.....
$D_{11}\times 10^5$	1.576 ±0.155	1.935 ±0.033	1.959 ±0.021	1.967 ±0.018	1.971 ±0.016	1.973 ±0.016	1.974 ±0.017	1.975 ±0.019	2.000
$D_{12}\times 10^5$	0.888 ±0.252	0.296 ±0.049	0.255 ±0.030	0.240 ±0.023	0.233 ±0.021	0.229 ±0.020	0.226 ±0.020	0.221 ±0.022	0.200
$D_{21}\times 10^5$	0.062 ±0.052	0.103 ±0.011	0.103 ±0.008	0.103 ±0.006	0.103 ±0.006	0.103 ±0.006	0.103 ±0.006	0.103 ±0.006	0.100
$D_{22}\times 10^5$	1.062 ±0.085	0.997 ±0.017	0.997 ±0.011	0.998 ±0.008	0.998 ±0.007	0.998 ±0.007	0.998 ±0.007	0.999 ±0.007	1.000
$\frac{\sigma^2_{ext}}{\sigma^2_{int}}$	0.72	1.07	1.08	1.08	1.08	1.07	1.08	1.09	.....
$(\Sigma\Delta^2_{ij})\times 10^{13}$	97.614	3.909	1.489	0.946	0.770	0.724	0.744	0.916	.....

Initial conditions: $\Delta X^\circ=0.025$; $\Delta Y^\circ=0.015$. Cell constant: $\beta=0.1$.
Total number of experiments in a set: 8.
Adopted errors: $E_{X,Y}=\pm 0.2\%$; $E_T=\pm 60$ s; $E_{\Delta X^\circ,\Delta Y^\circ}=\pm 0.1\%$; $E_\beta=0.1\%$.
*Same set of random numbers used for each column.

TABLE 2. *Effect of number of experiments in a set on the estimated values and errors of the diffusion coefficients**

Number of experiments in a set	3		5		8		True diff. coeffs.
$D_{11} \times 10^5$	2.005 ±0.027	1.938 ±0.026	2.051 ±0.015	2.010 ±0.022	2.002 ±0.010	1.973 ±0.016	2.000
$D_{12} \times 10^5$	0.197 ±0.029	0.261 ±0.028	0.151 ±0.018	0.202 ±0.025	0.189 ±0.012	0.228 ±0.020	0.200
$D_{21} \times 10^5$	0.114 ±0.009	0.088 ±0.009	0.097 ±0.005	0.096 ±0.008	0.103 ±0.003	0.103 ±0.006	0.100
$D_{22} \times 10^5$	0.986 ±0.010	1.012 ±0.010	1.003 ±0.006	1.004 ±0.009	0.994 ±0.004	0.998 ±0.007	1.000
$\frac{\sigma^2_{ext}}{\sigma^2_{int}}$	0.58	0.58	0.47	0.99	0.40	1.08	.....

Initial conditions: $\Delta X^\circ = 0.025$; $\Delta Y^\circ = 0.015$. Cell constant; $\beta = 0.1$.
Longest experiment in each set: 516 hr.
Adopted errors: $E_{X,Y} = \pm 0.2\%$; $E_T = \pm 60$ s; $E_{\Delta X^\circ, \Delta Y^\circ} = \pm 0.1\%$; $E_\beta = \pm 0.1\%$.

*Entries in subcolumns are extreme values of D_{ij} obtained with 6 to 10 sets of randomized data.

eters are given in the figure caption. The lower curve corresponds to the example given in table 1; however, both plots are restricted to the regions adjacent to the minimum. Values for D_{ij} estimated from the experimental sets represented by the points between arrows in figure 1 do not differ appreciably.

The actual position of the minimum in $\Sigma\Delta^2_{ij}$ for a given system shifts for different values of the cell constant, β, but it always occurs at approximately the same values of R_1 and R_2. In the absence of analytical expressions to calculate optimum diffusion times in ternary systems, the procedure reported here can be used to determine the duration for which a minimum in the errors for D_{ij} is obtained. This approach, of course, requires estimates for the values of D_{ij}, errors in the observables, initial conditions, and the cell constant. With these parameters, curves like those in figure 1 can be computed and a decision about the diffusion time can be made.

The effect of the number of experiments in a set on the estimated values of D_{ij} is shown in table 2. Calculations for this table were made using the same initial conditions and set of parameters used in table 1. The longest time used in any particular set was 516 hr, and the time increment for the N singular experiments was $516/N$. The calculations were carried out several times for each set using different sets of random numbers for the estimation of the "experimental" observations. Results for the two sets of calculations displaying the maximum differences in D_{ij} are given in the table. It is apparent that as the number of experiments in each set is increased, the variations in D_{ij} and Δ_{ij} due to experimental errors decrease although the duration of the longest experiment in all the sets was the same, 516 hr.

The errors in the observables not only affect the estimated values for D_{ij} and Δ_{ij}, but also the time at which a minimum in $\Sigma\Delta^2_{ij}$ is obtained for a given system. Such effects are shown in table 3; the values for D_{ij} were calculated from sets having an experiment with a maximum duration equal to the time for which a minimum in $\Sigma\Delta^2_{ij}$ was observed. With large errors in the observables, the values for D_{ij} obtained by the adjustment procedure may be very inaccurate; this situation is particularly true for the cross-term diffusion coefficients. Although definite shifts in the location of the minima in $\Sigma\Delta^2_{ij}$ are apparent, they are hardly significant for experimental planning.

TABLE 3. *Effect of errors in observables on the estimated values and errors of the diffusion coefficients*

$E_{X,Y}$	2.0%*	0.2%*	0.02%*	True diff. coeffs.
$D_{11} \times 10^5$	1.742 ±0.147	1.973 ±0.016	1.997 ±0.002	2.000
$D_{12} \times 10^5$	0.465 ±0.181	0.228 ±0.020	0.203 ±0.002	0.200
$D_{21} \times 10^5$	0.130 ±0.055	0.103 ±0.006	0.100 ±0.001	0.100
$D_{22} \times 10^5$	0.978 ±0.068	0.998 ±0.007	1.000 ±0.001	1.000
$(\Sigma\Delta^2_{ij}) \times 10^{13}$	62.025	0.723	0.008	.....
Duration of longest experiment, hr	532	516	536	.....

Initial conditions: $\Delta X^\circ = 0.025$; $\Delta Y^\circ = 0.015$. Cell constant: $\beta = 0.1$.
Total number of experiments in a set: 8.
Adopted errors: $E_{\Delta X^\circ, \Delta Y^\circ} = \pm 0.1\%$; $E_\beta = \pm 0.1\%$; $E_T = \pm 60$ s.
*Same set of random numbers used for each column.

The adjustment procedure described in this paper was applied to the diffusion data reported by Kelly [1] for the ternary system mannitol (1) – NaCl (2) – H_2O, using the condition eqs (6) and (7). Kelly had obtained the values for D_{ij} from the results of two experimental arrangements with initial conditions given at the head of table 4. His results and the results obtained by the present procedure are shown, side by side, in the same table.

There is satisfactory agreement between the results obtained by the present procedure and those obtained by Kelly for systems where he could calculate diffusion coefficients, with the exception of the value for D_{11} in the system 2–A. The values for D_{ij} estimated from Kelly's experimental data for system 1–A should have agreed, in theory, with those obtained from the experimental data for the system 1–B. The cause of these discrepancies is that, usually, when one of the components has zero initial concentration gradient, the amount diffused is so small that a reliable estimation of the D_{ij} is impossible.

The discrepancies in systems 2–A and 2–B are explained on the same basis; however, the large value for the ratio $\sigma^2_{ext}/\sigma^2_{int}$ for system 2–A suggests that the error variances used for the observables are very different from those actually existing in this system; for this reason, the values for D_{ij} obtained from this experiment are questionable.

Cussler and Dunlop [4] also estimated D_{ij} from Kelly's data. It is not clear in their publication whether they combined the data for systems 1–A and 1–B or estimated D_{ij} from each arrangement separately. The values they obtained are in good agreement with those obtained by the present method and reported in table 4, with the exception of the value for D_{21} which is about 5 percent lower than the figure reported here. Significant differences, however, do exist between the errors reported by Cussler and Dunlop and those obtained in the present investigation. This is not surprising because in their unweighted least squares procedure, those investigators arrived at estimates of errors for the D_{ij} by a bound method. Their reported error figures correspond to the maximum difference between the D_{ij} calculated considering the nominal value of the observables and the D_{ij} obtained through similar calculation but using the values of the observables as the nominal values minus their errors and plus their errors, respectively. The procedure given in this paper to calculate Δ_{ij} is not only time saving but also it has a sound statistical basis.

The authors are indebted to L. J. Gosting, Institute for Enzyme Research, Wisconsin University, Madison, Wisconsin, for making available to them the material of reference (1) and to R. P. Wendt, Department of Chemistry, Loyola University, New Orleans, Louisiana, for his suggestions and critical review of the manuscript.

TABLE 4. *Comparison of Kelly's estimated values of the diffusion coefficients with those estimated by the present procedure using Kelly's experimental data for the system mannitol* (X) – NaCl (Y) – H_2O

Average conc.	$\bar{X}=0.2M$; $\bar{Y}=1.5M$				$\bar{X}=0.2M$; $\bar{Y}=3.0M$			
Initial conditions	$\Delta X^\circ=0.4$ $\Delta Y^\circ=0.0$		$\Delta X^\circ=0.0$ $\Delta Y^\circ=0.5$		$\Delta X^\circ=0.4$ $\Delta Y^\circ=0.0$		$\Delta X^\circ=0.0$ $\Delta Y^\circ=1.0$	
System	1 – A 5 experiments		1 – B 4 experiments		2 – A 6 experiments		2 – B 3 experiments	
	This paper	Ref. (1)	This paper	Ref. (1)	This paper	Ref. (1)	This paper	Ref. (1)
$D_{11}\times10^5$	0.557 ±0.003	0.559 ±0.004	1.148 ±0.246	.....	1.006 ±0.016	0.448 ±0.006	0.439 ±0.625	.....
$D_{12}\times10^5$	0.025 ±0.039	.....	0.018 ±0.002	0.016 ±0.010	0.512 ±0.066	.....	0.013 ±0.003	0.013 ±0.008
$D_{21}\times10^5$	0.232 ±0.017	0.232 ±0.001	0.138 ±1.918	.....	0.494 ±0.072	0.456 ±0.003	−0.040 ±9.969	.....
$D_{22}\times10^5$	1.556 ±0.230	.....	1.388 ±0.013	1.390 ±0.002	1.122 ±0.291	.....	1.469 ±0.048	1.469 ±0.003
$\frac{\sigma^2_{ext}}{\sigma^2_{int}}$	5.20	.....	4.32	.....	167.18	.....	38.98	.....

$E_{X^\circ,Y^\circ}=\pm0.02\%$; $E_{X,Y}=\pm0.02\%$; $E_T=\pm60$ s; $E_\beta=0.1\%$.

4. References

[1] Kelly, F. J., Ph. D. Thesis, University of New England, Armidale, N.S.W., Australia (1961).

[2] Kelly, F. J., and Stokes, R. H., Electrolytes, pp. 96–100, B. Pesce, Ed. (Pergamon Press Ltd., Oxford, 1962).

[3] Burchard, J. K., and Toor, H. L., J. Phys. Chem. **66,** 2015 (1962).

[4] Cussler, E. L., Jr., and Dunlop, P. J., J. Phys. Chem. **70,** 1880 (1966).

[5] Onsager, L., Ann. N.Y. Acad. Sci., **46,** 241 (1945).

[6] Kirkwood, J. G., Baldwin, R. L., Dunlop, R. J., Gosting, L. J., and Kegeles, G., J. Chem. Phys. **33,** 1505 (1960).

[7] Gilliland, E. R., Baddour, R. F., and Goldstein, D. J., Can. J. Chem. Eng. **35,** 10 (1957).

[8] Deming, W. E., Statistical Adjustment of Data, pp. 49–58 and pp. 128–147 (John Wiley & Sons, Inc., New York, New York, 1943) (Reprinted by Dover Publications, New York, New York, 1964.)

[9] Guest, P. G., Numerical Methods of Curve Fitting, pp. 370–381 (Cambridge, University Press, Cambridge, England, 1961).

[10] Birge, R. T., Phys. Review **40,** 207 (1932).

[11] Box, G. E. P., Bull. Inst. Internat. Statistique **36,** 215 (1958).

[12] Hartley, H. O., Technometrics **3,** 269 (1961).

[13] Strand, T. G., Kohl, D. A., and Bonham, R. A., J. Chem. Phys. **39,** 1307 (1963).

[14] Robinson, R. L., Jr., Edmister, W. C., and Dullien, F. A. L., J. Phys. Chem. **69,** 258 (1965).

[15] Van Geet, A. L., and Adamson, A. W., J. Phys. Chem. **68,** 238 (1964).

(Paper 73A1–533)

324-194 O–69—4

JOURNAL OF RESEARCH of the National Bureau of Standards—A. Physics and Chemistry
Vol. 73A, No. 1, January–February 1969

Calculated Line Strengths for the Transition Array $(3d^3 + 3d^2 4s) - 3d^2 4p$ in Ti II

H. Mendlowitz

Department of Physics, Howard University*

and

Institute for Basic Standards, National Bureau of Standards, Washington, D.C. 20234

(August 27, 1968)

The transition array for the transitions between the configurations $(3d^3 + 3d^2 4s)$ and $3d^2 4p$ in Ti II are presented here. The relative line strengths have been calculated in the intermediate coupling scheme, taking into account interaction between configurations. The relative phase and magnitude of the radial transition integrals $(s-p)$ and $(d-p)$ for the jumping electron in the *LS* coupling have been determined empirically.

Key Words: Calculated line strengths; configuration interaction; intermediate coupling; Ti II; $3d^3$, $3d^2 4s$, $3d^2 4p$ configurations; transition array.

The line strengths for transitions between levels A and B are defined as in Condon and Shortley [1] as

$$\mathcal{S}(A, B) = \sum_{a,b} |(a|\mathbf{P}|b)|^2, \tag{1}$$

where the sum is over all the states which are the sublevels of the levels A and B. In this note, we first calculated the square roots of the relative strengths of the transitions between two given configurations in the *LS* representation and then transformed to the physical representation. It is assumed that the dipole approximation is valid. In this approximation the transition operator $\mathbf{P}$ is given by

$$\mathbf{P} = -\sum_j e\mathbf{r}_j \tag{2}$$

where the sum is taken over all the electrons involved in the transition. The matrix elements for the transition can be readily calculated except for a radial integral factor common to all the matrix elements of the transition array [2, 3].

The radial integral depends upon the quantum numbers of the jumping electron in the upper and lower levels of the transition. In cases where the interaction between configurations is negligible, one has only one radial integral to consider in the *LS* representation. Therefore, upon transforming to the intermediate coupling scheme, the relative transition strengths are easily obtained. However, in the case of Ti II, the interaction between the configurations is important, so one has to consider more than one radial integral for the jumping electron. In Ti II, transitions between the following configurations may be important:

(1) $3d^3 - 3d^2 4p$,

(2) $3d^2 4s - 3d^2 4p$.

The state $|a)$ may then be expressed as a superposition of the eigenstates $|K)$ of the various configurations. Thus,

$$|a) = \sum_K |K)(K|a), \tag{3}$$

where we have summed over the configurations K, and $(K|a)$ is the set of expansion coefficients. The matrix element of the transition between states a and b can be written as

$$(b|\mathbf{P}|a) = \sum_K \sum_{K'} (b|K')(K'|\mathbf{P}|K)(K|a), \tag{4}$$

where $(K'|\mathbf{P}|K)$ are the matrix elements of the transition operator $\mathbf{P}$ expressed in the representation where the configurations K' and K are good quantum

*Supported in part by National Science Foundation and Physics Branch of Office of Naval Research.

numbers. In Ti II, this refers to the transition array in the *LS* representation for each configuration of the lower state separately. The matrix element for the transition can then be expressed as

$$(b|\mathbf{P}|a)=\sum_{\substack{\alpha\\\beta}}(a|3d^24p,\beta)(3d^24p\beta|\mathbf{P}|3d^3,\alpha)(3d^3,\alpha|a)$$

$$+\sum_{\substack{\alpha\\\beta'}}(b|3d^24p\beta')(3d^24p\beta'|\mathbf{P}|3d^24s\alpha')(3d^24s,\alpha'|a) \qquad (5)$$

where α, α' and β, β' are the sets of relevant quantum numbers in the *LS* representation. In each of the two sums in eq (5) there is a factorable radial integral factor $(nl\|P\|n'l')$, where nl and $n'l'$ are the radial and orbital angular momentum quantum numbers of the jumping electron. Each set of configurations has a different set of n, l; n', l'. It is the phase and magnitude of the ratio of these radial factors which must be determined to calculate the relative intensities.

The determination of the expansion coefficients $(K|a)$ and the relative phase and magnitude as well as comparison with experiments are discussed elsewhere [4]. In the table we show the strengths for the transition array for $3d^3+3d^24s-3d^24p$ for Ti II. The composition of the upper and lower level is described in terms of the dominant states in the *LS* representation. For each position in the array, the upper number is the relative strength of the transition. The next lower number is the wavelength corresponding to the transition obtained from Russell's classifications [5], whenever available. The lowest number gives the wavenumber corresponding to the transition. The relative strengths are given to three significant figures for the stronger transitions and only one significant figure for the weaker lines. The number of significant figures given is consistent with the results of the diagonalization of the energy matrix and the empirical determination of the ratio of the radial integral parameters [4]. The magnitudes of the radial integral parameters have been found to be equal within the approximations that have been used, so in this table, the magnitudes of the radial integral factor have been taken to be unity for simplicity. Those relative strengths listed as zero indicate that, on the scale employed here, these strengths are less than 5×10^{-5}.

TABLE 1. *Transition array for* $(3d^3+3d^24s)-3d^24p$ *in* Ti II *in intermediate coupling scheme with configuration interaction.*

The upper and lower levels are described in terms of the dominant states in the *LS* representation and the energy levels assigned in AEL [6]. For each position in the array, the upper number is the relative strength of the transition with the normalization of the radial integral parameter for the jumping electron in the *d-p* transition taken as unity. The next lower number is the wavelength corresponding to the transition obtained from Russell's classification when available. The lowest number is the wave number of the transition.

		$(3d^3+3d^24s)$				
	1/2 / 1/2	a^2P 9850.90	a^4P 9363.71	a^2S 21338.0	b^2P 16515.79	b^4P 9872.87
$(3d^24p)$	z^2S°	0.0004	0.0000	0.0000	0.30	0.0001
		3624.82	3561.92	6212.29	4779.95	3627.70
	37430.55	27579.65	28066.84	16092.55	20914.76	27557.68
	$^2P^\circ$	0.0003	0.0000	0.66	0.003	0.0000
	(63210.1)	53359.20	53846.39	41872.10	46694.31	53337.23
	y^2P°	0.21	0.02	0.004	0.23	0.003
		2806.50			3452.47	
	45472.89	35621.99	36109.18	24134.89	28957.10	35600.02
	z^2P°	0.06	0.003	0.005	0.02	0.002
		3352.06	3298.20	5452.02	4316.80	
	39674.64	29823.74	30310.93	18336.64	23158.85	29801.77
	z^4P°	0.003	0.01	0.0000	0.0001	0.10
			3063.48	4839.22		3112.05
	41996.74	32145.84	32633.03	20658.74	25480.95	32123.87
	y^4D°	0.005	0.01	0.0000	0.0000	0.55
						3282.33
	40330.25	30479.35	30966.54	18992.25	23814.46	30457.38
	z^4D°	0.007	0.08	0.0000	0.0000	0.008
		4407.68	4314.98			4411.94
	32532.38	22681.48	23168.67	11194.38	16016.59	22659.51

TABLE 1.—Continued

$(3d^3 + 3d^24s)$

3/2 / 1/2	a^2P	a^4P	d_1^2D	b_3^2D	b^4F	b^2P	b^4P	a^2D	a^4F	D^2D
	9975.92	9395.76	(32358.5)	12628.77	907.96	16625.25	9930.74	8710.47	0	24961.34
$z^2S°$	0.26	0.04	0.0000	0.002	0.0000	0.18	0.03	0.02	0.0000	0.0001
	3641.33	3566.00				4805.10		3480.89		
37430.55	27454.63	28034.79	5072.05	24801.78	36522.59	20805.30	27499.81	28720.08	37430.55	12469.21
$^2P°$	0.0008	0.0001	0.14	0.03	0.0000	0.002	0.0001	0.0002	0.0000	0.02
(63210.1)	53234.18	53814.34	30851.60	50581.33	62302.14	46584.85	53279.36	54499.63	63210.10	38248.76
$y^2P°$	0.01	0.002	0.14	0.06	0.0000	0.22	0.002	0.001	0.0000	0.04
				3043.85		3465.58		2719.39		4873.95
45472.89	35496.97	36077.13	13114.39	32844.12	44564.93	28847.64	35542.15	36762.42	45472.89	20511.55
$z^2P°$	0.09	0.02	0.0008	0.002	0.0001	0.002	0.01	0.69	0.0003	0.008
	3366.17			3696.38		4337.32		3228.60		
39674.64	29698.72	30278.88	7316.14	27045.87	38766.68	23049.39	29743.90	30964.17	39674.64	14715.30
$z^4P°$	0.02	0.07	0.0000	0.0001	0.0000	0.0001	0.54	0.0000	0.0000	0.0000
	3122.10	3066.52					3117.67			
41996.74	32020.82	32600.98	9638.24	29367.97	41088.78	25371.49	32066.00	33286.27	41996.74	17035.40
$y^4D°$	0.01	0.002	0.0000	0.0000	0.08	0.0001	0.09	0.0008	0.01	0.0000
					2535.87		3288.58		2478.77	
40330.25	30354.33	30934.49	7971.75	27701.48	39422.29	23705.00	30399.51	31619.78	40330.25	15368.91
$z^4D°$	0.0005	0.02	0.0000	0.0000	0.16	0.0000	0.002	0.0000	0.66	0.0000
	4432.10	4320.95			3161.20				3072.97	
32532.38	22556.46	23136.62	173.88	19903.61	31624.42	15907.13	22601.64	23821.91	32532.38	7571.04

$(3d^24p)$

TABLE 1.—Continued

$(3d^3 + 3d^2 4s)$

1/2 / 3/2	a^2P	a^4P	a^2S	b^2P	b^4P
	9850.90	9363.71	21338.0	16515.79	9872.87
z^4S°	0.03	0.09	0.0005	0.0006	0.20
		3260.26			3315.32
40027.28	30176.38	30663.57	18689.28	23511.49	30154.41
$^2P^\circ$	0.0006	0.0000	1.32	0.0007	0.0000
(63284.3)	53433.40	53920.59	41946.30	46768.51	53411.43
y^2P°	0.007	0.0006	0.007	0.14	0.0000
				3443.38	
45548.90	35698.00	36185.19	24210.90	29033.11	35676.03
z^2P°	0.04	0.02	0.01	0.002	0.01
		3306.04	5473.52	4330.25	3362.66
39602.90	29752.00	30239.19	18264.90	23087.11	29730.03
z^4P°	0.0008	0.07	0.0001	0.0001	0.52
	3103.00	3056.74			3105.08
42068.85	32217.95	32705.14	20730.85	25553.06	32195.98
$(3d^2 4p)$					
x^2D°	0.13	0.01	0.0001	0.86	0.001
	2851.10	2812.05		3520.25	
44914.80	35063.90	35551.09	23576.80	28399.01	35041.93
y^2D°	0.05	0.004	0.0003	0.05	0.008
	3402.42				3404.99
39233.44	29382.54	29869.73	17895.44	22717.65	29360.57
z^2D°	0.18	0.03	0.0000	0.01	0.0004
	4563.77	4464.47		6559.58	4568.30
31756.50	21905.60	22392.79	10418.50	15240.71	21883.63
y^4D°	0.02	0.005	0.0000	0.001	0.56
	3269.75				3272.08
40425.80	30574.90	31062.09	19087.80	23910.01	30552.93
z^4D°	0.03	0.06	0.0000	0.0006	0.01
	4394.06	4301.93			4398.31
32602.51	22751.61	23238.80	11264.51	16086.72	22729.64
z^4F°	0.0003	0.0000	0.0000	0.0000	0.0000
30836.52	20985.62	21472.81	9498.52	14320.73	20963.65

TABLE 1.—Continued

$(3d^3 + 3d^24s)$

3/2 / 3/2	a^2P	a^4P	$d^2_{\frac{1}{2}}D$	b^2_5D	b^4F	b^2P	b^4P	a^2D	a^4F	C^2D
	9975.92	9395.76	(32358.5)	12628.77	907.96	16625.25	9930.74	8710.47	0	24961.34
$z^4S°$	0.0004	0.18	0.0002	0.005	0.0000	0.007	0.52	0.009	0.0000	0.0000
		3263.68					3321.70	3192.26		
40027.28	30051.36	30631.52	7668.78	27398.51	39119.32	23402.03	30096.54	31316.81	40027.28	15065.94
$^2P°$	0.0003	0.0000	0.03	0.003	0.0000	0.008	0.0000	0.004	0.0000	0.004
(63284.3)	53308.38	53888.54	30925.80	50655.53	62376.34	46659.05	53353.56	54573.83	63284.3	38322.96
$y^2P°$	0.50	0.06	0.04	0.02	0.0000	0.63	0.08	0.001	0.0000	0.01
		2765.22		3036.78		3456.39		2713.76		
45548.90	35572.98	36153.14	13190.40	32920.13	44640.94	28923.65	35618.16	36838.43	45548.90	20587.56
$z^2P°$	0.12	0.05	0.0001	0.07	0.0000	0.06	0.002	0.002	0.0001	0.0000
	3374.35			3706.23		4350.83	3369.20	3236.12		
39602.90	29626.98	30207.14	7244.40	26974.13	38694.94	22977.65	29672.16	30892.43	39602.90	14641.56
$z^4P°$	0.04	0.02	0.0000	0.0001	0.0000	0.0002	0.14	0.0000	0.0000	0.0000
	3115.09	3059.74					3110.67			
42068.85	32092.93	32673.09	9710.35	29440.08	41160.89	25443.60	32138.11	33358.38	42068.85	17107.51
$(3d^24p)$										
$x^2D°$	0.03	0.007	0.06	0.0005	0.0000	0.07	0.008	0.16	0.0000	0.02
	2861.29	2814.61		3096.43		3533.85		2761.29		5010.21
44914.80	34938.88	35519.04	12556.30	32286.03	44006.84	28289.55	34984.06	36204.33	44914.80	19953.46
$y^2D°$	0.03	0.02	0.02	0.008	0.0008	0.04	0.01	1.19	0.0000	0.004
	3416.95	3350.53		3757.69		4421.95		3275.38		
39233.44	29257.52	29837.68	6874.94	26604.67	38325.48	22608.19	29302.70	30522.97	39233.44	14272.10
$z^2D°$	0.002	0.01	0.01	0.18	0.001	0.04	0.001	0.002	0.03	0.0004
	4589.95	4470.88		5226.56	3240.72		4580.46	4337.92	3148.04	
31756.50	21780.58	22360.74		19127.73	30848.54	15131.25	21825.76	23046.03	31756.50	6795.16
$y^4D°$	0.07	0.009	0.0008	0.0001	0.03	0.001	0.57	0.02	0.004	0.0001
				3596.55	2529.86		3278.29			
40425.80	30449.88	31030.04	8067.30	27797.03	39517.84	23800.55	30495.06	31715.33	40425.80	15464.46
$z^4D°$	0.02	0.09	0.0008	0.009	0.07	0.002	0.004	0.0001	0.23	0.0000
	4418.33	4307.90			3154.20		4409.53	4184.33	3066.36	
32602.51	22626.59	23206.75	244.01	19973.74	31694.55	15977.26	22671.77	23892.04	32602.51	7641.17
$z^4F°$	0.0000	0.0000	0.0001	0.0003	0.32	0.0001	0.0000	0.0000	1.07	0.0000
					3340.34				3241.99	
30836.52	20860.60	21440.76		18207.75	29928.56	14211.27	20905.78	22126.05	30836.52	5875.18

TABLE 1.—Continued

$(3d^3 + 3d^24s)$

	3/2 / 5/2	a^2P	a^4P	d^2_3D	b^2_3D	b^4F	b^2P	b^4P	a^2D	a^4F	C^2D
		9975.92	9395.76	(32358.5)	12628.77	907.96	16625.25	9930.74	8710.47	0	24961.34
$(3d^24p)$	$z^4P°$	0.02	0.07	0.0000	0.001	0.0000	0.001	0.55	0.0000	0.0000	0.0000
			3046.69					3097.19			
	42208.84	32232.92	32813.08	9850.34	29580.07	41300.88	25583.59	32278.10	33498.37	42208.84	17247.50
	$x^2D°$	0.19	0.02	0.01	0.02	0.0000	1.39	0.03	0.02	0.0000	0.002
		2862.32	2815.57		3097.63		3535.41		2762.22		
	44902.42	34926.50	35506.66	12543.92	32273.65	43994.46	28277.17	34971.68	36191.95	44902.42	19941.08
	$y^2D°$	0.07	0.04	0.001	0.10	0.0001	0.07	0.10	0.11	0.0000	0.002
		3388.76			3723.60		4374.82		3249.37		
	39476.87	29500.95	30081.11	7118.37	26848.10	38568.91	22851.62	29546.13	30766.40	39476.87	14515.53
	$z^2D°$	0.24	0.13	0.004	0.02	0.0003	0.02	0.02	0.006	0.003	0.0000
		4533.97	4417.72		5154.07		6491.68	4524.72	4287.88	3121.60	
	32025.50	22049.58	22629.74		19396.73	31117.54	15400.25	22094.76	23315.03	32025.50	7064.16
	$y^4D°$	0.28	0.005	0.0000	0.0000	0.002	0.004	1.11	0.0000	0.0003	0.0000
		3266.41			3576.37	2519.79		3261.59	3136.75		
	40581.80	30605.88	31186.04	8223.30	27953.03	39673.84	23956.55	30651.06	31871.33	40581.80	15620.46
	$z^4D°$	0.08	0.12	0.0003	0.002	0.005	0.003	0.06	0.0004	0.01	0.0000
		4399.77	4290.23					4391.02		3057.40	
	32697.94	22722.02	23302.18	339.44	20069.17	31789.98	16072.69	22767.20	23987.47	32697.94	7736.60
	$y^2F°$	0.01	0.005	0.003	0.23	0.0001	0.001	0.001	1.35	0.0000	0.02
		3337.79			3662.24				3202.54		6680.26
	39926.83	29950.91	30531.07	7568.33	27298.06	39018.87	23301.58	29996.09	31216.36	39926.83	14965.49
	$z^2F°$	0.002	0.0001	0.02	0.02	0.005	0.0005	0.0000	0.21	0.0000	0.0001
		4708.65	4583.44		5381.02				4443.80	3203.44	
	31207.44	21231.52	21811.68		18578.67	30299.48	14582.19	21276.70	22496.97	31207.44	6246.10
	$x^2F°$	0.0003	0.0002	0.20	0.03	0.0000	0.0006	0.0001	0.009	0.0000	0.04
		2655.30			2856.62				2568.98		4411.08
	47625.17	37649.25	38229.41	15266.67	34996.40	46717.21	30999.92	37694.43	38914.70	47625.17	22663.83
	$z^4F°$	0.0001	0.0000	0.0007	0.001	0.08	0.0000	0.0001	0.007	0.26	0.0000
			4636.34			3326.76			4493.52	3229.19	
	30958.70	20982.78	21562.94		18329.93	30050.74	14333.45	21027.96	22248.23	30958.70	5997.36
	$z^4G°$	0.0000	0.0000	0.0001	0.0000	0.06	0.0000	0.0000	0.001	1.72	0.0000
						3491.05			4798.52	3383.76	
	29544.37	19568.45	20148.61		16915.60	28636.41	12919.12	19613.63	20833.90	29544.37	4583.03

TABLE 1.—Continued

$(3d^3 + 3d^24s)$

5/2 / 3/2	a^4P	d^2D	d_1^2D	b^2F	b^4F	b^4P	a^2D	a^2F	a^4F	C^2D
	9518.05	(32362.7)	12758.15	20951.77	983.80	10024.74	8744.27	4628.61	93.94	25193.04
$z^4S°$	0.35	0.0000	0.0000	0.0000	0.0001	0.63	0.02	0.0002	0.0000	0.0008
	3276.76					3332.11	3195.71			
40027.28	30509.23	7664.58	27269.13	19075.51	39043.48	30002.54	31283.01	35398.67	39933.34	14834.24
$^2P°$	0.0000	0.24	0.06	0.0000	0.0000	0.0000	0.0001	0.0000	0.0000	0.05
(63284.3)	53766.25	30921.60	50526.15	42332.53	62300.50	53259.56	54540.03	58655.69	63190.36	38091.26
$y^2P°$	0.0000	0.23	0.08	0.006	0.0000	0.0000	0.004	0.0003	0.0000	0.07
			3048.77	4064.40			2716.25			4911.19
45548.90	36030.85	13186.20	32790.75	24597.13	44565.10	35524.16	36804.63	40920.29	45454.96	20355.86
$z^2P°$	0.004	0.0008	0.008	0.0000	0.0001	0.007	1.41	0.003	0.0003	0.02
			3724.08			3379.92	3239.66	2858.40		
39602.90	30084.85	7240.20	26844.75	18651.13	38619.10	29578.16	30858.63	34974.29	39508.96	14409.86
$z^4P°$	0.08	0.0000	0.001	0.0000	0.0000	0.64	0.0002	0.0001	0.0000	0.0001
	3071.24					3119.80				
42068.85	32550.80	9706.15	29310.70	21117.08	41085.05	32044.11	33324.58	37440.24	41974.91	16875.81
$(3d^24p)$										
$x^2D°$	0.0000	0.02	0.02	0.62	0.0000	0.0001	0.009	0.04	0.0000	0.004
			3108.93	4171.90				2481.49		5069.12
44914.80	35396.75	12552.10	32156.65	23963.03	43931.00	34890.06	36170.53	40286.19	44820.86	19721.76
$y^2D°$	0.003	0.0007	0.07	0.0004	0.005	0.0000	0.003	0.08	0.0005	0.0000
			3776.06			3422.69	3278.92	2888.93		
39233.44	29715.39	6870.74	26475.29	18281.67	38249.64	29208.70	30489.17	34604.83	39139.50	14040.40
$z^2D°$	0.0004	0.002	0.008	0.01	0.01	0.0003	0.01	1.10	0.05	0.0000
			5262.14				4344.29	3685.19	3157.39	
31756.50	22238.45		18998.35	10804.73	30772.70	21731.76	23012.23	27127.89	31662.56	6563.46
$y^4D°$	0.003	0.0000	0.003	0.0000	0.13	0.07	0.001	0.002	0.02	0.0000
					2534.62	3288.42			2478.64	
40425.80	30907.75	8063.10	27667.65	19474.03	39442.00	30401.06	31681.53	35797.19	40331.86	15232.76
$z^4D°$	0.01	0.0001	0.0005	0.0005	0.23	0.0007	0.001	0.06	1.01	0.0000
	4330.71				3161.77		4190.29	3573.74	3075.22	
32602.51	23084.46	239.81	19844.36	11650.74	31618.71	22577.77	23858.24	27973.90	32508.57	7409.47
$z^4F°$	0.0000	0.0000	0.0001	0.0000	0.08	0.0000	0.0000	0.003	0.26	0.0000
					3348.82			3814.57	3251.91	
30836.52	21318.47		18078.37	9884.75	29852.72	20811.78	22092.25	26207.91	30742.58	5643.48

TABLE 1.—Continued

$(3d^3 + 3d^24s)$

$(3d^24p)$ 5/2 / 5/2	a^4P	d_1^2D	b_3^2D	b^2F	b^4F	b^4P	a^2D	a^2F	a^4F	C^2D
	9518.05	(32362.7)	12758.15	20951.77	983.80	10024.74	8744.27	4628.61	93.94	25193.04
z^4P°	0.17	0.0004	0.0006	0.0000	0.0000	1.45	0.0002	0.0000	0.0000	0.0000
	3058.09					3106.23	2987.38			
42208.84	32690.79	9846.14	29450.69	21257.07	41225.04	32184.10	33464.57	37580.23	42114.90	17015.80
x^2D°	0.0004	0.10	0.0009	0.04	0.0000	0.004	0.26	0.009	0.0000	0.05
			3110.11				2764.80			5072.30
44902.42	35384.37	12539.72	32144.27	23950.65	43918.62	34877.68	36158.15	40273.81	44808.48	19709.38
y^2D°	0.001	0.03	0.0000	0.0000	0.002	0.02	1.72	0.0001	0.0001	0.006
	336.98		3741.64					2868.74		
39476.87	29958.82	7114.17	26718.72	18525.10	38493.07	29452.13	30732.60	34848.26	39382.93	14283.83
z^2D°	0.01	0.02	0.22	0.0005	0.007	0.0001	0.001	0.008	0.06	0.0008
			5188.70		3220.48	4544.01	4294.12		3130.80	
32025.50	22507.45		19267.35	11073.73	31041.70	22000.76	23281.23	27396.89	31931.56	6832.46
y^4D°	0.01	0.002	0.001	0.0006	0.04	0.53	0.07	0.001	0.005	0.0003
			3593.11		2524.64	3271.65		2780.55	2469.15	
40581.80	31063.75	8219.10	27823.65	19630.03	39598.00	30557.06	31837.53	35953.19	40487.86	15388.76
z^4D°	0.08	0.003	0.03	0.0000	0.08	0.01	0.0002	0.008	0.27	0.0001
	4312.87		5013.69		3152.25	4409.23	4173.55	3561.59	3066.22	
32697.94	23179.89	335.24	19939.79	11746.17	31714.14	22673.20	23953.67	28069.33	32604.00	7504.90
y^2F°	0.0009	0.004	0.03	0.08	0.0008	0.002	0.21	0.12	0.0001	0.0002
				5268.63			3206.00	2832.16		
39926.83	30408.78	7564.13	27168.68	18975.06	38943.03	29902.09	31182.56	35298.22	39832.89	14733.79
z^2F°	0.0002	0.002	0.04	0.12	0.02	0.0000	0.0008	1.70	0.05	0.0002
			5418.77		3307.72	4719.51	4450.49	3761.32	3213.14	
31207.44	21689.39		18449.29	10255.67	30223.64	21182.70	22463.17	26578.83	31113.50	6014.40
x^2F°	0.0000	0.02	0.0001	0.26	0.0000	0.0001	0.002	0.01	0.0000	0.005
				3748.01						4456.62
47625.17	38107.12	15262.47	34867.02	26673.40	46641.37	37600.43	38880.90	42996.56	47531.23	22432.13
z^4F°	0.0000	0.0000	0.0004	0.005	0.39	0.0000	0.0001	0.05	1.36	0.0000
					3335.20			3796.88	3239.04	
30958.70	21440.65		18200.55	10006.93	29974.90	20933.96	22214.43	26330.09	30864.72	5765.66
z^4G°	0.0000	0.0000	0.0001	0.0005	0.01	0.0000	0.0000	0.008	0.26	0.0000
					3500.33			4012.39	3394.58	
29544.37	20026.32		16786.22	8592.60	28560.57	19519.63	20800.10	24915.76	29450.43	4351.33

TABLE 1.—Continued

$(3d^3 + 3d^24s)$

5/2 / 7/2	a^4P	d_1^2D	b_3^2D	b^2F	b^4F	b^4P	a^2D	a^2F	a^4F	C^2D
	9518.05	(32362.7)	12758.15	20951.77	983.80	10024.74	8744.27	4628.61	93.94	25193.04
$y^4D°$	0.04	0.0002	0.02	0.0000	0.002	2.59	0.01	0.0002	0.0002	0.001
	3195.99		3565.33		2510.90	3248.60	3118.85	2763.90		
	40798.37	31280.32	8435.67	28040.22	19846.60	39814.57	30773.63	32054.10	36169.76	40704.43	15605.33
$z^4D°$	0.42	0.0000	0.0005	0.0000	0.004	0.04	0.001	0.0002	0.01	0.0000
	4300.05					4395.86	4161.54		3059.73	
	32767.02	23248.97	404.32	20008.87	11815.25	31783.22	22742.28	24022.75	28138.41	32673.08	7573.98
$y^2F°$	0.0005	0.005	0.33	0.002	0.0001	0.03	2.07	0.008	0.0001	0.03
			3659.76				3190.87			6717.89
	40074.71	30556.66	7712.01	27316.56	19122.94	39090.91	30049.97	31330.44	35446.10	39980.77	14881.67
$z^2F°$	0.0002	0.03	0.04	0.0003	0.004	0.004	0.33	0.08	0.0004	0.0001
			5336.81		3276.98	4657.20	4395.04	3721.64	3184.09	
	31490.82	21972.77		18732.67	10539.05	30507.02	21466.08	22746.55	26862.21	31396.88	6297.78
$x^2F°$	0.0002	0.28	0.05	0.01	0.0000	0.0002	0.01	0.0000	0.0000	0.06
			2880.28	3770.40			2581.73			4488.32
	47466.80	37948.75	15104.10	34708.65	26515.03	46483.00	37442.06	38722.53	42838.19	47372.86	22273.76
$(3d^24p)$										
$z^4F°$	0.0002	0.0007	0.001	0.0000	0.11	0.0002	0.007	0.004	0.33	0.0000
					3318.03		4469.15		3222.84	
	31113.61	21595.56		18355.46	10161.84	30129.81	21088.87	22369.34	26485.00	31019.67	5920.57
$z^2G°$	0.0000	0.0000	0.0001	0.03	0.0000	0.0000	0.0000	2.45	0.0001	0.0000
								3341.88	2901.94	
	34543.36	25025.31	2180.66	21785.21	13591.59	33559.56	24518.62	25799.09	29914.75	34449.42	9350.32
$y^2G°$	0.0000	0.0000	0.0002	0.20	0.0000	0.0000	0.0009	0.07	0.0000	0.0000
				4386.86				2555.99		
	43740.77	34222.72	11378.07	30982.62	22789.00	42756.97	33716.03	34996.50	39112.16	43646.83	18547.73
$z^4G°$	0.0000	0.0000	0.0000	0.0000	0.07	0.0000	0.0006	0.0002	2.32	0.0000
					3477.18		4762.78	3982.01	3372.80	
	29734.45	20216.40		16976.30	8782.68	28750.65	19709.71	20990.18	25105.84	29640.51	4541.41

TABLE 1.—Continued

$(3d^3+3d^24s)$

7/2 / 5/2	b^2F	b^4F	a^2G	a^2F	a^4F	b^2G
	20891.88	1087.21	8997.69	4897.60	225.47	15265.60
$z^4P°$	0.0000	0.0001	0.0000	0.0007	0.0000	0.0000
42208.84	21316.96	41121.63	33211.15	37311.24	41983.37	26943.24
$x^2D°$	0.89	0.0000	0.0004	0.07	0.0000	0.0007
	4163.65			2498.94		
44902.42	24010.54	43815.21	35904.73	40004.82	44676.95	29636.82
$y^2D°$	0.003	0.01	0.009	0.11	0.001	0.002
		2604.11	3279.98	2891.07	2546.88	
39476.87	18584.99	38389.66	30479.18	34579.27	39251.40	24211.27
$z^2D°$	0.01	0.05	0.005	1.52	0.19	0.0000
		3231.32	4341.39	3685.20	3143.76	
32025.50	11133.62	30938.29	23027.81	27127.90	31800.03	16759.90
$y^4D°$	0.0000	0.19	0.004	0.004	0.02	0.0007
		2531.25			2477.21	
40581.80	19689.92	39494.59	31584.11	35684.20	40356.33	25316.20
$(3d^24p)$						
$z^4D°$	0.002	0.33	0.0001	0.21	1.44	0.0000
		3162.57		3596.05	3078.64	
32697.94	11806.06	31610.73	23700.25	27800.34	32472.47	17432.34
$y^2F°$	0.004	0.003	0.57	0.001	0.0005	0.09
		2573.91	3232.28	2853.93	2518.06	4053.84
39926.83	19034.95	38839.62	30929.14	35029.23	39701.36	24661.23
$z^2F°$	0.001	0.002	0.23	0.02	0.02	0.0000
		3319.08	4501.27	3799.78	3226.76	
31207.44	10315.56	30120.23	22209.75	26309.84	30981.97	15941.84
$x^2F°$	0.01	0.0000	0.0000	0.0000	0.0000	2.04
	3739.50					3089.40
47625.17	26733.29	46537.96	38627.48	42727.57	47399.70	32359.57
$z^4F°$	0.0000	0.11	0.009	0.004	0.32	0.0000
		3346.73		3836.10	3252.91	
30958.70	10066.82	29871.49	21961.01	26061.10	30733.23	15693.10
$z^4G°$	0.0000	0.0005	0.0006	0.0002	0.009	0.0000
		3513.08	4865.62	4056.20	3409.81	
29544.37	8652.49	28457.16	20546.68	24646.77	29318.90	14278.77

TABLE 1.—Continued

$(3d^3 + 3d^2 4s)$

7/2 / 7/2	b^2F	b^4F	a^2G	a^2F	a^4F	b^2G
	20891.88	1087.21	8997.69	4897.60	225.47	15265.60
$y^4D°$	0.003	0.03	0.001	0.005	0.004	0.0001
		2517.43		2784.67	2464.00	
40798.37	19906.49	39711.16	31800.68	35900.77	40572.90	25532.77
$z^4D°$	0.0004	0.07	0.0000	0.006	0.24	0.0000
		3155.67		3587.13	3072.11	
32767.02	11875.14	31679.81	23769.33	27869.42	32451.55	17501.42
$y^2F°$	0.10	0.002	0.03	0.17	0.0002	0.002
	5211.58			2841.94		
40074.71	19182.83	38987.50	31077.02	35177.11	39849.24	24809.11
$z^2F°$	0.17	0.02	0.007	2.21	0.04	0.001
		3288.13	4444.56	3759.30	3197.52	
31490.82	10598.94	30403.61	22493.13	26593.22	31265.35	16225.22
$x^2F°$	0.36	0.0000	0.01	0.01	0.0000	0.08
	3761.89					3104.60
47466.80	26574.92	46379.59	38469.11	42569.20	47241.33	32201.20
$(3d^2 4p)$						
$z^4F°$	0.005	0.58	0.0001	0.05	2.04	0.0000
		3329.46		3813.39	3236.57	
31113.61	10221.73	30026.40	22115.92	26216.01	30888.14	15848.01
$z^2G°$	0.0004	0.0001	0.31	0.09	0.0005	0.18
			3913.46	3372.21	2913.08	5185.90
34543.36	13651.48	33456.15	25545.67	29645.76	34317.89	19277.76
$y^2G°$	0.003	0.0000	0.008	0.005	0.0000	2.63
			2877.44	2573.72		3510.84
43740.77	22848.89	42653.56	34743.08	38843.17	43515.30	28475.17
$z^4G°$	0.0002	0.02	0.0001	0.003	0.33	0.0000
		3489.74		4025.14	3387.84	
29734.45	8842.57	28647.24	20736.76	24836.85	29508.98	14468.85

TABLE 1.—Continued

$(3d^3 + 3d^24s)$

	7/2 / 9/2, 11/2	b^2F	b^4F	a^2G	a^2F	a^4F	b^2G
		20891.88	1087.21	8997.69	4897.60	225.47	15265.60
$(3d^24p)$	$z^4F°$	0.0000	0.09 3308.81	0.0000	0.002	0.24 3217.06	0.0000
	31300.92	10409.04	30213.71	22303.23	26403.32	31075.45	16035.32
	$z^2G°$	0.04	0.0000	0.01	3.16 3349.04	0.0001 2895.81	0.0007
	34748.50	13856.62	33661.29	25750.81	29850.90	34523.03	19482.90
	$y^2G°$	0.25 4367.66	0.0000	0.01 2874.68	0.10 2571.03	0.0000	0.05 3505.91
	43780.99	22889.11	42693.78	34783.30	38883.39	43555.52	28515.39
	$z^4G°$	0.0000	0.10 3461.50	0.0000	0.0000	3.09 3361.21	0.0000
	29968.08	9076.20	28880.87	20970.39	25070.48	29742.61	14702.48
	$z^2H°$	0.0001	0.0000	0.02 2725.78	0.0000	0.0000	3.30 3287.66
	45673.75	24781.87	44586.54	36676.06	40776.15	45448.28	30408.15

TABLE 1.—Continued

$(3d^3+3d^24s)$

$(3d^24p)$	9/2, , 11/2 / 7/2	b^4F 1215.58	a^2G 9118.15	a^2H 12676.99	a^4F 393.22	b^2G 15257.53
	$y^4D°$ 40798.37	0.28 2525.60 39582.79	0.03 31680.22	0.0000 28121.38	0.04 2474.22 40405.15	0.006 25540.84
	$z^4D°$ 32767.02	0.56 3168.52 31551.44	0.0007 23648.87	0.0000 20090.03	2.36 3088.02 32373.80	0.0000 17509.49
	$y^2F°$ 40074.71	0.01 38859.13	0.70 3229.42 30956.56	0.002 3648.87 27397.72	0.003 2519.31 39681.49	0.12 4028.34 24817.18
	$z^2F°$ 31490.82	0.0001 3302.09 30275.24	0.30 4468.50 22372.67	0.0001 18813.83	0.02 3214.75 31097.60	0.0000 16233.29
	$x^2F°$ 47466.80	0.0000 46251.22	0.0000 38348.65	0.0001 34789.81	0.0000 47073.58	2.63 3103.80 32209.27
	$z^4F°$ 31113.61	0.09 3343.77 29898.03	0.009 4545.14 21995.46	0.0001 18436.62	0.24 3254.25 30720.39	0.0000 15856.08
	$z^2G°$ 34543.36	0.0000 33327.78	0.03 3932.02 25425.21	0.66 4571.98 21866.37	0.0000 34150.14	0.001 5183.73 19285.83
	$y^2G°$ 43740.77	0.0000 42525.19	0.01 2887.46 34622.62	0.90 3218.27 31063.78	0.0000 43347.55	0.06 3509.85 28483.24
	$z^4G°$ 29734.45	0.0005 28518,87	0.0002 20616.30	0.0003 17057.46	0.006 3407.20 29341.23	0.0000 14476.92

TABLE 1.—Concluded

$(3d^3 + 3d^24s)$

$(3d^24p)$ 9/2, 11/2 \ 9/2, 11/2	b^4F	a^2G	a^2H	a^4F	b^2G	a^2H
	1215.58	9118.15	12676.99	393.22	15257.53	12774.81
$z^4F°$	0.91	0.0001	0.0000	3.10	0.0004	0.0001
	3322.94			3234.52		
31300.92	30085.34	22182.77	18623.93	30907.70	16043.39	18526.11
$z^2G°$	0.0005	0.38	0.02	0.003	0.24	0.81
		3900.54	4529.46	2909.92	5129.15	4549.63
34748.50	33532.92	25630.35	22071.51	34355.28	19490.97	21973.69
$y^2G°$	0.0000	0.01	0.03	0.0000	3.33	1.09
		2884.11	3214.12		3504.89	3224.24
43780.99	42565.41	34662.84	31104.00	43387.77	28523.46	31006.18
$z^4G°$	0.01	0.0000	0.0000	0.35	0.0000	0.30
	3476.99			3380.28		
29968.08	28752.50	20849.93	17291.09	29574.86	14710.55	17193.27
$z^2H°$	0.0000	0.004	0.0000	0.0009	0.05	0.009
			3029.73		3286.78	3038.71
45673.75	44458.17	36555.60	32996.76	45280.53	30416.22	32898.94
$z^4G°$	0.13	0.0000	0.0000	4.00	0.0000	0.0000
	3444.31			3349.41		
30240.68	29025.10	21122.53	17563.69	29847.46	14983.15	17465.87
$z^2H°$	0.0000	0.02	0.01	0.0000	4.02	0.47
		2717.29	3008.33		3261.60	3017.19
45908.56	44692.98	36790.41	33231.57	45515.34	30651.03	33133.75

References

[1] Condon, E. U., and Shortley, G. H., The Theory of Atomic Spectra (Cambridge Univ. Press, New York, 1935).
[2] Mendlowitz, H., Astroph. J. **138,** 1277 (1963).
[3] Mendlowitz, H., Astroph. J. **141,** 573 (1966).
[4] Mendlowitz, H., Astroph. J. **154,** 1099 (1968).
[5] Russell, H. N., Astroph. J. **46,** 283 (1927).
[6] Moore, C. E., Atomic Energy Levels, NBS Circ. 467 (1949).

(Paper 73A1–534)

JOURNAL OF RESEARCH of the National Bureau of Standards—A. Physics and Chemistry
Vol. 73A, No. 1, January–February 1969

Morphological Stability of a Cylinder

Sam R. Coriell and Stephen C. Hardy

Institute for Materials Research, National Bureau of Standards, Washington, D.C. 20234

(August 27, 1968)

The stability of the shape of a solid cylinder crystallizing in a supercooled liquid is treated. The effects of solute diffusion, slightly anisotropic surface tension and interface kinetics are included. The resulting stability equations are applied to the specific case of ice cylinders.

Key Words: Cylinder; ice; interface kinetics; morphological stability; solute diffusion; surface tension.

1. Introduction

The stability of the shape of a solid growing by diffusion or heat flow was first studied by Mullins and Sekerka [1][1], who determined the stability criteria for a sphere. The cylindrical geometry has been treated by Coriell and Parker [2] and Kotler and Tiller [3]. These studies assumed that the interface properties were isotropic. Cahn [4] has taken account of slightly anisotropic surface free energy for the sphere. Recently, we have made experimental studies [5, 6] of the morphological stability of ice cylinders. In connection with this experimental program, it appears desirable to work out the stability of a cylindrical shape taking account of slightly anisotropic surface tension and interface kinetics. In this paper we treat the case of a cylinder crystallizing from a binary melt; it is assumed that the surface tension and kinetic coefficient are slightly anisotropic. For the case of isotropic interface properties, the problem reduces to the case previously treated by Kotler and Tiller [3].

Although our calculation is general, we are particularly interested in the case of an ice cylinder growing from pure water and from water with impurities added. We present some specific calculations for these cases.

2. Formulation and Calculation

We wish to solve Laplace's equation [1, 2] for the temperature T and concentration C of impurity. The subscripts S and L denote solid and liquid, respectively, while a subscript I denotes that the quantity is to be evaluated at the interface. We assume a slightly perturbed cylinder of shape [2]

$$r = R + \delta e^{ik\Phi} e^{i2\pi z/\lambda}, \tag{1}$$

where r, Φ, and z are the usual cylindrical coordinates, R is the radius of the unperturbed cylinder, δ is the amplitude of the perturbation ($\delta/R \ll 1$), and k and λ determine the shape of the perturbation. Neglecting diffusion in the solid, the equations to be solved are

$$\nabla^2 T_L = \nabla^2 T_S = \nabla^2 C_L = 0 \tag{2}$$

with the auxiliary equations

$$T_L(R_b) = T_b \tag{3a}$$

$$T_S(0) - \text{finite} \tag{3b}$$

$$T_{LI} = T_{SI} \tag{3c}$$

$$C_L(R_c) = C_b \tag{3d}$$

$$v = \frac{k_S}{L_v}\left(\frac{\partial T_S}{\partial r}\right)_I - \frac{k_L}{L_v}\left(\frac{\partial T_L}{\partial r}\right)_I \tag{3e}$$

$$v = \left\{\sum_k \mu_k e^{ik\Phi}\right\}\{T_e - T_{LI}\} \tag{3f}$$

$$v = \frac{-D_L}{C_{LI}(1-j)}\left(\frac{\partial C_L}{\partial r}\right)_I \tag{3g}$$

$$v = \dot{R} + \dot{\delta} e^{ik\Phi} e^{i2\pi z/\lambda} \tag{3h}$$

$$T_e = T_M - T_M K\left\{\sum_k \Gamma_k e^{ik\Phi}\right\} - mC_{LI} \tag{3i}$$

[1] Figures in brackets indicate the literature references at the end of this paper.

324-194 O-69—5

and

$$K=\frac{1}{R}+\frac{\delta}{R^2}\,(k^2+k_z^2-1)e^{ik\Phi}e^{i2\pi z/\lambda}. \tag{3j}$$

In the above equations R_b is the bath radius, T_b (a constant) is the temperature at R_b, R_c is the radius at which the concentration of impurity is C_b (a constant), v is the velocity of the interface, k_S and k_L are the thermal conductivities of the solid and liquid, respectively, L_v is the latent heat per unit volume of the solid, the $\left(\sum_k \mu_k e^{ik\Phi}\right)$ is the slightly anisotropic linear kinetic coefficient,[2] T_e is the equilibrium temperature of the interface, D_L is the solute diffusion coefficient, j is the partition coefficient (the ratio of the equilibrium concentration of solute on the solid side of the interface to that on the liquid side of the interface), $\dot{R}$ and $\dot{\delta}$ are the rate of growth of the unperturbed cylinder and the perturbation, respectively, T_M is the melting point of a flat interface, K is the curvature of the perturbed cylinder, the $\left(\sum_k \Gamma_k e^{ik\Phi}\right)$ is the slightly anisotropic capillary constant, m is the freezing point lowering constant, and $k_z=2\pi R/\lambda$. The solution of Laplace's equation in cylindrical coordinates is of the form $C_1+C_2\ \ln\ r+e^{ik\Phi}e^{i2\pi z/\lambda}[C_3I_k(k_zr/R)+C_4K_k(k_zr/R)]$ where the C's are constants and I_k and K_k are modified Bessel functions. A solution of this form is written for T_L, T_S, and C_L and the constants are determined by the boundary conditions. Since we are treating small perturbations and slightly anisotropic surface tension and interface kinetics, we neglect all terms that are greater than first order in δ, μ_k, and Γ_k $(k\neq 0)$, i.e., we omit terms containing δ^2, $\delta\mu_k$, $\delta\Gamma_k$, $\Gamma_k\mu_k$, etc., $(k\neq 0)$. Although the calculation is tedious, it is straightforward and we will not reproduce the details here. We define $A_b=\ln\,(R_b/R)$, $A_c=\ln\,(R_c/R)$,

$$\Delta T=T_M-(T_M\Gamma_0/R)-T_b, \qquad \Delta\theta=\Delta T-mC_b$$

$$\beta_A=(k_L/RL_v\mu_0)+A_b, \qquad \xi=[(1-j)k_LA_C]/[DL_v]$$

$$A_1=[K_k(k_zR_b/R)/I_k(k_zR_b/R)],$$

$$D_1=[K_k(k_zR_c/R)/I_k(k_zR_c/R)],$$

$$J_A=-k_z\{[K_k'(k_z)-A_1I_k'(k_z)]/[K_k(k_z)-A_1I_k(k_z)]\},$$

$$J_D=-k_z\{[K_k'(k_z)-D_1I_k'(k_z)]/[K_k(k_z)-D_1I_k(k_z)]\},$$

$$H_I=k_zI_k'(k_z)/I_k(k_z),$$

where the prime indicates the derivative with respect to k_z. The results of the calculation are

$$\dot{R}=(k_L/RL_vA_b)\,(DT), \tag{4a}$$

where (DT) is given by

$$(DT)=A_b\left[\frac{1}{2\xi}+\frac{\Delta T}{2\beta_A}\right]-\left|A_b\left\{\left[\frac{1}{2\xi}+\frac{\Delta T}{2\beta_A}\right]^2-\frac{\Delta\theta}{\beta_A\xi}\right\}^{1/2}\right|. \tag{4b}$$

For the ratio $(\dot{\delta}/\delta)/(\dot{R}/R)$ we obtain

$$\frac{\dot{\delta R}}{\delta\dot{R}}=\left\{1+\frac{\alpha}{\mu_0}+\frac{m\alpha}{\nu}\right\}^{-1}\left\{J_A-1+\frac{m\alpha}{\nu}\,(J_D-1)+\frac{[J_A+(k_S/k_L)H_I]A_b}{(DT)}\left[\frac{\dot{R}R\mu_k}{\delta\mu_0^2}-\frac{T_M\Gamma_k}{\delta}-\frac{T_M\Gamma_0(k^2+k_z^2-1)}{R}\right]\right\}, \tag{4c}$$

where $\alpha=(k_L/L_VR)\,(J_A+k_SH_I/k_L)$

and

$$\nu=\frac{k_LA_C}{L_VRC_b\xi}\left[1-\frac{\xi(DT)}{A_b}\right]\left[J_D-\frac{\xi(DT)}{A_CA_b}\right].$$

In the above equations Γ_k and $\mu_k(k\neq 0)$ are zero if $k_z\neq 0$, i.e., the anisotropic terms only effect Φ-type perturbations and have no effect on perturbations along the axis of the cylinder. This follows, for example, since there are no terms of the form $\Gamma_{k,\,k_z}e^{ik\Phi}e^{i2\pi z/\lambda}$ in eq (3i) (see footnote 2).

Thus one of the important results of this calculation is that the growth rate of z-perturbations is independent of slightly anisotropic surface tension and kinetic coefficient.

Discussion

The general results of our stability analysis are given by eqs (4a–c). In this section, we apply these equations to the special case of ice cylinders (oriented with the c-axis of ice parallel to the cylinder axis) growing in slightly supercooled water ($\Delta T\cong 0.1$ °C). We also consider the case in which impurities have been added to the water. We are interested in the case where R lies between 0.04 cm and 0.25 cm; the bath radius R_b in most of the experimental work was 0.875 cm. Under the above conditions we can simplify the equations by neglecting interface kinetics, i.e., we take $1+\frac{\alpha}{\mu_0}\cong 1$. This implies that $(k_L/RL_V)\,(J_A+H_Ik_S/k_L)\ll\mu_0$; typically $(J_A+H_Ik_S/k_L)<100$ and the above approximation is valid if $\mu_0\gg .05$ cm deg^{-1} sec^{-1}.

[2] The kinetic coefficient and the capillary constant can be written in this form since we are only considering first order terms in the perturbation amplitude and in the anisotropy. In general, for example, the kinetic coefficient μ can be expanded as

$$\mu=\sum_k\int dk_z\mu_k(k_z)e^{ik\Phi'}e^{ik_zz'(k)}$$

where Φ' and z' give the orientation of the surface. For a slightly perturbed cylinder, the orientational coordinates z' and Φ' are related to the space coordinates z and Φ by $z'=0+\delta a_1$ and $\Phi'=\Phi+\delta a_2$, where a_1 and a_2 are functions of Φ and z. Substituting these expressions in the expansion of μ, expanding the exponentials, neglecting terms of the order $\mu_k(k_z)\delta$, and performing the integral over k_z we obtain $\mu=\Sigma\mu_ke^{ik\Phi}$, where $\mu_k=\int dk_z\mu_z(k_z)$. A similar procedure gives $\Gamma=\sum_k\Gamma_ke^{ik\Phi}$; here Γ is $(1/L_V)(\gamma+d^2\gamma/d\Phi^2)$ where γ is the surface tension.

Although the interface kinetic coefficient for ice growing perpendicular to the c-axis is not known, a lower bound can be obtained from bath undercooling measurements. For example, Lindenmeyer et al. [7], observed a growth velocity of 1 cm sec^{-1} at a bath undercooling of 2 °C. Assuming a linear law, this gives $\mu_0 > .5$ cm sec^{-1} deg^{-1} [8]. Since μ_0 may be orders of magnitude greater than this, it appears valid to neglect interface kinetics. It follows that $\beta_A \cong A_b$.

It is almost always (and certainly under the experimental conditions of interest) valid to neglect the A_1 and D_1 terms in the definition of J_A and J_D. Defining $H_K = -k_z K_k'(k_z)/(K_k(k_z))$, we then have $J_A \cong H_K \cong J_D$. With this approximation and the neglect of interface kinetics, eqs (4b) and (4c) can be written

$$(DT) = \tfrac{1}{2}([(A_b/\xi) + \Delta T] - |\{[A_b/\xi) + \Delta T]^2 - 4\Delta\theta A_b/\xi\}^{1/2}|) \qquad (5a)$$

and

$$\frac{\dot{\delta R}}{\delta \dot{R}} = H_K - 1 + \frac{[H_K + (k_S/k_L)H_1]A_b}{(1 + m\alpha/\nu)DT} \times \left[\frac{\dot{R}R\mu_k}{\delta\mu_0^2} - \frac{T_M\Gamma_k}{\delta} - \frac{T_M\Gamma_0(k^2 + k_z^2 - 1)}{R}\right]. \qquad (5b)$$

For pure water, there is further simplification, viz, taking $m = 0$ and $\xi \to 0$,

$$(DT) = \Delta T \qquad (6a)$$

and

$$\frac{\dot{\delta R}}{\delta \dot{R}} = H_K - 1 + \frac{[H_K + (k_S/k_L)H_1]A_b}{DT} \times \left[\frac{\dot{R}R\mu_k}{\delta\mu_0^2} - \frac{T_M\Gamma_k}{\delta} - \frac{T_M\Gamma_0(k^2 + k_z^2 - 1)}{R}\right]. \qquad (6b)$$

Recalling that for a $k_z \neq 0$ perturbation $\mu_k = 0$ and $\Gamma_k = 0$ ($k \neq 0$), eq (6b) becomes

$$\frac{\dot{\delta R}}{\delta \dot{R}} = H_K - 1 - \frac{T_M\Gamma_0(k^2 + k_z^2 - 1)A_b[H_K + (k_S/k_L)H_1]}{R(DT)}. \qquad (6c)$$

This equation has been used in references 5 and 6 to analyze the experimental data.

We now give a brief discussion of the choice of the bath boundary conditions, i.e., the choice of R_b and R_c; we also discuss the use of Laplace's equation. For an infinite bath, the choice of these parameters has been previously discussed [2]. For an infinite bath $R_b = R_\lambda$ where $R_\lambda = R/(1.33\lambda)$ and λ satisfies

$$\lambda^2 e^{\lambda^2} Ei(-\lambda^2) + S = 0.$$

In the above equation Ei is the exponential integral function and for heat flow $S = S_T = C_v(T_I - T_b)/L_v$ and for impurity diffusion [9] $S = S_c = (C_{LI} - C_b)/C_{LI}(1 - j)$. In these equations T_b and C_b are the temperature and concentration at infinity, respectively, and C_v is the specific heat per unit volume of the liquid. In order for Laplace's equation to be valid, it is necessary that $S_T \ll 1$ and $S_c \ll 1$. Since $S_T \cong \left(\frac{1}{73}\right)\Delta T$, it is clear that for $\Delta T < 1$, $S_T \ll 1$. Using the solution of the diffusion equation, we may rewrite S_c as $S_c = (A_c/A_b)(k_1/DL_v)DT$. Taking $k_L = 1.33(10^{-3})$ cal cm^{-1} deg^{-1} sec^{-1}, $L_v = 73.4$ cal cm^{-3}, $D = 10^{-5}$ cm^2 sec^{-1}, and $(A_c/A_b) \cong 1$, we have $S_c \cong 1.8$ (DT). For $DT = 0.1$, $S_c \cong 0.2$, and Laplace's equation is a reasonable approximation. For larger (DT) and for smaller diffusion constants, there may well be deviations from Laplace's equation.

In the actual experiments the temperature is maintained at T_b at some radius, say R_a. If $R_a < R_\lambda$, it seems reasonable to take $R_b = R_a$ and this has been done [5, 6]. If $R_a > R_\lambda$, it is better to take $R_b = R_\lambda$. If this were not done, i.e., if instead we let $R_b = R_a$ when $R_a > R_\lambda$, then from eq (4a) we would predict that $\dot{R}$ is larger when $T_L(\infty) = T_b$ than when $T_L(R_a) = T_b$. This is obviously wrong and hence for $R_a > R_\lambda$ we take $R_b = R_\lambda$. When $R_a < R_\lambda$, there is a certain error in taking $R_b = R_a$, but this error lies within the experimental error in measuring ΔT and $\dot{R}$. The choice of R_c is even more complicated since the average concentration in the liquid changes as solute is rejected from the ice. Fortunately for many cases the results are not very sensitive to the choice of R_c and for calculational purposes we take $R_c = R_a$. The proper choice of R_c and R_b can be studied experimentally by comparing the observed growth rate $\dot{R}$ of the unperturbed cylinder with the theoretical $\dot{R}$.

We present some calculations of δ as a function of R for the special case where $(\dot{\delta R}/\delta\dot{R})$ is given by eq (6c). Following Cahn [4] we use the relationship $(\dot{\delta R}/\delta\dot{R}) = (R/\delta)(d\delta/dR)$. Denoting the right hand side of eq (6c) by $f(R)$, we have

$$\frac{d\ln\delta}{dR} = \frac{f(R)}{R}. \qquad (7a)$$

Integrating yields

$$\ln(\delta/\delta_0) = \int_{R_0}^{R} \frac{f(x)}{x}\,dx, \qquad (7b)$$

where δ_0 is the value of δ at $R = R_0$. The integral has been evaluated numerically for various values of the parameters occurring in $f(R)$. In many cases over small ranges of R, $\ln\delta$ is to a good approximation linear with R. This is illustrated in table 1 which gives $(d\ln\delta/dR)$ as a function of R. From table 1, it is seen that $(d\ln\delta/dR)$ changes very slowly with R. Since in the experimental measurements of δ versus R, R varies by about 0.02 to 0.03 cm and R is greater than 0.120 cm, it is to be expected that plots of the experimental data in the form $\ln\delta$ versus R will appear linear.

Of interest is the wavelength dependence of the δ versus R curves. This is shown in table 2 for three different wavelengths. We can consider δ/δ_0 as an amplification factor, that is, it gives the relative magnitude of δ at R as compared to δ at R_0. As seen from the table, these amplification factors are very large. Experimentally values of δ of $3(10^{-3})$ cm have been observed at $R \cong 0.175$ cm. Extrapolating to $R = 0.05$ cm gives a value of $\delta \cong 10^{-7}$ cm as the size of the initial perturbation. It is clear from table 2 that the amplification factor is a function of wavelength. For small R, perturbations with $\lambda = 0.045$ cm are amplified slightly more than perturbations corresponding to the other wavelengths of the table. For larger R, however, the amplification is greatest for $\lambda = 0.055$. Calculations similar to these will be useful in attempting to predict the wavelength of the perturbation which appears on a growing cylinder. However, such a prediction requires some assumption about the initial distribution of the amplitudes of the perturbations of various wavelengths.

We wish to discuss the effect of solute on the stability equations. It is interesting that for no anisotropy and zero surface tension, the addition of solute has no effect on $(\dot{\delta}/\delta)/(\dot{R}/R)$, i.e., eqs (5b) and (6b) are identical. The addition of solute changes the unperturbed growth rate by changing DT. For a bath undercooling $\Delta T = 0.1$, the value of (DT) for various values of mc_b are given in table 3.

Also of interest is the factor $1 + (m\alpha/\nu)$ appearing in eq (5b). It can be shown that

$$(m\alpha/\nu) \cong (k_L/DL_\nu)(mc_b)(1 + k_S/k_L) \cong 9\ (mc_b).$$

Thus for $mc_b < 0.1$ deg., $1 + (m\alpha/\nu)$ varies from 1 to 2. Since DT varies more rapidly than this, the main effect of adding solute is to decrease DT and thus to increase the magnitude of the last term in eq (5b). Thus for fixed ΔT adding solute makes $(\dot{\delta}/\delta)/(\dot{R}/R)$ smaller, thus stabilizing the cylinder. On the other hand for fixed (DT), which corresponds to not changing the unperturbed velocity $\dot{R}$, the addition of solute increases $(\dot{\delta}/\delta)/(\dot{R}/R)$ and consequently makes the cylinder more unstable. The above statements assume that the Γ_0 term is the dominant term inside the bracket of eq (5b) and that the addition of solute does not change the physical properties such as the surface tension. If solute is adsorbed at the interface, one expects a lowering of the surface tension. One method of studying such effects is to add a very small amount of solute, e.g., 10^{-4} M NaCl in which case $mc_b \cong 4(10^{-4})$. From the preceding calculations, it is clear that $DT \cong \Delta T$ and $1 + (m\alpha/\nu) \cong 1$ so that eqs (6a) and (6b) can be used. Thus any difference between experimental results for distilled water and water containing 10^{-4} M of impurities should probably be attributed to a change in the surface tension due to adsorption at the interface.

In summary, we have analyzed the stability of a solid cylinder growing by heat flow into a binary melt and have taken account of any small anisotropy in the interface properties. In particular, we have provided a theoretical framework for the experimental study of the stability of ice cylinders.

TABLE 1. *(d ln δ/dR) as a function of* R *for* $\lambda = 0.055$ *cm;* $\gamma = 0.018$ *J/m² and* $\Delta T = 0.1$ *deg.*

R(cm)	$(d \ln \delta/dR)$ (cm^{-1})
0.100	85.8
.110	84.3
.120	82.9
.130	81.7
.140	80.7
.150	79.7
.160	78.9
.170	78.1
.180	77.4
.190	76.8
.200	76.3

TABLE 2. *Effect of wavelength on* δ/δ_0 *for* $\gamma = 0.018$ *J/m² and* $\Delta T = 0.1$ *deg.*

R(cm)	(δ/δ_0)		
	$\lambda = 0.045$ cm	$\lambda = 0.055$ cm	$\lambda = 0.065$ cm
0.050	1.00	1.00	1.00
.075	$1.08(10^1)$	$1.07(10^1)$	9.88
.100	$9.85(10^1)$	$9.70(10^1)$	$8.16(10^1)$
.125	$7.80(10^2)$	$7.91(10^2)$	$6.07(10^2)$
.150	$5.53(10^3)$	$5.99(10^3)$	$4.22(10^3)$
.175	$3.59(10^4)$	$4.28(10^4)$	$2.80(10^4)$
.200	$2.17(10^5)$	$2.93(10^5)$	$1.80(10^5)$

TABLE 3. *Value of effective undercooling* (DT) *as a function of added solute for bath undercooling* $\Delta T = 0.1$ °C ($\xi/A_b = 1.8$ deg^{-1} *used in the calculation)*

mc_b	DT
0.001	0.0988
.01	.0881
.02	.0768
.04	.0556
.06	.0359
.08	.0174

4. References

[1] Mullins, W. W., and Sekerka, R. F., J. Appl. Phys. **34,** 323 (1963).
[2] Coriell, S. R., and Parker, R. L., J. Appl. Phys. **36,** 632 (1965).
[3] Kotler, G. R., and Tiller, W. A., Crystal Growth, Supplement to J. Phys. Chem. Solids, edited by H. S. Peiser (Pergamon Press, Oxford, 1967), p. 721.
[4] Cahn, J., Ref. 3, p. 681.
[5] Hardy, S. C., and Coriell, S. R., J. Appl. Phys. **39,** 3505 (1968).
[6] Hardy, S. C., and Coriell, S. R., Proceedings of the 1968 International Conference on Crystal Growth.
[7] Lindenmeyer, C. S., Orrok, G. T., Jackson, K. A., and Chalmers, B., J. Chem. Phys. **27,** 822 (1957).
[8] In a paper presented at the 1968 International Conference on Crystal Growth, Kotler and Tarshis obtain a value of 16 cm/sec. deg. for μ_0 from a theoretical analysis of dendritic growth experiments.
[9] Frank, F. C., Proc. Roy. Soc. (London) **A201,** 586 (1950).

(Paper 73A1–535)

JOURNAL OF RESEARCH of the National Bureau of Standards—A. Physics and Chemistry
Vol. 73A, No. 1, January–February 1969

Distorted Tetrahedra in Strontium Copper Åkermanite

Jun Ito and H. Steffen Peiser

Institute for Materials Research, National Bureau of Standards, Washington, D.C. 20234

(September 26, 1968)

New analogs of åkermanite: $Sr_2CuSi_2O_7$ and $Sr_2CdSi_2O_7$ as well as many previously synthesized analogs were obtained by a simple technique consisting of heating in air of precipitated gels of the right composition. X-ray data revealed an anomaly of the Cu^{2+} and (to a lesser extent) Fe^{2+} åkermanites which is explained by a simple geometric argument in terms of a small ($\sim 3°$) angular distortion of the oxygen tetrahedron surrounding the smaller divalent cation. This interpretation is consistent with previous theoretical discussions and Mössbauer data on the iron analog prepared for this study. Single crystals of cobalt åkermanites can be grown from a sodium tungstate flux.

Key Words: Åkermanite; crystal chemistry; crystal growth; cupric silicate; flux growth; ion polyhedron distortion; melilite; Mössbauer spectroscopy; silicate gels; silicate synthesis; x-ray powder data.

1. Introduction

Nuclear magnetic resonance, Mössbauer and other spectroscopies are providing highly sensitive techniques for exploring symmetries and distortions of ionic polyhedra in crystals [1, 2].[1] Too few have been the crystal-chemical studies based on geometric considerations and specifically aimed at exploring symmetries of ionic environments. The purpose of this investigation was to present an example for demonstrating the power of one simple crystal-chemical method and to reveal data bearing upon their limitations especially in sensitivity. The method consists in the synthesis of a number of isostructural compounds followed by measurement and interpretation of their accurate lattice or structural parameters. The specific aim in our example is to look for distortion of tetrahedra of divalent copper ions in silicates having the melilite structure. Divalent copper ion usually causes strong distortion in both octahedral and tetrahedral sites [3, 4].

2. Syntheses and Cell Data

The structure of åkermanite type minerals,

$$M_2^{2+}(8)M^{2+}(4)Si_2O_7;$$

$M^{2+}(8) = Ca$, Sr and Ba, $M^{2+}(4) = Cd$, Mn, Fe^{2+}, Zn, Cu, Co, Mg, and Be, was determined by Warren [5] and Smith [6]. It consists of two equivalent (SiO_4) tetrahedra sharing a corner on a twofold axis to form a Si_2O_7 group, and one [$M^{2+}O_4$] tetrahedron located at the corners and the *C*-face centers of the tetragonal P42m cell. These tetrahedra are arranged in a sheet-like pattern parallel to (001). The sheets are held together along *c* by weaker $M^{2+}(8)$–0 linkages (fig. 1a).

Two new analogs, $Sr_2CuSi_2O_7$ and $Sr_2CdSi_2O_7$ were synthesized by heating in air precipitated gels of the right composition. The following compounds with the åkermanite structure were also synthesized but these have been reported previously: $Ca_2BeSi_2O_7$ [7, 8], $Ca_2MgSi_2O_7$ [9, 10], $Ca_2ZnSi_2O_7$ [11], $Sr_2ZnSi_2O_7$ [12], $Ca_2CoSi_2O_7$ and $Sr_2CoSi_2O_7$ [13], and $Sr_2FeSi_2O_7$, $Sr_2MnSi_2O_7$, $Ba_2FeSi_2O_7$, $Ba_2MnSi_2O_7$ [14]. The other analogs such as $Ca_2CuSi_2O_7$, $Ca_2NiSi_2O_7$ and $Sr_2NiSi_2O_7$ could not be obtained by our method of synthesis.

The compositional stability range for åkermanite-type compounds thus obtained is illustrated in terms of $M^{2+}(8)$ and $M^{2+}(4)$ ions in figure 2. The unit-cell dimensions measured by the x-ray method, conditions for the syntheses, and some of the physical properties are given in table 1. Indexed *d*-spacings, standardized internally with Si, for Sr, Cu- and Sr, Cd åkermanites are given in table 2.

All the unit-cell dimensions and the *c*/*a* ratio are plotted against the recognized value of the ionic radius [15] of the smaller cation of each Sr-analog in figure 3. All the data used in these diagrams are taken from the compounds synthesized for this study by the same method. The variation of the unit-cell dimensions for each of the analogs relative to the established ionic radii is fairly smooth except for those of the Cu^{2+}- and Fe^{2+}-analogs (fig. 3).

[1] Figures in brackets indicate the literature references at the end of this paper.

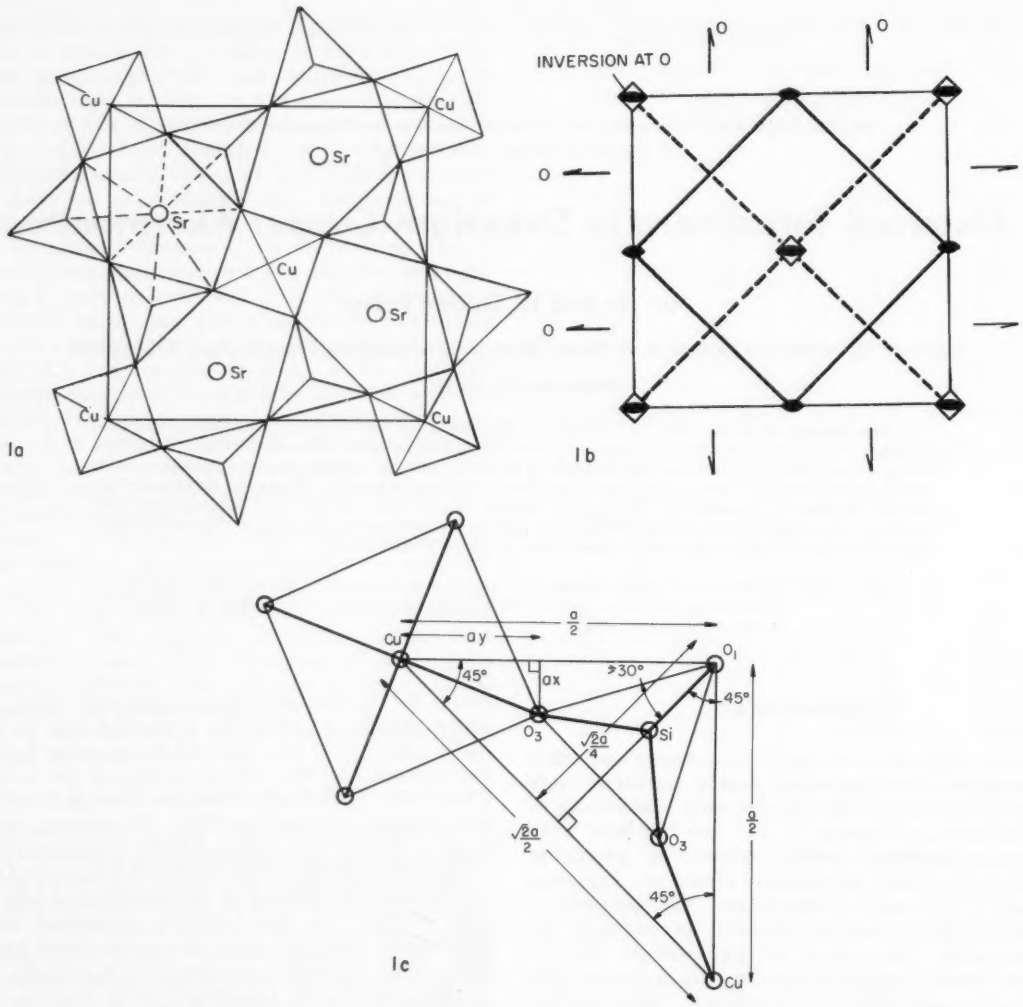

FIGURE 1. *(a) The structure of Sr,Cu-åkermanite projected on (001) [after references 5 and 6]. (b) Symmetry of Sr,Cu-åkermanite structure ($P\bar{4}2_1m$) (Notation as in International Crystallographic Tables, Kynoch Press, 1952). (c) Schematic detail of geometry of (001) sheet (difference in size of tetrahedra exaggerated).*

3. Geometric Considerations

The geometry of the (001) sheet (fig. 1a) of oxygen tetrahedra is overdetermined by:

(i) The *a*-cell parameter directly and accurately measurable by x-ray powder data.

(ii) The established space-group symmetry, $P\bar{4}2_1m$, including a twofold axis parallel to the *z* axis on which lies the unique oxygen of the Si_2O_7 group; the $\bar{4}$ inversion point on which the $M^{2+}(4)$ ion is situated; and the diagonal mirror plane parallel to the *z* axis ensuring for example that the O_1-Si direction projected on (001) is at 45° to the *x* and *y* axes. (See fig. 1b.)

(iii) The sum of the ionic radii; with an uncertainty of about 1 percent in some values for

$$R_{M\text{-}O} = \{R[M^{2+}(4)] + R[O^{2-}]\},$$

for example when M^{2+} is Cu.

(iv) The "tetrahedral angles" $2\varphi_{Si}$ and $2\varphi_M$ bisected by the *z*-axis direction. It is unlikely that $2\varphi_{Si}$ departs greatly from 109½°, and even if it did it would be even less likely to be greatly dependent on the nature of the $M^{2+}(4)$ ion. Angle $2\varphi_M$ is thus the only "tetrahedral angle" subject to wide variations.

Algebraically the three variable cell coordinates (*xyz*) for the oxygen (O_3 in fig. 1a) shared by the Si and M^{2+} tetrahedra are related by five independent equations (see fig. 1c). The first two are derived from the horizontal tetrahedron edge; the third relates to an inclined tetrahedron edge; the fourth and fifth are

TABLE 1. *The unit-cell dimensions, the physical properties, and the conditions for the syntheses of åkermanites*

$CuK_{\alpha_1} = 1.54050 \times 10^{-10}$ m(Å)

Formulas	a in $m \times 10^{-10}$ (Å)	c in $m \times 10^{-10}$ (Å)	c/a	V in $m^3 \times 10^{-30}$ (Å^3)	Sp. Gr.	Temp. (°C)	Pressure bars	Time hr	Index of refraction N (mean value)	Color
$Ca_2CoSi_2O_7$	7.835	5.025	0.6413	309.9	3.26	950	1	24	1.650	Blue.
$Ca_2ZnSi_2O_7$	7.829	5.017	.6408	307.5	.....	1100	1	20	.....	Colorless.
$Ca_2MgSi_2O_7$	7.800	5.012	.6425	304.9	.....	1050	1	20	.....	Colorless.
$Ca_2BeSi_2O_7$	7.416	4.995	.6735	274.7	.....	1050	1	20	.....	Colorless.
$Sr_2CdSi_2O_7$	8.228	5.188	.6305	351.2	.....	900	1	20	1.67	Colorless.
$Sr_2MnSi_2O_7$	8.121	5.164	.6358	339.7	.....	750	3,000	48	1.645	Greenish white.
$Sr_2FeSi_2O_7$	8.108	5.122	.6317	336.7	.....	750	3,000	48	1.665	Dark brown.
$Sr_2CuSi_2O_7$	8.087	5.076	.6276	331.9	.....	950	1	20	.....	Black.
$Sr_2CoSi_2O_7$	8.021	5.157	.6428	331.7	3.98	950	1	48	.....	Dark blue.
$Sr_2ZnSi_2O_7$	7.999	5.169	.6462	330.7	.....	1100	1	20	.....	Colorless.
$Sr_2MgSi_2O_7$	7.999	5.156	.6445	329.9	.....	900	1	20	.....	Colorless.

TABLE 2. *X-ray powder data for* Sr, Cu- *and* Sr, Cd-*åkermanites*

(Cu, K radiation, Ni filtered). Space Group, $P\bar{4}2_1m$ tetragonal

	$Sr_2CuSi_2O_7$			$Sr_2CdSi_2O_7$		
hkl	d in $m \times 10^{-10}$ (Å) obs.	I/I_0	d in $m \times 10^{-10}$ (Å) calc.	d in $m \times 10^{-10}$ (Å) obs.	I/I_0	d in $m \times 10^{-10}$ (Å) calc.
101	4.296	3	4.299	4.38	2	4.38
111	3.798	50	3.797	3.864	60	3.869
210	3.616	8	3.616	3.689	5	3.689
201	3.162	80	3.162	3.222	80	3.228
211	2.947	100	2.945	3.005	100	3.006
220	2.857	20	2.858	2.913	50	2.910
310	2.556	60	2.556	2.609	50	2.602
221	2.490	10	2.491	2.529	10	2.536
102	2.419	10	2.422	2.475	3	2.472
301	.....	.....	.....	2.420	5	2.422
112	2.313	8	2.320	.....	.....	.....
311	2.285	5	2.288	2.325	5	2.323
212	2.077	50	2.077	2.119	20	2.121
400	2.021	2	2.021	2.059	25	2.059
410	1.961	30	1.961	2.001	10	1.997
330	.....	.....	.....	1.937	15	1.940
222	1.898	40	1.898	1.932	15	1.936
401	1.878	10	1.880	1.919	3	1.912
411	1.829	20	1.830	1.862	10	1.863
420	1.808	5	1.808	.....	.....	.....
312	1.801	50	1.802	1.837	50	1.836
331	1.784	25	1.785	1.814	30	1.816
113	1.621	3	1.623	1.656	5	1.657
203	1.561	5	1.561	1.594	8	1.594
213	1.533	30	1.533	1.567	3	1.565
511	1.515	10	1.515	1.547	5	1.541
223	1.458	5	1.457	1.485	2	1.485
303	.....	.....	.....	1.462	5	1.461

$a = 8.087 \times 10^{-10}$m(Å); $c = 5.076 \times 10^{-10}$m(Å); $a = 8.228 \times 10^{-10}$m(Å); $c = 5.188 \times 10^{-10}$m(Å).

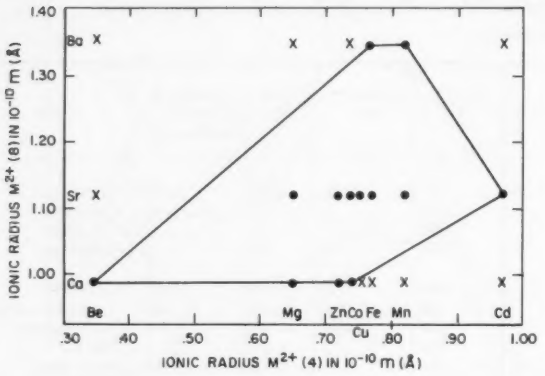

FIGURE 2. *Compositional stability range for the compounds with åkermanite structure, in terms of the divalent tetrahedral cations and the divalent octahedral cations.*

Ionic radii given by Ahrens.
X, Melilite not found.
●, Melilite found.

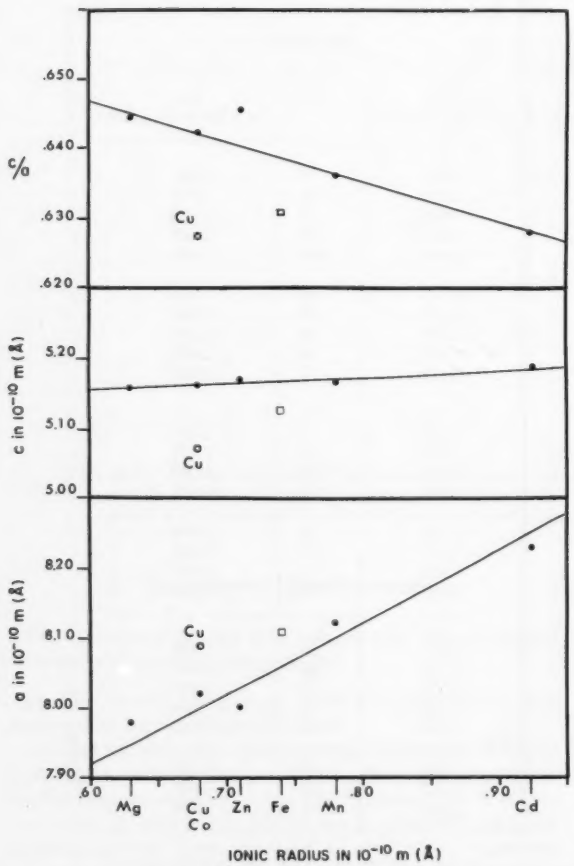

FIGURE 3. *Unit-cell dimensions of the Sr-analogs of åkermanite versus the ionic radii (4-fold coordination).*

Ahren's [15] values (6-fold coordination) were used multiplied by a factor of 0.95.

projections of horizontal tetrahedron edges on cell diagonals in (001):

$$a^2(x^2+y^2) - R^2_{M\text{-}O} \sin^2 \varphi_M = 0 \tag{1}$$

$$a^2(\tfrac{1}{2}-x-y)^2 - 2R^2_{Si\text{-}O} \sin^2 \varphi_{Si} = 0 \tag{2}$$

$$a^2(x^2+y^2) + \frac{a^2}{4} - a^2y + c^2z^2 - 4R^2_{Si\text{-}O} \sin^2 \varphi_{Si} = 0 \tag{3}$$

$$R_{M\text{-}O} \sin \varphi_M \cos\left[\tan^{-1}\left(\frac{x}{y}\right) - \frac{\pi}{4}\right] + R_{Si\text{-}O} \sin \varphi_{Si} - \frac{\sqrt{2}a}{4} = 0 \tag{4}$$

$$-R_{M\text{-}O} \sin \varphi_M \sin\left[\tan^{-1}\left(\frac{x}{y}\right) - \frac{\pi}{4}\right] + \left\{a^2(x^2+y^2) + \frac{a^2}{4} - a^2y\right\}^{1/2} \left\{\cos\left[\tan^{-1}\left(\frac{x}{\frac{1}{2}-y}\right) - \frac{\pi}{4}\right]\right\} - \frac{\sqrt{2}a}{4} = 0 \tag{5}$$

Since from simple crystal chemical considerations $0 \ll \frac{x}{y} < 1$, $\cos\left[\tan^{-1}\left(\frac{x}{y}\right) - \frac{\pi}{4}\right]$ is an insensitive function of the other variables and, $0.71 \ll \cos\left[\tan^{-1}\left(\frac{x}{y}\right) - \frac{\pi}{4}\right] < 1$. Differentiating (4) and allowing only for departures $\Delta R_{M\text{-}O}$ and $\Delta\varphi_M$ from established values of $R_{M\text{-}O}$ and φ_M leads to a value of a, differing by Δa from the anticipated value:

$$0.9\ (\sin \varphi_M \Delta R_{M\text{-}O} + R_{M\text{-}O} \cos \varphi_M \Delta\varphi_M) \approx \frac{\sqrt{2}}{4} \Delta a \tag{6}$$

If then an unusual value for a were alone due to an unusual value for $R_{M\text{-}O}$ the magnitude would be $\Delta R_{M\text{-}O} = 0.48\Delta a$. For Cu,Sr-åkermanite Δa observed is 0.087 Å (see fig. 3) whence the change in Cu-ion radius would be about 0.04 Å. Such a change is improbable so that the observed unusual value for a is more likely to be explained, at least in greater part, by a distortion of the tetrahedron.

There is stronger evidence still for this view: the signs of Δa, Δc and $R_{M\text{-}O}$ must be alike, unless $|\Delta\varphi_M| > 0$. The observed Δa and Δc are of opposite sign. The discrepancy in a thus is mostly due to a distortion of the $M^{2+}(4)$ tetrahedron. If $\Delta R_{M\text{-}O} = 0$;

$$\Delta\varphi_M \frac{\sqrt{2}\Delta a}{4 \times 0.9 R_{M\text{-}O} \cos \varphi_M} \approx +1.7°$$

corresponding to a "tetrahedral angle" of about 113°. The magnitude of this distortion is not at all unlikely.

There exists another method for estimating φ_M on the additional assumption that the closeness of stacking of the successive layers of SiO_4 and $M^{2+}O_4$ tetrahedra is unaffected by small changes in φ_M. Under those conditions the discrepancy, Δc, between the

observed and expected values of c is due to an expansion (or, if Δc is negative, a contraction) of the $M^{2+}O_4$ tetrahedra parallel to the z axis. By simple geometry it follows that $\Delta c \approx -2R_{M\text{-}O} \sin \varphi_M \Delta\varphi_M$. For Cu, Sr-åkermanite we observe $\Delta c = -0.09$ Å (fig. 3) corresponding to $\Delta\varphi_M \approx +1.6°$ in excellent agreement with the value deduced from Δa.

The $\bar{4}$ symmetry requires that all the $M^{2+}(4)$–O_4 "tetrahedral angles" not bisected by the z-axis direction are equal to one another, and from simple geometry that half "tetrahedral angle" φ' is related to φ by $\cos^2 \varphi + 2 \cos^2 \varphi' = 1$. Differentiating we obtain $\Delta\varphi' \approx \frac{1}{2}\Delta\varphi$, we would thus deduce for Cu, Sr-åkermanite that $\Delta\varphi' = -0.8°$.

4. Discussion

Anomalous shrinkage of the M^{2+} tetrahedra along the c axis in Sr, Cu-åkermanite, and their elongation along the a axis can best explain the observations (fig. 3). This view is consistent with the prediction by Dunitz and Orgel [3] of distorted Cu^{2+} tetrahedra in the structure. For the divalent copper ion with nine d-electrons, the nonbonding e orbitals are fully occupied, and the antibonding t_2 orbitals are partially occupied. A distortion which flattens the tetrahedron along the c axis will remove the orbital degeneracy. Wide departure from the normal c/a ratio in the case of the tetrahedral Cu^{2+} ion would then be directly related to the appreciable flattening of the coordination tetrahedron.

The divalent nickel ion does not form the åkermanite structure. This can also be explained by the molecular orbital theory, because the tetrahedra of Ni^{2+} ion with 8 d-electrons should elongate differently from the tetrahedra of the Cu^{2+} ion [3]. Elongation parallel to one twofold axis of the tetrahedron, caused by Ni^{2+} ions, leads to a rodlike distortion of the tetrahedron. It is not difficult to see that the åkermanite structure is much less able to accommodate such a distortion which would lead to gaps between adjacent (in the c-direction) $M^{2+}(8)$ ions. The compression of the tetrahedron parallel to one twofold axis, as occurs for the Cu^{2+} ion, causes a disklike distortion which probably facilitates good packing in the åkermanite structure. Furthermore, Ni^{2+} ion is known to have greater stabilization energy (Wells, 1962) in octahedral coordination than in tetrahedral coordination. Therefore, Ni^{2+} ion tends to form more stable octahedral compounds such as Ni_2SiO_4 (olivine). Superior stability of copper 4-fold planar coordination was demonstrated by Papst for instance in Egyptian blue (square quadricovalent cupric copper) ($CaCuSi_4O_{10}$) [16].

Instability of Ca, Cu-åkermanite can also be explained. The longer $M^{2+}(8)$–O distances, required by the flattening of Cu^{2+} tetrahedra, can be filled by Sr^{2+} but plausibly not by the smaller Ca^{2+} ion. However, similar though less prominent unit-cell flattening is observed for Sr, Fe^{2+}-åkermanite. In gillespite also, Fe^{2+} forms simple square coordination but it was found to be rather unstable compared to the Cu^{2+} compound.

Mössbauer spectroscopical examination on our Sr, Fe^{2+}-åkermanite was carried out by J. J. Spijkerman (private communication) at the National Bureau of Standards. The results showed that this compound contains Fe^{2+} and that the divalent Fe^{2+} ion is unusually distorted. These findings appear to be entirely consistent with our crystal-chemical conclusions. The same Mössbauer study also showed that this compound contains 10 to 20 percent of its iron as ferric iron (J. J. Spijkerman, private communication). The anomaly observed for its unit-cell dimension could be due to isomorphous replacement of Fe^{2+} and Si^{4+} by two Fe^{3+} ions, and, therefore, cannot be discussed with confidence comparable with that applicable to the Cu^{2+} analog.

5. Appended Note on Preliminary Experiments on the Growth of Large Crystals of Åkermanites

Co analogs of Ca and Sr åkermanite were grown in a sodium tungstate flux at temperatures from 1,200 to 1,000 °C for the Sr-analogs, and from 1050 to 850 °C for the Ca-analogs. The flux/charge ratio used was approximately 10/1. Deep blue platy {001} crystals up to 5 mm in size, often twinned on {110}, were obtained. This platy crystal habit of growth indicates strongest bonding forces within sheets parallel to {100} (fig. 1). Relative stability of these Co-analogs can be attributed to the symmetrical and fully occupied $(e)^4$ level and the half filled $(t_2)^3$ orbitals in the Co^{2+} ion with 7 d-electrons which shows undistorted tetrahedra. Single crystal growth of the copper analogs was not achieved. Sr, Cu-åkermanite when synthesized often is accompanied by $SrSiO_3$ or the Sr analog of Egyptian blue, $SrCuSiO_4$ (also with Cu^{2+} tetrahedra) [16].

We gratefully acknowledge J. J. Spijkerman's Mössbauer study and partial support from the Advanced Research Projects Agency of the Department of Defense.

6. References

[1] Aleksandrov, N. N., and Skripov, F. I., Structure investigations in crystals by the method of nuclear magnetic resonance. Advances in Physical Sciences, USSR (translated from Uspekhi Fiziches Kikh Nauk) **4,** 947–976 (1962).

[2] Greenwood, N. N., The Mössbauer spectra of chemical compounds. Chemistry in Britain **3,** 56–71 (1967).

[3] Dunitz, J. D., and Orgel, L. E., Electronic properties of transitional metal oxides–I. J. Phys. Chem. Solids **3,** 20–29 (1957).

[4] Orgel, L. E., and Dunitz, J. D., Stereochemistry of cupric compounds. Nature **179,** 462–465 (1957).

[5] Warren, B. E., The structure of melilite (Ca, $Na)_2$ (Mg, Al) (Si, $Al)_2O_7$. Z. Krist. **74,** 131–138 (1930).

[6] Smith, J. V., Reexamination of the crystal structure of melilite, Am. Mineralogist **38,** 643–661 (1953).

[7] Goria, C., Struttura dela Berillo Åkermanite. Atti accad. sci. Torino **88,** 153–160 (1953–1954).

[8] Christie, O. H. J., On sub solidus relation of silicates. III. A, Contribution to the chemistry of mellilites, Norsk Geol. Tidsskr **42,** 1–206 (1962) Band 1–2.

[9] Osborn, E. G., and Shairer, J. F., The ternary system pseudo wollastonite-åkermanite-gehlenite. Am. J. Sci. **239,** 715–763 (1941).
[10] Guy, E., and Osborn, E. G., X-ray data on synthetic mellilites, Am. Mineralogist **34,** 717–722 (1949).
[11] Klasens, H. A., Hoextra, A. H., and Cox, A. P. M., Ultraviolet fluorescence of some ternary silicates activated with lead. J. Electrochem. Soc. **104,** 93–100 (1957).
[12] Segnit, E. R., The system CaO–ZnO–SiO_2, J. Am. Ceram. Soc. **37,** 274–277 (1954).
[13] Brisi, C., and Abbattista, F., Ricerche sulle Meliliti, Note III, Silicati a Struttura Melilitica Contenenti Cobalte, Anali di Chimica **50,** 1435–1437 (1960).
[14] Brisi, C., and Abbattista, F., Composti a Struttura Melilitica Ferro e Manganese Bivalenti. Atti accad. sci. Torino **95,** 263–271 (1960–1961).
[15] Ahrens, L. H., The use of ionization potentials, Part 1. Ionic radii of the elements, Geochim. Cosmochim. Acta **2,** 155–169 (1952).
[16] Pabst, A., Structures of some tetragonal sheet silicates. Acta Cryst. **12,** 733–739 (1959).

(Paper 73A1–536)

JOURNAL OF RESEARCH of the National Bureau of Standards—A. Physics and Chemistry
Vol. 73A, No. 1, January–February 1969

Tritium-Labeled Compounds XII. Note on the Synthesis of D-Glucose-2-*t* and D-Mannose-2-*t*

Horace S. Isbell,* Harriet L. Frush, C. W. R. Wade, and A. J. Fatiadi

Institute for Materials Research, National Bureau of Standards, Washington, D.C. 20234

(July 9, 1968)

D-Glucose-2-*t* and D-mannose-2-*t* have been synthesized from sodium 2-*keto*-D-gluconate (sodium D-*arabino*-hexulosonate). Reduction of the salt with lithium borohydride-*t* produced the epimeric, 2-labeled aldonic acids in almost equal proportions. The acids, separated by carrier techniques, were lactonized, and the lactones were reduced with sodium amalgam to the corresponding sugars. The specificity of the labeling was established by converting each sugar into D-*arabino*-hexulose phenylosazone and determining that the osazone was substantially tritium-free.

Key Words: D-Gluconic-2-*t* acid, synthesis of; D-Glucose-2-*t*, synthesis and radioanalysis of; D-Mannonic-2-*t* acid, synthesis of; D-Mannose-2-*t*, synthesis and analysis of; Sodium 2-*keto*-D-gluconate, reduction with lithium borohydride-*t*; sugars, tritium-labeled; tritium-labeled compounds, D-mannose-2-*t* and D-glucose-2-*t*.

1. Introduction

In connection with a study of the behavior of sugars in alkaline solution [1],[1] several sugars labeled with tritium on C–2 were needed. Syntheses of D-glucose-2-*t* and D-mannose-2-*t* began with sodium 2-*keto*-D-gluconate (sodium D-*arabino*-hexulosonate); reduction of the ketonic carbonyl group with lithium borohydride-*t* provided a mixture of 2-labeled D-gluconic and D-mannonic acid. The acids were separated and lactonized, and the lactones were reduced with sodium amalgam by the procedures previously developed for preparing the corresponding ^{14}C-labeled sugars [2] [2].

Because the reduction of sodium 2-*keto*-D-gluconate with lithium borohydride-*t* was conducted in alkaline solution, it seemed possible that a C–2—C–3 enolization might have occurred and resulted in products having some tritium on C–3 as well as on C–2. However, the absence of tritium at positions other than C–2 was established by converting the labeled D-glucose and D-mannose into their common phenylosazone (D-*arabino*-hexulose phenylosazone). After three recrystallizations, the phenylosazone from each sugar was found to be essentially free of tritium, indicating the absence of labeling on C–3, C–4, C–5, and C–6. Absence of labeling on C–1 of the sugars may be assumed because the introduction of hydrogen on C–1 (by reduction of the lactone with sodium amalgam) was carried out as a separate step after the labeling had been completed. Hence the D-glucose and D-mannose must be labeled exclusively on C–2.

2. Experimental Procedures

2.1. Reduction of Sodium 2-*keto*-D-Gluconate With Lithium Borohydride-*t*

Sodium 2-*keto*-D-gluconate monohydrate was prepared from calcium 2-*keto*-D-gluconate monohydrate [3] [4] by treating the latter with an equivalent proportion of sodium oxalate, removing the calcium oxalate precipitated, and crystallizing the sodium 2-*keto*-D-gluconate monohydrate from the resulting solution.

A magnetic stirring-bar, 936 mg (4 mmoles) of sodium 2-*keto*-D-gluconate monohydrate, 10 mg of sodium carbonate, and 4 ml of water were placed in a 100-ml, round-bottomed flask having a small side-arm provided with a rubber cap suitable for perforation by a hypodermic needle. The solution was frozen, and the flask was evacuated on a vacuum manifold [5]. The flask was then closed off, the frozen solution was melted,

*Present address: Chemistry Department, American University, Washington, D.C. 20016.

[1] Figures in brackets indicate the references at the end of this paper.

[2] A similar reduction of sodium 2-*keto*-D-galactonate (sodium D-*lyxo*-hexulosonate), followed by procedures analogous to those described in ref. 3, yielded D-galactose-2-*t* and D-talose-2-*t*.

[3] The authors thank Peter Regna of Chas. Pfizer & Co., Inc., for the calcium 2-*keto*-D-gluconate used in this work.

and stirring was begun. With the flask in an ice-bath, 2-ml of a 0.5-*M* solution of lithium borohydride-*t* in dry tetrahydrofuran (40 mCi) was added by injection with a hypodermic needle through the capped side-arm. Stirring was continued for 2 hr at 0 °C, and the mixture was kept overnight at room temperature.

Aqueous acetic acid (1 ml of 5%) was injected to decompose any unreacted lithium borohydride-*t*, and, after the solution had been refrozen, hydrogen-*t* was collected in the manifold. The solvent was removed by freeze-drying (and was ultimately discarded in the manner approved for radioactive waste). The residue, dissolved in water, was passed through a small column of a strongly acidic cation-exchange resin (10 ml), and the effluent was evaporated to dryness under vacuum. Boric acid was removed from the residue as methyl borate by several successive additions of methanol, each followed by evaporation under vacuum.

An aqueous solution of the labeled products (volume 25 ml) was found to contain 18.9 mCi of radioactivity. The proportions of labeled D-gluconic and D-mannonic acid in the solution were determined by isotope dilution: a 100-μl aliquot was added to an aqueous solution containing 200 mg of barium D-gluconate trihydrate. This solution was then neutralized with aqueous barium hydroxide, and concentrated. The carrier crop was crystallized from aqueous methanol–isopropyl alcohol, and recrystallized three times. A second 100-μl aliquot was added to a solution of 200 mg of D-mannono-1,4-lactone. This solution was treated with aqueous sodium hydroxide sufficient to produce a faint, permanent, pink color with phenolphthalein indicator and was then passed through a small column (5 ml) of the cation-exchange resin; the effluent was evaporated to dryness under vacuum. The residue was dissolved in methanol, and the solution was heated at 70 °C for 1 hr to effect lactonization. The solvent was evaporated, and the lactone was crystallized and twice recrystallized, from methanol–isopropyl alcohol. Radioactivity found from the assay of the carriers: D-gluconic-*2-t* acid, 8.83 mCi (46.7% of the labeled products); D-mannonic-*2-t* acid, 9.91 mCi (52.4%).

2.2. Preparation of Barium D-Gluconate-2-*t* and D-Glucose-2-*t*

The solution containing D-gluconic-*2-t* and D-mannonic-*2-t* acid was neutralized with barium hydroxide and concentrated. Crystallization of barium D-gluconate was initiated by the addition of ethanol to incipient turbidity, and the resulting crystals were separated and recrystallized. The combined mother liquor was depleted of D-gluconate-*2-t* ions by five additional crystallizations with nonradioactive barium D-gluconate used as carrier (total, 2.5 g). Each carrier crop was recrystallized, and the mother liquors were combined for the next carrier crystallization. The first crystals and the carrier crops were selectively combined and recrystallized to give the following quantities of barium D-gluconate-*2-t* monohydrate: 1.155 g (5,700 μCi); 1.460 g (1,290 μCi); and 1.100 g (320 μCi); total yield, 83 percent of the D-gluconic-*2-t* acid found by analysis.

The two main crops of barium D-gluconate-*2-t* trihydrate (6,990 μCi) were converted into D-glucono-1,5-lactone-*2-t*, and this was reduced with sodium amalgam in the presence of sodium hydrogen oxalate by the procedure previously described for the preparation of D-glucose-*2-*^{14}C [2]. The yield of α-D-glucose-*2-t* (5,430 μCi) was approximately 78 percent of the barium D-gluconate-*2-t*, or 65 percent of the quantity initially found by analysis.

2.3. Preparation of D-Mannono-1,4-lactone-2-*t* and D-Mannose-2-*t*

Nonradioactive calcium D-mannonate dihydrate (1 g) was added to the mother liquor that had been depleted of its barium D-gluconate-*2-t*. An aqueous solution of the mixture was passed through 25 ml of the cation-exchange resin, and the effluent was evaporated under vacuum. The residue was digested for 1 hr in methanol at 70 °C, and the solution was then cooled, nucleated with D-mannono-1,4-lactone, and kept in a desiccator for several days. Crystalline D-mannono-1,4-lactone-*2-t* deposited and was separated. Residual, labeled lactone was isolated from the mother liquor in carrier crops by several co-crystallizations with nonradioactive D-mannono-1,4-lactone; yield, 7.48 mCi, or approximately 75 percent of the quantity found by analysis. The crops were combined, recrystallized, and then reduced in 1-mmole portions by the method described for the preparation of α-D-mannose-*2-*^{14}C [2]. The yield of α-D-mannose-*2-t* was approximately 65 percent of the labeled lactone employed, or 49 percent of the D-mannonic-*2-t* acid found by analysis.

2.4. Preparation of D-*arabino*-Hexulose Phenylosazone from D-Glucose-2-*t*

A mixture containing 100 mg of D-glucose-*2-t* (11.53 μCi), 200 mg of phenylhydrazine hydrochloride, and 300 mg of anhydrous sodium acetate was dissolved in 4 ml of water in a 15-ml centrifuge tube, and the solution was kept in a boiling-water bath for 20 min. The resulting suspension of yellow crystals was diluted with 4 ml of water, kept in ice-water for 30 min, and then centrifuged; the separated crystals were washed twice with 3-ml portions of water. To recrystallize the product, the moist crystals were dissolved in 3 ml of 2:1 (*v/v*) methyl Cellosolve–tetrahydrofuran, and water was added drop-wise, with stirring, to give a total volume of about 12 ml. The resulting, fluffy precipitate was centrifuged and washed as before. The recrystallization process was twice repeated, and the separated crystals were dried in a vacuum desiccator.

For analysis, 3.5 mg of the phenylosazone, in a standard liquid-scintillation bottle, was dissolved in one drop of tetrahydrofuran, and 10 ml of a scintillation mixture containing *p*-dioxane was added; the solution was assayed in a liquid-scintillation spectrometer. The radioactivity of the phenylosazone was 1.84 d/s per

milligram; the radioactivity of the equivalent quantity of the parent D-glucose-*2-t* (0.503 mg) had been 2145 d/s. Hence retention of radioactivity by the D-*arabino*-hexulose phenylosazone was less than 0.1 percent, and the compound was substantially tritium-free.

2.5. Preparation of D-*arabino*-Hexulose Phenylosazone From D-Mannose-2-*t*

A solution of 200 mg of phenylhydrazine hydrochloride and 300 mg of sodium acetate in 10 ml of water was treated with sufficient acetic acid to bring the pH to 4.6. To this solution was added 100 mg of D-mannose-*2-t* (containing 8.16 μCi of radioactivity), and the solution was heated in a boiling-water bath for 1 hr. A colorless precipitate of D-mannose phenylhydrazone formed at first and redissolved, and the yellow phenylosazone then precipitated. The suspension was diluted with 5 ml of water, cooled in ice-water, and centrifuged. The precipitate was washed, and recrystallized three times, as described for the phenylosazone of D-glucose-*2-t*. The radioactivity, measured with 5.2 mg of the dried phenylosazone, was scarcely greater than that of the background.

3. References

[1] Isbell, H. S., and Frush, H. L., Abstracts Papers, Am. Chem. Soc. Meeting, **155,** C25 (1968).

[2] Isbell, H. S., Frush, H. L., and Schaffer, R., J. Res. NBS **54,** 201 (1955)RP2581.

[3] Isbell, H. S., Frush, H. L., and Holt, N. B., J. Res. NBS **53,** 217 (1954)RP2536.

[4] Regna, P. P., and Caldwell, B. P., J. Am. Chem. Soc. **66,** 243 (1944).

[5] Isbell, H. S., and Moyer, J. D., J. Res. NBS **63A** (Phys. and Chem.), No. 2, 177 (1959).

(Paper 73A1–537)

JOURNAL OF RESEARCH of the National Bureau of Standards—A. Physics and Chemistry
Vol. 73A, No. 1, January–February 1969

A Survey of Blemishes on Processed Microfilm

C. S. McCamy, S. R. Wiley,* and J. A. Speckman

Institute for Basic Standards, National Bureau of Standards, Washington, D.C. 20234

(July 23, 1968)

As part of an investigation of the formation of six types of redox blemishes on microfilm, 7411 rolls of microfilmed records in 36 Federal Government agencies were microscopically inspected by 34 inspectors trained by the National Archives and the National Bureau of Standards. About 350,000 observations were statistically analyzed. Careful photographic processing, adequate washing, careful handling, cool and dry storage in inert containers, and adequate ventilation, are among the conditions that have been found beneficial in preventing blemish formation. Data are compiled in an appendix.

Key Words: Aging blemishes; archival records; blemishes; microfilm blemishes; microscopic spots; redox blemishes.

1. Introduction

About 1961, spots and other blemishes were observed on some commercial microfilms and an industrial laboratory undertook an investigation. By the end of 1962 it was clear that the phenomenon was quite widespread and that these blemishes were of a type not previously known. The matter came to the attention of the National Bureau of Standards in the first days of 1963 and studies were immediately initiated. Thousands of rolls of microfilmed Government records were microscopically inspected and the findings were classified by blemish type.

That preliminary survey clarified the problems and established the need for a broader survey than could be made directly by the NBS staff. Two objectives were sought: an appraisal of the condition of the millions of rolls of microfilmed Federal records and the discovery of relationships among pertinent variables which would assist in determining the causes of blemish formation and in formulating recommendations for action to prevent further attack.

To assist in unifying research on this problem, a handbook naming and describing the blemishes and methods of sampling collections and inspecting films was published [1].[1]

With the cooperation of the National Archives, 100 inspectors were trained to sample collections, inspect the films microscopically, and report their findings. About one-third of these participated in the survey reported here. Inspections were made in 36 Federal Government microfilming facilities.

1.1. Inspection Procedure

Information was obtained from the files of the agency holding the microfilm, from the original source of the materials, or from people who had been involved with the preparation and storage of the materials. Unfortunately, there were few if any records of the conditions of processing and storage over the years. The need for such records was not previously apparent, however obvious it may now be. Other information was found on the labels of the storage containers or was obtained by inspecting the film with the unaided eye. Although some blemishes are visible to the unaided eye, it was found necessary to use a microscope to inspect the films. A complete description of the inspection technique is given in reference 1.

The microfilming facilities of a number of other government agencies and private institutions were visited by one of the authors (Wiley). These included processing laboratories and storage facilities in all climatic areas of the United States. In a number of instances the data reported on the inspection sheets may not have been properly interpreted if the mass inspections and statistical reports were not followed by inspection of many facilities by a trained observer. Furthermore, these field trips included non-government facilities, from which information would not otherwise have been obtained.

2. Classification of Blemishes

Many kinds of defects and blemishes can appear on processed microfilm. This study was initiated because of the discovery of apparently related types of blemishes of unknown origin in some commercial

*Current address: U.S. Army Map Service, Washington, D.C. 20315.

[1] Figures in brackets indicate the literature references at the end of this paper.

collections. These blemishes have been referred to by many names: "microscopic spots" or "microspots," even though many are clearly visible to the unaided eye and many aren't spots; "measles," a totally inappropriate term because the blemishes bear no relationship to the human disease by that name, the blemishes were not caused by any biological activity, and this term has already been used in photographic engineering for some time for the effect better known as the "half-tone effect"; "J-type blemishes" or "J-spots," a shorthand allusion to Project Jupiter, the name assigned to the project at NBS during the first months; and "aging blemishes," the name which seemed to describe them most accurately. However, after considerable investigation we know that the oxidation and reduction of silver are the principal reactions and we can induce such reactions in a day or so [2, 3, 4, 5, 6, 7]. Therefore we feel that the name "redox blemishes" is the most accurate descriptor.

These blemishes were classified in six types as follows:

Type 1

Type 1 redox blemishes are circular spots, usually 50 to 150 micrometers in diameter, with sharp boundaries. Concentric light and dark rings are common. Spots normally occur as reduced density in high-density "background" areas, but may make incursions into low-density lines or characters. They are usually brown, orange, reddish, or yellow in color. It is common to find many spots about the same size on a sample. The circular boundaries of two or more spots may intersect. The spots are often seen centered on scratches in the emulsion, sometimes closely packed like beads on a string. They sometimes occur in higher concentration at steep density gradients between high- and low-density regions, sometimes being so closely packed as to give the appearance of a continuous band. By reflected light, the spots may display a silvery sheen.

Type 2

Type 2 are defects in the light lines forming the characters themselves, rather than in the high-density "background." The lines making up the characters become lighter, yellowish, and broader. The boundaries of the defect are sharp.

Type 3

Type 3 are very small spots, about 10 to 15 micrometers across. When they occur, there is usually a large number per unit of area. They usually range from pale yellow to orange in color. Their boundaries are sharp. By reflected light, the spots may display a silvery sheen.

Type 4

Type 4 blemishes are spots of less regular shape than type 1 but about the same size or a little larger, usually lighter in color, and less sharply bounded. A circular central "nucleus" is common. These spots occur in high-density "background" areas. They do not make incursions on low-density characters; on the contrary, their shapes may be very distorted to accommodate to the spaces between characters or parts of characters.

Type 5

Type 5 is a reddening of the dark background in the immediate neighborhood of lighter characters. The boundaries of the discoloration are very diffuse. The shape is not regular, being determined by the shape of the characters or line of characters with which the discoloration is associated.

Type 6

Type 6 is a reddish, orange, or yellow spot of reduced density, lightest at the center and gradually blending into the surrounding background. An irregular opaque or crystalline particle is commonly observed on the surface of the film at the center of the spot. The sizes of the spots may vary considerably, even within a small region.

3. Reporting

The incidence of a type of blemish could have been reported on the basis of the percentage of rolls affected but this method would not indicate the severity of the attack. In recording severity, it was necessary to consider the blemishes to be of two major kinds: *spot blemishes* (types 1, 3, 4, and 6) and *character-associated blemishes* (types 2 and 5). The concentration of *spot blemishes* was indicated by the number of spots per square centimeter. Five classes of severity were assigned numerical designations from 1 to 5, a severity of 1 was less than one spot per square centimeter, 2 was 1 to 8, 3 was 8 to 63, 4 was 63 to 500, and 5 was over 500. A severity of "zero" meant that no blemishes were found. After measuring the microscope field, the inspectors soon learned to recognize the severity on sight. Five severities of character-associated blemishes were defined as follows:

1. Blemishes barely detectable, have no effect on the original shape and size of the characters.
2. Blemishes clearly visible, coloration change clearly visible, but shape and size of characters unchanged.
3. Blemishes well developed. Lines or parts of lines making up characters changed, but general shape of characters is unchanged.
4. Blemishes have altered the shape and size of characters to the extent that individual characters could not be identified with certainty out of context. Characters can be identified in context.
5. Blemishes have so altered the size and shape of characters that they cannot be identified with certainty even in context. This constitutes information loss, on a given roll, in the practical sense. Information from other rolls of microfilm should not be considered part of the context.

The findings were reported on General Services Administration forms 1990 and 1990A, shown in the appendix. Form 1990A was prepared for each roll inspected. Three parts of each roll were inspected:

the leader, where only types 1, 3, 4, and 6 were possible, frames next to the leader, and center frames. The 16 severity ratings were reported along with answers to 32 questions concerning characteristics of the given roll of film, the conditions under which it had been stored, and the presence of certain common defects. Form 1990 was a summary of the findings for a stratum.

4. Statistical Analysis

The main purpose of the analysis was to discover factors or combinations of factors considered likely to affect the formation of blemishes. The data were grouped into categories on the basis of one or more of the 32 items reported on the inspection sheets and calculations were performed to summarize information on the incidence and severity of the blemishes for each category. For this purpose, each roll was considered to have 2 severity scores: the total severity score for the leader (the sum of the severities for the 4 different types of blemishes); and the total severity score for the information section (the sum of the 12 severities for the 6 different types of blemishes and for the 2 positions). For each category, the following information was tabulated:

n, the total number of rolls in the category
k_L, the number of rolls with blemishes on the leader
k_I, the number of rolls with blemishes on the information section
f_L, the fraction of rolls with blemishes on the leader
f_I, the fraction of rolls with blemishes on the information section
$\bar{x}_L$, the average, over k_L rolls, of the total severity score for the leader
$\bar{x}_I$, the average, over k_I rolls, of the total severity score for the information section.

In the statistical analysis it was not practical to consider all possible combinations of factors. For this reason, there is the possibility that differences could result from the coincidence of some unrecognized factor with other factors under study.

Statistical analysis is based on the assumption of random sampling. Since the rolls of film were usually selected by the inspectors and the procedures probably varied among inspectors, randomness is not as well assured as it might be in controlled experiments in a single laboratory.

The severity ratings gave no indication of whether a given severity was localized in a small area or was characteristic of the whole roll. Thus the choice of location for inspection could materially affect the results if the severity varied greatly over the roll. For the purpose of appraising the condition of a collection of microfilms, the total quantity of film affected might be of considerably more interest than it would be for the present purpose. It is of scientific interest to know that the physical and chemical conditions for blemish formation were present, even if on a small area, although it would have been desirable to know the extent as well.

The information involving storage conditions was not as reliable as we would have liked. For example, reported temperatures and humidities were usually estimated rather than measured. Data for films which were known to have been stored under more than one set of conditions were not included in the tabulations for storage conditions.

On the basis of these considerations, it is believed that two reported severity scores should not be considered significantly different unless their difference is 1 or more.

The significance of comparisons of fractions defective depends on the number of rolls in the sample and the fractions involved. The standard deviation s of a fraction defective f in a random sample containing n rolls is given in table I. The fractions defective in two different classes may be considered significantly different if the difference between the fractions exceeds twice the sum of the standard deviations of the fractions.

When the results were first tabulated, the fraction of rolls blemished in agencies 15 and 16 was so high that these agencies were visited and the conditions there were carefully reviewed. All of the defective films were processed by a particular type of processing machine that had small tanks, inadequate provision for removal of solutions from the film between baths, and inadequate washing capability. It was customary to load dry chemicals into the tanks rather than to dissolve them first, as is usually done. The machine is no longer on the market. In one agency, this type of processor was replaced years ago, by a machine with better washing and drying and the film processed by the new machine has not become blemished. In view of this apparent explanation of the consistently high incidence of blemishes at agencies 15 and 16 and the overriding influence that these data had on the analysis, many of the computations were done a second time, omitting the data from these agencies.

Finally, due to the inherent nature of this type of data, one should be cautioned not to draw conclusions concerning the causes of blemishes solely on the basis of the statistical significance of the data. The tabulations point out possible causes for the redox blemishes, but they must be interpreted in the light of technical knowledge of microfilms and, whenever possible, backed up by laboratory experience.

TABLE I. *Standard deviation* s *of a fraction defective* f *in a sample of* n *rolls*

n	f=0.1 or 0.9	0.3 or 0.7	0.5
25	0.06	0.09	0.10
50	.04	.06	.07
100	.03	.04	.05
200	.02	.03	.04
500	.01	.02	.03
1000	.01	.01	.02

Values not tabulated can be computed, using the relationship:

$$s^2 = f(1-f)/n.$$

324-194 O-69—6

5. Results

The statistical results are summarized and discussed in this section. For what value they may have for further study, all of the tables of numerical results are given in the appendix. The discussions of results in this section are given the same numbers as the corresponding tables in the appendix. Not all tables in the appendix are discussed here.

To facilitate encoding the data for the computer, a number was assigned to each reporting government agency, inspector, processing facility, and film supplier. The agency identification was a valuable aid in further studies but the data were obtained with the understanding that agencies would not be identified in published reports. The identity of inspectors was of little interest except for a detailed analysis of the statistical nature of the data, for which purpose the numerical identification is even more convenient than names. It is not our policy to publish comparisons of the merits of commercial products and services; therefore, we would not, without some compelling reason, identify the processing service facilities or film suppliers in a comparative study such as this. The statistics refer almost entirely to films manufactured in this country. Thus, to avoid misunderstanding or misuse of data, several of the factors are identified by number only.

To conserve space in the tables in which the results were classified by agency, agencies reporting no blemishes were not listed, although the data relative to these agencies were used in the analysis, where appropriate.

1. Agency. Two agencies, 15 and 16, reported an incidence of blemishes far in excess of all others. Both had used a processing machine which left chemicals on the film. After installation of a different type of machine in one of these agencies, all subsequently processed films were free of blemishes.

Of 36 agencies, 20 found no blemishes on information areas, 13 of the 20 having inspected 25 rolls or more; and 17 found no blemishes on leaders, 13 of these having inspected 25 rolls or more.

2. Agency and Inspector. Agencies 31, 40, 52, and 92 each had enough inspections made by different inspectors to permit statistical comparison among inspectors. The reporting within these agencies was consistent, indicating, in all probability, adequate training, good coordination of criteria of judgment, and careful exercise of observation and judgement.

3. Processing Facility. Two agencies, 15 and 16, which processed their own films (processors 47 and 14, respectively), had over 90 percent blemished films. Film from three facilities had 25 to 52 percent, four had 10 to 24 percent, and two had 1 to 10 percent. Of 42 processing facilities, 25 had processed films with no blemishes on leaders and 26 had none on information areas.

4. Agency and Processing Facility. Known unsatisfactory characteristics of the processing machines at agencies 15 and 16 account for the high incidence of blemishes reported there. Agency 31 reported very high incidence and high severity on 1499 films processed at facility 20, but only half the incidence and less severity on films processed by facility 41. Since these films were stored and handled alike, there is a clear indication that processing conditions can be important determinants of blemish-forming potential.

5. Film Manufacturer. This section and the associated table in the appendix are entitled "Film Manufacturer" because that was the information requested in the survey. However, the data actually refer to *brand names*, since they were what were known to the inspectors. In some cases one manufacturer's product might be known by two names. We know that two of the brands (6 and 10) considered in the present analysis were manufactured by the same company and there may be other such cases. Both the frequency and severity of blemishes reported for these two brands of film were substantially different, indicating that variables other than the kind of film made the difference. This example illustrates very well the need for caution in the interpretation of the statistics.

6. Agency and Film Manufacturer. In an experiment designed to test films, the film brands would be equally distributed among all the other pertinent variables, but in practical experience we expect that certain combinations of films and processors would be sold by the same dealers and would be used together. There would be some tendency for one agency to continue to use the same brand, reordering from the same dealer as long as the price and quality were satisfactory. Then all the processing, handling, and storage conditions associated with that agency would be correlated with that film brand. The consistently bad results at agencies 15 and 16 were associated with 5 different brands of film. The consistently good results at agency 81 were associated with 4 brands. Under good conditions, all films were good; under bad conditions, they were all bad. Thus, we find no basis for ranking the various brands of film on the basis of their tendency to withstand the formation of blemishes. Agencies reporting no blemishes are not included in table 6.

7. Year of Purchase. The frequency of observed blemishes increased with the time since the film was purchased. This accounts in part for the fact that microfilms were in use for many years before redox blemishes were discovered. There was no distinct trend of severity with time.

8. Year Processed. Since films were usually processed soon after they were purchased, the statistics are similar for time since purchase and time since processing.

9. Frequency of Use. The incidence of blemishes and their severity are both inversely related to the frequency of use. This suggests that the stagnant atmosphere associated with disuse promotes blemish formation, while the ventilation associated with use is beneficial.

10. Type of Container. One-third of all films stored in cans were at agencies 15 and 16. At these agencies practically all films were blemished, so these agencies account for almost all blemished film found in cans. With these agencies omitted, the blemish frequency

on the leaders of film stored in cardboard containers was twelve times that on films stored in cans. The frequency of blemishes on the information sections of films stored in cardboard containers was 3.2 times that of films stored in cans. The severity on films stored in cardboard containers was about twice as bad as that on films in cans. In most cases, there was no way of knowing whether or not films had always been stored in the containers in which they were found at the time of inspection.

11. Type of Reel. Cardboard reels were associated with substantially more blemishes than were other types of reels. The severity was also substantially higher for these reels on information areas but not on leaders.

12. Temperature. There was a significant but not monotonic increase in blemish frequency and severity with increasing maximum temperature. There was a significant increase in blemish frequency and severity with increasing minimum temperature.

13. Relative Humidity. Aside from agencies 15 and 16, the effect of humidity on blemish incidence was quite pronounced. When the maximum humidity was 51 to 60 percent, there were 11 times as many blemished leaders and 19 times as many blemished information sections as there were when the maximum humidity was 20 to 50 percent. The 55 rolls stored at humidities ranging as high as 71 to 80 percent had been in storage only a short time. Among 526 rolls of film for which the minimum storage humidity was less than 40 percent, there was only 1 blemished leader and no blemished information frames, whereas among the 1472 rolls for which the minimum humidity was over 40 percent, there were 477 blemished leaders and 283 films with blemished information areas.

In the arid southwestern part of the United States, Wiley observed a collection of films, including several brands processed in many places over a twenty-five year period and stored in cans or paper boxes. The storage temperature was thought to exceed 100 °F frequently but the humidity was always low. No redox blemishes were found on these films.

14. Air Conditioning. Aside from agencies 15 and 16, films stored in nonair-conditioned spaces had 8 times as many blemished leaders and twice as many blemished information sections. The severity was also substantially greater, being nearly twice as severe for information sections.

15. Storage Location. Office storage was associated with substantially fewer blemished leaders and less severely affected leaders than any other type of storage area listed. On the other hand, this advantage was not observed with respect to blemishes on information sections of the films.

16. Humidification Trays. Unfortunately, the question asked in the survey did not elicit the required information. Respondents indicated the current practice but said nothing about usage in the past. About three fourths of the positive answers were with reference to films stored in metal cans which would nearly nullify the effects of humidifying the cabinets. The validity of any inferences drawn from these data would be questionable.

17. Type of Leader. The eight reports of blemishes on plastic leaders must be erroneous, but they were not considered of sufficient interest to investigate. The number of reports of clear-and-plastic leaders was too small for valid statistical inference. The films without leaders had a higher incidence of blemishes on information sections than films with leaders, the criterion of significance of the difference being barely exceeded. The incidence of blemishes on the leader varied from one type of leader to another by a factor of 49 with a corresponding change by a factor of only 1.2 in the incidence on information frames. Thus a leader appears beneficial and it seems to make little difference which of these kinds is used.

18. Length of Leader. Films without leaders had a blemish incidence rate 2 to 3 times that for films with leaders. Films with leaders more than 5 ft. long had a little lower incidence than those with shorter leaders.

19 and 20. Number of Splices. The combined statistics for agencies other than 15 and 16 indicate very low incidence on information areas when more than 5 splices were made. The statistical analysis was, however, dominated by the very numerous splices on unblemished film at agency 52. When the data were analyzed by agency, out of 8 agencies that had many splices and some blemishes, 6 displayed an increase in incidence on information areas with increasing number of splices. More splicing implies more handling and, in most cases, more fingerprinting and other contamination. In agency 52, films were spliced carefully and handled with gloves. At agency 52, the incidence decreased with the number of splices. This suggests, as did the data on Frequency of Use and Storage Location, that more active files benefit from better ventilation. Table 20 lists only those agencies reporting some blemishes.

21. Type of Splice. Rolls with overlap splices had 2 to 3 times the blemish rate of rolls with butt splices and higher severity.

22. Type of Band. Most of the films examined had no string, paper, rubber or other band to hold the coil tight. The slight differences observed when bands were employed are not significant because of the small number of such cases.

23. Chemical Residues. At agencies 15 and 16, practically all films had blemishes and chemical residues but elsewhere the incidence of blemishes was independent of such residues.

24. Silvery Sheen on Leaders. The incidence and severity of blemishes on leaders and information areas were significantly greater when a silvery sheen appeared on the leader.

25. Silvery Sheen on Dense Areas. Where a silvery sheen appeared on dense areas of the information section, the incidence and severity of blemishes on information areas increased greatly.

26. Discoloration or Fading. Apart from agencies 15 and 16 where many films were discolored and faded, this defect was so infrequent that correlations are not significant.

324-194 O-69—7

27. Water Spots. Reports of water spots were associated with an increased incidence of blemishes on information areas, however, on the leaders the trend was in the opposite direction.

28. Other Blemishes. When agencies 15 and 16 were included, reports of other kinds of blemishes were associated with considerable increases in the incidence of redox blemishes on both leaders and information areas. Without agencies 15 and 16, the trend was opposite.

6. Summary

Clean and uniform processing conditions, including adequate washing, have always been considered essential to the preparation of permanent record films. The data emphasize this point. More emphasis must now be placed on cool and dry storage in containers that do not evolve chemicals that cause blemish formation. Ventilation appeared desirable, but this factor probably would not have been important were it not for the widespread use of cardboard containers for the storage of microfilm.

The authors are grateful to the administrators of the many agencies which set up programs to cooperate with us in this survey, to the many records officers and others who conducted the actual inspections, to the personnel of the Bureau of the Census who encoded all of the information on punched cards, and to the personnel of NBS who provided computer services.

7. Appendix

The following symbols are used in the tables in this appendix:

n number of rolls of film inspected
k number of rolls of film with blemishes
f fraction of films with blemishes (expressed in decimal notation)
$\bar{x}$ average, over k rolls, of the total severity score.

Agencies, inspectors, processing facilities, and film suppliers are identified by number only and the identities are not available for publication.

TABLE 1. *Summary of results classified by agency*

Agency	n	Leader			Information section		
		k	f	$\bar{x}$	k	f	$\bar{x}$
10	1	0	0.	.....	0	0.	.....
11	60	0	0.	.....	0	0.	.....
12	54	0	0.	.....	0	0.	.....
13	28	0	0.	.....	0	0.	.....
14	501	0	0.	.....	0	0.	.....
15	142	116	.82	1.72	116	.82	3.51
16	246	221	.90	3.67	243	.99	8.59
17	34	0	0.	.....	0	0.	.....
18	99	0	0.	.....	0	0.	.....
19	123	0	0.	.....	0	0.	.....
20	25	0	0.	.....	0	0.	.....
21	94	0	0.	.....	0	0.	.....
22	200	0	0.	.....	0	0.	.....
31	1668	870	.52	4.69	472	.28	7.51
40	301	20	.07	1.15	15	.05	3.67
51	209	59	.28	5.19	109	.52	2.63
52	1545	384	.25	5.97	98	.06	5.32
61	628	87	.14	3.41	103	.16	2.84
62	116	16	.14	3.88	15	.13	6.13
63	405	37	.09	3.76	70	.17	3.71
71	100	27	.27	3.44	23	.23	3.35
72	35	0	0.	.....	0	0.	.....
73	65	11	.17	2.00	10	.15	3.30
81	13	2	.15	2.00	0	0.	.....
82	9	1	.11	4.00	0	0.	.....
83	11	1	.09	3.00	0	0.	.....
84	31	0	0.	.....	0	0.	.....
86	6	0	0.	.....	0	0.	.....
87	3	0	0.	.....	0	0.	.....
91	102	0	0.	.....	0	0.	.....
92	159	3	.02	3.00	11	.07	4.27
101	10	4	.40	5.00	6	.60	4.67
102	6	1	.17	5.00	0	0.	.....
103	82	12	.15	2.24	7	.09	2.45
111	299	34	.11	2.88	146	.49	4.43
121	1	0	0.	.....	1	1.00	3.00

TABLE 2. *Summary of results classified by agency and inspector*

Agency	Inspector	n	Leader			Information section		
			k	f	$\bar{x}$	k	f	$\bar{x}$
15								
	231	142	116	0.82	1.72	116	0.82	3.51
16								
	230	245	220	.90	3.66	242	.99	8.57
	232	1	1	1.00	6.00	1	1.00	12.00
31								
	10	34	27	.79	4.48	4	.12	7.25
	140	622	320	.51	4.62	155	.25	7.44
	141	1	0	0.	.....	0	0.	.....
	161	419	227	.54	4.89	148	.35	8.02
	233	592	296	.50	4.62	165	.28	7.12
40								
	110	101	2	.02	1.50	10	.10	3.20
	194	100	2	.02	1.00	0	0.	.....
	300	100	16	.16	1.12	5	.05	4.60
51								
	20	1	0	0.	.....	0	0.	.....
	30	208	59	.28	5.19	109	.52	2.63
52								
	25	398	92	.23	5.59	29	.07	5.38
	111	339	84	.25	6.05	23	.07	4.13
	200	372	96	.26	6.00	22	.06	5.59
	260	370	108	.29	6.36	22	.06	6.59
61								
	20	628	87	.14	3.41	103	.16	2.84
62								
	20	116	16	.14	3.88	15	.13	6.13
63								
	20	405	37	.09	3.76	70	.17	3.71
71								
	21	100	27	.27	3.44	23	.23	3.35
73								
	130	65	11	.17	2.00	10	.15	3.30
81								
	20	13	2	.15	2.00	0	0.	.....
82								
	20	9	1	.11	4.00	0	0.	.....
83								
	20	11	1	.09	3.00	0	0.	.....
92								
	31	48	3	.06	3.00	6	.13	4.67
	150	110	0	0.	.....	5	.05	3.80
	180	1	0	0.	.....	0	0.	.....
101								
	50	3	2	.67	7.50	3	1.00	6.00
	120	7	2	.29	2.50	3	.43	3.33
102								
	120	6	1	.17	5.00	0	0.	.....
103								
	20	6	0	0.	.....	0	0.	.....
	120	82	12	.15	2.08	7	.09	2.29
111								
	190	299	34	.11	2.88	146	.49	4.43

TABLE 3. *Summary of results classified by processing facility*

Processor	n	Leader			Information section		
		k	f	$\bar{x}$	k	f	$\bar{x}$
1	26	0	0.	.....	0	0.	.....
2	4	0	0.	.....	0	0.	.....
3	3	0	0.	.....	0	0.	.....
4	60	0	0.	.....	0	0.	.....
5	100	0	0.	.....	0	0.	.....
6	88	0	0.	.....	0	0.	.....
7	290	19	.07	1.16	14	.05	3.79
8	2	0	0.	.....	0	0.	.....
9	1	0	0.	.....	0	0.	.....
10	5	1	.20	5.00	1	.20	4.00
11	26	0	0.	.....	0	0.	.....
12	9	1	.11	4.00	0	0.	.....
13	26	0	0.	.....	0	0.	.....
14	232	209	.90	3.62	230	.99	8.71
15	91	0	0.	.....	0	0.	.....
16	7	0	0.	.....	0	0.	.....
17	40	7	.17	2.14	9	.22	3.44
18	235	25	.11	3.20	122	.52	4.44
19	158	3	.02	3.00	11	.07	4.27
20	1720	832	.48	4.68	451	.26	7.54
21	34	0	0.	.....	0	0.	.....
22	1	0	0.	.....	0	0.	.....
23	17	0	0.	.....	0	0.	.....
24	328	35	.11	3.86	64	.20	3.78
25	1903	444	.23	5.76	195	.10	4.12
26	1	0	0.	.....	1	1.00	3.00
27	13	3	.23	2.00	1	.08	4.00
28	11	0	0.	.....	0	0.	.....
29	1	0	0.	.....	0	0.	.....
30	4	2	.50	2.00	1	.25	4.00
31	1	0	0.	.....	0	0.	.....
32	1	1	1.00	6.00	1	1.00	3.00
33	1	0	0.	.....	0	0.	.....
34	32	0	0.	.....	0	0.	.....
40	277	0	0.	.....	0	0.	.....
41	173	47	.27	4.32	25	.14	6.12
42	5	1	.20	8.00	0	0.	.....
43	4	0	0.	.....	0	0.	.....
44	83	0	0.	.....	0	0.	.....
45	171	0	0.	.....	0	0.	.....
46	1	1	1.00	2.00	1	1.00	4.00
47	114	114	1.00	1.72	114	1.00	3.50

TABLE 4. *Summary of results classified by agency and processing facility*

Agency	Processor	n	Leader			Information section		
			k	f	$\bar{x}$	k	f	$\bar{x}$
15								
	46	1	1	1.00	2.00	1	1.00	4.00
	47	114	114	1.00	1.72	114	1.00	3.50
16								
	14	232	209	.90	3.62	230	.99	8.71
31								
	10	1	1	1.00	5.00	1	1.00	4.00
	20	1499	824	.55	4.70	446	.30	7.59
	41	167	45	.27	4.42	25	.15	6.12
40								
	7	290	19	.07	1.16	14	.05	3.79
51								
	25	103	28	.27	6.11	59	.57	2.61
52								
	20	1	1	1.00	6.00	0	0.	.....
	25	1539	382	.25	5.97	98	.06	5.32
61								
	20	2	0	0.	.....	1	.50	3.00
	25	73	0	0.	.....	2	.03	2.50
62								
	25	6	5	.83	3.20	3	.50	3.00
	32	1	1	1.00	6.00	1	1.00	3.00
63								
	20	9	0	0.	.....	3	.33	2.67
	24	328	35	.11	3.86	64	.20	3.78
71								
	25	84	19	.23	2.74	23	.27	3.35
	42	1	1	1.00	8.00	0	0.	.....
73								
	25	20	0	0.	.....	0	0.	.....
	27	13	3	.23	2.00	1	.08	4.00
	30	4	2	.50	2.00	1	.25	4.00
81								
	20	2	0	0.	.....	0	0.	.....
	41	6	2	.33	2.00	0	0.	.....
82								
	12	9	1	.11	4.00	0	0.	.....
83								
	10	4	0	0.	.....	0	0.	.....
	25	3	1	.33	3.00	0	0.	.....
	42	4	0	0.	.....	0	0.	.....
92								
	19	158	3	.02	3.00	11	.07	4.27
101								
	25	10	4	.40	5.00	6	.60	4.67
102								
	25	6	1	.17	5.00	0	0.	.....
103								
	20	10	7	.70	2.29	1	.10	3.00
	25	28	4	.14	1.75	4	.14	2.50
111								
	17	40	7	.17	2.14	9	.22	3.44
	18	235	25	.11	3.20	122	.52	4.44
121								
	26	1	0	0.	.....	1	1.00	3.00

TABLE 5. *Summary of results classified by manufacturer*

Manufacturer	n	Leader			Information section		
		k	f	$\bar{x}$	k	f	$\bar{x}$
1	177	117	0.66	3.24	104	0.59	7.52
2	107	6	.06	1.50	7	.07	2.43
3	97	3	.03	3.33	7	.07	8.86
4	1093	297	.27	3.17	298	.27	5.98
5	2	0	0.	.....	0	0.	.....
6	5238	1453	.28	4.86	989	.19	5.56
8	7	0	0.	.....	0	0.	.....
9	70	0	0.	.....	0	0.	.....
10	391	0	0.	.....	1	0.	3.00
11	94	0	0.	.....	0	0.	.....

TABLE 5A. *Summary of results classified by manufacturer*
Agencies 15 and 16 omitted

Manufacturer	n	Leader			Information section		
		k	f	$\bar{x}$	k	f	$\bar{x}$
1	110	62	0.56	3.5	39	0.35	5.0
2	102	1	.01	2.0	2	.02	2.5
3	90	0	0.	.....	0	0.	.....
4	853	63	.07	4.2	58	.07	4.9
5	2	0	0.	.....	0	0.	.....
6	5189	1432	.28	4.9	967	.19	5.5
8	7	0	0.	.....	0	0.	.....
9	70	0	0.	.....	0	0.	.....
10	391	0	0.	.....	1	0.	3.0
11	94	0	0.	.....	0	0.	.....

TABLE 6. *Summary of results classified by Agency and film manufacturer*

Agency	Film manufacturer	n	Leader			Information section		
			k	f	$\bar{x}$	k	f	$\bar{x}$
15								
	4	116	116	1.00	1.72	116	1.00	3.51
	6	26	0	0.	.....	0	0.	.....
16								
	1	67	55	.82	3.00	65	.97	9.03
	2	5	5	1.00	1.40	5	1.00	2.40
	3	7	3	.43	3.33	7	1.00	8.86
	4	124	118	.95	4.02	124	1.00	8.78
	6	23	21	.91	4.19	22	.96	6.82

TABLE 6. *Summary of results classified by Agency and film manufacturer*—Continued

Agency	Film manufacturer	n	Leader			Information section		
			k	f	$\bar{x}$	k	f	$\bar{x}$
31								
	4	169	46	.27	4.39	26	.15	6.27
	6	1498	823	.55	4.70	446	.30	7.58
40								
	1	49	18	.37	1.11	3	.06	3.33
	4	129	2	.02	1.50	8	.06	3.12
	6	94	0	0.	.....	2	.02	8.50
	10	19	0	0.	.....	0	0.	.....
51								
	4	3	2	.67	4.50	3	1.00	2.00
	6	203	56	.28	5.29	103	.51	2.68
52								
	4	1	0	0.	.....	0	0.	.....
	6	1541	384	.25	5.97	98	.06	5.32
	8	2	0	0.	.....	0	0.	.....
61								
	1	48	35	.73	4.49	27	.56	4.00
	4	73	2	.03	2.00	1	.01	2.00
	6	501	49	.10	2.67	73	.15	2.41
62								
	1	10	9	.90	4.11	9	.90	8.56
	2	7	0	0.	.....	0	0.	.....
	4	21	1	.05	3.00	2	.10	1.50
	5	2	0	0.	.....	0	0.	.....
	6	68	6	.09	3.67	4	.06	3.00
	8	1	0	0.	.....	0	0.	.....
63								
	4	19	0	0.	.....	0	0.	.....
	6	386	37	.10	3.76	70	.18	3.71
71								
	4	17	8	.47	5.12	0	0.	.....
	6	83	19	.23	2.74	23	.28	3.35
73								
	6	40	4	.10	2.00	5	.13	3.80
81								
	1	2	0	0.	.....	0	0.	.....
	2	3	0	0.	.....	0	0.	.....
	4	4	2	.50	2.00	0	0.	.....
	6	2	0	0.	.....	0	0.	.....
82								
	6	9	1	.11	4.00	0	0.	.....
83								
	2	4	0	0.	.....	0	0.	.....
	4	5	0	0.	.....	0	0.	.....
	6	2	1	.50	3.00	0	0.	.....
92								
	3	31	0	0.	.....	0	0.	.....
	6	127	3	.02	3.00	11	.09	4.27
	10	1	0	0.	.....	0	0.	.....
101								
	6	10	4	.40	5.00	6	.60	4.67
102								
	6	6	1	.17	5.00	0	0.	.....
103								
	2	2	1	.50	2.00	1	.50	2.00
	4	1	0	0.	.....	1	1.00	1.00
	6	44	11	.25	2.09	5	.11	2.60
111								
	1	1	0	0.	.....	0	0.	.....
	2	1	0	0.	.....	1	1.00	3.00
	3	1	0	0.	.....	0	0.	.....
	4	20	0	0.	.....	17	.85	5.00
	6	261	33	.13	2.88	121	.46	4.29
121								
	10	1	0	0.	.....	1	1.00	3.00

TABLE 7. *Summary of results classified by year of purchase*

Years	n	Leader			Information section		
		k	f	$\bar{x}$	k	f	$\bar{x}$
1901–1945	346	137	0.40	4.66	181	0.52	6.03
1946–1950	1203	478	.40	4.64	300	.25	6.08
1951–1955	1640	472	.29	4.69	256	.16	4.60
1956–1960	1487	420	.28	4.52	349	.23	6.52
1961–1965	513	110	.21	3.26	67	.13	6.76

TABLE 7A. *Summary of results classified by year of purchase*
Agencies 15 and 16 omitted

Years	n	Leader			Information section		
		k	f	$\bar{x}$	k	f	$\bar{x}$
1901–1945	346	137	0.40	4.7	181	0.52	6.0
1946–1950	1142	417	.37	5.0	239	.21	6.2
1951–1955	1555	392	.25	5.2	172	.11	4.3
1956–1960	1381	326	.24	4.8	247	.18	6.1
1961–1965	438	65	.15	3.7	16	.04	3.8

TABLE 8. *Summary of results classified by year processed*

Years	n	Leader			Information section		
		k	f	$\bar{x}$	k	f	$\bar{x}$
1901–1945	361	69	0.19	4.20	111	0.31	3.76
1946–1950	1610	646	.40	4.65	455	.28	6.25
1951–1955	1836	507	.28	4.64	249	.14	4.69
1956–1960	1856	417	.22	4.51	381	.21	6.42
1961–1965	801	127	.16	3.37	78	.10	6.68

TABLE 8A. *Summary of results classified by year processed*
Agencies 15 and 16 omitted

Years	n	Leader			Information section		
		k	f	$\bar{x}$	k	f	$\bar{x}$
1901–1945	361	69	0.19	4.2	111	0.31	3.8
1946–1950	1549	585	.38	4.9	394	.25	6.3
1951–1955	1754	430	.25	5.1	168	.10	4.4
1956–1960	1748	321	.18	4.8	277	.16	6.0
1961–1965	726	82	.11	3.8	27	.04	4.7

TABLE 9. *Summary of results classified by frequency of use*

Frequency of use	n	Leader			Information section		
		k	f	$\bar{x}$	k	f	$\bar{x}$
Daily	127	4	0.03	1.50	3	0.02	2.67
Frequently	1002	94	.09	3.80	187	.19	3.06
Infrequently	2540	479	.19	4.52	371	.15	5.54
Dead storage	3730	1328	.36	4.48	881	.24	6.53

TABLE 9A. *Summary of results classified by frequency of use*
Agencies 15 and 16 omitted

Frequency of use	n	Leader			Information section		
		k	f	$\bar{x}$	k	f	$\bar{x}$
Daily	127	4	0.03	1.5	3	0.02	2.7
Frequently	1002	94	.09	3.8	187	.19	3.1
Infrequently	2415	362	.15	4.8	246	.10	4.2
Dead storage	3467	1108	.32	4.8	647	.19	6.6

TABLE 10. *Summary of results classified by type of container*

Type of container	n	Leader			Information section		
		k	f	$\bar{x}$	k	f	$\bar{x}$
Metal can	519	166	0.32	3.66	191	0.37	8.35
Cardboard container	6643	1645	.25	4.62	1149	.17	5.38
Other	65	49	.75	3.45	57	.88	7.47
Metal can cardboard container	175	44	.25	2.30	46	.26	3.98

TABLE 10A. *Summary of results classified by type of container*
Agencies 15 and 16 omitted

Type of container	n	Leader			Information section		
		k	f	$\bar{x}$	k	f	$\bar{x}$
Metal can	347	8	0.02	2.9	19	0.05	2.7
Cardboard container	6528	1558	.24	4.8	1061	.16	5.5
Other	7	0	0.	.....	1	.14	4.0
Metal can cardboard container	134	3	.02	7.3	5	.04	4.4

TABLE 11. *Summary of results classified by type of reel*

Type of reel	n	Leader			Information section		
		k	f	$\bar{x}$	k	f	$\bar{x}$
Metal	3965	1163	0.29	4.41	840	0.21	5.74
Plastic	2353	521	.22	4.63	411	.17	5.49
Core only	618	51	.08	4.51	27	.04	6.63
Other	112	59	.53	3.41	76	.68	6.45
Cardboard	218	88	.40	4.50	65	.30	7.09
Metal and plastic	67	0	0.	.....	0	0.	.....

TABLE 11A. *Summary of results classified by type of reel*
Agencies 15 and 16 omitted

Type of reel	n	Leader			Information section		
		k	f	$\bar{x}$	k	f	$\bar{x}$
Metal	3676	888	0.24	4.9	551	0.15	5.1
Plastic	2317	511	.22	4.6	402	.17	5.5
Core only	618	51	.08	4.5	27	.04	6.6
Other	52	10	.19	3.7	18	.35	2.7
Cardboard	218	88	.40	4.5	65	.30	7.1
Metal and plastic	67	0	0.	.....	0	0.	.....

TABLE 12–1. *Summary of results classified by maximum temperature*

Temperature (°F)	n	Leader			Information section		
		k	f	$\bar{x}$	k	f	$\bar{x}$
61–70	59	7	0.12	2.00	5	0.08	2.80
71–75	231	5	.02	2.20	44	.19	4.59
76–80	1325	287	.22	3.67	315	.24	7.49
81–85	841	423	.50	4.45	169	.20	7.88

TABLE 12–2. *Summary of results classified by minimum temperature*

Temperature (°F)	n	Leader			Information section		
		k	f	$\bar{x}$	k	f	$\bar{x}$
40–55	88	0	0.	.....	0	0.	.....
56–65	321	23	.07	1.39	10	.03	3.70
66–75	2047	699	.34	4.19	523	.26	7.40

TABLE 12A–1. *Summary of results classified by maximum temperature*
Agencies 15 and 16 omitted

Temperature (°F)	n	Leader			Information section		
		k	f	$\bar{x}$	k	f	$\bar{x}$
61–70	59	7	0.12	2.0	5	0.08	2.8
71–75	231	5	.02	2.2	44	.19	4.6
76–80	1056	67	.06	3.7	75	.07	4.0
81–85	841	423	.50	4.4	169	.20	7.9

TABLE 12A–2. *Summary of results classified by minimum temperature*
Agencies 15 and 16 omitted

Temperature (°F)	n	Leader			Information section		
		k	f	$\bar{x}$	k	f	$\bar{x}$
40–55	62	0	0.	.....	0	0.	.....
56–65	321	23	.07	1.4	10	.03	3.7
66–75	1804	479	.27	4.4	283	.16	6.4

TABLE 13–1. *Summary of results classified by maximum humidity*

Relative humidity (%)	n	Leader			Information section		
		k	f	$\bar{x}$	k	f	$\bar{x}$
20–50	776	230	0.30	3.9	235	0.30	8.5
51–60	1513	478	.32	4.3	283	.19	6.3
61–70	0	.....	.....	.....	.....	.....	.....
71–80	55	0	0.	.....	0	0.	.....
81–95	1	0	0.	.....	0	0.	.....

TABLE 13–2. *Summary of results classified by minimum humidity*

Relative humidity (%)	n	Leader			Information section		
		k	f	$\bar{x}$	k	f	$\bar{x}$
1–30	691	194	0.28	3.8	205	0.30	8.7
31–40	93	18	.19	2.3	24	.26	7.6
>40	1472	477	.32	4.3	283	.19	6.3

TABLE 13A–1. *Summary of results classified by maximum humidity*
Agencies 15 and 16 omitted

Relative humidity (%)	n	Leader			Information section		
		k	f	$\bar{x}$	k	f	$\bar{x}$
20–50	544	19	0.03	5.5	6	0.01	5.8
51–60	1487	478	.32	4.3	283	.19	6.3
61–70	0	.....	.....	.....	.....	.....	.....
71–80	55	0	0.	.....	0	0.	.....
81–95	1	0	0.	.....	0	0.	.....

TABLE 13A–2. *Summary of results classified by minimum humidity*
Agencies 15 and 16 omitted

Relative humidity (%)	n	Leader			Information section		
		k	f	$\bar{x}$	k	f	$\bar{x}$
1–30	485	1	0.	4.0	0	0.	.....
31–40	41	0	0.	.....	0	0.	.....
>40	1472	477	.32	4.3	283	0.19	6.3

TABLE 14. *Summary of results classified by use of air conditioning*

Air conditioning used?	n	Leader			Information section		
		k	f	$\bar{x}$	k	f	$\bar{x}$
Yes	1508	278	0.18	3.51	356	0.24	7.13
No	1132	450	.40	4.46	184	.16	7.59

TABLE 14A. *Summary of results classified by use of air conditioning*
Agencies 15 and 16 omitted

Air conditioning used?	n	Leader			Information section		
		k	f	$\bar{x}$	k	f	$\bar{x}$
Yes	1266	59	0.05	3.0	117	0.09	4.2
No	1106	449	.41	4.5	183	.17	7.6

TABLE 15. *Summary of results classified by storage location*

Storage location	n	Leader			Information section		
		k	f	$\bar{x}$	k	f	$\bar{x}$
Vault	1688	655	0.39	4.10	408	0.24	8.22
Office	830	55	.07	3.44	123	.15	4.21
Basement	10	1	.10	5.00	1	.10	1.00
Other	22	0	0.	.....	0	0.	.....
Underground or mine	141	26	.18	4.58	11	.08	4.46

TABLE 15A. *Summary of results classified by storage location*
Agencies 15 and 16 omitted

Storage location	n	Leader			Information section		
		k	f	$\bar{x}$	k	f	$\bar{x}$
Vault	1425	440	0.31	4.3	174	0.12	7.8
Office	827	52	.06	3.4	120	.15	4.0
Basement	10	1	.10	5.0	1	.10	1.0
Other	22	0	0.	.....	0	0.	.....
Underground or mine	141	26	.18	4.6	11	.08	4.5

TABLE 16. *Summary of results classified by use of humidification trays*

Humidification trays?	n	Leader			Information section		
		k	f	$\bar{x}$	k	f	$\bar{x}$
Yes	78	6	0.08	4.83	6	0.08	4.67
No	2532	721	.28	4.10	529	21	7.36

TABLE 16A. *Summary of results classified by use of humidification trays*
Agencies 15 and 16 omitted

Humidification trays?	n	Leader			Information section		
		k	f	$\bar{x}$	k	f	$\bar{x}$
Yes	78	6	0.08	4.8	6	0.08	4.7
No	2264	501	.22	4.3	289	.13	6.3

TABLE 17. *Summary of results classified by type of leader*

Type of leader	n	Leader			Information section		
		k	f	$\bar{x}$	k	f	$\bar{x}$
Fogged	923	274	0.30	3.52	239	0.26	7.10
Clear	3427	187	.05	2.49	648	.19	5.26
Plastic	68	8	.12	3.75	11	.16	5.64
Fogged and clear	2913	1428	.49	4.89	522	.18	5.99
No leader	38	.....	.....	.....	13	.34	2.38
Clear and plastic	4	1	.25	10.00	2	.50	2.00

TABLE 17A. *Summary of results classified by type of leader*
Agencies 15 and 16 omitted

Type of leader	n	Leader			Information section		
		k	f	$\bar{x}$	k	f	$\bar{x}$
Fogged	758	117	0.15	3.5	75	0.10	4.9
Clear	3220	19	.01	2.7	469	.15	5.1
Plastic	65	5	.08	2.0	8	.12	2.9
Fogged and clear	2907	1424	.49	4.9	516	.18	6.0
No leader	38	0	0.	.....	13	.34	2.4
Clear and plastic	4	1	.25	10.0	2	.50	2.0

TABLE 18. *Summary of results classified by length of leader*

Length (ft)	n	Leader			Information section		
		k	f	$\bar{x}$	k	f	$\bar{x}$
0	38	.....	.....	.....	13	0.34	2.38
1–2	2295	184	0.08	3.53	438	.19	4.98
3–5	3733	1326	.36	4.38	773	.21	5.93
> 5	1024	377	.37	5.21	194	.19	7.34

TABLE 18A. *Summary of results classified by length of leader*
Agencies 15 and 16 omitted

Length (ft)	n	Leader			Information section		
		k	f	$\bar{x}$	k	f	$\bar{x}$
0	38	.....	.....	.....	13	0.34	2.38
1–2	2203	102	0.05	3.7	348	.16	4.2
3–5	3517	1144	.33	4.7	583	.17	6.1
> 5	958	316	.33	5.5	128	.13	6.2

TABLE 19. *Summary of results classified by number of splices*

Number of splices	n	Leader			Information section		
		k	f	$\bar{x}$	k	f	$\bar{x}$
None	3902	1175	0.30	4.27	859	0.22	5.55
1–5	2176	577	.27	4.74	480	.22	6.22
6–10	344	52	.15	5.58	25	.07	5.48
> 10	548	55	.10	4.76	35	.06	5.43

TABLE 19A. *Summary of results classified by number of splices*
Agencies 15 and 16 omitted

Number of splices	n	Leader			Information section		
		k	f	$\bar{x}$	k	f	$\bar{x}$
None	3577	900	0.25	4.7	563	0.16	5.1
1–5	2140	541	.25	4.8	444	.21	6.0
6–10	342	50	.15	5.5	23	.07	5.0
> 10	548	55	.10	4.8	35	.06	5.4

TABLE 20. *Summary of results classified by agency and number of splices*

Agency	Number of splices	n	Leader			Information section		
			k	f	$\bar{x}$	k	f	$\bar{x}$
15	0	137	111	0.81	1.7	111	0.81	3.5
	1 to 5	5	5	1.00	1.4	5	1.00	2.8
16	0	188	164	.87	3.5	185	.98	8.3
	1 to 5	31	31	1.00	4.1	31	1.00	10.5
	6 to 10	2	2	1.00	6.5	2	1.00	10.5
31	0	800	429	.54	4.6	204	.25	7.1
	1 to 5	813	419	.52	4.8	256	.31	7.7
	6 to 10	21	7	.33	5.0	4	.19	11.2
	>10	6	1	.17	4.0	3	.50	11.7
40	0	212	15	.07	1.1	4	.02	2.2
	1 to 5	60	2	.03	1.0	5	.08	5.4
	6 to 10	12	0	0.	.....	2	.17	1.5
	> 10	12	2	.17	1.5	4	.33	4.0
51	0	157	46	.29	5.1	67	.43	2.6
	1 to 5	40	9	.22	4.8	35	.88	2.7
	6 to 10	1	1	1.00	10.0	1	1.00	2.0
	> 10	1	1	1.00	5.0	1	1.00	2.0
52	0	334	228	.68	6.2	29	.09	5.8
	1 to 5	478	62	.13	6.3	36	.08	4.9
	6 to 10	217	42	.19	5.5	10	.05	5.0
	>10	511	51	.10	4.9	23	.05	5.5
61	0	394	77	.20	3.5	67	.17	3.2
	1 to 5	192	7	.04	3.3	23	.12	2.3
	6 to 10	14	0	0.	.....	4	.29	2.5
	>10	10	0	0.	.....	4	.40	2.5
62	0	93	15	.16	3.9	14	.15	6.5
	1 to 5	16	1	.06	3.0	1	.06	1.0
	6 to 10	1	0	0.	.....	0	0.	.....
63	0	206	16	.08	3.8	46	.22	3.8
	1 to 5	195	20	.10	3.7	22	.11	3.5
71	0	32	15	.47	3.7	3	.09	3.3
	1 to 5	68	12	.18	3.1	20	.29	3.4
73	0	54	6	.11	2.0	6	.11	3.8
	1 to 5	9	5	.56	2.0	4	.44	2.5
	6 to 10	1	0	0.	.....	0	0.	.....
81	0	11	2	.18	2.0	0	0.	.....
	1 to 5	1	0	0.	.....	0	0.	.....
	6 to 10	0	.....	.....	.....	.....	.....	.....
	> 10	1	0	0.	.....	0	0.	.....
82	0	4	1	.25	4.0	0	0.	.....
	1 to 5	5	0	0.	.....	0	0.	.....
83	0	8	0	0.	.....	0	0.	.....
	1 to 5	3	1	.33	3.0	0	0.	.....
92	0	128	3	.02	3.0	8	.06	4.2
	1 to 5	12	0	0.	.....	0	0.	.....
101	0	7	3	.43	6.0	3	.43	3.7
	1 to 5	3	1	.33	2.0	3	1.00	5.7
102	0	6	1	.17	5.0	0	0.	.....
103	0	16	11	.69	2.1	6	.38	2.2
	1 to 5	7	1	.14	2.0	1	.14	3.0
111	0	236	32	.14	2.9	105	.44	4.6
	1 to 5	56	1	.02	3.0	38	.68	4.0
	6 to 10	4	0	0.	.....	2	.50	3.0
	> 10	1	0	0.	.....	0	0.	.....
121	0	1	0	0.	.....	1	1.00	3.0

TABLE 21. *Summary of results classified by type of splice*

Type of splice	n	Leader			Information section		
		k	f	$\bar{x}$	k	f	$\bar{x}$
Overlap	1491	487	0.33	4.87	350	0.23	6.45
Butt	1221	149	.12	4.69	139	.11	4.51
Other	67	2	.03	6.00	4	.06	2.50
Overlap and butt	189	27	.14	4.63	25	.13	8.60
Overlap and other	6	0	0.	.....	0	0.	.....
Butt and other	26	4	.15	4.25	4	.15	3.25

TABLE 21A. *Summary of results classified by type of splice*
Agencies 15 and 16 omitted

Type of splice	n	Leader			Information section		
		k	f	$\bar{x}$	k	f	$\bar{x}$
Overlap	1481	477	0.32	4.9	340	0.23	6.5
Butt	1215	143	.12	4.8	133	.11	4.4
Other	67	2	.03	6.0	4	.06	2.5
Overlap and butt	189	27	.14	4.6	25	.13	8.6
Overlap and other	6	0	0.	.....	0	0.	.....
Butt and other	26	4	.15	4.2	4	.15	3.2

TABLE 22. *Summary of results classified by type of band*

Type of band	n	Leader			Information section		
		k	f	$\bar{x}$	k	f	$\bar{x}$
None	6877	1703	0.25	4.61	1209	0.18	5.72
String	16	0	0.	.....	0	0.	.....
Rubber band	348	161	.46	3.24	177	.51	6.46
Other	45	29	.64	2.17	35	.78	7.34
Paper	15	2	.13	2.50	1	.07	7.00

TABLE 22A. *Summary of results classified by type of band*
Agencies 15 and 16 omitted

Type of band	n	Leader			Information section		
		k	f	$\bar{x}$	k	f	$\bar{x}$
None	6679	1541	0.23	4.8	1037	0.16	5.6
String	16	0	0.	.....	0	0.	.....
Rubber band	195	15	.08	2.7	25	.13	2.3
Other	9	1	.11	1.0	1	.11	2.0
Paper	15	2	.13	2.5	1	.07	7.0

TABLE 23. *Summary of results classified by presence or absence of chemical residues*

Chemical residue?	n	Leader			Information section		
		k	f	$\bar{x}$	k	f	$\bar{x}$
Yes	500	298	0.60	3.49	304	0.61	7.34
No	6495	1554	.24	4.67	1081	.17	5.49

TABLE 23A. *Summary of results classified by presence or absence of chemical residues*
Agencies 15 and 16 omitted

Chemical residue?	n	Leader			Information section		
		k	f	$\bar{x}$	k	f	$\bar{x}$
Yes	229	50	0.22	4.1	37	0.16	3.8
No	6383	1468	.23	4.8	994	.16	5.6

TABLE 24. *Summary of results classified by presence or absence of silvery sheen on leaders*

Sheen on leader?	n	Leader			Information section		
		k	f	$\bar{x}$	k	f	$\bar{x}$
Yes	1042	791	0.76	5.33	397	0.38	7.74
No	5912	1054	.18	3.86	970	.16	5.08

TABLE 24A. *Summary of results classified by presence or absence of silvery sheen on leaders*
Agencies 15 and 16 omitted

Sheen on leader?	n	Leader			Information section		
		k	f	$\bar{x}$	k	f	$\bar{x}$
Yes	874	629	0.72	5.6	230	0.26	6.5
No	5710	888	.16	4.2	796	.14	5.2

TABLE 25. *Summary of results classified by presence or absence of silvery sheen on dense area*

Sheen on dense area?	n	Leader			Information section		
		k	f	$\bar{x}$	k	f	$\bar{x}$
Yes	284	158	0.56	4.50	192	0.68	10.56
No	6705	1691	.25	4.50	1183	.18	5.10

TABLE 25A. *Summary of results classified by presence or absence of silvery sheen on dense area*
Agencies 15 and 16 omitted

Sheen on dense area?	n	Leader			Information section		
		k	f	$\bar{x}$	k	f	$\bar{x}$
Yes	168	50	0.30	5.5	76	0.45	11.2
No	6449	1471	.23	4.8	956	.15	5.0

TABLE 26. *Summary of results classified by presence or absence of discoloration or fading*

Discoloration or fading?	n	Leader			Information section		
		k	f	$\bar{x}$	k	f	$\bar{x}$
Yes	192	112	0.58	3.58	125	0.65	8.10
No	6798	1736	.26	4.55	1255	.18	5.62

TABLE 26A. *Summary of results classified by presence or absence of discoloration or fading*
Agencies 15 and 16 omitted

Discoloration or fading?	n	Leader			Information section		
		k	f	$\bar{x}$	k	f	$\bar{x}$
Yes	83	14	0.17	4.6	17	0.20	8.1
No	6535	1507	.23	4.8	1019	.16	5.5

TABLE 27. *Summary of results classified by presence or absence of water spots*

Water spots?	n	Leader			Information section		
		k	f	$\bar{x}$	k	f	$\bar{x}$
Yes	718	180	0.25	2.24	291	0.41	4.52
No	6297	1663	.26	4.74	1077	.17	6.18

TABLE 27A. *Summary of results classified by presence or absence of water spots*
Agencies 15 and 16 omitted

Water spots?	n	Leader			Information section		
		k	f	$\bar{x}$	k	f	$\bar{x}$
Yes	590	57	0.10	2.9	165	0.28	4.4
No	6062	1467	.24	4.9	869	.14	5.7

TABLE 28. *Summary of results classified by presence or absence of other blemishes*

Other blemishes?	n	Leader			Information section		
		k	f	$\bar{x}$	k	f	$\bar{x}$
Yes	281	136	0.48	4.02	150	0.53	9.01
No	6241	1629	.26	4.58	1109	.18	5.70

TABLE 28A. *Summary of results classified by presence or absence of other blemishes*

Agencies 15 and 16 omitted

Other blemishes?	n	Leader			Information section		
		k	f	$\bar{x}$	k	f	$\bar{x}$
Yes	149	16	0.11	3.6	18	0.12	5.6
No	6036	1437	.24	4.9	913	.15	5.8

TABLE 29. *Summary of results classified by agency and type of leader*

Agency	Type of leader	n	Leader			Information section		
			k	f	$\bar{x}$	k	f	$\bar{x}$
15	Fogged	33	33	1.00	1.7	33	1.00	3.4
	Clear	107	81	.76	1.8	81	.76	3.6
	Fogged and clear	1	1	1.00	1.0	1	1.00	2.0
16	Fogged	132	124	.94	4.0	131	.99	9.3
	Clear	100	87	.87	3.1	98	.98	7.5
	Plastic	3	3	1.00	6.7	3	1.00	13.0
	Fogged and clear	5	3	.60	3.3	5	1.00	7.2
31	Fogged	11	6	.55	4.7	4	.36	11.8
	Clear	376	4	.01	2.5	130	.35	8.8
	Fogged and clear	1281	860	.67	4.7	338	.26	7.0
40	Fogged	99	16	.16	1.1	4	.04	4.8
	Clear	162	0	0.	.....	6	.04	2.8
	Fogged and clear	38	4	.11	1.2	4	.11	2.8
51	Fogged	5	5	1.00	4.4	5	1.00	3.6
	Clear	120	3	.02	3.0	71	.59	2.6
	Plastic	1	0	0.	.....	0	0.	.....
	Fogged and clear	69	48	.70	5.3	23	.33	2.6
	No leader	8	.....	.....	.....	7	.88	2.6
	Clear and plastic	2	1	.50	10.0	1	.50	2.0
52	Fogged	62	28	.45	5.6	14	.23	6.4
	Clear	609	2	.00	4.5	15	.02	5.2
	Plastic	21	0	0.	.....	0	0.	.....
	Fogged and clear	841	354	.42	6.0	69	.08	5.1
	No leader	6	.....	.....	.....	0	0.	.....
	Clear and plastic	1	0	0.	.....	0	0.	.....
61	Fogged	14	3	.21	3.3	3	.21	2.3
	Clear	299	3	.01	2.3	44	.15	2.3
	Fogged and clear	306	81	.26	3.5	55	.18	3.3
	No leader	7	.....	.....	.....	1	.14	2.0
62	Fogged	4	2	.50	3.5	2	.50	3.5
	Clear	65	1	.02	4.0	4	.06	5.5
	Fogged and clear	37	13	.35	3.9	9	.24	7.0
	No leader	4	.....	.....	.....	0	0.	.....
63	Clear	310	1	.00	3.0	59	.19	3.8
	Fogged and clear	93	35	.38	3.8	10	.11	3.4
71	Fogged	8	6	.75	4.0	0	0.	.....
	Clear	36	0	0.	.....	18	.50	3.1
	Fogged and clear	56	21	.38	3.3	5	.09	4.4
73	Fogged	4	3	.75	2.0	2	.50	4.0
	Clear	29	3	.10	2.0	4	.14	3.8
	Plastic	29	5	.17	2.0	4	.14	2.5
81	Fogged	2	0	0.	.....	0	0.	.....
	Clear	4	0	0.	.....	0	0.	.....
	Fogged and clear	7	2	.29	2.0	0	0.	.....
82	Fogged	1	0	0.	.....	0	0.	.....
	Clear	6	0	0.	.....	0	0.	.....
	Fogged and clear	2	1	.50	4.0	0	0.	.....
83	Fogged	1	0	0.	.....	0	0.	.....
	Clear	7	0	0.	.....	0	0.	.....
	Fogged and clear	3	1	.33	3.0	0	0.	.....
92	Fogged	71	1	.01	3.0	2	.03	3.0
	Clear	61	0	0.	.....	7	.11	4.6
	Plastic	1	0	0.	.....	0	0.	.....
	Fogged and clear	25	2	.08	3.0	2	.08	4.5
101	Fogged	4	4	1.00	5.0	4	1.00	3.2
	Clear	2	0	0.	.....	2	1.00	7.5
	Fogged and clear	4	0	0.	.....	0	0.	.....
102	Fogged and clear	6	1	.17	5.0	0	0.	.....
103	Fogged	38	11	.29	2.1	4	.11	2.5
	Clear	48	0	0.	.....	2	.04	1.5
	Fogged and clear	2	1	.50	2.0	1	.50	3.0
111	Fogged	90	32	.36	2.9	31	.34	4.5
	Clear	194	2	.01	2.0	106	.55	4.6
	Plastic	7	0	0.	.....	4	.57	3.2
	No leader	7	.....	.....	.....	4	.57	2.0
	Clear and plastic	1	0	0.	.....	1	1.00	2.0

TABLE 30. *Summary of results classified by type of leader and length of leader*

Type of leader	Length	n	Leader			Information section		
			k	f	$\bar{x}$	k	f	$\bar{x}$
Fogged	1 to 2 ft	262	53	0.20	3.92	50	0.19	6.10
	3 to 5 ft	450	144	.32	3.11	109	.24	6.52
	>5 ft	160	70	.44	3.90	13	.46	8.44
Clear	1 to 2 ft	1780	71	.04	3.04	342	.19	4.96
	3 to 5 ft	1284	102	.08	2.13	271	.21	5.58
	>5 ft	236	5	.02	2.20	20	.08	6.45
Plastic	1 to 2 ft	44	6	.14	3.50	9	.20	5.11
	3 to 5 ft	14	1	.07	7.00	1	.07	14.00
	>5 ft	6	0	0.	.....	0	0.	.....
Fogged and clear.	1 to 2 ft	203	53	.26	3.85	35	.17	3.66
	3 to 5 ft	1972	1075	.55	4.76	388	.20	6.01
	>5 ft	617	300	.49	5.55	99	.16	6.74
Clear and plastic.	1 to 2 ft	1	0	0.	.....	1	1.00	2.00
	3 to 5 ft	2	0	0.	.....	0	0.	.....
	>5 ft	1	1	1.00	10.0	1	1.00	2.00

TABLE 31. *Summary of results classified by agency and type of splice*

Agency	Type of splice	n	Leader			Information section		
			k	f	$\bar{x}$	k	f	$\bar{x}$
15	Overlap	5	5	1.00	1.4	5	1.00	2.8
16	Overlap	5	5	1.00	3.4	5	1.00	10.2
	Butt	6	6	1.00	3.2	6	1.00	8.0
31	Overlap	711	380	.53	4.9	226	.32	7.5
	Butt	86	45	.52	4.4	24	.28	9.2
	Overlap and butt	58	11	.19	4.8	18	.31	10.3
40	Overlap	10	1	.10	1.0	2	.20	8.5
	Butt	58	1	.02	1.0	6	.10	3.3
	Other	3	0	0.	.....	1	.33	3.0
	Overlap and other	1	0	0.	.....	0	0.	.....
	Butt and other	10	1	.10	2.0	2	.20	3.0
51	Overlap	3	0	0.	.....	3	1.00	3.7
	Butt	37	9	.24	4.8	32	.86	2.8
	Other	2	1	.50	10.0	2	1.00	2.0
52	Overlap	324	71	.22	6.1	46	.14	5.8
	Butt	714	69	.10	5.4	16	.02	3.6
	Other	12	0	0.	.....	0	0.	.....
	Overlap and butt	128	16	.13	4.5	6	.05	4.7
	Overlap and other	1	0	0.	.....	0	0.	.....
61	Overlap	150	5	.03	2.6	21	.14	2.4
	Butt	39	0	0.	.....	8	.21	2.1
	Other	18	1	.06	2.0	0	0.	.....
61—Con.	Overlap and butt	2	0	0.	.....	1	0.50	1.0
	Overlap and other	4	0	0.	.....	0	0.	.....
	Butt and other	1	1	1.00	8.0	1	1.00	5.0
62	Overlap	7	1	.14	3.0	0	0.	.....
	Butt	7	0	0.	.....	1	.14	1.0
	Other	3	0	0.	.....	0	0.	.....
63	Overlap	13	0	0.	.....	3	.23	3.0
	Butt	162	17	.10	3.8	17	.10	3.6
	Other	4	0	0.	.....	1	.25	3.0
	Butt and other	15	2	.13	3.5	1	.07	2.0
71	Overlap	67	12	.18	3.1	20	.30	3.4
	Other	1	0	0.	.....	0	0.	.....
73	Overlap	10	5	.50	2.0	4	.40	2.5
81	Overlap	1	0	0.	.....	0	0.	.....
	Other	1	0	0.	.....	0	0.	.....
82	Overlap	5	0	0.	.....	0	0.	.....
83	Overlap	1	1	1.00	3.0	0	0.	.....
	Other	2	0	0.	.....	0	0.	.....
92	Overlap	11	0	0.	.....	0	0.	.....
	Butt	1	0	0.	.....	0	0.	.....
101	Overlap	3	1	.33	2.0	3	1.00	5.7
103	Butt	7	1	.14	2.0	1	.14	3.0
111	Overlap	26	0	0.	.....	12	.46	4.2
	Butt	36	1	.03	3.0	28	.78	3.8

TABLE 32. *Summary of results classified by agency and type of band*

Agency	Type of band	n	Leader			Information section		
			k	f	$\bar{x}$	k	f	$\bar{x}$
15	None	100	74	0.74	1.6	74	0.74	3.3
	Rubber band	42	42	1.00	1.9	42	1.00	3.9
16	None	98	88	.90	3.9	98	1.00	9.2
	Rubber band	111	104	.94	3.8	110	.99	8.4
	Other	36	28	.78	2.2	34	.94	7.5
31	None	1666	868	.52	4.7	472	.28	7.5
40	None	280	20	.07	1.2	14	.05	3.8
	Rubber band	15	0	0.	.....	0	0.	.....
	Other	3	0	0.	.....	1	.33	2.0
51	None	185	52	.28	5.4	92	.50	2.8
	Rubber band	18	3	.17	2.3	16	.89	1.9
	Other	3	1	.33	1.0	0	0.	.....
	Paper	2	2	1.00	2.5	0	0.	.....
52	None	1545	384	.25	6.0	98	.06	5.3
61	None	595	81	.14	3.4	86	.14	3.0
	Rubber band	4	1	.25	3.0	1	.25	2.0
62	None	81	10	.12	4.3	11	.14	7.5
	Rubber band	24	5	.21	3.2	4	.17	2.5
	Paper	2	0	0.	.....	0	0.	.....
63	None	399	36	.09	3.8	67	.17	3.7
	Other	1	0	0.	.....	0	0.	.....
71	None	100	27	.27	3.4	23	.23	3.3
73	None	58	9	.16	2.0	8	.14	3.6
	Rubber band	6	2	.33	2.0	2	.33	2.0
81	None	7	2	.29	2.0	0	0.	.....
	Rubber band	6	0	0.	.....	0	0.	.....
82	None	4	0	0.	.....	0	0.	.....
	Rubber band	5	1	.20	4.0	0	0.	.....
83	Rubber band	11	1	.09	3.0	0	0.	.....
92	None	120	3	.02	3.0	10	.08	4.2
	Rubber band	37	0	0.	.....	1	.03	5.0
101	None	10	4	.40	5.0	6	.60	4.7
102	None	6	1	.17	5.0	0	0.	.....
103	None	41	11	.27	2.2	7	.17	2.3
	Rubber band	1	1	1.00	1.0	0	0.	.....
	Other	1	0	0.	.....	0	0.	.....
	Paper	4	0	0.	.....	0	0.	.....
111	None	294	33	.11	2.9	143	.49	4.4
	Rubber band	1	1	1.00	3.0	1	1.00	5.0
	Paper	2	0	0.	.....	1	.50	7.0

TABLE 33. *Summary of results classified by storage location and year of purchase*

Agencies 15 and 16 omitted

Storage and year of purchase	n	Leader			Information section		
		k	f	$\bar{x}$	k	f	$\bar{x}$
Vault							
1901–1945	232	111	0.48	4.6	143	0.62	6.6
1946–1950	655	341	.52	4.9	186	.28	6.9
1951–1955	571	157	.27	4.6	68	.12	5.1
1956–1960	555	226	.41	4.4	128	.23	8.2
1961–1965	281	49	.17	3.5	5	.02	2.6
Office							
1901–1945	56	12	.21	2.9	22	.39	3.5
1946–1950	69	6	.09	2.8	6	.09	5.3
1951–1955	314	23	.07	3.0	66	.21	3.9
1956–1960	380	24	.06	3.6	48	.13	3.8
1961–1965	57	1	.02	2.0	0	0.	.....
Basement							
1901–1945	18	9	.50	4.7	0	0.	.....
1946–1950	53	13	.25	3.2	23	.43	3.3
1951–1955	2	0	0.	.....	0	0.	.....
1956–1960	3	2	.67	10.0	1	.33	1.0
1961–1965	17	3	.18	4.3	3	.18	2.3
Underground or mine							
1901–1945	188	53	.28	5.2	53	.28	5.3
1946–1950	342	56	.16	6.1	10	.03	3.7
1951–1955	531	208	.39	6.0	13	.02	2.9
1956–1960	373	59	.16	6.7	18	.05	7.6
1961–1965	60	11	.18	4.3	6	.10	6.0
Other							
1901–1945	2	0	0.	.....	1	.50	4.0
1946–1950	8	0	0.	.....	1	.13	2.0
1951–1955	114	0	0.	.....	8	.07	5.9
1956–1960	11	0	0.	.....	0	0.	.....
1961–1965	18	0	0.	.....	0	0.	.....

TABLE 34. *Summary of results classified by type of container and maximum humidity*

Agencies 15 and 16 omitted

Container and maximum humidity	n	Leader			Information section		
		k	f	$\bar{x}$	k	f	$\bar{x}$
Metal can—Percent:							
20–50	13	0	0.	.....	0	0.	.....
51–60	41	0	0.	.....	0	0.	.....
Cardboard container—Percent:							
20–50	488	19	.04	5.5	6	.01	5.8
51–60	1443	478	.33	4.3	282	.20	6.3
61–70	0	.....	.....	.....	.....	.....	.....
71–80	55	0	0.	.....	0	0.	.....
Metal can and cardboard container—Percent:							
20–50	37	0	0.	.....	0	0.	.....
51–60	3	0	0.	.....	1	.33	4.0
Other—Percent:							
20–50	6	0	0.	.....	0	0.	.....

TABLE 35. *Summary of results classified by type of container and maximum temperature*

Agencies 15 and 16 omitted

Container and maximum temperature	n	Leader			Information section		
		k	f	$\bar{x}$	k	f	$\bar{x}$
Metal can—Percent:							
61–70	6	0	0.	.....	0	0.	.....
71–75	8	0	0.	.....	0	0.	.....
76–80	101	0	0.	.....	0	0.	.....
Cardboard container—Percent:							
61–70	47	7	.15	2.0	5	.11	2.8
71–75	221	5	.02	2.2	44	.20	4.6
76–80	954	67	.07	3.7	74	.08	4.0
81–85	804	423	.53	4.4	169	.21	7.9
Metal can and cardboard container—Percent:							
61–70	0	0	0.	.....	0	0.	.....
71–75	2	0	0.	.....	0	0.	.....
76–80	1	0	0.	.....	1	1.00	4.00
81–85	37	0	0.	.....	0	0.	.....
Other—Percent:							
71–75	6	0	0.	.....	0	0.	.....

TABLE 36. *Summary of results classified by manufacturer and processor*

Manufacturer	Processor	n	Leader			Information section		
			k	f	$\bar{x}$	k	f	$\bar{x}$
1	7	47	17	0.36	1.1	3	0.06	3.3
	14	67	55	.82	3.0	65	.97	9.0
	18	1	0	0.	.....	0	0.	.....
2	14	5	5	1.00	1.4	5	1.00	2.4
	18	1	0	0.	.....	1	1.00	3.0
	25	1	1	1.00	2.0	0	0.	.....
	41	3	0	0.	.....	0	0.	.....
	42	4	0	0.	.....	0	0.	.....
3	14	7	3	.43	3.3	7	1.00	8.9
	18	1	0	0.	.....	0	0.	.....
	19	31	0	0.	.....	0	0.	.....
4	7	126	2	.02	1.5	7	.06	3.3
	10	4	0	0.	.....	0	0.	.....
	14	124	118	.95	4.0	124	1.00	8.8
	18	16	0	0.	.....	13	.81	4.4
	20	1	1	1.00	3.0	1	1.00	10.0
	25	3	0	0.	.....	0	0.	.....
	41	170	47	.28	4.3	25	.15	6.1
	42	1	1	1.00	8.0	0	0.	.....
	46	1	1	1.00	2.0	1	1.00	4.0
	47	114	114	1.00	1.7	114	1.00	3.5
6	7	88	0	0.	.....	2	.02	8.5
	10	1	1	1.00	5.0	1	1.00	4.0
	12	9	1	.11	4.0	0	0.	.....
	14	10	9	.90	3.8	10	1.00	7.3
	17	39	7	.18	2.1	9	.23	3.4
	18	203	24	.12	3.2	102	.50	4.4
	19	126	3	.02	3.0	11	.09	4.3
	20	1534	830	.54	4.7	450	.29	7.5
	24	328	35	.11	3.9	64	.20	3.8
	25	1886	443	.23	5.8	193	.10	4.2
	27	9	1	.11	2.0	0	0.	.....
	32	1	1	1.00	6.0	1	1.00	3.0
8	25	2	0	0.	.....	0	0.	.....
10	7	19	0	0.	.....	0	0.	.....
	19	1	0	0.	.....	0	0.	.....
	20	183	0	0.	.....	0	0.	.....
	26	1	0	0.	.....	1	1.00	3.0

TABLE 37. *Summary of results classified by activity of use and year of purchase*

Agencies 15 and 16 omitted

Activity and year of purchase	n	Leader			Information section		
		k	f	$\bar{x}$	k	f	$\bar{x}$
Daily							
1901–1945	8	3	0.38	1.0	2	0.25	1.0
1946–1950	11	1	.09	3.0	1	.09	6.0
1951–1955	20	0	0.	.....	0	0.	.....
1956–1960	21	0	0.	.....	0	0.	.....
1961–1965	7	0	0.	.....	0	0.	.....
Frequently							
1901–1945	25	4	.16	4.5	8	.32	4.2
1946–1950	102	10	.10	4.6	19	.19	3.6
1951–1955	84	7	.08	4.1	19	.23	2.4
1956–1960	216	18	.08	5.4	56	.26	2.8
1961–1965	50	4	.08	3.8	3	.06	1.7
Infrequently							
1901–1945	171	35	.20	4.4	45	.26	5.6
1946–1950	168	17	.10	4.4	7	.04	4.7
1951–1955	837	200	.24	5.8	80	.10	4.0
1956–1960	629	45	.07	2.7	49	.08	3.8
1961–1965	145	4	.03	2.8	2	.01	3.0
Dead storage							
1901–1945	296	143	.48	4.8	166	.56	6.2
1946–1950	860	389	.45	5.0	211	.25	6.5
1951–1955	612	185	.30	4.6	73	.12	5.0
1956–1960	512	262	.51	5.1	141	.28	8.2
1961–1965	236	57	.24	3.7	11	.05	4.5

8. References

[1] McCamy, C. S., Inspection of processed photographic record films for aging blemishes, NBS Handbook 96, U.S. Govt. Printing Office, Washington, D.C. 20402 (Jan. 24, 1964).

[2] Henn, R. W., and Wiest, D. G., Microscopic spots in processed microfilm, Phot. Sci. Eng. **7**, 253 (1963).

[3] James, T. H., The stability of silver filaments, Phot. Sci. Eng. **9**, 121 (1965).

[4] Henn, R. W., Wiest, D. G., and Mack, Bernadette D., Microscopic spots in processed microfilm: The effect of iodide, Phot. Sci. Eng. **9**, 167 (1965).

[5] McCamy, C. S., and Pope, C. I., Current research on preservation of archival records on silver-gelatin type microfilm in roll form, J. Res. NBS **69A** (Phys. and Chem.), No. 5, 385 (1965).

[6] Henn, R. W., and Mack, B. D., A gold protective treatment for microfilm, Phot. Sci. Eng. **9**, 378 (1965).

[7] Henn, R. W., and Wiest, D. G., Properties of gold-treated microfilm images, Phot. Sci. Eng. **10**, 15 (1966).

[8] Pope, C. I., Blemish formation in processed microfilm, J. Res. NBS, **72A** (Phys. and Chem.), No. 3, 251 (1968).

(Paper 73A1–538)

NOTE: The General Services Administration forms 1990A and 1990 are shown on the following pages.

GENERAL SERVICES ADMINISTRATION

MICROFILM BLEMISH INSPECTION WORKSHEET

PAGE OF PAGES

INSTRUCTIONS.-Prepare a separate worksheet for each roll of microfilm selected for inspection. *(See GSA Form 1990, Report on Microfilm Blemishes, for instructions concerning stratum and sample selection.)* Number worksheets in consecutive order within each stratum inspected. SUBMIT ALL WORKSHEETS WITH REPORT.

NAME

1. DEPARTMENT OR AGENCY

2. BUREAU OR SERVICE

ROLL IDENTIFICATION

3. COLLECTION TITLE

4. SERIES

5. ROLL NO.

6. STRATUM *(Name or number)*

FILM DATA

7. FILM SIZE
☐ a. 16MM ☐ b. 35MM ☐ c. OTHER *(Specify)*

8. NAME OF MANUFACTURER

9. BRAND NAME OF FILM

10. YEAR OF MANUFACTURE OR PURCHASE

11. FILM PROCESSED BY *(Name, city and State)*

YEAR PROCESSED

STORAGE AND USE DATA

12. ACTIVITY OF STRATUM
☐ a. DAILY ☐ b. FREQUENTLY ☐ c. INFREQUENTLY ☐ d. DEAD STORAGE

13. TYPE OF CONTAINER
☐ a. METAL CAN ☐ b. CARDBOARD CONTAINER ☐ c. OTHER *(Specify)*

14. TYPE OF REEL
☐ a. METAL ☐ b. PLASTIC ☐ c. CORE ONLY ☐ d. OTHER *(Specify)*

15. STORAGE CONDITIONS

		(1) MAX.	(2) MIN.
a.	TEMPERATURE		
b.	HUMIDITY	(1) MAX.	(2) MIN.
c.	AIRCONDITIONED	☐ (1) YES	☐ (2) NO

16. STORAGE LOCATION
☐ a. VAULT ☐ b. OFFICE SPACE ☐ c. BASEMENT ☐ d. OTHER *(Specify)*

17. ARE HUMIDIFICATION TRAYS STILL USED?
☐ a. YES ☐ b. NO

18. DO THE DATA RECORDED IN ITEMS 12 THOUGH 17 REPRESENT CONDITIONS UNDER WHICH FILM HAS BEEN MAINTAINED SINCE IT WAS PROCESSED?
☐ a. YES ☐ b. NO *(If "NO," describe significant deviations on reverse)*

INSPECTION DATA

19. TYPE OF LEADER
☐ a. FOGGED FILM ☐ b. CLEAR FILM ☐ c. PLASTIC

20. LENGTH OF LEADER *(Feet)*

21. NUMBER OF SPLICES
☐ a. NONE ☐ b. 1-5 ☐ c. 6-10 ☐ d. 11 OR MORE

22. PURPOSE OF SPLICES
☐ a. REPAIR ☐ b. ADD ON

23. TYPE OF SPLICE
☐ a. OVERLAP ☐ b. BUTT ☐ c. OTHER *(Specify)*

24. TYPE OF BAND USED ON ROLL
☐ a. NONE ☐ b. STRING ☐ c. RUBBER BAND ☐ d. OTHER *(Specify)*

25. SPOT AND CHARACTER-ASSOCIATED BLEMISHES FOUND

a. LEADER				b. FRAMES NEXT TO LEADER				c. CENTER FRAMES			
TYPE	SEVERITY	TYPE	SEVERITY	TYPE	SEVERITY	TYPE	SEVERITY	TYPE	SEVERITY	TYPE	SEVERITY
☐ 1				☐ 1		☐ 2		☐ 1		☐ 2	
☐ 3		☐ 4		☐ 3		☐ 4		☐ 3		☐ 4	
		☐ 6		☐ 5		☐ 6		☐ 5		☐ 6	

26. OTHER BLEMISHES AND IMPERFECTIONS FOUND

a. CHEMICAL RESIDUE ☐ (1) YES ☐ (2) NO

b. SILVERY SHEEN ON LEADER ☐ (1) YES ☐ (2) NO

c. SILVERY SHEEN ON DENSE AREAS ☐ (1) YES ☐ (2) NO

d. DISCOLORATION OR FADING ☐ (1) YES ☐ (2) NO

e. WATER SPOTS ☐ (1) YES ☐ (2) NO

f. OTHER ☐ (1) YES *(Explain on reverse)* ☐ (2) NO

27. ARE THERE ANY APPARENT CAUSES FOR THE BLEMISHES FOUND ON THIS ROLL?
☐ a. YES *(Explain on reverse)* ☐ b. NO

INSPECTED BY

28. NAME AND TITLE

TELEPHONE NO.

DATE

USCOMM-DC GSA DC 64-9749

GSA FORM JAN 64 1990A

GENERAL SERVICES ADMINISTRATION

REPORT ON MICROFILM BLEMISHES

REPORT NO.

INSTRUCTIONS.-Prepare a separate report summarizing worksheet data for each stratum of microfilm inspected. Before inspection, divide microfilm holdings into separate homogenous groups (stratum) which are distinguished by photographically significant differences, such as processing date or place, storage conditions, film size, and film make. Inspections should be on a sample basis. The sample should be 1/1000 of the stratum but not less than 100 rolls. Inspect complete stratum if less than 100 rolls.

NAME

1. DEPARTMENT OR AGENCY

2. BUREAU OR SERVICE

3. COLLECTION TITLE

4. SERIES

5. STRATUM *(Name or no.)*

6. NUMBER OF ROLLS IN STRATUM

7. NUMBER OF ROLLS IN SAMPLE

IDENTIFICATION OF FILM INSPECTED

8. CHARACTERISTICS OF THE STRATUM

SUMMARY OF BLEMISHES FOUND

9. BLEMISHES FOUND IN STRATUM

TYPE (1)	(a) LEADER		(b) FRAMES NEXT TO LEADER		(c) CENTER FRAMES	
	NUMBER OF ROLLS (2)	% OF SAMPLE (COL. (2) ÷ ITEM 7) (3)	NUMBER OF ROLLS (4)	% OF SAMPLE (COL. (4) ÷ ITEM 7) (5)	NUMBER OF ROLLS (6)	% OF SAMPLE (COL. (6) ÷ ITEM 7) (7)
1						
2						
3						
4						
5						
6						

10. SUMMARIZE ON REVERSE SIDE, APPARENT CAUSES FOR BLEMISHES AS REPORTED IN ITEM 26 OF THE MICROFILM BLEMISH INSPECTION WORKSHEET (GSA FORM 1990A) FOR THIS STRATUM.

PREPARED BY

11. NAME | TITLE | TELEPHONE NO. | DATE

GSA DC 64-9750

GSA FORM JAN 64 1990

JOURNAL OF RESEARCH of the National Bureau of Standards—A. Physics and Chemistry
Vol. 73A, No. 1, January–February 1969

Publications of the National Bureau of Standards*

Selected Abstracts

Carter, G. C., Bennett, L. H., Cuthill, J. R., Kahan, D. J., **The NBS alloy data center: Function, bibliographic system, related data centers, and reference books,** *Tech. Note 464 (Aug. 1968), $1.25.*
The Alloy Data Center, part of the National Standard Reference Data System, has two primary functions. One is to stimulate cooperation and coordination among the existing data centers in the area of the physical properties of well characterized alloys. The final data generated by these centers for publication should be consistent with one another where correlation or possible overlap exists. The other purpose is the collection (from publications as well as private communications), evaluation, and publication of data in some areas where special competence exists in the Alloy Physics Section. Of interest to the center are metals, semimetals, intermetallic compounds, and alloys. Excluded are those materials which have ill-defined constitutions and heat treatments. An automated system has been developed to meet the bibliographic needs of the center. This system will be described as well as the specific properties of interest. The system presently contains a complete annotated file on papers dealing with NMR Knight shift measurements. The soft X-ray spectroscopy compilation is being kept up-to-date with the same system.

Key Words: Alloys; annotation; automated; bibliography; data; indexing; information; Knight shifts; metals; NMR; soft X-ray spectroscopy.

Colson, J. P., Clark, E. S., **Tables of solutions to Bragg's equation for copper, cobalt, iron and chromium K^- radiation and small diffraction angles,** *Tech. Note 461 (Aug. 1968), 50 cents.*

Tables of solutions to Bragg's equation are presented for the $K\bar{\alpha}$ radiation of Cu(1.541838 Å*), Co(1.790260 Å*), Fe(1.937355 Å*), and Cr(2.291002 Å*). The value of 2θ is increased in increments of 0.001 degree from 0.001 to 2.999 degrees and in increments of 0.00001 radian from 0.00002 to 0.04999 radian. The solutions are rounded off to five digits.

Key Words: Bragg's equation; Co; Cr; Cu; Fe; $K\bar{\alpha}$ radiation; small angle.

Cord, M. S., Lojko, M. S., Petersen, J. D., **Microwave spectral tables, Volume V. Spectral line listing,** *Mono. 70, Volume V (June 1968), $4.75.*
This volume is a listing of the spectral lines reported in Volumes I, III, and IV of the Microwave Spectral Tables. These lines are listed according to ascending magnitude of frequency and should provide a ready reference.

Key Words: Microwave spectra; molecular spectra; spectral lines; rotational quantum numbers; diatomic molecules; polyatomic molecules; hyperfine.

Davis, M. M., **Acid-base behavior in aprotic organic solvents,** *Mono. 105 (Aug. 1968), $2.25.*
A unified picture of acid-base behavior in aprotic organic solvents is presented, based on an extensive survey of the literature and experimental results of the author and associates. Evidence given to support this picture includes data pertaining to colligative properties of acids, bases, and salts and also conductance, dielectric constants, distribution between immiscible solvents, and spectral absorption in the infrared, visible, and ultraviolet. The acids upon which attention is centered are proton-donor compounds that are measurably ionized in water, such as aliphatic and aromatic carboxylic acids, substituted phenols, and mineral acids. The bases of principal interest are likewise compounds capable of forming ions in water, for example, aliphatic and aromatic amines and derivatives of guanidine or pyridine. The solvents emphasized are hydrocarbons and halohydrocarbons, but data for dipolar aprotic solvents (for example, acetone, acetonitrile, and nitrobenzene) are included. Contrasts in acid-base behavior and in acidity and basicity scales in aprotic and water-like solvents are discussed.
The role of hydrogen bonding in aprotic solvents is discussed at length. Important types of hydrogen-bonded structures include chelate rings; self-associated acids, bases, and salts; hydrogen-bonded ion pairs; and homo- and heteroconjugate cations and anions. Examples are given in which hydrogen bonding of these types affects such properties as the absorption spectrum of a salt, the catalytic effect of an acid, and the accurate location of a titration endpoint.

Key Words: Acid-base behavior; acidity and basicity scales; aprotic organic solvents; hydrogen bonding; titrations.

Fraction, G. F., Walker, J. C., Tauber, S. J., **Connection tables from Wiswesser chemical structure notations—a partial algorithm,** *Tech. Note 432 (Sept. 1968), 65 cents.*
An algorithm has been developed for transforming certain types of Wiswesser organic structure notations into connection tables. Acyclic and benzene structures are treated, and provision has been made for all of the types of contractions used by the Wiswesser notation system. A separate algorithm is presented for treating linearly fused ring aggregates. A syntax has been developed to describe those portions of Wiswesser notations which refer to non-benzene ring systems.

Key Words: Acyclic; benzene; chemical structure notations; connection tables; contractions; ring system; syntax analysis; transformation algorithm; Wiswesser.

Goldman, D. T., Ed., **Neutron cross sections and technology,** *Proc. Conf., Washington, D.C., Mar. 4–7, 1968, Spec. Publ. 299 Sept. 1968), $10.50 set of 2 volumes.*
The Second Conference on Neutron Cross Sections and Technology was held in Washington, D.C. on March 4–7, 1968. Papers from this Conference have been published in two volumes, as follows: Volume I, Sessions A–D, pages 1–640; Volume II, Sessions E–H, pages 641–1337. These volumes contain the texts of the invited and contributed papers of the Conference. Topics covered include: The need for neutron data in fields of science and technology; standard data and flux measurements; the determination of neutron cross sections by theoretical and experimental techniques; a presentation of recently measured data and their utilization in a variety of applications.

Key Words: Cross sections; neutrons; nuclear data; nuclear technology; reactors.

Haar, L., **Thermodynamic properties of ammonia as an ideal gas,** *NSRDS–NBS 19 (Aug. 1968), 20 cents.*
Thermodynamic functions for ammonia as an ideal gas at one atmosphere pressure have been evaluated. The contribution of the highly anharmonic out-of-plane vibrational mode, including its large

324-194 O - 69 - 8

coupling with rotation and its coupling with the other vibrational modes, is considered in detail. Tables of C_p°/R, $(H^\circ - E_0^\circ)/RT$, $(E_0^\circ - G^\circ)/RT$, and S°/R have been calculated at closely spaced intervals from 50 to 5000 °K within an overall uncertainty of less than 0.1 percent at 1000 °K.

Key Words: Ammonia; ideal gas; thermodynamic functions.

Heinrich, K. F. J., Ed., **Quantitative electron probe microanalysis,** *Proc. Seminar, National Bureau of Standards, Gaithersburg, Md., June 12–13, 1967, Spec. Publ. 298 (Oct. 1968), $3.00.*
A seminar was held at the National Bureau of Standards in June 1967 to examine critically the factors involved in quantitative electron-probe microanalysis. Major consideration was given to proposed methods for data evaluation, and to requirements for further work in theory, in measurement, and in the preparation of standards. This volume contains a series of invited papers which formed the basis of discussion at the seminar. Topics covered include corrections for the atomic number effect, for x-ray absorption, and for fluorescence by characteristic lines and the continuum. The various ways to derive a simplified model of the complex electron-target interaction are critically analyzed by several authors, and the accuracy of several proposed methods is compared by error histograms constructed on the basis of hundreds of analyses of materials of known composition. Applications to the analysis of biological specimens and to problems of stereometric analysis are also discussed.

Key Words: Atomic number effect; biological specimens; electron probe; microanalysis; electron scattering; fluorescence by the continuum; quantitative analysis; stereometric analysis; x-ray absorption; x-ray emission.

Johnston, H. S., **Gas phase reaction kinetics of neutral oxygen species,** *NSRDS–NBS 20 (Sept. 1968), 45 cents.*
The available data for reactions among neutral oxygen species, oxygen atoms, oxygen molecules and ozone, have been reviewed. Selected data have been reanalyzed and used to establish values for the rates of these reactions:

$O_2 + M \rightarrow O + O + M$——($M = O_2$, Ar)
$O + O + M \rightarrow O_2 + M$——($M = O_2$)
$O_3 + M \rightarrow O + O_2 + M$——($M = O_2$, O_3, He, Ar, N_2, CO_2)
$O + O_2 + M \rightarrow O_3 + M$——($M = O_2$, O_3, He, Ar, N_2, CO_2)
$O + O_3 \rightarrow O_2 + O_2$
$O + O_2 \rightarrow O + O_2$ (isotopic exchange)

Key words: Chemical kinetics; dissociation; isotopic exchange; oxygen atom; oxygen molecule; ozone; recombination; review.

Menis, O., Ed., **Analytical Coordination Chemistry Section: Summary of activities July 1967 to June 1968,** *Tech. Note. 454 (July 1968), 55 cents.*
This annual report outlines the progress made in titrimetry, gravimetry, flame emission, atomic absorption and fluorescence, spectophotometry, spectrofluorometry and the determination of gases in metals in conjunction with the analysis of Standard Reference Materials. It describes recent developments in instrumentation and in sample dissolution techniques and discusses some unique applications of coordination systems and ternary complexes.
In flame spectroscopy considerable progress was made in the development and testing of electrodeless discharge lamps, Xe-arc continuum sources, a.c. scanning systems, resonance detectors and improved nebulizer-burner combinations. The relative merits of flame emission, atomic absorption and atomic fluorescence were evaluated from theoretical and practical standpoints. Specialized instrumentation was also developed for use in thermal analysis studies and in spectrofluorometry. In the area of gases in metals, a new inert gas fusion apparatus having a unique sampling valve and gas flow system was constructed and coupled to a high sensitivity gas chromatograph. In addition, a new commercial inert gas fusion apparatus was tested and a vacuum fusion unit modified to permit more readily the successive determination of oxygen and nitrogen.
Studies were made of the dissolution of refractory materials containing volatile or easily hydrolizable components. Sealed Teflon-lined bombs and quartz tubes were successfully applied to the determination of trace nitrides in steels and niobium alloys and of antimony at the 10–50 ppm level in ferrous alloys. The latter was prerequisite to the provision of standards for correlating the presence of trace antimony in rotor blades with power turbine failures. Teflon-lined bombs were also used for the dissolution of clays prior to the determination of trace components.
The formation and extraction of ternary complex systems were investigated to provide enhanced spectrophotometric and spectrofluorometric sensitivity for trace metal determination. Improvement in the detection limits of existing procedures were effected by the use of micro-volume techniques. Also, the utilization of recently developed spectrofluorometric chelating agents have yielded significant improvement in sensitivity. Beryllium, for example, was readily determined in resin beads at the 50 picogram level.
Finally, a large number of Standard Reference Materials and potential standards were certified for their major, minor and trace constituents. These included clays, tungsten-molybdenum compacts, neutron flux glasses, aluminum alloys, organo-metallic compounds, ferrous alloys, solder, and high-purity and doped zinc, platinum and gold. Many of the values obtained were confirmed by independent methods.

Key words: Atomic absorption and atomic fluorescence spectrometry; differential thermal analysis; flame emission; gases in metals; gravimetry and titrimetry; spectrophotometry and spectrofluorometry; standard reference materials.

Moore, C. E., **Bibliography on the analyses of optical spectra. Section 1. ^{1}H–^{23}V,** *Spec. Publ. 306 (Sept. 1968), $1.00.*
The three published volumes on "Atomic Energy Levels," NBS Circ. 467, contain for each spectrum the bibliography that was used in compiling the data. The present work is a continuation of these bibliographies arranged in the same form. The time interval is the span from the respective dates of the earlier publications to the present. The selection of references is restricted to those needed for the preparation of revised tables of atomic energy levels and multiplets.
The bibliography is being published in three Sections each of which covers the same elements as the respective volumes of AEL. The present Section contains reference lists for the elements 1 H through 23 V, corresponding to Volume I. The spectra of a given element are listed in order of increasing stage of ionization. Listings are included for spectra of the 23 elements.
The original papers have been examined for nearly all of the quoted references. A selected list of general literature references is also included.

Key Words: Spectra, atomic; analyses of atomic spectra; elements, spectra of H through V; bibliography, atomic spectra; atomic spectra, H through V; references to atomic spectra.

Muhlenhaupt, R. C., Strobridge, T. R., **An analysis of the Brayton cycle as a cryogenic refrigerator,** *Tech. Note 366 (Aug. 1968), $1.25.*
The performance of a Brayton-cycle refrigerator has been computed taking into account the efficiencies of the various components. The results are presented in graphical form. These charts give the input power requirements, mass flow rate, pertinent temperatures, and allow selection of the optimum high pressure for a given set of component characteristics.

Key Words: Brayton; cryogenics; refrigeration.

NBS frequency and time broadcast services radio stations WWV, WWVH, WWVB, WWVL, *Spec. Publ. 236, 1968 edition (1968), 15 cents. (Supersedes Misc. Publ. 236, 1967 edition).*
Detailed descriptions are given of the technical services provided by the National Bureau of Standards radio stations WWV, WWVH, WWVB, and WWVL. These services are: 1. Standard radio frequencies; 2. Standard audio frequencies; 3. Standard musical pitch; 4. Standard time intervals; 5. Time signals; 6. UT2 corrections; 7. Radio propagation forecasts; and 8. Geophysical alerts. In order to provide users with the best possible services, occasional changes in the broadcasting schedules are required. This publication shows the schedules in effect on January 1, 1968. Annual revisions will be made. Current data relating to standard frequencies and

time signals are available monthly in the Time and Frequency Services Bulletin. Advance notices of changes occurring between revisions will be sent to users of NBS broadcast services who request such notice on the basis of need.

Key Words: Broadcast of standard frequencies; high frequency; low frequency; standard frequencies; time signals; very low frequency.

Scribner, B. F., Ed., **Spectrochemical Analysis Section: Summary of Activities July 1967 to June 1968,** *Tech. Note 452 (Sept. 1968), $1.00.*
A summary is given of activities of the NBS spectrochemical Analysis Section for the year July 1967 through June 1968. This covers research activities, improvement in equipment, and applications in analysis including the certification of standard reference materials. In optical spectrometry studies were completed on the plasma torch as a means of excitation of solutions, and on computer programs for the calibration of photographic emulsions. In electron probe microanalysis a matrix scanner for automatic point-by-point grid scans was tested and a lithium-drifted silicon detector was installed for non-diffractive x-ray dispersion. A study was made of color composites for combining the information of three x-ray area scans. In quantitative probe analysis, measurements were made of x-ray mass attenuation coefficients, and a study of atomic number corrections is underway. In x-ray fluorescence considerable improvement was realized by replacement of electronics by solid state circuitry, and methods are being studied for corrections of interelement effects, utilizing the digital computer. Spark source mass spectrometry was applied, by means of chemical separations and by isotope dilution techniques, to the accurate determination of impurities in zinc, platinum, and gold. A critical study was made of the uniformity of response of ion-sensitive emulsions over the area of the plates used in the mass spectrometry. Improvements in the Section's equipment and further developments in computer applications are also discussed. Listings are given of 23 publications and 19 talks by members of the Section during the year.

Key Words: Computing; digital readout; electron probe; emulsion calibration; emulsion sensitivity; gold analysis; isotope dilution method; x-ray mass attenuation coefficients; microprobe grid scanner; optical spectrometry; plasma torch; platinum analysis; preconcentration; silicon detector; spark source mass spectrometry; spectrochemical analysis; standard reference materials; time-shared computer; x-ray absorption coefficients; x-ray fluorescence analysis; zinc analysis.

Swindells, J. F., Ed., **Precision measurement and calibration. Selected NBS papers on temperature,** *Spec. Publ. 300, Vol. 2 (Aug. 1968), $4.75.*
This volume is one of an extended series which brings together the previously published papers, monographs, abstracts, and bibliographies by NBS authors dealing with the precision measurement of specific physical quantities and the calibration of the related metrology equipment. The contents have been selected as being useful to the standards laboratories of the United States in tracing to NBS standards the accuracies of measurement needed for research work, factory production, or field evaluation.
Volume 2 contains reprints through June 1967 covering the general topics: Uncertainties, Temperature Scales, Resistance Thermometry, Thermoelectric Thermometry, Liquid-in-Glass Thermometry, Optical Pyrometry, and Spectroscopic Thermometry. A selected bibliography covering the period from January 1953 through December 1965 is included.

Key Words: Acoustical thermometry; cerous magnesium nitrate thermometer; error analysis; liquid-in-glass thermometry; reprints; resistance thermometry; spectroscopic thermometry; standards; temperature scales; thermoelectric thermometry.

Wachtman, J. B., Jr., Franklin, A. D., Ed., **Mass transport in oxides.** *Proceedings of a symposium held at Gaithersburg, Maryland, October 22–25, 1967, Spec. Publ. 296 (Aug. 1968), $3.00.*
This publication presents the Proceedings of the Conference on Mass Transport in Oxides, held at the National Bureau of Standards in Gaithersburg, Md., from October 22 to October 25, under the joint sponsorship of the Bureau and the Advanced Research Projects Agency. Invited papers reviewed mass transport in alkali and silver halides as background, and topics relating to oxides including point defects (both experiment and theory), lattice dynamics and ionic interactions, atomistic mechanisms of diffusion and ionic conduction, chemical diffusion, defect complexes, assessments of the experimental situation for diffusion and ionic conduction, and the availability of good research materials. In contributed papers, attention was focused on color centers in alkaline earth oxides, cation diffusion in MgO, transport of both cations and anions in transition metal oxides, and coulometric and emf techniques for obtaining transport data. A panel discussion summarized the work of the conference.

Key Words: Crystal defects; diffusion; ionic conductivity; mass transport; oxides; stoichiometry.

Armstrong, G. T., **Calorimetry, Encyclopaedic Dictionary of Physics,** *2d Supplementary Volume 2, 1–8 (Pergamon Press, Inc., New York, N.Y., Oct. 1967).*
This survey deals in separate sections with materials supplementary to articles on calorimetry appearing in the main work of the Encyclopaedic Dictionary of Physics. Separate sections treat the relationship of calorimetry to thermodynamics, applications of the results of calorimetric measurements, current (1965) areas of activity in the development of calorimetric instruments and procedures, and the scope of calorimetric work including national and international coordination.
A short article on Standard Samples for Calorimetry is appended.

Key Words: Calorimetric instruments and procedures; calorimetric measurements; calorimetry; calorimetry to thermodynamics; standard samples for chemistry.

Ausloos, P., Lias, S. G., **Primary modes of decomposition of superexcited n-alkane molecules** *(Proc. Intern. Conf. Photochemistry, München, Germany, Sept. 6–9, 1967), Ber. deut. Gunsenges. 72, No. 2, 187–195 (1968).*
Information is summarized concerning fragmentation of superexcited propane and n-butane molecules produced by photolysis of these compounds with 11.6–11.8 eV photons, which is about 0.5 and 1.0 eV above the ionization energies of the two compounds. The decomposition of the excited $[C_3H_8^+]^*$ and $[C_4H_{10}]^*$ ions which are formed either by direct ionization or by autoionization are quenched at pressures around 10 Torr. These ions can then be removed from the photolysis system through a charge transfer reaction with added NO or an H_2 transfer reaction with low concentrations of added ethylene. The modes of decomposition of the superexcited alkane molecules are derived from the isotopic analysis of the products formed upon irradiation of $CD_3CH_2CD_3$, $CH_3CD_2CH_3$, $CD_3CH_2CH_2CD_3$ and of the equimolar mixtures C_3H_8–C_3D_8 and C_4H_{10}–C_4D_{10}. Comparison of these results with studies at longer wavelengths demonstrates that although the modes of decomposition observed at the superexcitation energies are the same as those observed at excitation energies below the ionization energy, free radical producing processes occur with higher probability when the energy of the photon is increased.

Key Words: Superexcited molecules; primary processes; photolysis; alkanes; photoionization; ion-molecule reactions; free radical reaction.

Beaty, E. C., Patterson, P. L., **Mobilities and reaction rates in neon ions in neon,** *Phys. Rev.* **170,** *No. 1, 116–121 (June 5, 1968).*
The mobilities of Ne and Ne_2 ions in neon has been measured at 300 °K. The mobility of Ne^+ and Ne_2^+ at low E/p_0 are given by the equations: $K(Ne^+) = 4.07\,[1 + 8.0 \times 10^3\,(E/p_0)^2 + 2.0 \times 10^{-6}\,(E/p_0)^4]^{-1/8}$ and $K(Ne_2^+) = 6.14\quad[(1 + 8.3 \times 10^{-3}\quad(E/p_0)^2/(1 + 2.0 \times 10^{-3}\quad(E/p_0)^2 + 8.4 \times 10^{-6}\,(E/p_0)^4)]^{1/4}$. The Ne^+ was observed to convert to Ne_2^+ by a three-body reaction with a rate coefficient ranging from about 7×10^{-32} cm^6/sec at $E/p_0 = 2.0$ to abour 5×10^{-32} cm^6/sec at $E/p_0 = 6.0$.

Key Words: Neon; ion; mobilities; reaction; rates.

Bender, P. L., Alley, C. O., Currie, D. G., Faller, J. E., **Satellite geodesy using laser range measurements only,** *J. Geophys. Res.* **73,** *No. 16, 5353–5357 (Aug. 15, 1968).*
The potential accuracy of a 12-station worldwide geodetic network based on laser range measurements to an optical retro-reflector package on a high altitude satellite has been investigated. An accuracy of 15 cm in the range (one nanosec in the round-trip transit time) seems achievable with about 10 min of observations. The model

used consists of range measurements being made at about the same time from the 4 closest ground stations for each of 30 satellite positions. For the "ideal" case the stations were located at the 12 vertices of a regular icosahedron and the satellite positions were over the centers of the 30 edges. This gave an expected uncertainty of less than 45 cm in the distance between any 2 stations, with little dependence on satellite altitude over the range of 20,000 to 110,000 km. For 12 stations chosen from the Pageos Geometric Satellite Network, the expected accuracy for a satellite altitude of 110,000 km was found to be 60 cm or better for the distance between any 2 stations. The results indicate that the geometry can be "strong" even for high satellite altitudes if the satellite positions observed from a given ground station are well separated.

Key Words: Laser; satellite; geodesy; range worldwide; network.

Bennett, H. S., **F center in ionic crystals; semicontinuum polaron models,** *Phys. Rev.* **169,** *No. 3, 729–745 (May 15, 1968).*
The states of the F center are considered on the basis of a model which treats the movement of the nearest neighbors to the F center and the F electron in a self-consistent manner. The lattice is described in terms of classical ionic crystal theory and the F electron is treated according to the semi-continuum polaron theory. The absorption energy, the emission energy, the lifetime of the first excited state, the thermal activation energies, and the Huang Rhys factor are evaluated for two models (Hartree and quasi-adiabatic) which differ in the evaluation of the optical polarization. It is shown that the Hartree semi-continuum polaron model agrees best with the experimental results for NaCl, KCl, CaF_2, SrF_2, and BaF_2. In addition, these models show that among the above quantities the thermal activation energies and the lifetime of the first excited state are most sensitive to the physical content of a given model.

Key Words: *F* center; alkali halide; alkaline earth fluoride; alkaline earth oxide; polaron; ionic crystal; and semi-continuum model.

Bennett, J. A., **The initiation of fatigue microcracks under sequential bending and torsional loads,** *Trans. ASM* **61,** *No. 2, 210–218 (June 1968).*
Specimens of 6061–T6 aluminum alloy were stressed first in alternating torsion, then in reversed bending or vice versa. The development of cracks was observed by microscopic examination of replicas taken of the specimen surfaces at intervals during the tests. The results indicate that fatigue damage under uniaxial stress did not reduce the resistance to crack initiation in pure shear; the reverse was also true. Based on the number of cycles to initiate microcracks, the fatigue strength in terms of shear stress amplitude was 14% higher in torsion than in bending. Comparison of these results with earlier studies of environmental effects suggests that moisture influences the fatigue behavior of this alloy only after microcracks have formed.

Key Words: Fatigue strength; microcracks; aluminum alloy; bending; torsion; shear stress.

Bevan, A. W., Jr., Daniel, A. C., Mahler, R. J., **Indication of the effect of a magnon gap in the ^{19}F relaxation rate in antiferromagnetic CoF_2,** *Physics Letters* **25A,** *No. 7, 555–556 (Oct. 9, 1967).*
The F^{19} nuclear spin-lattice relaxation time in a CoF_2 single crystal has been measured in zero external magnetic field over the temperature range of 4° to 16 °K. The relaxation rate falls off exponentially, but faster than the $T^2 \exp(-T_{AE}/T)$ predicted using a simplified spin wave theory.

Key Words: CoF_2; antiferromagnetism; relaxation times; magnon gap.

Bullis, W. M., Brewer, F. H., Kolstad, C. D., Swartzendruber, L. J., **Temperature coefficient of resistivity of silicon and germanium near room temperature,** *Solid-State Electron.* **11,** *No. 7, 639–646 (July 1968).*
Temperature coefficients for the resistivity of n- and p-type germanium and silicon in the neighborhood of room temperature have been determined over a wide range of resistivity. Linear temperature coefficients have been found for the extrinsic exhaustion region ($< 5\ \Omega$.cm for germanium and $< 5000\ \Omega$.cm for silicon). The results are presented as plots of temperature coefficient against resistivity at 23 °C. The plots may be used in connection with measurements of resistivity on extrinsic germanium and silicon doped with the usual shallow impurities such as boron, aluminum, gallium, phosphorus, arsenic, and antimony. Accurate linear coefficients cannot be found for specimens doped with deep-lying impurities in sufficient amounts to affect the carrier density nor for specimens with resistivity in the transition region between extrinsic and intrinsic conduction.

Key Words: Temperature coefficients; resistivity; n-type; p-type; germanium; silicon; extrinsic exhaustion region.

Chang, T., Yang, G. C., **Temperature dependence of paramagnetic relaxation of Mo^{5+} in TiO_2,** *J. Chem. Phys.* **48,** *No. 6, 2546–2549 (Mar. 15, 1968).*
The relaxation rate of Mo^{5+} in TiO_2 was measured, by the measurement of line width at temperatures between 77 °K and 240 °K, and by the saturation and recovery method at temperatures at and below 4.2 °K. The line width is about 300 gauss at 240 °K, and 0.5 gauss at 77 °K. The relaxation time is about 5 sec. at 4.2 °K and about 100 min. at 1.05 °K. The temperature dependence of the relaxation rate is T^9 between 3 °K and 200 °K, T^5 between 1.5 °K and 3 °K, and T below 1.5 °K. At the linear dependence region, i.e., ~ 1 °K, the magnetic field dependence is H^4 as verified by experiments.

Key Words: Mo^{5+}; paramagnetic relaxation; temperature dependence; TiO_2.

Codling, K., Madden, R. P., **Structure in the $L_{II, III}$ absorption of aluminum and its oxides,** *Phys. Rev.* **167,** *No. 3, 587–591 (Mar. 1968).*
The $L_{II, III}$ region of absorption has been observed for thin films of evaporated aluminum, for amorphous (anodized) Al_2O_3 and for crystalline γ alumina) Al_2O_3. The spectra were obtained in high resolution (0.06 Å) using the NBS 180 MeV electron synchrotron as a background source. The $L_{II, III}$ absorption edges of Al are located with improved accuracy at 169.49 (±0.05)* Å and 170.49 (±0.05) Å. Structure on the high energy side is compatible with other recent observations. The $L_{II, III}$ absorption edge in Al_2O_3 is not split in high resolution and is located at 162.11 (±0.15) Å for the amorphous form and 160.15 (±0.15) Å for the γ alumina. Both forms show considerable structure on the high energy side of the edge. That observed for the amorphous form is in agreement with other recent observations, while the absorption structure in γ alumina (showing maxima at 78.0, 78.6, 79.5, 84 and 99 eV) has been found to be more complex.

*Estimated probable error.

Key Words: Aluminum; aluminum oxide; $L_{II, III}$ edges; soft X-ray; absorption spectrum.

Cooper, M. J., **Electric field effect on critical opalescence of dipolar binary mixture,** *J. Chem. Phys.* **48,** *No. 9, 4272–4277 (May 1, 1968).*
A modified van der Waals model is used to describe the effect of a time varying external electric field on the critical mixing point properties of a dipolar binary mixture. Assuming that the behavior of the concentration fluctuations about equilibrium is governed by linearized hydrodynamic equations and that the diffusion coefficient is determined by the instantaneous equilibrium state, the decay of the fluctuations is described. The relaxation time characterizing the electric field effect upon the light scattering by critical opalescence is related to the free relaxation of the concentration fluctuations.

Key Words: van der Waals; binary mixture; electric field effect; critical opalescence; excess concentration.

Daniel, A. C., Bevan, A. W., Jr., Mahler, R. J., **Nuclear spin-lattice relaxation in the antiferromagnets $CoCl_2 \cdot 2H_2O$ and $FeCl_2 \cdot 2H_2O$,** *J. Appl. Phys.* **39,** *No. 2, Part I, 496–497 (Feb. 1, 1968).*
Spin-lattice relaxation of protons in $CoCl_2 \cdot 2H_2O$ and $FeCl_2 \cdot 2H_2O$ has been measured over a temperature range of 1.3° to 12 °K in zero external magnetic field. The temperature dependence of the relaxation rate exhibits two relaxation processes, neither of which is adequately characterized by the T and T^3 laws previously reported for $CuCl_2 \cdot 2H_2O$. Additional T^{11} and $AT^2 \exp(-T_{AE}/T)$ dependences are required to fit our data which predicts a $T_{AE} = (42.8 \pm 1)$ °K for $CoCl_2 \cdot 2H_2O$ and a $T_{AE} = (4.18 \pm 0.2)$ °K for $FeCl_2 \cdot 2H_2O$.

Key Words: Spin-lattice relaxation time; antiferromagnetism; magnons; magnon energy gap.

Dean, J. W., Richards, R. J., **Hydrostatic pressure effects in carbon and germanium thermometers** (*Proc. 1967 Cryogenic Engineering Conf., Stanford University, Stanford, Calif., Aug. 21–23, 1967*), *Book, Advances in Cryogenic Engineering 13, 505–508 (Plenum Press Inc., New York, N.Y., 1968).*
This work describes measurements of the hydrostatic pressure coefficient of electrical resistivity for carbon and germanium thermometers in the range of 4 to 295 °K with experimental pressures up to 1000 psig (7.0×10^6 N/m²). Pressure coefficients were found to be independent of pressure but to vary with temperature from -0.65×10^{-5} to -1.1×10^{-5} psi^{-1} (-0.944×10^{-9} to -1.6×10^{-9} m²/N) for germanium and from -1.2×10^{-5} to -1.5×10^{-5} psi^{-1} (-1.74×10^{-9} to -2.18×10^{-9} m²/N) for carbon. These pressure coefficients result in resistance changes for a 1000 psig (7.0×10^6 N/m²) pressure at 20 °K that may be interpreted as temperature errors of 0.3 °K for carbon and 0.03 °K for germanium.

Key Words: Carbon; germanium; pressure effect; thermometer.

Dunn, G. H., **Photodissociation of H_2^+ and D_2^+: theory,** *Phys. Rev.* **172,** *No. 1, 1–7 (Aug. 5, 1968).*
Theory is described and calculations made for photodissociation cross sections of H_2^+ (D_2^+) from each of the ion's 19 (27) vibrational levels. Cross sections are summed over an assumed Franck-Condon distribution of initial vibrational states to give a predicted cross section for comparison with experiment. Auxiliary calculations are made of some of the cross sections using the common δ function approximation to the continuum radial wave functions, and a comparison made with the results using more exact wave functions shows very good agreement for photodissociation from the lowest vibrational levels, but very poor agreement for photodissociation from higher levels.

Key Words: Photodissociation; H_2^+; D_2^+; cross sections; vibrational levels; theory.

Gallagher, A., **Rubidium and cesium excitation transfer in nearly adiabatic collisions with inert gases,** *Phys. Rev.* **172,** *No. 1, 88–96 (Aug. 5, 1968).*
The cross sections for rubidium $5^2P_{1/2} \leftrightarrow 5^2P_{3/2}$ and cesium $6^2P_{1/2} \leftrightarrow 6^2P_{3/2}$ excitation transfer due to inert gas collisions have been measured. The temperature of the collision vessel has been varied from 300 °K to partially establish the velocity dependence of these cross sections (the alkali resonance line optical depths were always much less than one). The various cross sections exhibit a systematic behavior that can be combined to find the general shape of a "universal" cross section that ranges across six orders of magnitude, starting just below the threshold for "sudden" collisions. The surprisingly large influence of line broadening on these excitation transfer measurements has been removed as a source of error.

Key Words: Cross sections; collisions; rubidium; cesium; line broadening; velocity dependence; alkali resonance.

Heinrich, K. F. J., **Electron probe microanalysis by specimen current measurement** (*Proc. Fourth Intern. Symp. X-ray Optics and Microanalysis, Orsay, France, Sept. 7–10, 1965*), *Book, X-ray Optics and Microanalysis, Eds. R. Castaing, P. Deschamps, and J. Philibert, pp. 159–167 (Hermann, Paris, France, 1966).*
Under appropriate instrumental conditions, electron backscatter coefficients of elements and compounds can be determined quantitatively in the electron probe microanalyzer, without interference of low energy electrons. It is shown that there is a simple relation between the backscatter coefficient of a binary target and those of its constituents. This relation can be used for quantitative analysis of binary specimens. The advantages and limitations of this method are discussed, and a practical application of the technique for quantitative metallography is demonstrated. The backscatter coefficients of several elements have been experimentally determined at electron energies of 10, 20, 30, 40, and 49 keV.

Key Words: Electron backscatter; electron probe microanalysis; microanalysis; specimen; current.

Herron, J. T., Huie, R. E., **Arrhenius parameters for the reactions of atomic nitrogen with some olefins and acetylenes,** *J. Phys. Chem.* **72,** *No. 7, 2538–2540 (July 1968).*
The rates of reaction of atomic nitrogen with a series of olefins and acetylenes have been measured from 320 to 550 K. Pre-exponential factors and activation energies have been derived. In addition, upper limits are given for the rates of reaction of atomic nitrogen with several miscellaneous organic compounds.

Key Words: Atomic nitrogen; olefin; acetylene; rate constant; chemical kinetics; activation energy.

Hetzer, H. B., Robinson, R. A., Bates, R. G., **Dissociation constants of piperazinium ion and related thermodynamic quantities from 0 to 50°,** *J. Phys. Chem.* **72,** *2081–2086 (1968).*
The two thermodynamic dissociation constants of piperazinium ion at 11 temperatures from 0 to 50° have been determined from emf measurements of hydrogen-silver chloride cells without liquid junction. The first (acidic) dissociation constant (K_1) for the process $PzH_2^{++} + H_2O = H_3O^+ + PzH^+$ is given as a function of T (°K) by the equation $-\log K_1 = 952.111/T + 4.3919 - 0.007555T$. At 25°, $-\log K_1$ is 5.333, $\Delta H°$ is 31,080 J mole^{-1}, $\Delta S°$ is +2.2 J deg^{-1} mole^{-1}, and $\Delta C_p°$ is 86 J deg^{-1} mole^{-1}. The second (acidic) dissociation constant (K_2) for the process $PzH^+ + H_2O = H_3O^+ + Pz$ is given by the equation $-\log K_2 = 1656.59/T + 6.1316 - 0.006556T$. At 25°, $-\log K_2$ is 9.73_1, $\Delta H°$ is 42,870 J mole^{-1}, $\Delta S°$ is -42.6 *J deg*$^{-1}$ mole^{-1}, and $\Delta C_p°$ is 75 J deg^{-1} mole^{-1}. The results are compared with those for other protonated bases of similar structure.

Key Words: Piperazinium ion; piperazine; dissociation constant; ionization; thermodynamics of ionization; electrolyte; acid-base equilibria.

Hughes, E. E., Dorko, W. D., **Direct mass spectrometric determination of atmospheric carbon dioxide,** *Anal. Chem.* **40,** *No. 6, 866–869 (May 1968).*
The direct mass spectrometric determination of atmospheric carbon dioxide cannot be performed with any useful degree of accuracy because of the high concentration of oxygen in the atmosphere. By removing the oxygen with phosphorus it is possible to admit sufficiently high pressures of the remaining gas to determine the carbon dioxide with an inaccuracy of less than 1%. Since the argon content of the atmosphere is presumed constant, a direct comparison of the carbon dioxide to argon ratio should provide a fixed reference for future surveys. The method is rapid and requires little equipment other than a mass spectrometer. Results obtained on analysis of rural air in the vicinity of Washington, D.C., are presented.

Key Words: Atmospheric carbon dioxide; mass spectrometric atmosphere analysis; gas analysis; carbon dioxide.

Johannesen, R. B., Candela, G. A., Tsang, T., **Jahn-Teller distortion: magnetic studies of vanadium tetrachloride,** *J. Chem. Phys.* **48,** *No. 12, 5544–5549 (June 15, 1968).*
Paramagnetic resonance of polycrystalline VCl_4 diluted with $TiCl_4$ has been observed near 9, 24, and 36 GHz below 9 °K. Both g-values and hyperfine A-tensors are axially symmetric and temperature independent with the same principal axes; $g_{||} = 1.920$, $g_{\perp} = 1.899$, $|A_{||}| = 72$ G, $|A_{\perp}| = 120$ G. The average g-value obtained from susceptibility data is in agreement with the resonance value. The paramagnetic relaxation time T_1 varies with temperature as shown by the relaxation $T_1 = 2 \times 10^{-9} \exp(25/T)$ sec, indicating the presence of a potential barrier approximately 18 cm^{-1} in height. The results indicate a static Jahn-Teller distortion, but with large zero-point vibrations. This situation is in between Ballhausen-de Heer's ligand field and Ballhausen-Liehr's crystal field calculations.

Key Words: Hydrogen; molecular beam; field emission; condensa- magnetic susceptibility; vanadium tetrachloride; Jahn-Teller distortion; ligand field.

Klein, R., **The deposition of hydrogen beams on tungsten,** *Surface Sci.* **11,** *227–241 (1968).*
The deposition and chemisorption of hydrogen on tungsten have been investigated with a molecular beam apparatus to which a field emission microscope is attached. The FEM is operated immersed in liquid helium. The surface temperature of both the surface on which

the deposition is made, and the beam, can be varied independently. Advantage is taken of the formation of a sharp boundary line after spreading on a shadowed emitter to evaluate the effect of beam temperature on the condensation process. There is a very marked effect which suggests that the deposition depends on a critical velocity for the hydrogen molecule in the beam. This effect is found only for the second layer where the adsorption forces are relatively weak. The course of the deposition in the first layer can be followed from the characteristics of the electron emission from the tip as coverage proceeds.

•

Key Words: Hydrogen; molecular beam; field emission; condensation; tungsten.

Klemens, P. G., Jackson, J. L., **Diffusion of electrons on the Fermi surface. II. Longitudinal magnetoresistance of Ib metals,** *Physica* **31,** *1421–1427 (1965).*
Following Pippard the longitudinal high-field magnetoresistance is discussed in terms of belts on the Fermi sphere on which the deviation of the electron distribution from equilibrium must vanish. For the ideal resistance case the electron diffusion equation is solved with appropriate boundary conditions for a number of directions and neck radii, and the magnetoresistance is pointed out.

Key Words: Fermi surface; high-field magnetoresistance; magnetoresistance.

Kokoszka, G. F., Allen, H. C., Jr., Gordon, G., **Electron paramagnetic resonance spectra of two zinc-doped and nickel-doped copper chloride pyridine-N-oxide complexes,** *J. Chem. Phys.* **46,** *No. 8, 3020–3024 (Apr. 15, 1967).*
The electron paramagnetic resonance spectra of zinc-doped dichlorobispyridine-N-oxidecopper(II) $[(C_5H_5NO)_2Cu(Zn)Cl_2]$ and zinc-doped dichloromonoaquopyridine-N-oxidecopper(II) $[C_5H_5NOCu(Zn)Cl_2 \cdot H_2O]$ have been observed at liquid nitrogen temperature. The data could be fit to the usual $S=\frac{1}{2}$ Spin Hamiltonian. The g values obtained in this study for the copper-zinc pairs agree with the g values obtained for the copper-copper pairs in the pure material to within experimental uncertainty. Copper hyperfine splitting and chlorine superhyperfine splitting were also observed. The magnetic parameters for $(C_5H_5NO)_2Cu(Zn)Cl_2$ are $g_z=2.323$, $g_x=2.056$, $g_y=2.080$, $A_z=129\times10^{-4}$ cm^{-1}, $A_x=A_y<10\times10^{-4}$ cm^{-1}, $A'=25\times10^{-4}$ cm^{-1}, and $B'=7\times10^{-4}$ cm^{-1}, while for $C_5H_5NOCu(Zn)Cl_2 \cdot H_2O$ we obtain $g_z=2.306$, $g_x=2.056$, $g_y=2.083$, $A_z=139\times10^{-4}$ cm^{-1}, and $A_x=A_y<10\times10^{-4}$ cm^{-1}. An analysis of the data using a simple LCAO–MO approach suggests relatively strong metal-ligand bonds.
The data obtained from the study of nickel-doped $(C_5H_5NO)_2CuCl_2$ could be dit to an $S=\frac{1}{2}$ Spin Hamiltonian with the following magnetic parameters: $g_z=2.14$, $g_x=2.54$, $g_y=2.49$, $A_z=35\times10^{-4}$ cm^{-1}, and $A_x=A_y<7\times10^{-4}$ cm^{-1}. For nickel-doped $C_5H_5NOCuCl_2 \cdot H_2O$ we obtain $g_z=2.15$, $g_x=2.61$, $g_y=2.50$, $A_z=40\times10^{-4}$ cm^{-1}, and $A_x=A_y<7\times10^{-4}$ cm^{-1}. These are the first reported magnetic parameters from dimers which contain exchange coupled dissimilar transition metal ions.

Key Words: E.p.r. pair spectra; copper-nickel pairs; copper-zinc pairs; magnetic resonance; copper chloride-pyridine-N-oxide.

Lenzi, M., Okabe, H., **Photodissociation of NOCl and NO_2 in the vacuum untraviolet** (*Proc. Intern. Conf. Photochemistry, Munich, Germany, Sept. 6–9, 1967*), *Ber. deut. Bunsenges. Phys. Chem.* **72,** *No. 2, 169–173 (1968).*
The photodissociation of NOCl and NO_2 in the vacuum ultraviolet yields the electronically excited NO molecule which fluoresces in the near ultraviolet. The fluorescence spectrum, which lies mostly in the region 2200 to 4000 Å, extends below 2200 Å as the wavelength of incident light decreases. This is interpreted in terms of the production of the NO $C^2\Pi$, $D^2\Sigma^+$, $B'^2\Delta$, $E^2\Sigma^+$ along with the production of the NO $A^2\Sigma^+$, $B^2\Pi$ molecule. The fluoroescence intensity and the yield are measured as a function of incident wavelength. The fluorescence curves thus obtained are correlated with the absorption spectrum. The absorption coefficient of NOCl in the region 1100 to 2000 Å has been measured. The absorption spectrum between 1100 and 1700 Å may be divided into three regions each corresponding to the transitions providing the NO $A^2\Sigma^+$, NO $C^2\Pi$, $D^2\Sigma^+$ and NO $B'^2\Delta$, $E^2\Sigma^+$ molecule along with the ground state NO or other products. On the other hand the absorption by NO_2 in the spectral region from 1100 to 1450 Å involves not only transitions yielding the NO $A^2\Sigma^+$, $B^2\Pi$, NO $C^2\Pi$, $D^2\Sigma^+$ and NO $B'^2\Delta$, $E^2\Sigma^+$ but also those yielding different states which give products other than the electronically excited NO. The threshold energy of incident photon producing the NO $A^2\Sigma^+$, $B^2\Pi$ gives an upper limit of the bond dissociation energy. The bond energies obtained are $D(NO-Cl) \leq 1.77 \pm 0.05$ eV and $D(NO-O) \leq 3.22 \pm 0.05$ eV which are 0.17 eV and 0.10 eV higher than the respective values obtained from the heat of formation.

Key Words: Photodissociation; vacuum ultraviolet nitrosyl chloride; nitrogen dioxide; fluorescence excited states; absorption spectra.

McCulloh, K. E., **Franck-Condon calculations for double ionization of molecular hydrogen,** *J. Chem. Phys.* **48,** *No. 4, 2090–2093 (Mar. 1, 1968).*
The Franck-Condon radial overlap integral for transition from the ground vibronic state of H_2 to a state in the H_2^{+} continuum is expanded as an asymptotic series in powers of a small parameter. The initial semi-convergence of the series is sufficiently rapid to provide a convenient basis for computing the kinetic energy distribution for protons formed by double ionization of H_2. The results of these computations are presented. The analysis includes a derivation of the reflection approximation for the particular case of transition to the repulsive Coulomb potential curve. Preliminary results of a more general study indicate that this approximation can be applied to a much larger class of repulsive potentials. Previous forms of the reflection approximation, which have heretofore lacked theoretical foundation, are classified and discussed in relation to the derived approximation.

Key Words: Franck-Condon principle; reflection approximation; double ionization; H_2; proton; kinetic energy; theoretical.

McCulloh, K. E., Rosenstock, H. M., **Experimental test of the Franck-Condon principle:** *Double ionization of molecular hydrogen, J. Chem. Phys.* **48,** *No. 4, 2084–2089 (Mar. 1, 1968).*
The double ionization of molecular hydrogen by electron impact has been observed by coincidence detection of the resulting proton pairs in a system especially designed for absolute kinetic energy measurements. Monte Carlo calculations provided an accurate knowledge of the resolution with which the kinetic energy measurements were made. Experimental results agree closely with predictions based on accurate Franck-Condon overlap integrals for a model involving Morse oscillator wave functions for the molecule and Coulomb wave functions for the ion. In contrast, the reflection approximation and the harmonic oscillator approximation for molecular vibration, two approximations frequently made in such Franck-Condon calculations, do not agree well either with experiment or accurate calculations. Observations at electron energies of 0.5, 0.75, and 1 keV show that the kinetic energy distribution is independent of electron energy and suggest that the double ionization cross section is inversely proportional to electron energy in this range. These results are to be expected for a direct two-electron ejection mechanism for double ionization of H_2.

Key Words: Franck-Condon principle; double ionization; H_2; proton; kinetic energy; experimental.

Macek, J. H., **Application of the Fock expansion to doubly excited states of the helium atom,** *Phys. Rev.* **160,** *No. 1, 170–174 (Aug. 5, 1967).*
The origin of the plus and minus character of the ^1P and ^3P doubly excited states of helium which converge to the $n=2$ level is investigated in the close coupling approximation. It is found that the close coupling wave functions do exhibit the plus and minus character, and that the widths of these states are related to their plus and minus character in the case of the ^1P, but not for ^3P.

Key Words: Atomic physics; spectroscopy; theoretical physics; classification; levels; lifetimes.

Mann, D. E., Acquista, N., Linevsky, M. J., **An electronic band spectrum of yttrium monofluoride** (*Proc. 4th Rare Earth*

Research Conf., Phoenix, Ariz., Apr. 22–25, 1964), Book, Proceedings of the Fourth Conference on Rare Earth Research, pp. 363–372 (Gordon and Breach, New York, N.Y., 1965).
A system of 19 double-headed red-degraded bands has been observed in absorption in the range 3075–3300 Å when YF_3 is heated to about 2000 °C in a King furnace. They have been attributed to YF and a vibrational analysis made. The constants determined from measurements on the R heads are (in cm^{-1}): $\nu_{00}=31218.0$, $\omega_e''=633.5$, $\omega_e''x_e''=2.0$, $\omega_e'=539.0$, $\omega_e'x_e'=2.0$ A series of 10 diffuse bands in the range 2500–3000 Å was also seen in absorption. They have been tentatively ascribed to YF_2.

Key Words: Electronic band spectrum; rare earth research; yttrium monofluoride.

Mann, D. E., White, D., Seshadri, K. S., Dever, D. F., Linevsky, M. J., **The infrared spectra, structures and thermodynamics of gaseous LiO, Li_2O and Li_2O_2,** *J. Chem. Phys.* **39,** *2463–2473 (1963).*
The vapor above heated lithium oxide (Li_2O) has been investigated mass spectrometrically and by infrared matrix-isolation spectroscopy. The vapor composition and Knudsen effusion rates were measured as functions of temperature, and the matrix spectra of the principal lithium oxide species—Li_2O, LiO, Li_2O_2—identified and analyzed for different isotopic abundances. The predominant vapor species Li_2^7O is probably linear with r (Li–O) = 1.59 Å, and has fundamentals ν_1, ν_2, ν_3 at [760], [140], and 987 cm^{-1}, respectively. Its heat of formation $\Delta H_0^\circ(f) = -43.7 \pm 2.5$ kcal/mole. The diatomic molecule Li^7O has $\nu = 745$ cm^{-1}, an estimated bond length $r = 1.62$ Å, and $\Delta H_0^\circ(f) = +16.0 \pm 5$ kcal/mole. The previously undetected molecule $Li_2^7O_2$ is shown to resemble the alkali halide dimers in having a planar rhombic (V_h) structure for which the O–Li–O angle and Li–O bond length are estimated to be 116° and 1.90 Å, respectively. Its B_{2u} and B_{3u} frequencies are found at 324 and 522 cm^{-1}, respectively, in a krypton matrix. The remaining unobserved modes are estimated in cm^{-1} as follows: $\nu_1(A_g) = 400$, $\nu_2(A_g') = 250$, $\nu_3(B_{1g}) = 300$, $\nu_4(B_{1u}) = 270$. Its $\Delta H_0^\circ(f) = +27.5 + 6$ kcal/mole.

Key Words: Infrared matrix; infrared spectra; isolation spectroscopy; lithium oxide species; matrix spectra; spectroscopy.

Maryott, A. A., Birnbaum, G., **Line shape and collision effects in the microwave wing of far-infrared rotational lines,** *J. Chem. Phys.* **47,** *No. 9, 3200–3205 (Nov. 1967).*
The microwave absorption located very far in the low frequency wings of the rotational spectra of HCl and DCl has been measured in order to test the applicability of the Van Vleck-Weisskopf relation for pressure broadening in the region many line widths removed from the resonance frequencies. Data for mixtures of HCl with the foreign gases, He, H_2, Ar, N_2, CH_4, C_2H_6, CO, SF_6, and CO_2, are also reported. Results for the mixtures with He and H_2 are in accord with theory. Results for the remaining mixtures and the pure gases do not agree with predictions, the observed absorption being from two to eight times greater. These discrepancies suggest the presence of an additional absorption region which is centered at a lower frequency than the normal rotational spectrum and which may be attributed to interacting molecular pairs.

Key Words: Interacting molecular pairs; low frequency; microwave absorption; rotational spectra.

Miller, K. J., Krauss, M., **Inapplicability of the born exchange scattering amplitude for the He ($1^1S \rightarrow 2^3S$) transition,** *J. Chem. Phys.* **48,** *No. 6, 2611–2614 (Mar. 15, 1968).*
Differential cross-sections are calculated for the He($1^1S \rightarrow 2^3S$) transition within the Born-Oppenheimer approximation. The Bonham-Ochkur (OB) Approximation is compared to the exact exchange scattering amplitude and it is found to yield semiquantitative agreement, especially at high incident energies. However, the theoretical results show qualitatively different behavior from recent experimental results. Experimental differential cross-sections peak in the forward direction while theory predicts a maximum at large angles.

Key Words: Born exchange scattering amplitude; Bonham-Ochkur approximation; helium ($1^1S \rightarrow 2^3S$); differential cross-section.

Moiseiwitsch, B., Smith, S. J., **Electron impact excitation of atoms,** *Rev. Mod. Phys.* **40,** *No. 2, 238–353 (Apr. 1968).*
The experimental and theoretical literature about the electron impact excitation of atoms is reviewed. Theoretical methods ranging from the Bethe and Born approximations to the close coupling approximations are discussed and intercompared. Where possible, on theoretical grounds or through intercomparison, the reliability of the various methods is discussed.
A general critique of the optical method of measuring excitation functions is given, with the objective of promoting higher quality future experimental work. A critical study of existing experimental work leads to the conclusion that most workers have ignored important physical and instrumental effects, and it may be presumed that the data in the literature is subject to many unrecognized systematic errors. The literature on hydrogen and helium is discussed critically. The literature on the alkalis, heavy rare gases, mercury, cadmium and zinc is surveyed but the quality of the literature does not support critical review beyond some general comments about the physics of these atoms.

Key Words: Electron; atom; impact; excitation; theoretical; experimental; review; hydrogen; helium.

Mopsik, F. I., **Molecular and ionic interactions,** *1966 Digest of Literature on Dielectrics* **30,** *Chapt. 3, 62–90 (National Academy of Sciences-National Research Council, Washington, D.C., 1966).*
This year's chapter includes the literature covered by Physics Abstracts and Chemical Abstracts for the year 1966. The papers included are those, both theoretical and experimental, that are concerned with underlying dielectric phenomena. Papers that report values for dielectric parameters have been omitted unless there was a significant contribution to the understanding of dielectric theory. In particular, papers that should be adequately covered by the tables were not included.

Key Words: Dielectrics literature; digest of literature; molecular and ionic interactions; review of literature; dielectric theory; 1966 dielectrics literature.

Persson, K-B., Johnson, E. G., Jr., Uhlenbrock, D. A., **A theory for cyclotron harmonic radiation from plasmas,** *Phys. Fluids* **1,** *No. 3, 619–628 (Mar. 1968).*
A highly simplified hydrodynamic model for the cause of cyclotron harmonics radiation in a magnetized abnormal glow helium plasma is proposed. The high velocity electrons are treated as sources for the charge density waves in the plasma. With the very crucial existence of statistical fluctuations in the ion density, these waves act as sources for electromagnetic radiation. This radiation contains the cyclotron harmonics. Some numerical curves of the radiation spectra are shown for a number of plasma parameters.

Key Words: Electron cyclotron frequency; emission; harmonic; microwave and theory.

Rubin, R. J., **Momentum autocorrelation function of a heavy particle in a finite crystal,** *J. Am. Chem. Soc.* **90,** *3061–3063 (1968).*
The momentum autocorrelation function of a heavy particle in a finite one-dimensional crystal, $\rho_0^{(N)}(\tau)$, is compared with the same function in an infinite crystal, $\rho_0^{(\infty)}(\tau)$, by obtaining an explicit upper bound for the magnitude of the difference. $|\rho_0^{(N)}(\tau) - \rho_0^{(\infty)}(\tau)|$. The precise meaning of the statement that $\rho_0^{(\infty)}(\tau)$ is approximately a simple exponential is reviewed; and precise meaning is given to the statement that there is exponential damping in the case of a finite crystal.

Key Words: Brownian motion; correlation function; lattice dynamics.

Rybicki, G. B., Hummer, D. G., **Spectral line formation in variable-property media: the Riccati method,** *Astrophys. J.* **150,** *No. 2, 607–635 (Nov. 1967).*
A numerical method, based on the generalized Riccati transformation of Rybicki and Usher, is presented for the integration of the radiative transfer equation for spectral line formation by noncoherent scattering in inhomogeneous plane-parallel media. An asymptotic theory is developed which permits the application of this method to problems involving semi-infinite media. Numerical

results obtained by the Riccati method are used to discuss the effects of spatial variations in the Doppler width on lines formed by pure Doppler broadening.

Key Words: Variable-property media; Doppler width; radiative transfer media; Riccati method; spectral line formation.

Sadowski, W. L., **On some aspects of the eigenfunction expansion of the solution of the nonlinear Vlasov equation** (*Proc. Computer Simulation of Plasma and Many-Body Problems, Williamsburg, Va., Apr. 19–21, 1967*), *Natl. Aeronaut. Space Agency Spec. Publ. 153, 433–440 (1967)*.
The non-linear Vlasov equation governing a one-dimensional periodic plasma was solved numerically. The solutions were expanded into a double set of eigenfunctions. The x-dependence of the distribution function was expressed by Fourier series, while Hermite polynomials were used to express the v-dependence. These two sets are eigenfunctions of the differential operators and the partial differential equation reduces to an ordinary differential equation on a matrix of expansion coefficients.
Some of the results are discussed as well as the closure problems arising from the attempts to represent an infinite expansion in terms of a finite matrix. The effect of the Fokker-Planck term on the detailed description of particle trapping and on Landau damping is also discussed.

Key Words: Plasma physics; Landau damping; Vlasov equation; non-linear; eigenfunction; truncation; numerical solution.

Schindler, P. W., **Heterogeneous equilibria involving oxides, hydroxides, carbonates and hydroxide carbonates** (*Proc. Symp. Division of Water, Air and Waste Chemistry, 151st Meeting of the American Chemical Society, Pittsburgh, Pa., Mar. 1966*), *Book, Equilibrium Concepts in Natural Water Systems, Advances in Chemistry Series 67, 196–221 (American Chemical Society, New York, N.Y., 1967)*.
Part I discusses the experimental determination and graphical presentation of equilibrium data. Some emphasis is placed on the connection between "thermodynamic" constants (referring to pure water as standard state) and "stoichiometric" constants relating to aqueous solutions of constant ionic strength. Part II compares equilibria in stable and metastable systems. Recent experimental work on the effect of particle size upon solubility is summarized, and the changes of solubility in the presence of metastable modifications is discussed. An attempt is made to classify some major and minor constituents of sea water with respect to a possible control of their concentrations by simple solubility equilibria.

Key Words: Equilibria; Sea Water; Oxides; Hydroxides; Carbonates; Hydroxide Carbonates; Solubility.

Shapiro, J. T., Madden, R. P., **On the optical constants of polystyrene in the vacuum ultraviolet,** *J. Opt. Soc. Am.* **58,** *No. 6, 771–775 (June 1968)*.
The optical constants n and k for polystyrene in both thin film and bulk form have been measured by the reflectance vs angle of incidence technique in the wavelength region from 584 Å to 2,000 Å. Four angles of incidence were used, and the effects of monochromator polarization were eliminated experimentally. The results differ from previously published data for the bulk form. The energy loss function $-\mathrm{Im}(1/\epsilon)$ was calculated from n and k determined for the thin films and compared with values obtained previously by characteristic electron energy loss techniques. These two methods yield the same structure in the energy loss function; however there remains some difference in the magnitude of the 6.9 eV loss relative to the background.

Key Words: Polystyrene; optical constants; vacuum ultraviolet; reflectance electron energy loss.

Shuler, K. E., **Reaction cross sections, rate coefficients and nonequilibrium kinetics** (*Lecture, NATO Summer School on Theoretical Chemistry, Constance, Germany, Summer 1965*), *Book, Chemische Elementarprozesse, Ed. H. Hartmann, pp. 1–22 (Springer-Verlag, Berlin, Germany, 1968)*.
The observed rate of a chemical reaction is usually expressed through an empirical equation involving the concentration of reactants and/or products and a proportionality constant k, the *rate coefficient*. This rate coefficient is determined experimentally from measurements of the change of concentration of reactants and/or products with time. If the empirical rate equation correctly describes, *in all aspects*, the reaction under investigation, the rate coefficient should be independent of the concentration of the reactants and/or products and of the time and should depend only upon the temperature of the (isothermal) reaction system.
Recent advances in experimental techniques permit the measurement of the "efficiency" of elementary chemical collision processes leading to product formation as a function of the energy of the reactants (kinetic and internal) and the geometry of the encounter. The results of these measurements are expressed as *reaction cross sections*, σR. It is the purpose of these lectures to explore the relation between the macroscopic rate coefficient k and the microscopic reaction cross section σR.

Key Words: Cross sections; nonequilibrium kinetics; rate coefficients; reaction cross sections.

Silverman, S., **Reflections on bioengineering** (*Proc. Symp. Engineering Significance of the Biological Sciences, Pittsburgh, Pa., Jan. 25–27, 1967*), *Book, Bioengineering—An Engineering View, pp. 103–106 (San Francisco Press Inc., San Francisco, Calif., June 1968)*.
The role of Bioengineering in the contemporary scene is examined. The conviction is expressed that there is a real need for such an interdisciplinary development at this time. It is pointed out that Bioengineering must compete with other well-entrenched trends in science and technology in a budgetary environment that calls for thorough analysis and justification. There is, however, good evidence that the social needs should draw the necessary interest of gifted and competent people, and therefore sufficient Federal interest to support a growing program.

Key Words: Bioengineering; trends in science; technology; budgetary environment; social needs.

Smith, G. W., Becker, D. A., **Preparation of an NBS biological standard reference material for trace elemental analysis,** *Proc. Nuclear Activation Techniques in the Life Sciences, Amsterdam, The Netherlands, May 8–12, 1967, pp. 197–207 (International Atomic Energy Agency, Vienna, Austria, 1967)*.
A survey of leading U.S. biological, medical and forensic laboratories confirms the need for well characterized botanical, soft mammalian tissue, bone tissue and blood standards with elemental constituents at the 100 ppm level and below. The only sources of dried and sterilized tissue and blood known to the authors are certain U.S. drug concerns, whereas H. J. M. Bowen's kale has only been available since 1964 as a botanical comparison sample.
Before reliable analytical data can be obtained on a reference material, homogeneity must be established. Examples are given of this procedure, which is carried out routinely by the NBS on Standard Reference Materials. Honogeneity of Bowen's kale for chlorine (~ 4000 ppm), manganese (~ 14 ppm) and copper (~ 6 ppm) as well as for manganese in beef liver (~ 10 ppm) citrus leaf (~ 28 ppm) and oak leaf (~ 1000 ppm) are given. Measurements were made by neutron activation analysis both with and without chemical separation, using a Ge(Li) semiconductor detector. This technique was also used for the quantitative determination of the trace constituents chlorine and manganese, non-destructively. In addition, a destructive method was used for the elements arsenic and copper.
Analyses of variance, using the activation analysis data, indicate that all of the biological materials except the citrus leaves are homogeneous. Therefore, preparation under contract, of large lots of deciduous leaves and beef liver, will begin. Analyses for homogeneity and elemental content certification will be made by NBS activation analysis and other analytical competencies.

Key Words: Biological; trace; tissue; botanical; bone; blood; reference; neutron; activation; analysis; non-destructive; destructive; variance; leaves; liver; homogeneity.

Tisone, G. C., Branscomb, L. M., **Detachment of electrons from H^- and O^- negative ions by electron impact,** *Phys. Rev.* **170,** *No. 1, 169–183 (June 5, 1968)*.

The energy range for the electron detachment cross section for H^- has been extended from 500 eV down to 8.4 eV. The absolute cross section for detachment of electrons from atomic oxygen negative ions has been measured in the energy range of 7.1 to 487.1 eV. Results of these measurements are compared with Bethe-Born calculations of the cross section. This calculation with the semiclassical Coulomb correction is in qualitative agreement with the experimental results above 20 eV electron energy for both H^- and O^-, although the energy dependence of the H^- cross section from 100 to 500 eV is not consistent with the slope predicted theoretically for the high energy limit.

Key Words: Ionization cross section; hydrogen negative ion; crossed-charged beams; electron collisions; negative oxygen ion.

Truesdell, C., **The non-linear field theories of mechanics,** *Encyclopedia of Physicas III, Part 3, 602 pages (Springer-Verlag, Berlin, Germany, 1965).*
This treatise presents an organized development of theories of mechanical response of materials subject to large deformations. It contains as one of its chapters an exposition of everything now known about the general theory of finite elastic strain.

Key Words: Elastic strain; field theories; finite elastic strain; mechanical response; mechanics.

VanderHart, D. L., Gutowsky, H. S., Farrar, T. C., **Dipole-dipole interactions of a spin ½ nucleus with a quadrupole-coupled nucleus,** *J. Am. Chem. Soc.* **89,** *No. 19, 5056–5057 (Sept. 13, 1967).*
Line shapes for a two-spin $(\frac{1}{2}, \frac{1}{2})$ system having axial symmetry along the internuclear vector and quadrupole coupling at the spin ½ nucleus are calculated as a function of the ratio of the Zeeman to quadrupole interaction energies. It is shown that the spin-½ NMR line shape is frequency dependent and that the second moment of the spin-½ NMR spectrum may be as much as 1.84 times its value in the absence of quadrupole coupling. Reported values for M–H bond distances via NMR studies in transition-metal carbonyl hydrides may be too small.

Key Words: Frequency-dependent proton NMR line shapes; solids; bond-distance indirect quadrupole interaction.

Vriens, L., Kuyatt, C. E., Mielczarek, S. R., **Tests of born approximations; differential and total cross sections for elastic scattering of 100- to 400-eV electrons by helium,** *Phys. Rev.* **170,** *No. 1, 163–169 (June 1968).*
The angular dependence for elastic scattering of 100 to 400 eV electrons by helium atoms has been measured with a high resolution electron spectrometer. The angular range in the present measurement extends from 5° to 30°. The relative differential cross sections were put on an absolute basis using measured ratios of elastic and 2^1P scattered currents and known 2^1P cross sections. The differential cross sections were integrated to get total elastic scattering cross sections. Large deviations from the Born approximation are found, especially for small incident energies and small scattering angles. The agreement with more sophisticated calculations of Khare and Moiseiwitsch is better, but not yet satisfactory. Our results are in reasonable qualitative agreement with results of earlier experiments, but are quantitatively quite different and extend to smaller scattering angles.

Key Words: Born approximation; differential and total cross sections; elastic scattering; electrons; exchange; helium.

Wachtman, J. B., Jr., Brower, W. S., Farabaugh, E. N., **Elastic constants of single crystal calcium molybdate ($CaMoO_4$),** *J. Am. Ceram. Soc.* **51,** *No. 6, 341–344 (June 1968).*
The seven elastic compliances (and seven elastic constants) of single crystal calcium molybdate were determined by a resonance method. The compliance s_{16}, which is zero for higher symmetry tetragonal crystals, need not be zero for crystals of lower tetragonal symmetry and contributes significantly to the orientation dependence of the elastic moduli of calcium molybdate. The values of the compliances and their standard errors (based on 41 measurements) in units of $10^{-11}m^2/N(10^{-12}cm^2/dyn)$ are $s_{11} = .974 \pm .005$, $s_{33} = .958 \pm .004$, $s_{44} = 2.720 \pm .009$, $s_{66} = 2.276 \pm .024$, $s_{13} = -.308 \pm .009$, $s_{13} = -.249 \pm .009$, and $s_{16} = .418 \pm .011$.

Key Words: Calcium molybdate; compressibility; Debye temperature; elastic constants; shear modulus; Young's modulus.

Wang, F. E., DeSavage, B. F., Buehler, W. J., **The irreversible critical range in the TiNi transition,** *J. Appl. Phys.* **39,** *No. 5, 2166–2175 (Apr. 1968).*
Through an investigation of the transport and other related thermodynamic properties of TiNi at and around its "martensitic" transition temperature, the existence of a critical range extending over a 60 degree interval is characterized. Within this critical range, phase transition is second-order with anomalous heat capacity changes. Irreversibility of various properties within the critical range is interpreted in terms of irreversible shear movement of atoms.
By inference, based on transport data, the band structure of TiNi is a single or "nearly" single positive band within the temperature range investigated. The postulate that part of the valence electrons undergo a "covalent" ↔ "conduction" electronic state transformation, in the course of the 60 degree interval, second-order transition, is consistent in large measure with experimental data.

Key Words: Martensitic transition; covalent; electronic conduction; resistivity; Hall effect; magnetic susceptibility; order-disorder; phase transformation; localized; delocalized.

Younglove, B. A., **Polarizability, dielectric constant, pressure, and density of solid parahydrogen on the melting line,** *J. Chem. Phys.* **48,** *No. 9, 4181–4186 (May 1, 1968).*
Polarizibilities, calculated from measurements of the dielectric constant, are reported for solid parahydrogen on the melting line between 18 and 320 atmospheres (14.4 to 22.2 °K). Also new melting pressures below 17 °K are presented. Previously reported solid densities are adjusted slightly, using the new resulting pressure data. Liquid parahydrogen polarizibilities were determined over part of the density range of the solid and are seen to be slightly less than the solid polarizibilities.

Key Words: Polarizibility; dielectric constant; melting pressure; solid density; parahydrogen.

Zwanzig, R., Lauritzen, J. R., Jr., **Exact calculation of the partition function for a model of two-dimensional polymer crystallization by chain folding,** *J. Chem. Phys.* **48,** *No. 8, 3351–3360 (Apr. 15, 1968).*
A model of two-dimensional polymer crystallization by chain folding is treated by equilibrium statistical mechanics. The Laplace transform of the partition function with respect to the length of the polymer chain is obtained in exact analytical form. The model leads to thermodynamically well defined chain folded crystals. Under certain circumstances in the limit of an infinitely long polymer chain, the model shows a second order phase transtition from an "extended chain" crystal to the chain folded crystal.

Key Words: Polymer crystals; chain-folding; phase transition; equilibrium statistical mechanics; partition function.

Other NBS Publications

J. Res. NBS 72B (Math. Sci.), No. 4 (Oct.–Dec. 1968), 75 cents.

Principal submatrices VII: Further results concerning matrices with equal principal minors. R. C. Thompson.

On the multipliers of the Dedekind modular function. J. Lehner.

Minimax error selection of a discrete univariate distribution with prescribed componentwise bounds. A. J. Goldman and P. R. Meyers.

Minimax error selection of a discrete univariate distribution with prescribed componentwise ranking. A. J. Goldman.

On the signs of the ν-derivatives of the modified Bessel functions $I_\nu(x)$ and $K_\nu(x)$. D. O. Reudink.

Comparison of finite-difference computations of natural convection. K. E. Torrance.

Generalized inverses and solutions of linear systems. J. Z. Hearon.

J. Res. NBS 72C (Engr. and Instr.), No. 4 (Oct.–Dec. 1968), 75 cents.

Theoretical and experimental study on longitudinal impact of tapered rods. L. R. Hettche.

Analytical studies of probe conduction errors in ground temperature measurements. B. A. Peavy.

Nonlinear constrained optimization by a nonrandom complex method. R. A. Mitchell and K. L. Kaplan.

---

deMaine, P. A. D., Input/output packages for the systems 360 assembly language processor, Tech. Note 433 (Sept. 1968), 25 cents.

Eisele, J. W., Tech. Std. Coordinator, Fabrics for book covers, PS9–68 (Apr. 15, 1968), 10 cents.

Lovell, W. S., Thiel, L. M., Interferometric measurements of the complex dielectric constant of liquids, Tech. Note 369 (Aug. 1968), 50 cents.

Marsden, C. P., Tabulation of published data on Soviet electron devices through October 1967, Tech. Note 441 (July 1968), 55 cents. (Supersedes Tech. Note 265.)

Swanson, H. E., McMurdie, H. F., Morris, M. C., Evans, E. H., Standard X-ray diffraction powder patterns, Mono. 25, Sect. 6 (June 1968), 60 cents.

Tate, D. R., Acceleration due to gravity at the National Bureau of Standards, Mono. 107 (June 1968), 25 cents.

Watstein, D., Johnson, P. V., Experimental determination of eccentricity of floor loads applied to a bearing wall, Bldg. Sci. Series 14 (June 1968), 15 cents.

Wegstein, J. H., Rafferty, J. F., Pencak, W. J., Matching fingerprints by computer, Tech. Note 466 (July 1968), 20 cents.

Abrams, M. D., A comparative sampling of the systems for producing computer-drawn flow charts, Proc. 1968 ACM National Conf., Las Vegas, Nevada, Aug. 27–29, 1968, pp. 743–750 (Brandon/Systems Press, Inc., Princeton, N.J., 1968).

Ambs, W. J., Field-emission studies of the oxidation of clean nickel surfaces, Proc. 2nd Intern. Congress on Metallic Corrosion, New York, N.Y., Mar. 11–15, 1963, pp. 815–821 (Natl. Assoc. Corrosion Engr., Houston, Texas, 1966).

Ausloos, P., Rebbert, R. E., Lias, S. G., Structure and reactivity of propylions in gas-phase radiolysis, J. Am. Chem. Soc. **90,** No. 18, 5031–5033 (Aug. 28, 1968).

Bates, A. A., Responsibility in building research, Proc. Third Australian Building Research Cong., Melbourne, Australia, Aug. 1967, pp. 27–34 (1968).

Bates, R. G., Measurement of pH, Handbook of Biochemistry, Ed. H. A. Sober, pp. J100–J194 (Chemical Rubber Company, Cleveland, Ohio, 1967).

Bechtoldt, C. J., Ogburn, F., Smit, J., Structure and morphology of electrodeposited molybdenum dendrites, J. Electrochem. Soc. **115,** No. 8, 814–816 (Aug. 1968).

Bender, P. L., Branscomb, L. M., Credit for gravity apparatus, Phys. Today Letter **20,** No. 10, 17 (Oct. 1967).

Branscomb, L. M., The misinformation explosion: Is the literature worth reviewing? Sci. Res. **3,** No. 11, 49–52 (May 1968).

Broberg, J., Leiss, J., Schrack, R. A., Wyckoff, J. M., On-line handling system for the NBS linac, IEEE Trans. Nucl. Sci. **NS–11,** No. 3, 331–337 (June 1964).

Burke, P. G., Cooper, J. W., Ormonde, S., Electron-impact excitation of $n=2$ states in He, Phys. Rev. Letters **17,** No. 7, 345–348 (Aug. 15, 1966).

Bussey, H. E., Instrumentation and measurement, 1966 Digest of Literature on Dielectrics 30, Publ. 1496, 1–21 (National Academy of Sciences-National Research Council, Washington, D.C., 1966).

Chappell, S. E., Humphreys, J. C., Motz, J. W., Berger, M. J., Seltzer, S. M., Response of silicon transmission detectors to monoenergetic electrons, IEEE Trans. Nuclear Sci. **NS–15,** No. 3, 359 (June 1968).

Corliss, E. L. R., A mechanistic model for the limits of auditory preception, Proc. Symp. on Models for the Perception of Speech and Visual Form, Boston, Mass., Nov. 11–14, 1964, pp. 339–343 (Massachusetts Institute of Technology, Boston, Mass., 1967).

Davis, J. C., Faison, T. K., Achenbach, P. R., Errors in temperature measurement in moving air under isothermal conditions using thermocouples, thermistors and thermometers, ASHRAE Trans. **73,** Part I, VII 1.1 (1967).

Drechsel, D., Maximon, L. C., Potential model calculation for coplanar and non-coplanar proton-proton bremsstrahlung, Physics Letters **26B,** No. 8, 477–479 (Mar. 1968).

Drechsel, D., Seaborn, J. B., Greiner, W., Collective correlations in spherical nuclei and the structure of giant resonances, Phys. Rev. **162,** No. 4, 983–991 (Oct. 1967).

Durst, R. A., Ross, J. W., Jr., Electrochemical generation of fluoride ion by solid-state transference, Anal. Chem. **40,** No. 8, 1343–1344 (July 1968).

Evenson, K. M., The optical detection of stimulated emission in CN at 20-CM wavelength, Appl. Phys. Letters **12,** No. 8, 253–254 (Apr. 15, 1968).

Forbes, E. J., A graphic method of economic feasibility analysis, Proc. Inst. Electronics and Automation in Publishing, Washington, D.C., 1965), Book, Automation and Electronics in Publishing, Ed. L. H. Hattery and G. P. Bush, 3, Part IV, Chapt. 13, 129–140 (Spartan Books, Washington, D.C., 1965).

Forman, R. A., Cardona, M., Exciton electroreflectance in II–VI compounds, Proc. Intern. Conf. II–VI Semiconducting Compounds, Brown University, Providence, Rhode Island, Sept. 6–8, 1967, pp. 100–111 (W. A. Benjamin, Inc., New York, N.Y., 1967).

Fowler, H. A., Experiments in electron scattering, 1, Proc. Symp. Quantitative Aspects of Electron Microscopy, Walter Reed Institute of Pathology, Washington, D.C., 1965; Lab. Investigations **14,** No. 6, Part 2, 9–16 (1965).

Franklin, A. D., NBS dedicates new laboratory, J. Am. Ceramic Soc. **45,** No. 10, 841–842 (1966).

Freeman, D. H., Aiyar, A. S., Studies of ion exchange materials: homogeneous fractional sulfonation of copolymers of styrene and divinylbenzene, Anal. Chem. **39,** No. 10, 1141–1144 (Aug. 1967).

Freeman, D. H., Paulson, R. A., Chemical microstandards from ion exchange resin, Nature **218,** 563–564 (May 11, 1968).

Gammon, W. H., Remotes and displays, Proc. A Pioneer Presentation of a National Symposium on the Impact of Automation and Documentation, Denver, Colo., Apr. 27–29, 1967, p. 119 (1968).

Gammon, W. H., Security and privacy problems brought on by automation, Proc. A Pioneer Presentation of a National Symposium on the Impact of Automation and Documentation, Denver, Colorado, Apr. 27–29, 1967, pp. 74–75 (1968).

Gammon, W. H., Software as it relates to documentation, Proc. A Pioneer Presentation of a National Symposium on the Impact of Automation and Documentation, Denver, Colo., Apr. 27–29, 1967, pp. 14–22 (1968).

Gammon, W. H., What educators can expect from the center for Computer Sciences and Technology, Proc. Gen. Conf. Midwestern States Educational Information Project, Des Moines, Iowa, June 20, 1967, P. L. 89–10, Title V, Sect. 505, pp. 30–45 (Department of Public Instruction, State of Iowa, Des Moines, Iowa, 1967).

Gates, D. M., Keegan, H. J., Weidner, V. R., Spectral reflectance and planetary reconnaissance (Proc. Third Goddard Memorial Symp. Scientific Experiments – Manned Orbital Flights, Washington, D.C., Mar. 18–19, 1965), Book, Scientific Experiments for Manned Orbital Flights 4, 71–86 (Western Periodicals Co., North Hollywood, Calif., 1965).

Glasgow, A. R., Jr., High-temperature valve for corrosive gases, Anal. Chem. **38,** 1104 (July 1966).

Goldman, D. T., Reactor physicists emphasize need for neutron data, Phys. Today **21,** No. 8, 85–89 (Aug. 21, 1968).

Gould, H. A., Guernsey, R. L., Williams, R. H., Comment on the kinetic equation of a dilute gas with repulsive and attractive interactions, J. Chem. Phys. Letter **47,** No. 2, 872–873 (July 15, 1967).

Greenberg, L., Kleinian groups, Proc. Am. Math. Soc. **17,** No. 5, 1195–1198 (Oct. 1966).

Gugler, A. L., A study of the adherence of procelain enamel to aluminum, Proc. Procelain Enamel Institute Forum **29,** 202–208 (Nov. 1967).

Haber, S., A combination of Monte Carlo and classical methods for evaluating multiple integrals, Bull. Am. Math. Soc. **74,** No. 4, 683–686 (July 1968).

Hall, M. B., Little, W. E., A directional coupler with a readily calculable coupling ratio, IEEE Trans. Microwave Theory Tech. **MTT–15,** No. 11, 598–603 (Nov. 1967).

Harris, W. P. Low frequency dielectric behavior (Proc. Seventh Electrical Insulation Conf., Chicago, Ill., Oct. 16–19, 1967), IEEE Publ. 32C79–42, 123–125 (1967).

Heinrich, K. F. J., Scanning electron probe microanalysis, Am. Soc. Testing Mater. Spec. Tech. Publ. 430, 315–342 (1968).

Heinrich, K. F. J., Vieth, D., Yakowitz, H., Correction for nonlinearity of proportional counter systems in electron probe x-ray microanalysis, Advan. X-ray Anal. **9,** 208–220 (1966).

Herber, R. H., Spijkerman, J. J., Narrow-line source for ^{119}Sn

Mössbauer spectroscopy, J. Chem. Phys. **43,** No. 11, 4057–4059 (Dec. 1, 1965).
Herron, J. T., Huie, R. E., On the reaction of atomic nitrogen with carbon dioxide, J. Phys. Chem. **72,** No. 6, 2235–2236 (June 1968).
Hertelendy, P., An approximate theory governing symmetric motions of elastic rods of rectangular or square cross section, J. Appl. Mech. Paper No. 68–APM–10, pp. 333–341 (June 1968).
Hiza, M. J., Heck, C. K., Kidnay, A. J., Liquid-vapor and solid-vapor equilibrium in the system hydrogen-ethane (Proc. 1967 Cryogenic Engineering Conf., Stanford University, Stanford, Calif., Aug. 21–23, 1967), Book, Advances in Cryogenic Engineering 13, 343–356 (Plenum Press Inc., New York, N.Y., 1968).
Hobbs, A. M., Remarks on network simplification, J. Operations Res. **15,** No. 3, 548–551 (May–June 1967).
Hummer, D. G., Radiative transfer processes in planetary nebulae (Proc. Intern. Astronomical Union, Symp. No. 34, Tatranska Lomnica, Czechoslovakia, Sept. 4–8, 1967), Book, Planetary Nebulae, Ed. D. E. Osterbrock and C. R. O'Dell, pp. 166–184 (D. Reidel Publ. Co., Dordrecht, Amsterdam, The Netherlands, 1968).
Hummer, D. G., Mihalas, D., Line formation with non-coherent electron scattering in O and B stars, Astrophys. J. **150,** No. 1, L57–L59 (Oct. 1967).
Ito, J., Silicate apatities and oxyapatites, Am. Mineralogist **53,** 890–907 (May–June 1968).
Ito, J., Strontium rare-earth hydro-germanate and garnets, Mater. Res. Bull. **3,** 495–500 (1968).
Jackson, J. L., Coriell, S. R., Transport coefficients of composite materials, J. Appl. Phys. **39,** No. 5, 2349–2354 (Apr. 1968).
Kerns, D. M., Beatty, R. W., Book, Basic theory of waveguide junctions and introductory microwave network analysis, 150 pgs. (Pergamon Press Inc., London, England, 1967).
Kidnay, A. J., Hiza, M. J., Dickson, P. F., The adsorption isotherms of methane, nitrogen, hydrogen and their mixtures on charcoal at 76 °K (Proc. 1967 Cryogenic Engineering Conf., Stanford University, Stanford, Calif., Aug. 21–23, 1967), Book, Advances in Cryogenic Engineering 13, 397–408 (Plenum Press Inc., New York, N.Y., 1968).
Koch, H. W., Caswell, R. S., Muehlhause, C. O., Neutron measurement at the National Bureau of Standards, Nuclear News **10,** No. 11, 48–53 (Nov. 1967).
Kokoszka, G. F., Allen, H. C., Jr., Gordon, G., Magnetic and optical spectra of copper monochloracetate 2.5 hydrate, J. Chem. Phys. **47,** No. 1, 10–13 (July 1, 1967).
Kopec, C. S., Measurement of gears, Handbook of Industrial Metrology, Chapt. 15, pp. 424–450 (Prentice-Hall, Inc., Englewood Cliffs, N.J., 1967).
Krauss, M., Use of approximate Hartree-Fock calculations to estimate ionization potentials, Book, Advances in Mass Spectrometry 4, 575–578 (Elsevier Publ. Co., Amsterdam, The Netherlands, Aug. 14, 1967).
Kruger, J., The spectrum of corrosion research of the Corrosion Section of the National Bureau of Standards (Proc. 12th Annual Appalachian Underground Corrosion Short Course, West Virginia University, Morgantown, West Virginia, Oct. 1967), West Virginia University Tech. Bull. 86, 11–13 (1967).
Landgrebe, A. R., Pella, P. A., McClendon, D. T. DeVoe, J. R., Purdy, W. C., The application of substoichiometric radioisotopic dilution principles to controlled potential coulometry and solvent extraction, Anal. Chim. Acta **39,** 151–159 (1967).
Larsen, S. Y., Quantum-mechanical pair-correlation function of hard spheres, J. Chem. Phys. **48,** No. 4, 1701–1708 (Feb. 15, 1968).
Lederer, P. S., Performance testing, pressure transducers, Instr. Control System **40,** No. 9, 93–99 (Sept. 1967).
Leiss, J. E., Electron linear accelerators as sources of high intensity neutron bursts, Proc. Seminar on Intense Neutron Sources, Santa Fe, New Mexico, Sept. 19–23, 1966, Report No. CONF–660925, pp. 605–616 (1966).
Leiss, J. E., The NBS linac, Proc. Linear Accelerator Conf., Los Alamos, New Mexico, Oct. 3–7, 1966, Report No. LA–3609, p. 20 (1966).
Leslie, R. T., Kuehner, E. C., Ebulliometry, Treatise on Analytical Chemistry 8, Part D–5, Chapt. 89, 5085–5109 (1968).
Lightbody, J. W., Jr., Penner, S., A 12-channel semiconductor counter system for the NBS electron scattering spectrometer, IEEE Trans. Nucl. Sci. **NS–15,** 419–425 (June 1968).
Linzer, M., Forman, R. A., NMR studies of single crystal ND_4Cl, J. Chem. Phys. **46,** No. 12, 4690–4693 (June 15, 1968).
Litovitz, I., Macedo, P. B., Ultrasonic relaxation, viscosity, and free volume in molten glasses (Proc. Intern. Conf. Physics of Non-crystalline Solids, Delft, The Netherlands, July 6–10, 1964), Book, Physics of Non-crystalline solids, Ed. J. A. Prins, p. 220 (North Holland Publ. Co., Amsterdam, The Netherlands, 1965).
Loftus, T. P., Services and facilities for the calibration of soft x-ray detection instruments at the National Bureau of Standards (Proc. Conf. Detection and Measurement of X-radiation from Color Television Receivers, Washington, D.C., Mar. 28–29, 1968), Book, Conference on Detection and Measurement of X-radiation from Color Television Receivers, pp. 129–134 (U.S. Dept. Health, Education and Welfare, Washington, D.C., Mar. 1968).
Lonie, M., A report on body sizing for boys and students, Boys' and Young Men's Apparel Buyers' Assoc. J., p. 8 (1967).
Lutz, G. J., DeSoete, D. A., Determination of carbon in sodium by photon activation analysis, Anal. Chem. **40,** No. 4, 820–822 (Apr. 1968).
McMurdie, H. F., Progress in X-ray diffraction data compilations, Chapter in Fifty Years of Progress in Metallorgraphic Techniques, Am. Soc. Testing Mater. Spec. Tech. Publ. 430, 192–200 (1968).
Maeda, K., Young, J., Propagation of the pressure waves produced by auroras, J. Geomagnetism Geoelectricity **18,** No. 2, 275–299 (1966).
Mahaffey, C. T., Basic construction standards and a technical information center recommended at a Pan American seminar, ASA Mag. Std. **36,** No. 12, 375–377 (Dec. 1965).
Maienthal, E. J., Taylor, J. K., Improvement of polarographic precision by a comparative technique, Mikrochim. Acta **5,** 939–945 (1967).
Maki, A. G., Interpretation of the CS_2 laser transitions, Appl. Phys. Letters **11,** No. 6, 204–205 (Sept. 1967).
Marezio, M., Remeika, J. P., Zocchi, M., Cation distribution in the garnet $Eu_3Fe_{1.94}Ga_{3.06}O_{12}$, J. Chem. Phys. **48,** No. 3, 1094–1096 (Feb. 1968).
Margoshes, M., Selection of wavelengths for atomic absorption spectrometry, Anal. Chem. **39,** No. 10, 1093–1096 (Aug. 1967).
Marton, L., Photoelectricity, Encyclopedia of Physics, Ed. R. M. Besancon, pp. 512–514 (1966).
Mather, J. N., Invariance of the homology of a lattice, Proc. Am. Math. Soc. **17,** No. 5, 1120–1124 (Oct. 1966).
Melmed, A. J., Field emission microscopy, Book, Advances in Materials Research, Volume I. Experimental Methods, Ed. H. Herman, pp. 103–143 (Interscience Publ. Inc., New York, N.Y., 1967).
Melmed, A. J., Whiskers, thin films, and applications (real and imagined) to mass spectrometry and biological molecule imaging, Book, Field-Ion Microscopy, Ed. J. J. Hren and S. Ranganathan, pp. 183–212 (Plenum Press Inc., New York, N.Y., 1968).
Melmed, A. J., Layer, H. P., Kruger, J., Ellipsometry, low energy electron diffraction and field emission microscopy combined, Surface Sci. **9,** 476–483 (1968).
Moore, G. A., Automatic scanning and computer processes for the quantitative analysis of micrographs and equivalent subjects (Proc. Symp. Automatic Photo Interpretation, Washington, D.C., May 31–June 2, 1967), Book, Pictorial Pattern Recognition, Ed. G. C. Cheng, R. S. Ledley, D. K. Pollock, and A. Rosenfeld, pp. 275–326 (Thompson Book Co., Washington, D.C., 1968).
Mountain, R. D., Relaxation times for the volume viscosity of simple fluids, J. Chem. Phys. **48,** No. 5, 2189–2190 (Mar. 1, 1968).
Mountain, R. D., Zwanzig, R., Anomalous transport properties of a van der Waals gas, J. Chem. Phys. **48,** No. 4, 1451–1458 (Feb. 15, 1968).
Mulroy, W. J., Kusuda, T., Phillips, C. W., Survey on digital computer programs for heating and cooling load calculations, SICCAP Bull. **2,** No. 2, 4–8 (May 1968).
Newman, M., A bound for the number of conjugacy classes in a group, J. London Math. Soc. **43,** 108–110 (1968).
Odabasi, H., Spectrum of doubly ionized lanthanum (La III), J. Opt. Soc. Am **57,** 1459 (1967).
Olver, F. W. J., An extension of Millers's algorithm, Aplikace Mat. **13,** 174–176 (1968).
Parker, R. L., Report on the 1966 Boston International Conference on Crystal Growth, Proc. 1966 Intern. Union Crystallography, Moscow, U.S.S.R., July 12–21, 1966, 7, 341–354 (Academy of Sciences, Moscow, U.S.S.R., 1968).
Patty, O. L., Little, W. E., Zanboorie, M. H., Waveguide connector

measurements with a millimeter wave reflectometer, IEEE Trans. Microwave Theory Tech. **MTT-16,** No. 2, 121–123 (Feb. 1968).
Penner, S., Handling high-energy high-power electron beams, Record IEEE 9th Annual Symp. Electron, Ion and Laser Beam Technology, Berkeley, Calif., May 9–11, 1967, No. F-79, 50–61 (1967).
Penner, S., Handling high power electron beams, IEEE Trans. Nucl. Sci. **NS-14,** 908 (June 1967).
Penney, R. W., Phillips. C. W., Refrigeration requirements for truck bodies-effects of door usage, USDA Tech. Bull. No. 1375 (Superintendent of Documents, Government Printing Office, Washington, D.C. 20402, Nov. 1967, 10 cents).
Peterson, R. L., Ising chain as the basic cluster in effective-field theories of magnetism, Physics Letters **27A,** 177 (June 10, 1968).
Peterson, R. L., Suppressed spin-lattice relaxation, Phys. Rev. Letters **20,** No. 24, 1346–1348 (June 10, 1968).
Rhodes, I., The importance of the glossary storage in machine translation, Book, Machine Translation, Ed. A. D. Booth, pp. 431–449 (North-Holland Publ. Co., Amsterdam, The Netherlands, 1967).
Rhodes, I., The mighty man-computer team, Blanch Anniversary Volume, pp. 277–284 (Aerospace Research Laboratories, Office of Aerospace Research, U.S. Air Force, Arlington, Va., Feb. 1967).
Robbins, C. R., Synthetic $CaTiSiO_5$ and its germanium analogue ($CaTiGeO_5$), Mater. Res. Bull. **3,** 693–698 (1968).
Robbins, R. F., Reed, R. P., Tensile properties of neoprene below the glass transition temperature (Proc. 1967 Cryogenic Engineering Conf., Stanford University, Stanford, Calif., Aug. 21–23, 1967), Book, Advances in Cryogenic Engineering 13, 252–258 (Plenum Press Inc., New York, N.Y., 1968).
Roder, H. M., The thermal conductivity of helium gas at moderate pressures, Proc. Thermodynamik Symp., Heidelberg, Germany, Sept. 1967, Sponsored by the International Union of Pure and Applied Chemistry, Ed. K. L. Schafer, Paper No. VI-3, pp. 1–8 (1968).
Ronn, A. M., Laser induced infrared fluorescence, J. Chem. Phys. **48,** No. 1, 511–513 (Jan. 1968).
Schafft, H. A., Avoiding second breakdown, Proc. XIII Intern. Scientific Congress on Electronics, Rome, Italy, June 1966, pp. 119–130 (Rassegna Internazionale Elettronica Nucleare Teleradiocinematografica, Rome, Italy, 1966).
Scribner, B. F., Advances in excitation sources for spectrochemical analysis, Pure Appl. Chem. **10,** 579–594 (July 21, 1967).
Schwerdtfeger, W. J., Discussion of the paper, Method of estimating corrosion of highway culverts by means of polarization curves, by R. I. Lindberg, Highway Research Record No. 204, Metal Corrosion, Publ. 1535, p. 8 (National Research Council-National Academy of Sciences, Washington, D.C., 1967).
Sengers, J. V., Triple collision contribution to the transport coefficients of gases (Lectures presented at the Theoretical Physics Institute, University of Colorado, Boulder, Colo., Summer 1966), Book, Lectures in Theoretical Physics, Vol. IXC. Kinetic Theory, Ed. W. E. Brittin, pp. 335–374 (Gordon and Breach, New York, N.Y., 1967).
Shideler, R. W., Interfacing a teletypewriter to nuclear instruments used for computer-coupled activation analysis, Proc. 1965 Intern. Conf. Modern Trends in Activation Analysis, College Station, Texas, Apr. 1965, pp. 236–242 (1965).
Shimizu, A., Calculations of the penetration of gamma rays through slabs by the method of invariant imbedding, Nucl. Sci. Eng. **32,** 184–194 (May 1968).
Shimizu, A., Calculation of the penetration of gamma rays through two-layer slabs, Nucl. Sci. Eng. **32,** 385–391 (June 1968).
Simmon, J. H., Macedo, P. B., High temperature shear ultrasonic interferometer using sensitive phase-lock detection system, J. Acoust. Soc. Am. **43,** No. 6, 12–95–1301 (June 1968).
Spokas, O. E., The NBS linac master control and personnel protection system, IEEE Trans. Nucl. Sci. **NS-14,** 1016 (June 1967).
Stern, J., Aspect systems, Encyclopedia of Library and Information Science 1, 3200 (1967).
Sukle, D. J., Wells, J. S., EPR sample orientation servo, Rev. Sci. Instr. Notes **39,** No. 4, 604–605 (Apr. 1968).
Suzuki, G., Quantitative methods for decision making, Book, Management: Concepts and Practices, Ed. F. R. Brown, Chapt. VIII, pp. 155–193 (Industrial College of the Armed Forces, Washington, D.C., 1967).
Tighe, N. J., Hyman, A., Transmission electron microscopy of alumina ceramics (Proc. Intern. Symp. Anisotropy in Single-Crystal Refractory Compounds, Dayton, Ohio, June 13–15, 1967), Book, Anisotropy in Single-Crystal Refractory Compounds, Ed. F. W. Vahldiek and S. A. Mersol, 2, 121–136 (Plenum Press Inc., New York, N.Y., 1968).
Tschuikow-Roux, E., Photolysis of propene at 1470A, J. Phys. Chem. Note **71,** 2355 (1967).
Ugiansky, G. M., Ellinger, G. A., Corrosion of Monel 400 in high CO_2 well water, Corrosion **24,** No. 5, 134–136 (May 1968).
Ugiansky, G. M., Skolnick, L. P., Kruger, J., Stiefel, S. W., Rate-controlling step in stress corrosion cracking, Nature **218,** No. 5147, 1156–1157 (June 22, 1968).
Utech, H. P., Early, J. G., On the presence of thermal convection in the kinetics experiments of Rigney and Blakely, Acta Met. **15,** No. 7, 1238–1239 (1967).
Utech, H. P., Parker, R. L., Early, J. G., Coriell, S. R., The cam equation for a thermal-wave generator, J. Appl. Phys. **38,** No. 9, 3799–3800 (Aug. 1967).
Waclawski, B. J., Hughey, L. R., Madden, R. P., Effect of oxygen adsorption on the photoelectron yield from tungsten in the vacuum ultraviolet, Appl. Phys. Letters **10,** No. 11, 305–307 (June 1968).
Wahsweiler, H. G., Greiner, W., Danos, M., Continuum nuclear structure of O^{16} in the eigenchannel reaction theory, Phys. Rev. **170,** No. 4, 893–906 (June 20, 1968).
Wassink, H. W., Cyclotron harmonic emission along the field from a plasma, Phys. Fluids **11,** No. 3, 629–637 (Mar. 1968).
Watson, T. H., Flynn, D. R., Thermal conductivity and electrical resistivity of beryllium copper foil, Trans. Met. Soc. AIME **242,** 876–880 (May 1968).
Watson, T. W., Flynn, D. R., Thermal conductivity of four heat-resistant alloys, Trans. Met. Soc. AIME **242,** 844–846 (May 1968).
Weisman, H. M., Information and the discipline of communication sciences (Proc. American Documentation Institute Annual Meeting, New York, N.Y., Oct. 22–27, 1967), Book, Levels of Interaction Between Man and Information 4, 8–12 (Thompson Book Co., Washington, D.C., 1968).
Weissberg, A., Data handling systems, Proc. Second Conf. Technical Information Center Administration, St. David's, Pa., June 14–17, 1965, TICA 2, Ed. A. W. Elias, Chapt. 7, pp. 75–89 (Spartan Books, Washington, D. C., 1965).
Weitzel, D. H., Sindt, C. F., Daney, D. E., Hydrogen slush density reference system (Proc. 1967 Cryogenic Engineering Conf., Stanford University, Stanford, Calif., Aug. 21–23, 1967), Book, Advances in Cryogenic Engineering 13, 523–533 (Plenum Press Inc., New York, N.Y., 1968).
Wiederhorn, S. M., The influence of water vapor on crack propagation in soda-lime glass, J. Am. Ceram. Soc. **50,** No. 8, 407 (1967).
Wiese, W. L., Transition probabilities for prominent Ar I lines (Proc. 8th Intern. Conf. Phenomena in Ionized Gases, Vienna, Austria, Aug. 27–Sept. 2, 1967), Book, 8th International Conference on Phenomena in Ionized Gases, p. 447 (Springer Verlag, Vienna, Austria, Sept. 1967).
Winogradoff, N. H., Neill, A. H., Band tailing effects and the temperature dependence of radiative recombination in compensated, epitaxial GaAs laser junctions, IEEE J. Quantum Elect. **QE-4,** No. 4, 111–113 (Apr. 1968).
Wyckoff, J. M., On-line transformations of high resolution spectra, IEEE Trans. Nucl. Sci. **NS-14,** 634 (Feb. 1967).
Wyckoff, J. M., Radioactivity produced by a linac, IEEE Trans. Nucl. Sci. **NS-14,** 990 (June 1967).
Yakowitz, H. Vieth, D. L., Heinrich, F. J., Michaelis, R. E., Homogeneity characterization of NBS spectrometric standards. II: Cartridge brass and low-alloy steel (Proc. 14th Annual Conf. Applications of X-ray Analysis, University of Denver, Denver Research Inst., Denver, Colo., Aug. 25–27, 1965), Book, Advances in X-ray Analysis, Ed. G. R. Mallett, M. Fay, and W. M. Mueller, 9, 289–303 (Plenum Press Inc., New York, N.Y., 1966).
Yee, K. W., Deslattes, R. D., Transistorized current stabilizer for X-ray tubes with directly heated cathodes, Rev. Sci. Instr. **38,** No. 5, 637–638 (May 1967).
Yolken, H. T., Kruger, J., Thermal regeneration of oxide covered iron {100} and {110} surfaces, J. Electrochem. Soc. **114,** No. 8, 796–799 (Aug. 1967).
Yolken, H. T., Kruger, J., Calvert, J. P., Hydrogen in passive films on Fe, Corrosion Sci. **8,** 103–108 (1968).

**Publications for which a price is indicated are available by purchase from the Superintendent of Documents, U. S. Government Printing Office, Washington, D.C. 20402 (foreign postage, one-fourth additional). The NBS non-periodical series are also available from the Clearinghouse for Federal Scientific and Technical Information, Springfield, Va. 22151. Reprints from outside journals and the NBS Journal of Research may often be obtained directly from the authors.*

U.S. GOVERNMENT PRINTING OFFICE : 1969 OL—324-194

UNITED STATES
GOVERNMENT PRINTING OFFICE
DIVISION OF PUBLIC DOCUMENTS
WASHINGTON, D.C. 20402

OFFICIAL BUSINESS

SJR-A OCT 46129
UNIVERSITY MICROFILMS INC
ATTN SERIALS SECTION
300 NORTH ZEEB RD
ANN ARBOR MICH 48106

FICE

JOURNAL OF RESEARCH of the National Bureau of Standards Vol. 73A, No. 1 January–February 1969
A. Physics and Chemistry

Contents

Page

Specific heats of oxygen at coexistence. Robert D. Goodwin and Lloyd A. Weber. 1

Specific heats C_v of fluid oxygen from the triple point to 300 K at pressures to 350 atmospheres. Robert D. Goodwin and Lloyd A. Weber. 15

Thermodynamic properties of fluid oxygen at temperatures to 250 K and pressures to 350 atmospheres on isochores at 1.3 to 3.0 times critical density. Robert D. Goodwin. 25

Two new standards for the pH scale. Bert R. Staples and Roger G. Bates. 37

Calculation of diffusion coefficients in ternary systems from diaphragm cell experiments. P. R. Patel, E. C. Moreno, and T. M. Gregory. 43

Calculated line strength for the transition array $(3d^3+3d^24s)$-$3d^24p$ in Ti II. H. Mendlowitz. 51

Morphological stability of a cylinder. Sam R. Coriell and Stephen C. Hardy. 65

Distorted tetrahedra in strontium copper åkermanite. Jun Ito and H. Steffen Peiser. 69

Tritium-labeled compounds XII. Note on the synthesis of D-glucose-2-t and D-mannose-2-t. Horace S. Isbell, Harriet L. Frush, C. W. R. Wade, and A. J. Fatiadi. 75

A Survey of blemishes on processed microfilm. C. S. McCamy, S. R. Wiley, and J. A. Speckman. 79

Publications of the National Bureau of Standards. 99

Library of Congress Catalog Card Number: 62–37059

For sale by the Superintendent of Documents, U.S. Government Printing Office, Washington, D.C. 20402. Price $1.00 (single copy). Subscription price: $6 a year; $1.25 additional for foreign mailing.
UNITED STATES GOVERNMENT PRINTING OFFICE, WASHINGTON : 1969